Design and Synthesis of Novel Photoswitches for the Platform Concept

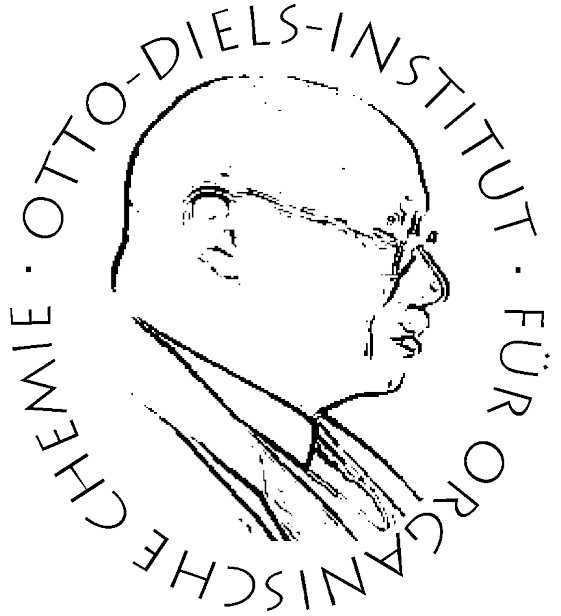

DISSERTATION

zur Erlangung des Doktorgrades
der Mathematisch-Naturwissenschaftlichen-Fakultät
der Christian-Albrechts-Universität
zu Kiel

vorgelegt von

Melanie Hammerich

Otto Diels-Institut für Organische Chemie
Kiel 2016

Referent: Prof. Dr. Rainer Herges
Koreferent: Prof. Dr. Frank Sönnichsen

Tag der mündlichen Prüfung: 13.10.2016
Zum Druck genehmigt: 13.10.2016

gez. Prof. Dr. Natascha Oppelt, Dekanin

Die vorliegende Arbeit wurde unter Anleitung von
Prof. Dr. Rainer Herges
am Otto Diels-Institut für Organische Chemie
der Christian-Albrechts-Universität
im Zeitraum von April 2012 bis Juli 2016 angefertigt.

Teile dieser Arbeit entstanden unter Kooperation im
Sonderforschungsbereich 677 „Funktion durch Schalten“.

Hiermit erkläre ich, Melanie Hammerich, dass ich die vorliegende Doktorarbeit selbstständig und nur mit den angegebenen Hilfsmitteln angefertigt habe. Diese Dissertation ist nach Inhalt und Form - abgesehen von der Beratung durch meinen Betreuer Herrn Prof. Dr. Rainer Herges - durch mich eigenständig nach den Regeln guter wissenschaftlicher Praxis der Deutschen Forschungsgemeinschaft verfasst worden. Sie hat weder in Auszügen noch in ganzer Form einer anderen Stelle im Rahmen eines Prüfungsverfahrens vorgelegen. Es handelt sich um meinen ersten Promotionsversuch.

Kiel, 28.07.2016

Melanie Hammerich

Danksagung

Der erste Dank gebührt Prof. Dr. Rainer Herges für die Bereitstellung des spannenden und interessanten Themas. In den vier Jahren meiner Doktorarbeit nahm er sich stets die Zeit in anregenden Diskussionen neue Lösungsansätze zu entwickeln. Sehr dankbar bin ich für die zahlreichen Konferenzreisen, die mir während meiner Promotion ermöglicht wurden.

Obendrein möchte ich mich bei Prof. Dr. Frank Sönnichsen bedanken, der mit stets hilfreichen Ideen auch die schwierigsten analytischen Probleme zu lösen wusste und des Weiteren immer offen für wissenschaftliche Diskussionen war. Zudem möchte ich mich für die Übernahme der Zweitkorrektur bedanken.

Ein großer Dank gilt Vanessa Kahl für die Hilfe bei allem Organisatorischen und den seelischen Beistand in all den Jahren. Der spektroskopischen Abteilung möchte ich meine Wertschätzung ausdrücken für die Aufnahme der zahlreichen Spektren.

Insbesondere möchte ich mich beim AK Herges bedanken – Wettbewerbe mit sonderbaren Regeln, die Kaffeepausen, FABs, Mett-Frühstück, einige AK-Ausflüge sorgten dafür, dass diese Zeit nie langweilig wurde. Ausdrücklich dem verrücktesten Labor im ganzen Institut - R217 – möchte ich für das spaßige Arbeiten danken. Dazu wären die paar Monate im Kabuff ohne Schütti, der geduldig meine Pöbeleien ertragen hat, nicht dieselben gewesen. Cosima, Torben, Fynn, Janine, Lisa, Widukind und Jonas möchte ich für die fleißige Unterstützung bei ihren Bachelorarbeiten, F3-Praktika und als Koch-Hiwi danken.

Eine große Hilfe beim Schreiben dieser Arbeit waren die stets nützlichen Korrekturen, die ich von Torsten, Lisa, Anna, Schütti und Jens erhalten habe. Für das geduldige Lösen so mancher LaTeX-Probleme möchte ich mich bei Flo bedanken.

Bei meinen Kommilitonen möchte ich mich für den Zusammenhalt in all den Jahren und die Ermutigungen nie aufzugeben bedanken. Vor allem bei „der Herde“ möchte ich mich für die lustigen Donnerstagabende bedanken, die ich sehr vermissen werde. Claudia, Carolin, Jessica, Anne, Gernot und Kim – vielen Dank für die tolle Zeit. Die Treffen mit meinen Nichtchemikern Anna, Karim, Katharina und Gesa jeden Mittwochabend sorgten stets für Aufheiterung durch legendäre Siedler-von-Catan-Schlachten beim Pizzaessen.

Talina, Nicolai (AG Magnussen), Ian Howard (Karlsruhe) und Xianghui Zhang (Bielefeld, es existiert wirklich!) danke ich für die vielen interessanten Kooperationsprojekte.

Nadine und meinen Eltern möchte ich für die Unterstützung in all den Jahren danken. Die Ruhepausen bei euch waren immer die beste Erholung in stressigen Zeiten. Für all eure Hilfe möchte ich mich herzlich bedanken. Ohne euch hätte ich das alles nicht geschafft!

Abstract

The platform concept based on triazatriangulenes (TATA) offers a novel method to prepare functionalized gold surfaces (Au(111)). The large planar cations are used as molecular anchors that form highly ordered, hexagonal monolayers if absorbed to the gold surface. Furthermore, the distance between the platforms ensures the functionality of the mounted molecules. The three components, platform, spacer and functional unit, can be exchanged according to the desired application.
Within this thesis three different photoswitchable units were designed and investigated to achieve a unidirectional movement on the surface. Both the lateral movement of the adsorbed molecules about the surface and the transport of nanoparticles was the goal of this work. Thus, particularly suited photoswitchable molecules were designed towards this end. To achieve a lateral movement of the molecules on the surface an azobenzene moiety was spanned between two TATA platforms parallel to the surface. Two different molecules were synthesized which could both be switched to high percentage (>95 %) to the corresponding *cis* configuration and several switching cycles show no fatigue or decay.
For the realization of an artificial ciliated epithelium an imine-functionalized monolayer on a Au(111) surface was developed. Therefore, six imine-functionalized TATA platforms were synthesized and their photochemical properties were investigated in solution. The *cis* isomers could be accumulated upon irradiation with 365 nm up to 50 %, which was verified by low temperature ^{1}H NMR and UV/vis spectroscopy (215-233 K). Rate constants for the back isomerization were determined for several temperatures and hence, the half-life at room temperature could be extrapolated as $t_{1/2}$=0.58 s. The formation of highly ordered monolayers was confirmed by scanning tunneling microscopy and UV/vis measurements of these surfaces showed the integrity of the photoswitchable unit.

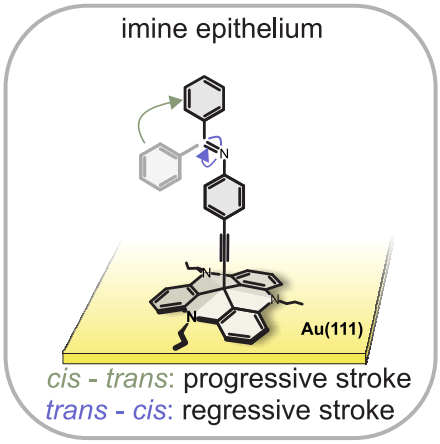

Futhermore, the synthesis of a new class of photoswitches was realized. These heterodiazocines exhibit outstanding photochemical properties whereas the synthesis is simplified with respect to the parent diazocines. Hence, a new approach for the synthesis of unsymmetric diazocines was developed. Moreover, these diazocines can be efficiently switched with light in the near infrared region which opens up applications as *in vivo* photoswitchable drugs and functional materials.

Kurzzusammenfassung

Das auf Triazatriangulenen (TATA) basierende Plattform-Konzept bietet eine neue Möglichkeit zur Funktionalisierung von Au(111)-Oberflächen. Die verwendeten großen, planaren Kationen bilden hoch geordnete, hexagonale Monolagen auf Au(111). Durch den räumlichen Abstand der Plattformen zueinander bleibt die Funktionalität der aufgebrachten Moleküle erhalten. Da es sich um ein modulares System handelt, können die drei Komponenten, Plattform, Abstandhalter und funktionelle Einheit, je nach Anwendung ausgetauscht werden.

Um eine gerichtete Bewegung über eine Oberfläche zu realisieren, wurden innerhalb dieser Dissertation drei verschiedene photoschaltbare Einheiten entworfen und untersucht. Ziel war dabei sowohl die laterale Bewegung des adsorbierten Moleküls, als auch der Transport von Nanopartikeln. Dafür wurde die photoschaltbare Einheit für die jeweilige Anwendung konzipiert. Um eine laterale Bewegung der adsorbierten Moleküle zu erreichen, wurde eine Azobenzol-Einheit zwischen zwei TATA-Plattformen parallel zur Oberfläche aufgespannt. Beide auf diese Weise erhaltenen Moleküle ließen sich zu hohen Anteilen (>95 %) in das *cis*-Isomer überführen und zeigten über mehrere Schaltzyklen keine Anzeichen von Zerfall oder Ermüdung.

Für die Realisierung eines künstlichen Flimmerepithels wurde ein Imin-funktionalisierter Monolayer auf einer Au(111)-Oberfläche entworfen. Hierfür wurden sechs verschiedene Imin-funktionalisierte TATA-Plattformen hergestellt und auf ihre photochemischen Eigenschaften in Lösung untersucht. Mit Tieftemperatur ^{1}H-NMR- und UV/vis-Spektroskopie (215-233 K) konnte beim Belichten mit 365 nm die Bildung der *cis*-Isomere zu 50 % nachgewiesen werden und die Geschwindigkeitskonstanten der Rückisomerisierung für verschiedene Temperaturen bestimmt werden. Damit konnte die Halbwertszeit der *cis*-Konfiguraton für Raumtemperatur auf $t_{1/2}$=0.58 s hochgerechnet werden. Mit Rastertunnelmikroskopieaufnahmen konnte die Bildung hochgeordneter Monolagen nachgewiesen werden. Ferner zeigten UV/vis-Messungen der Oberflächen die Unversehrtheit der photoschaltbaren Einheit nach der Adsorption.

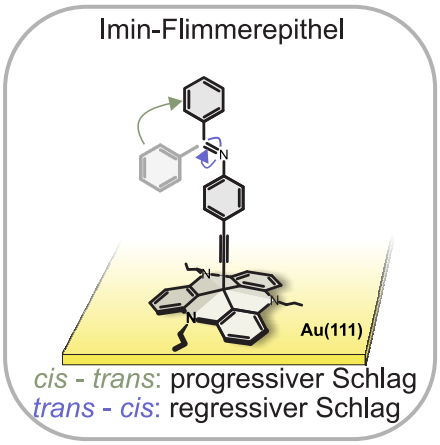

Weiterhin konnte in dieser Arbeit eine neue Klasse von Photoschaltern entwickelt werden. Die hergestellten Heterodiazocine besitzen herausragende photochemische Eigenschaften, während ihre Synthese im Vergleich zum Stammsystem deutlich vereinfacht werden konnte. Somit konnte ein neuer Ansatz für die Synthese unsymmetrischer Diazocine entwickelt werden. Die überragende Eigenschaft im biooptischen Fenster zu schalten, prädestiniert diese Moleküle für den Einsatz in Photopharmaka und in funktionellen Materialien.

Contents

1 Introduction

Locomotion represents one of the most important processes in nature and a variety of different mechanisms can be found in biological systems.[1,2] Depending on the environment, the size of the object or the possibilities of the degrees of freedom nature evolved a perfectly fitting movement mechanism for each organism.[3] To understand the general systematics of movement behind this diversity is the first challenge to mimic these natural processes on a molecular scale. PURCELL realized that it is necessary for a forward movement to break the time reversal symmetry.[4,5] Therefore two partial movements are required to avoid that the object returns to the place of origin. Only in this case it could be prevented that the dislocation obtained in the first step of the periodic movement is revoked in the second part. This is shown schematically in the graphic below (Figure 1.1).

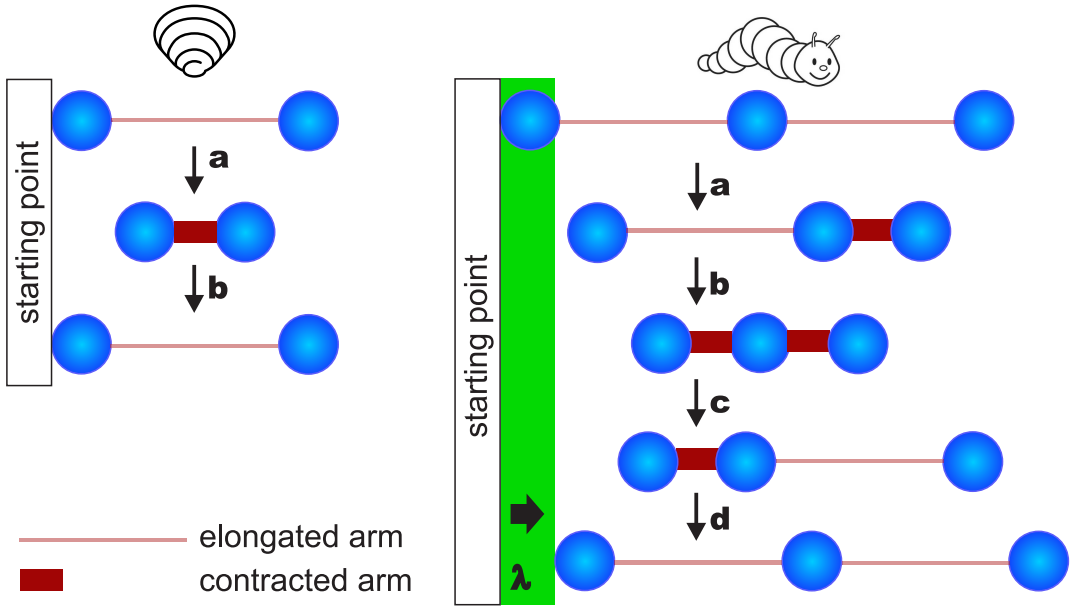

Figure 1.1: Schematic depiction of an object with one (left) and two (right) degrees of freedom: the object on the left failed to move forward as with the revision of the first movement the object reaches the starting point again; the object on the right, however, moves forward as the time reversal symmetry is broken by alternate movement of both joints.[4,5]

The left object only contains one degree of freedom whereby it moves forward in the first step of the periodic movement (step a) but only ends up at the starting point again when the movement is reverted in the second part of motion (step b). If the object, however, possesses two degrees of freedom the time reversal symmetry can be broken while using both joints in turn. After the object is contracted by shortening of joint 1 (step a), the back movement to the original position can be prohibited as the second joint is shortened as well and the whole object is contracted a second time. With this second part the time reversal symmetry is broken and after inversion of both movements (step c and d), the object moves forward the distance of the stretch λ marked in green. The swimming movement of a mussel sets an illustrative example for the first case. By opening the seashells the mussel can swim forward but returns immediately to the original position by closing the shell. As opposed to this, a spanworm can move forward by using two different moving steps, while first crawling forward by pulling the rump close to the head and subsequently stretching. The replication of this natural directed motion is one great challenge in current research.

1.1 Photoswitches as Molecular Joints

To mimic a natural movement on a molecular scale a molecular unit that can perform a reversible geometry change between two configurations is required. One common strategy to manipulate the constitution of molecules utilizes switchable units.[6] As a result the molecule can be transformed between two species by an external stimulus whereby the properties of the molecules such as geometry, dipole moment or conjugation are changed.[7]

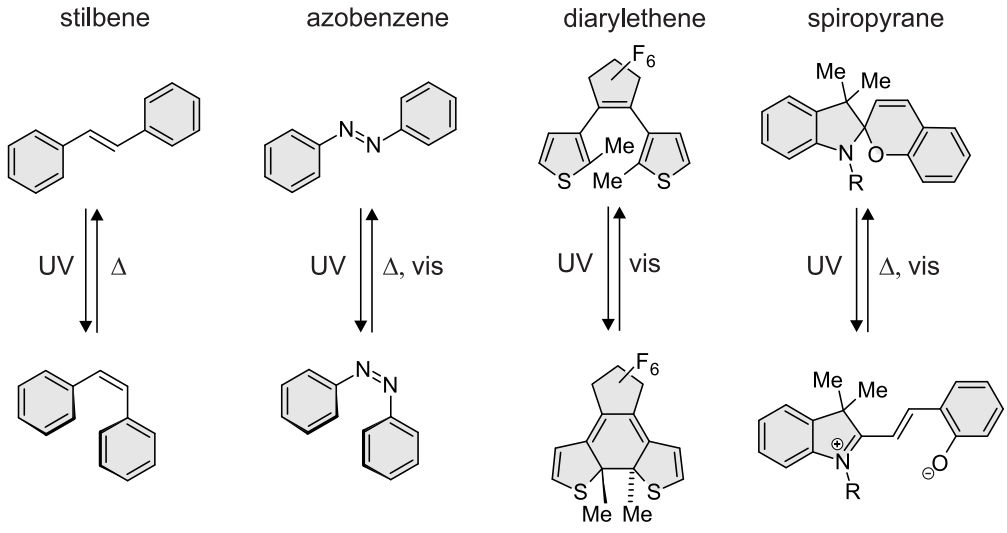

Figure 1.2: Structures of the ground state and the meta stable form of the most common photoswitches with the required region of light for the isomerization, from left to right: stilbene, azobenzene, diarylethene and spiropyrane.

The widespread use of photoswitches is based on several favorable properties: Firstly, light as an external stimulus can be fine-tuned with regard to wavelength and intensity, and secondly, the stimulus is bioorthogonal. A large variety of photoswitches has already been developed, the most prominent examples being stilbene,[8] azobenzene,[9] diarylethene[10] and spiropyranes[11] (Figure 1.2).

1.1.1 Azobenzene

To change the structure of a molecule by switching, azobenzenes offer the best opportunities as they provide a large variation in geometry. The switching mechanism of azobenzene is based on a *cis* → *trans* isomerization of the N=N double bond (Figure 1.3).[12] Upon isomerization, the distance of the *para* carbon atoms shortened by about 4 Å.[13–15] Additionally the geometry is changed from a planar configuration to a twisted form in the *cis* isomer. The switching to the *cis* isomer is induced by irradiation with light of 365 nm into the ππ* band.[16] In this process the ππ* band of the *cis* isomer is hypsochromically shifted and decreases in intensity. Simultaneously the previously forbidden nπ* transition is allowed for the *cis* isomer and the intensity of its absorption band increases.[17,18] The isomerization can proceed via different mechanisms.[19–22] One reaction pathway follows the inversion of one N−C single bond.[23,24] For the alternative route the isomerization is performed by rotation of the N=N double bond.[25,26] Whether the inversion or rotation mechanism occurs could not be conclusively resolved to date.[27] Current research suggests that the mechanism depends on the substitution of the azobenzene.[28] Next to these two mechanisms a third isomerization mechanism (hula-twist) was found for some azobenzenes that constitute a combination of the beforehand described mechanisms.[29]

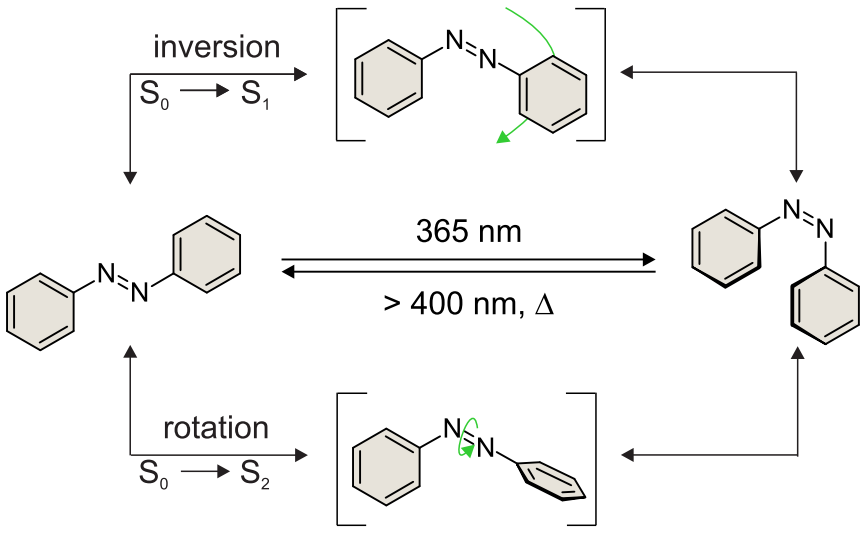

Figure 1.3: The switching between *trans* and *cis* isomer of azobenzenes can occur via inversion (excited state S_1) or rotation (excited state S_2). It is assumed that forward and back reaction proceed by the same mechanism.[9]

The *trans* isomer can be reobtained again by irradiation with visible light (400-450 nm), electrochemically or thermally.[9,16,30] The light-induced conversion from the *cis* to the *trans* isomer follows the same mechanism as the *cis* → *trans* isomerization. Therefore azobenzenes are not suitable for a unidirectional movement.

1.1.2 Imine

Imines achieve similar isomerization of the C=N double bond upon irradiation,[31] but the mechanism of the *trans* → *cis* isomerization differs from the back reaction (Figure 1.4).[32–34] Whereas the isomerization to the meta stable *cis* configuration occurs via a bond rotation, the back reaction to the thermodynamically more stable *trans* isomer follows an inversion mechanism. As the activation barrier is about 20 kJ/mol lower than for azobenzenes the thermal back reaction is extremely fast and the *trans* isomer is obtained back within seconds.[31,35–37] In comparison to azobenzenes the substitution of one nitrogen atom to a CH group leads to a distorted geometry of the imine and the aniline ring is twisted out of plane by about 41-55° depending on the substitution,[38] leading to a hypsochromic shift of the ππ* band.[39–41] As a result the *trans* isomer exhibits a dipole moment of 1.57 D.[42,43] By switching the imine to the *cis* isomer the molecule gets more twisted and the dipole moment rises to 2.18 D.[44]

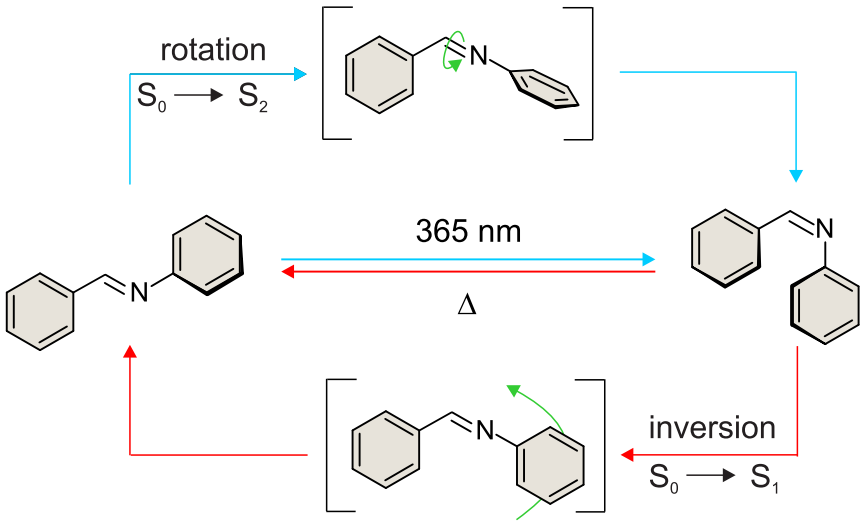

Figure 1.4: The forward reaction to the *cis* isomer occurs via rotation around the C=N double bond upon irradiation with 365 nm by excitation into the S_2 state (blue arrows), whereas the thermal back reaction follows an inversion mechanism of the C−N single bond by excitation into the S_1 state (red arrows).

Due to the different mechanisms of forward and back reaction as well as the fast back isomerization, imines are suitable candidates for a unidirectional movement on a molecular scale.[45,46]

1.1.3 Diazocine

One approach to enhance the effect of the switching movement is the suppression of conformational freedom in the photoswitchable unit. As in azobenzenes both phenyl rings can rotate around the single bond the stroke of the switching movement is reduced in efficiency. This rotation can be prohibited if both *ortho* positions are connected via an ethylene bridge. The so called diazocines exhibit excellent photochemical properties. The synthesis of the parent system was already published in 1910 by DUVAL[47] but the potential as a photoswitch was not discovered before the publication of TEMPS in 2009.[48,49] Due to the applied constraints the thermodynamically more stable form constitutes in the *cis* isomer. By switching the diazocine with 400 nm to the *trans* isomer the absorption of the nπ* band is shifted bathochromically by about 100 nm. The good separation of the nπ* bands within the diazocine leads to a change in color from yellow (*cis* isomer) to red (*trans* isomer) and to an almost complete conversion to the respective isomer (Figure 1.5).[50,51] The quantum yields of both switching processes ($\phi_{ZE} = 72 \pm 4$ % and $\phi_{EZ} = 50 \pm 10$ %) are considerably exceeding the respective values for azobenzenes ($\phi_{ZE} = 53$ % and $\phi_{EZ} = 24$ %).[52] Thereto diazocines proved a high photostability as they show no sign of photo degradation or fatigue.

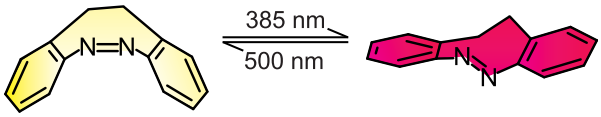

Figure 1.5: Isomerization to the *trans* configuration can be accomplished by irradiation with blue light, the *cis* isomer can be obtained with green light.

1.1.4 Photochromic Compounds Switchable with Visible Light

However, most employed photoswitches to date face the problem that UV light is mandatory as trigger for at least one photoinduced step whereby after some switching cycles photo degradation occurs. Consequently, the development and improvement of photoswitches that isomerize upon irradiation with visible light has been of great interest in recent years.[53–56] A huge challenge is caused by the synthesis of photoswitches within the bio-optical window ($\lambda > 650$ nm)[57,58] as those molecules would be of great interest in biological and medical applications, due to minimal absorption of blood in the region between 600 and 1100 nm.[59,60]

Beside the previously discussed diazocines a few azobenzenes could be improved to switch in the visible region of light. Nearly simultaneously WOOLLEY (OMe substitution)[61?] and HECHT (fluoro substitution)[62–65] published their ortho substituted azobenzenes (Figure 1.6). This substitution pattern leads to a non planar geometry in the *trans* configuration. As a result the nnπ* transitions of the *trans* isomers are no longer spin forbidden and in addition the nπ* transitions of both configurations are separated. Therefore, the nπ* band of the *trans* isomer shifts considerably to longer wavelengths whereby the nπ* band of the *cis* isomer remains nearly unchanged compared to common azobenzenes. Switching to the *cis* isomer can be accomplished by irradiation with green

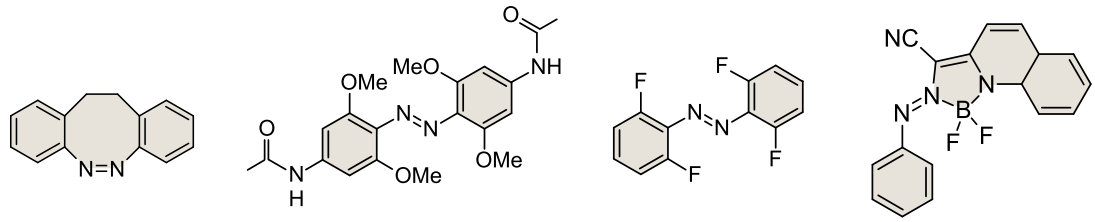

Figure 1.6: Enhanced azobenzenes that can be switched in both directions with visible light, from left to right: diazocine, *ortho* substituted azobenzenes from WOOLLEY and HECHT, BF_2-azobenzene by APRAHAMIAN.

light; the *trans* isomer is obtained with blue light. In comparison to diazocines the separation of both nπ* bands is distinctively smaller ($\sim$40 nm). Hence, the switching efficiency of these compounds slightly decreases. A completely new approach was introduced by the APRAHAMIAN group. Their BF_2 complexed azobenzenes exhibit a strong bathochromic absorption shift (λ_1 = 570 nm, λ_2 = 450 nm).[58,66]

1.2 Functionalized Metal Surfaces

To detect a unidirectional movement of photoswitchable molecules, it is favorable to anchor the photoswitches firmly to a rigid reference frame. To achieve this goal, self-assembled monolayers (SAMs) are widely used to immobilize molecules on metal surfaces.[67] Metal single crystals exhibit almost perfect surfaces without crystallographic defects, enabling the formation of highly ordered two-dimensional frameworks.[68,69] Additionally they can be investigated by a wide range of surface analytic methods like scanning tunneling microscopy (STM), UV/vis, infrared reflection absorption spectroscopy (IRRAS) or surface-enhanced raman scattering (SERS). A frequently employed surface is the Au(111) surface.[70,71] Apart from the previously described properties the easy preparation of the SAMs plays an important role. The most established method uses alkane thiols to anchor the functional molecules to the gold surface.[72–74] Sulfur has a high affinity to gold whereby the alkane thiols build tightly bound SAMs on Au(111) surfaces. The functionalized monolayers are prepared by the immersion of a Au(111) surface into a solution of the corresponding alkane thiol, resulting in spontaneous adsorption of the molecules on the surface.[75–77] The extremely dense packing in these monolayers ensures a nearly perpendicular orientation of the molecules on the surface.[78] Thus, the distance between the functional groups is very small on the surface (Figure 1.7). Consequently, sterically demanding reactions e.g. *trans* $\rightarrow$ *cis* isomerization can be hindered by the small distance between the functional groups on the surface and are only feasible to a minor degree.[79–83] Mixed monolayers with shorter alkane thiols slightly improve the situation. By implementation of the shorter alkane thiols the distance between the functional molecules is increased and *cis* $\rightarrow$ *trans* isomerization (e.g. azobenzene) is enabled. However, the preparation of highly ordered monolayers is impossible as the distribution on the surface is statistical and the ratio of the functional molecule can deviate

from the proportion in solution.[81,84] Moreover, after some time phase separation occurs and densely packed monolayers are obtained again.[84–86] To solve these problems several strategies have been developed e.g. unsymmetrical disulfides and thioethers, bulky groups attached to the functional molecules, tripods and calixarenes.[87] Despite these efforts the preparation of highly ordered monolayers with distinct distances between the functional molecules still remains challenging.

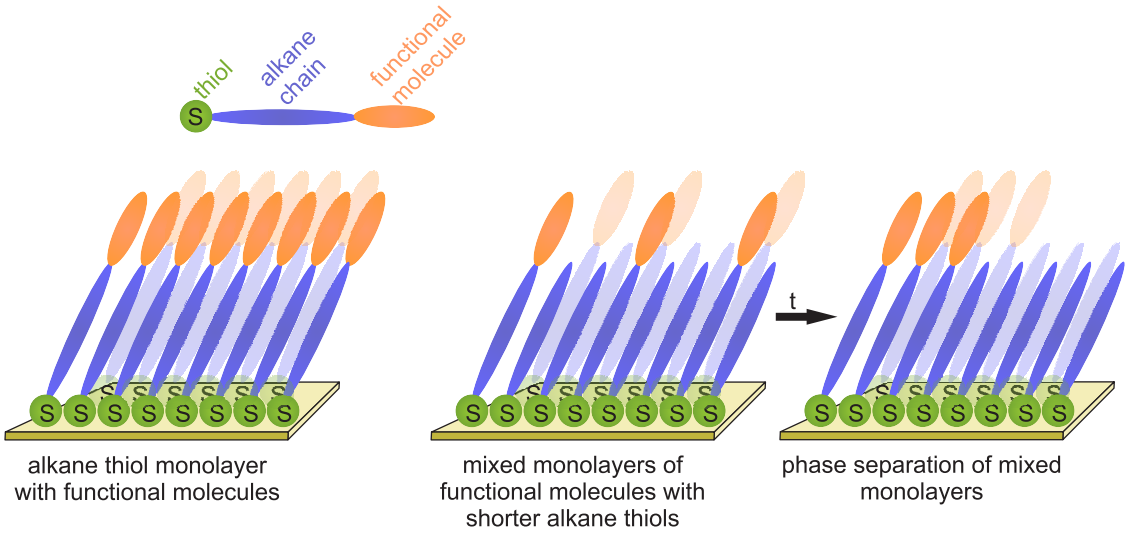

Figure 1.7: Alkane thiol based monolayers on Au(111) form highly packed SAMs which prevents sterically demanding reactions due to the small distance between molecules. Mixed monolayers with shorter alkane thiols added to the preparation solution are one approach to solve this problem as the free volume for the functional molecules is enhanced. After some time phase separation occurs and highly packed islands are obtained again.

A solution is provided by the platform concept that was developed by HERGES *et al.* as it proved to be an efficient method to prepare highly ordered functionalized Au(111) surfaces.[88] The attachment of the functional molecules to the metal surface is achieved by triazatriangulenium (TATA) cations. The planar systems form highly ordered hexagonal monolayers upon adsorption to a Au(111) surface by dipping the metal surface into a solution of the platform or its derivatives. The platforms are adsorbed on the surface by dispersive interaction as opposed to alkane thiols that are covalently attached to the metal surface. According to calculations the platforms can be moved over the surface with almost no barrier,[89] whereby the binding site with the phenyl rings and nitrogen atoms of the TATA located on top of the gold atoms are slightly favored.[90] The distance between the neighboring platforms can be adjusted by the length of the alkyl chains (Figure 1.8).

Thereby the distance change proceeds stepwise and not continuously with enlargement of the alkyl chains. As a consequence, only three different super structures ($\sqrt{13} \times \sqrt{13}$, $\sqrt{19} \times \sqrt{19}$ and $\sqrt{21} \times \sqrt{21}$) were observed for TATA platforms.[90] The crossovers occur between the propyl and butyl chain, as well as between decyl and dodecyl platforms. The undecyl TATA platform constitutes the only exception as it can form both $\sqrt{19} \times \sqrt{19}$ and $\sqrt{21} \times \sqrt{21}$ super structures.

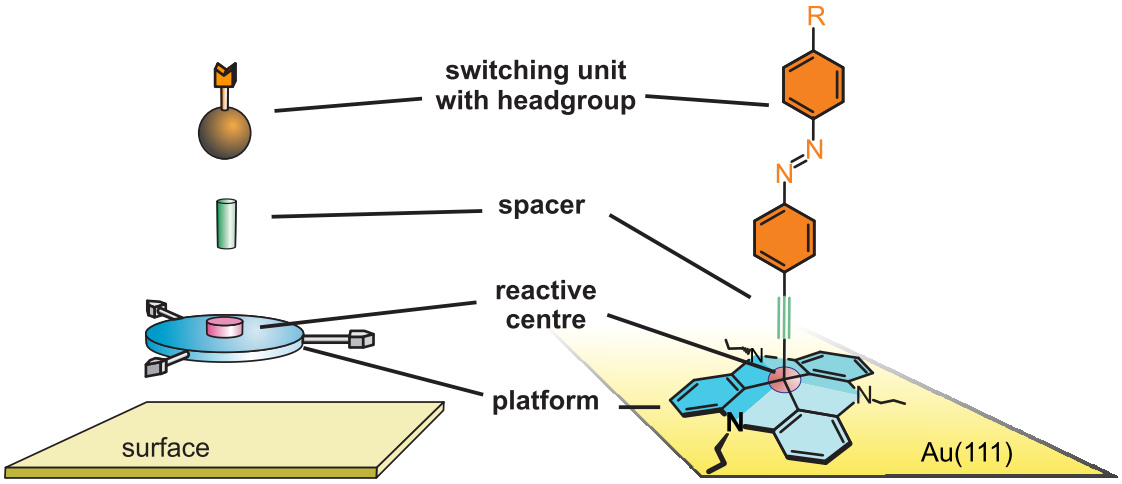

Figure 1.8: Sketch (left) and an exemplary molecule (right) for the platform concept: triazatriangulenium cations are used as platforms to bind firmly to a metal surface. The center of these platforms can be functionalized with a spacer unit that ensures the free rotation of the functional molecules and the orthogonal alignment of the setup. The distance between the platforms can be adjusted by the length of the alkyl chains.[91,92]

Functionalization of the platforms has no influence on the formed super structure[93] and can be easily realized by reaction of a TATA platform with a nucleophile.[94] To ensure an efficient distance between functional molecule and TATA platform, vertical spacer units are used, whereby ethynyl spacers proved to be particularly feasible. The functional molecules are attached orthogonally, freely rotatable and decoupled from the metal surface. Thus, the switching efficiency and quantum yields coincided with the values obtained for the switches in solution.[95] TATA platforms could already be successfully functionalized with porphyrins,[96–98] azobenzenes[88,91,94], diazocines[92,99] and molecular wires.[100] The switching of the azobenzene units could be verified with UV/vis,[101] SERS,[102] IRRAS,[103] cyclic voltammetry,[95] near edge X-ray absorption fine structure (NEXAFS)[104] and chronoamperometry.[95] However, the transport of nanoparticles could not be realized yet with the existing molecules. The synthesis of TATA functionalized molecules that are enabled to perform a unidirectional motion is therefore particularly interesting.

2 Scope

The platform concept provides a broad variety of possibilities for the realization of molecular systems that are enabled to perform different kinds of motion. As it is a modular system the three components (platform, spacer, functional unit) can be adapted depending on the desired application.[88,91,92,94] The focus of this work lies on the functional unit to realize a unidirectional movement. To this end, three photoswitchable molecules will be investigated as potential elements of triazatriangulenium (TATA) based molecular machines.

2.1 Lateral Movement above a Surface

The vertical functionalization of metal surfaces with photoswitches is well understood and a range of strategies on this topic has been developed.[87] However, for the lateral functionalization of surfaces only a few approaches have been reported.[105–107] As the platform concept provides the facility for vertical as well as horizontal functionalization the bridging of two TATA platforms with an azobenzene unit has to be be realized in this work. It is crucial for the design of molecules of this type that both TATA platforms can bind to the Au(111) surface in either configuration of the photoswitchable moiety. Furthermore, as photochromic compounds become inactive while adsorbed directly to a metal surface, the bridging unit is supposed to have a sufficient distance to the metal surface.[108] Supported by density functional theory (DFT) calculations the molecules were designed to archive a change of the distance between the platforms by switching the azobenzene moiety (Figure 2.1).

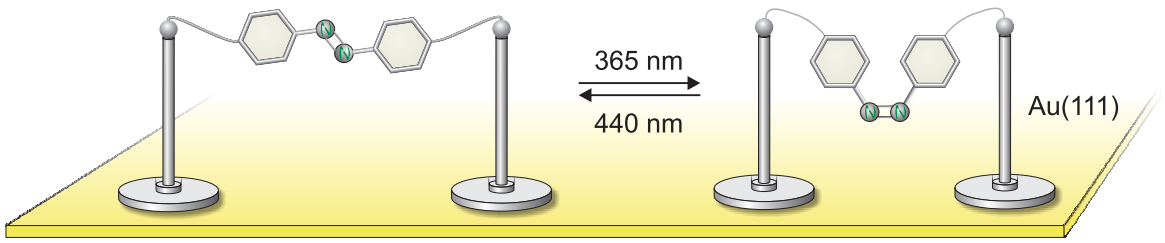

Figure 2.1: Scheme of the molecular muscle: two TATA platforms are linked laterally by an azobenzene unit and, therefore, the distance between the centers of the platforms can be adjusted by light.[109]

The *trans* configuration exhibits a distance of 18.9 Å between the two central carbon atoms of the platforms, whereas the detachment is shortened to 15.6 Å in the *cis* isomer. This motion resembles the contraction of a muscle. The aim of this project is to synthesize two molecular muscles on the basis of propyl- and octyl-TATA to investigate the influence on the lattice constant in the corresponding scanning tunneling microscopy (STM) experiment. After successful synthesis the photophysical properties of the molecular muscle have to be investigated in solution with ^{1}H NMR and UV/vis spectroscopy to check if the *cis* isomer can be formed. Subsequently, STM measurements have to be performed to show the movement above the surface.

2.2 Imines as Artificial Ciliated Epithelium

Furthermore, within the scope of this work is the functionalization of TATA platforms to achieve a unidirectional transport of nanoparticles above a surface. Azobenzenes are the most widely used photoswitches as they can be applied manifoldly and exhibit reliable photophysical properties. Nevertheless, some disadvantages hamper the application as an artificial ciliated epithelium. The main problem is caused by the undirected movement of the molecules during the switching process. Both directions of the isomerization perform the same stroke movement and, therefore, no directed transport of particles can be achieved by irradiation.

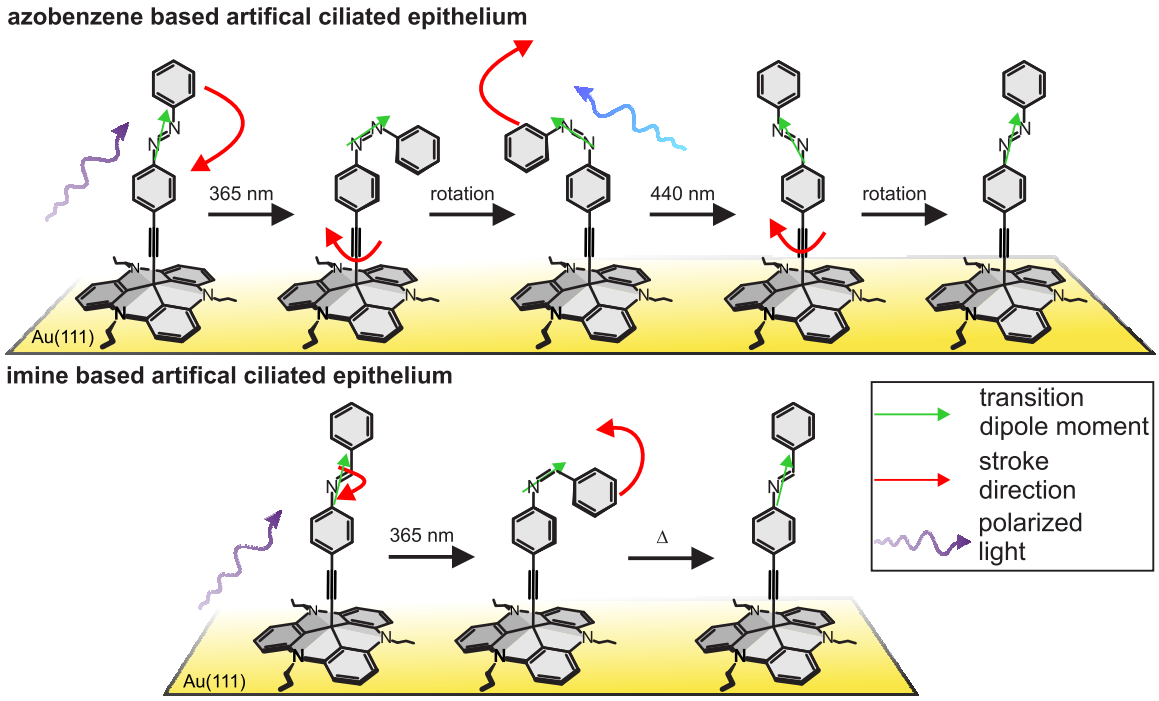

Figure 2.2: Comparison between an azobenzene and an imine-based artificial ciliated epithelium: (top) azobenzenes only have the ability to perform a unidirectional motion by using polarized light and a rotation step in turn, (bottom) as the switching mechanism of imines is inherently unidirectional and the back isomerization ensues thermally, the setup is simplified dramatically.

Nanotransport should be possible yet by using polarized light for isomerization. As isomerization is most efficient if the transition dipole moment is orientated parallel to the incident light beam, the stroke movement is only conducted by the molecules that are positioned accordingly.[110,111] As the azobenzene moiety is able to rotate freely, the back isomerization can be accomplished from the opposite direction. Thus, a unidirectional movement can be achieved but the efficiency is low as only few properly oriented molecules are effective.[91] To increase the efficiency of the switching process the aim of this project is to exchange the azobenzene moiety by an imine. Imines have the great advantage that their *trans* → *cis* isomerization occurs in a unidirectional motion. Consequently, only one polarized light beam is needed in this setup as the *cis* → *trans* isomerization ensues thermally (Figure 2.2).

2.3 Heterobridged Diazocines

Another disadvantage of azobenzenes originates from the high flexibility of the molecules. Due to the C−N single bonds the phenyl rings can rotate freely, and hence, the efficiency of the stroke is reduced. This problem was solved by using ethyl-bridged azobenzenes (diazocines) as photoswitches. The implementation of a second bridging unit yielded a chiral photoswitch that can only switch in one direction.[92,99,112] Although these molecules offer high potential as unidirectional photoswitches, the difficult synthesis restricts the application so far. A major drawback of this compounds is the contruction of the ethyl bridge for unsymmetrical molecules as the radical approach that is used so far leads to low yields and many side products that are difficult to separate.[92] Therefore, in this work new bridging units shall be developed that can be synthesized with higher yields, whereas the excellent photochemical properties of the diazocines are preserved. One approach to achieve this goal is to incorporate heteroatoms, e.g. oxygen or sulfur, into the ethyl bridge. Furthermore, the ring closure *via* azobenzene synthesis shall be improved with respect to yield as well as reliability since a large amount of the desired product is lost in this step. After successful synthesis the photophysical properties of the molecules shall be examined and compared to the parent system (Figure 2.3).

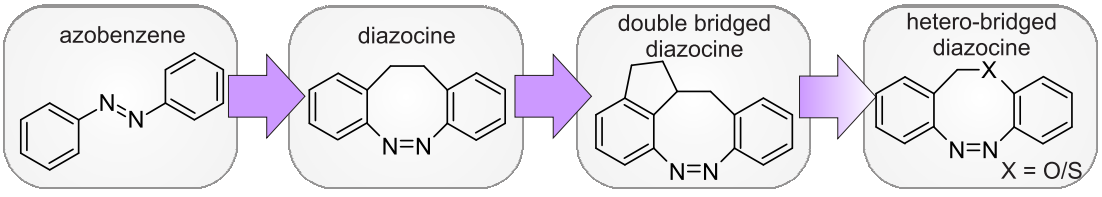

Figure 2.3: The photophysical properties of azobenzenes could be improved tremendously by bridging with an ethyl unit; further developments have been made by an additional second bridge; to simplify the synthesis of diazocines new bridging units shall be investigated.

3 Lateral Movement above a Surface

Many approaches for the orthogonal functionalization of metal surfaces were developed successfully, whereas only few examples for the lateral alignment have been reported. To achieve a lateral orientation of functional molecules certain requirements have to be fulfilled: primarily two posts are necessary to span the molecules above the surface. Secondly, both posts need to be capable of binding to the metal surface. Preferably the distance between both posts is supposed to coincide with the length of the functional molecules to avoid tension within the molecule.

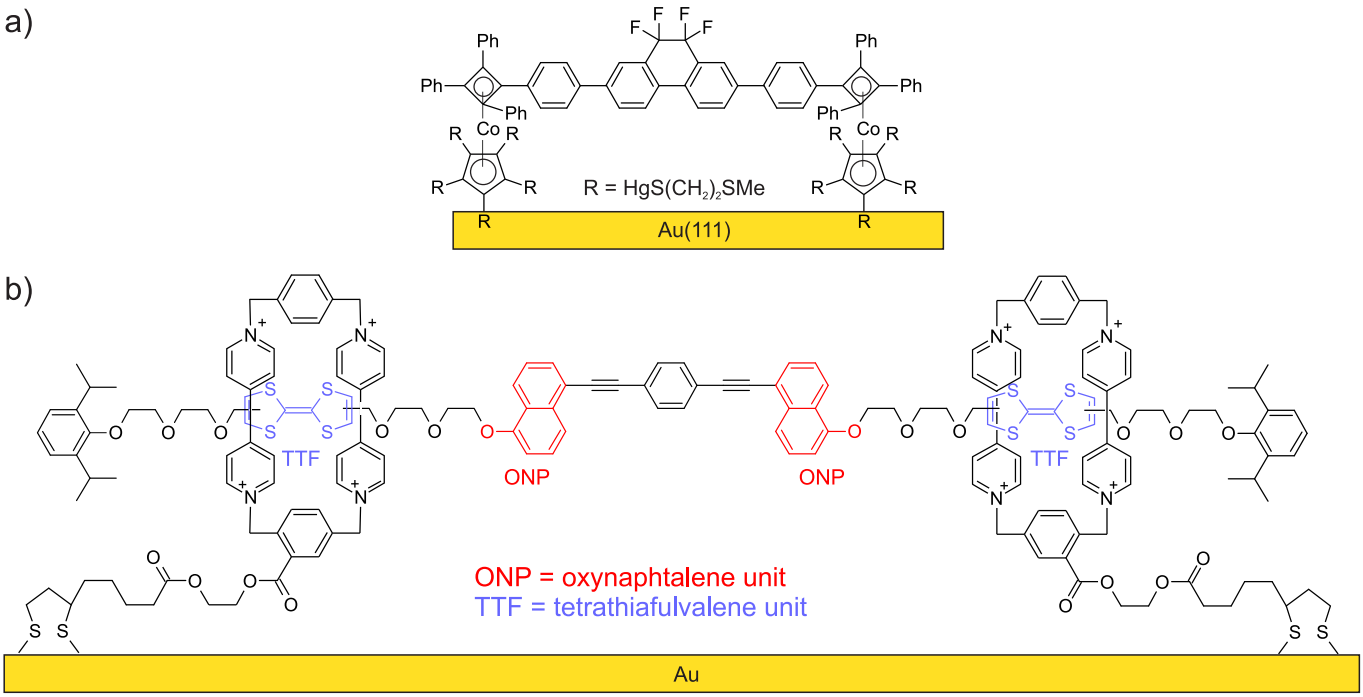

Figure 3.1: a) Molecular rotator published by MICHL: the molecule binds to the Au(111) surface by a ferrocene-thiol-linker, b) molecular muscle designed by STODDART based on rotaxane units that can be moved by oxidation/reduction. In the reduced form the cyclophanes bind to the tetrathiofulvene units (TTF, blue), by oxidation the binding positions are shifted to the oxynaphthalene units (ONP, red).[106,107,113]

With this approach MICHL synthesized a molecular altitudinal rotator that is spanned above a Au(111) surface. Two cobalt ferrocene ligands are used as posts that are linked to the Au(111) surface by thiol alkane chains. Therefore, the dipolar unit exhibits the required distance to the surface and can rotate around the horizontal axis (Figure 3.1).[106] Based on a rotaxane scaffold STODDART realized a molecular muscle spanned above a Au(111) surface. The position of the

cyclophan units can be switched by reduction/oxidation between the tetrathiofulvene units (TTP) and the oxynaphthalene units (ONP). Hence, the distance between the two cyclophane units is shortend by about 1.4 nm. As the cyclophane units are covalently linked to the surface, the distance change causes a bending of the gold surface.[107,113] Both systems exhibit already fascinating properties as functionalized surfaces, however, a lateral structure with a photoswtichable moiety could not be realized until now. The main challenge is that photochromic compounds become inactive if adsorbed directly to a metal surface.[108] Therfore, spacing groups are required that ensure the necessary distance to the surface. A first attempt of a lateral functionalization was presented by GRILL by adsorbing *tert*-butyl functionalized azobenzenes upon a Au(111) surface.[105] The azobenzene could be switched to the *cis* configuration with an electric field but for the isomerization with light the *tert*-butyl spacers are not large enough to prevent the quenching of the photochemical properties. To achieve a photochemical isomerization of a laterally oriented azobenzene moiety the spacer units have to be enlarged distinctly.

3.1 Laterally Mounted Azobenzenes on Platforms

Melanie Hammerich and Rainer Herges

J. Org. Chem. **2015**, *80*, 11233–11236.

DOI: 10.1021/acs.joc.5b02262

Scientific contribution to this paper:

All syntheses of the molecules and the characterization of the photoswitching in solution were performed by me. DFT-calculations were conducted by Prof. Dr. R. Herges. The manuscript was written by Prof. Dr. R. Herges and me.

Summary

We report on the synthesis of muscle type molecules which provide the possibility of a lateral movement about a surface. The molecules consist of two platform (TATA) elements linked by an azobenzene unit. In previous works it could be shown that TATA platforms build nearly perfectly ordered hexagonal monolayers on Au(111), providing the required distance of the functional molecules among themselves and according to the surface. The quantum chemical (DFT) supported design of the bridging azobenzene unit has to meet two requirements. Firstly, the azobenzene moiety may not adsorb to the gold surface for an efficient switching process and secondly, adsorption of the TATA platforms may not be impaired in either configuration of the azobenzene. DFT calculations showed that the distance between the two central carbon atoms of the TATA platforms changes upon irradiation with 365 nm about 3.3 Å (Figure 3.2).

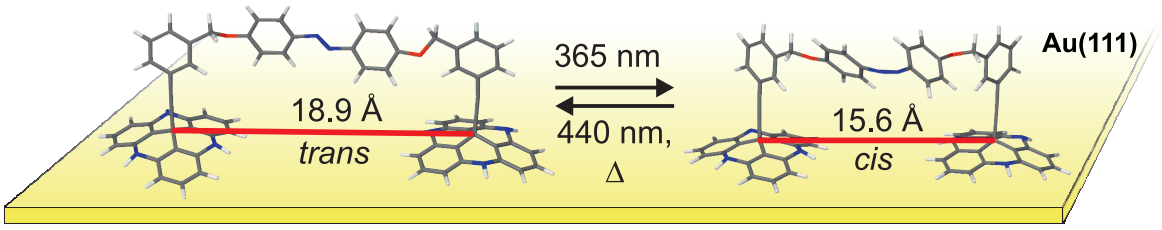

Figure 3.2: According to DFT calculations the distance between the central carbon atoms of the platforms changes about 3.3 Å by irradiation with 365 nm.

The syntheses of both molecules were achieved in an eight step convergent synthesis. The bridging azobenzene unit was synthesized in a four step synthesis with an overall yield of 24 %. The following functionalization of propyl- and octyl-TATA gains the molecular muscle in 27 % and 38 % yield, respectively. Photophysical properties were investigated by UV/vis and ^{1}H NMR spectroscopy, showing the high efficiency of the switching to the *cis* isomer (> 95 %). The switching process is fatigue resistant and showed no sign of decay of the molecules.

JOC The Journal of Organic Chemistry

Brief Communication

pubs.acs.org/joc

Laterally Mounted Azobenzenes on Platforms

Melanie Hammerich and Rainer Herges*

Otto Diels-Institute for Organic Chemistry, University of Kiel, Otto-Hahn-Platz 4, Kiel D-24119, Germany

Supporting Information

ABSTRACT: Triazatriangulenium ions have previously been used as platforms to prepare self-assembled monolayers of functional molecules such as azobenzenes with vertical orientation and that are free-standing on gold surfaces. We have now prepared azobenzenes that are spanned between two posts which are attached on two platforms. Absorbed on a gold surface, the azobenzene should be laterally oriented at a distance of more than 4 Å above and thus electronically decoupled from the surface, and the system should perform a muscle-type movement upon isomerization.

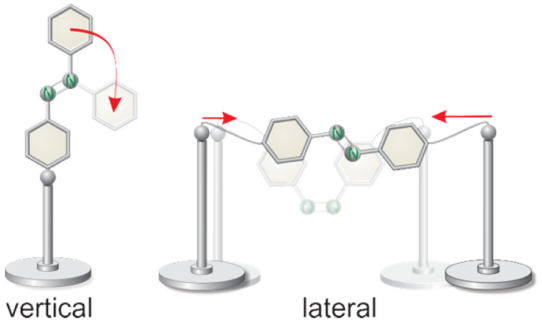

Photoactive molecules such as photochromic compounds or fluorescent dyes with their chromophores directly absorbed to a metal surface usually become photochemically inactive because their excited states are quenched by the metal.[1] A number of strategies have been used to attach functional molecules such as azobenzenes to metal surfaces using spacer groups which prevent direct contact and thus reduce electronic coupling to the surface.[2,3] Probably the most widely used method toward this end are alkanethiol spacer groups.[4−6] The sulfur attaches to the gold and in a densely packed monolayer the alkane chains prevent the chromophore on top from coupling with the surface underneath. Usually, self-assembled monolayers are formed by just dipping the gold surface into a dilute solution of the absorbate.[7] However, the free volumes in the densely packed monolayers often are not sufficient for a sterically demanding reaction (e.g., *cis*−*trans* isomerization of azobenzene),[8] and highly ordered monolayers are difficult to prepare because of the large degree of conformational freedom of the alkane chains.[9] A very successful strategy to enforce a defined (lateral) distance between the functional units and a vertical distance to the surface is the platform approach. Particularly suitable as molecular platforms are triazatriangulenium (TATA) ions.[10,11] The large π system has a high affinity to atomically flat gold surfaces. Even though the interaction with the Au(111) surface is almost exclusively dispersive, the binding energies of TATA platforms are similar to the affinity of thiols which attach via covalent bonds.[11] Dilute solutions of TATA form almost perfectly ordered monolayers on Au(111).[12,13] The size of the platform and thus the distance of the platforms to their next neighbors on the surface can be controlled by the size of the substituents at the nitrogen atoms.[14] The central carbon atom which formally bears the positive charge reacts with a number of carbanions that thus are covalently attached perpendicular to the plane of the platform. Ethynyl and phenyl groups are suitable spacers on top of which functional groups such as azobenzenes are attached.[15] The rigid, upright, and free-standing azobenzenes exhibit the same efficiency (extinction and quantum yield) in photochemical *cis*−*trans* isomerizations as the free azobenzenes in solution.[16] Whereas several strategies for a vertical attachment of functional molecules on surfaces have been developed,[17] very few approaches for a lateral orientation above the surface (without direct contact) have been published.[18−20] Our platform approach which has been successful for vertical mounting is particularly suitable for lateral mounting as well. We have designed and synthesized a compound which is able to span an azobenzene between two platforms and hold it above the surface. According to DFT calculations, the platforms slide over the surface with almost no barrier.[21] Upon alternating irradiation with UV and visible light, the azobenzene reversibly isomerizes (*cis trans* isomerization), and consequently, the distance between the platforms should contract and expand in a muscle-type movement.

According to PM3 model calculations, the structure shown in Figure 1 is a good candidate for the realization of the anticipated function. The *trans* isomer **1** ***trans*** exhibits a distance of 18.9 Å between the two centers of the TATA platforms. By switching the azobenzene to the *cis* isomer **1** ***cis*** the distance of the two platforms is reduced to 15.6 Å. To avoid strain, particularly in the cis form, the azobenzene unit is attached to the posts (phenylethynyl units) via flexible $-OCH_2-$ linkers.

For the sake of simplicity, the calculations have been performed without substitution at the angular nitrogen atoms. However, alkyl chains such as *n*-propyl and *n*-octyl are needed for the synthesis. For obvious reasons, the platforms should be

Received: September 28, 2015
Published: November 9, 2015

DOI: 10.1021/acs.joc.5b02262
J. Org. Chem. 2015, 80, 11233−11236

The Journal of Organic Chemistry Brief Communication

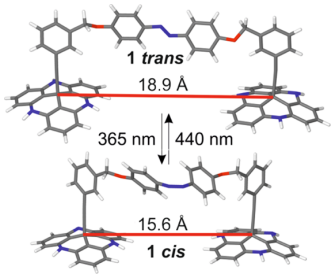

Figure 1. PM3-calculated geometries (fully optimized with the constraint that all angular nitrogen atoms are held in a plane) (top: *trans*, bottom: *cis*) of the "molecular muscle". By switching between the azobenzene isomers **1** ***trans*/*cis*** the distance between the platforms changes by about 3.3 Å (18.9 Å *trans* to 15.6 Å *cis*).

small enough not to hinder the contraction movement upon *trans* to *cis* isomerization. According to previous studies, the intermolecular spacing of the *n*-propyl-substituted platform in self-assembled monolayers is 11.0 ± 0.5 Å, and *n*-octyl TATA exhibits a spacing of 13.0 ± 0.5 Å.[10,14] Therefore, both platforms are sufficiently small to allow the muscle-type contraction on a gold surface.

The preparation of azobenzene **7** was achieved in a four-step synthesis (Scheme 1). *p*-Nitrophenol (**3**) reacts with benzyl

Scheme 1. Synthesis of the Azobenzene Unit[a]

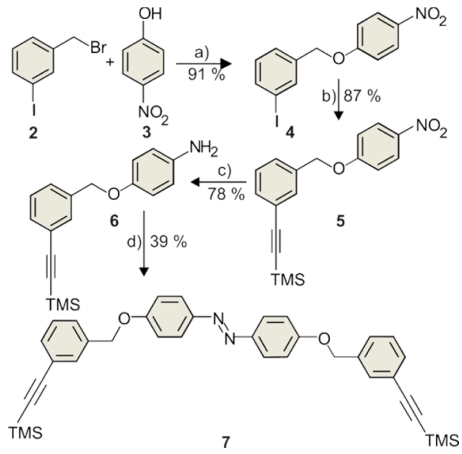

[a]Reagents and conditions: (a) K_2CO_3, acetone, 15 h, reflux; (b) TMSA, NEt_3, Cu(I)I, $Pd(PPh_3)Cl_2$ 40 °C 4 h, then rt 15 h ; (c) $SnCl_2$, EtOH, AcOH, 4 h, 80 °C; (d) Cu(I)Cl, pyridine, O_2, 18 h, rt.

bromide **2** forming ether **4** (91%). Sonogashira coupling with trimethylsilylacetylene gives compound **5** (87%). The standard reductive azobenzene coupling with zinc and barium hydroxide in ethanol was not successful.[22] Therefore, the nitro group was reduced with tin(II) chloride in ethanol yielding the corresponding amine **6** (78%). The oxidative azobenzene coupling was accomplished in pyridine with copper(I)chloride and air leading to the azobenzene linker **7** (39%).

The triazatriangulenium (TATA) platforms (**8a**/**b**) were synthesized according to a procedure from Laursen and Krebs in a three-step synthesis.[23]

Functionalization of the two TATA platforms (Scheme 2) was achieved by deprotection of the terminal silyl-protected

Scheme 2. Synthesis of the Molecular Muscle[a]

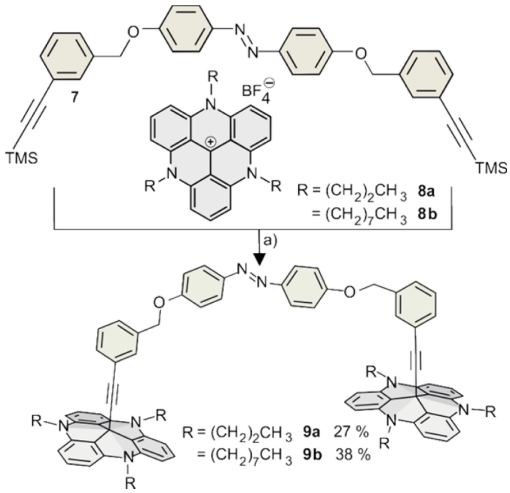

[a]Reagents and conditions: (a) KOH, THF, 16 h.

alkyne groups of the azobenzene unit with potassium hydroxide and in situ reaction with the cationic center of the platform to form the molecular muscles **9a**/**b** (**9a**, 27%; **9b**, 38%), which are indefinitely stable in toluene in the dark and as pure solids but instable in halogenated and acidic solvents.

The photophysical properties and particularly the switching behavior of compounds **9a**/**b** were determined in solution. UV/vis spectra and the photostationary states were measured upon irradiation at 365 and 440 nm (Figure 2).

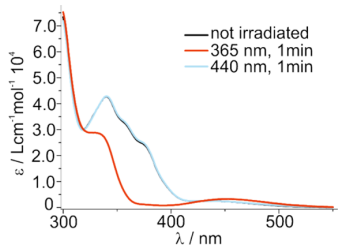

Figure 2. UV−vis spectrum of **9b** (29.1 μmol/L in toluene): black curve, pure *trans* isomer; red curve, photostationary equilibrium at 365 nm (~95% *cis*); blue curve, photostationary equilibrium at 440 nm.

Both substances show a strong ππ* band that decreases and shifts to shorter wavelengths upon irradiation with 365 nm, whereas the intensity of the nπ* band increases. This is in agreement with the UV spectra of typical azobenzenes.[24] After irradiation at 440 nm the solution exhibits the spectrum of the pure *trans* isomer.

Photostationary states were determined after irradiation in deuterated toluene with light of the wavelengths of 365 nm (*cis*) and 470 nm (*trans*) for 10 min. The *cis*/*trans* ratios were measured by ^{1}H NMR. Half-lives of the thermal back-isomerizations were determined by ^{1}H NMR measurements (Table 1).

In summary, we present the synthesis of a muscle-type molecule. An azobenzene unit is attached to molecular platforms at both *para* positions. According to previous studies, the platforms should absorb to Au(111) surfaces and therefore

DOI: 10.1021/acs.joc.5b02262
J. Org. Chem. 2015, 80, 11233−11236

The Journal of Organic Chemistry Brief Communication

Table 1. Photostationary States (PSS) of Azobenzenes in Toluene upon Irradiation with 365 nm (*Cis*) and 470 nm (*Trans*) Determined with ^{1}H NMR Spectroscopy (Toluene, 2 mmol/L)

	PSS at 365 nm (% *cis*)	PSS at 470 nm (% *trans*)	$t_{1/2}$ (h) (300 K)
9a	95	72	23.8
9b	95	76	21.4

should span the azobenzene at a distance of 4 Å above the surface. Photophysical experiments in solution exhibit a high switching efficiency and low fatigue of the photochromic system.

EXPERIMENTAL SECTION

General Experimental Methods. Acetone was dried and distilled from phosphorous pentoxide. Triethylamine was dried and distilled from calcium hydride, and tetrahydrofuran was dried and distilled from sodium/benzophenone. All compounds were characterized using ^{1}H and ^{13}C NMR spectroscopy. The signals were assigned using 2D spectroscopy. For ^{1}H and ^{13}C NMR assignment we performed HSQC and HMBC.

1-[(3-Iodophenyl)methoxy]-4-nitrobenzene (4). Potassium carbonate (3.77 g, 27.3 mmol) was added to a solution of 4-nitrophenol (**3**, 0.8 g, 5.75 mmol) in 25 mL of acetone under nitrogen atmosphere and stirred for 1 h at room temperature. 3-Iodobenzyl bromide (**2**, 1.76 g, 5.46 mmol) was added to the suspension and heated to 60 °C for 15 h. The solid was removed and the solvent evaporated. The solid was dissolved in ethyl acetate and washed with water and brine. The solution was dried over magnesium sulfate and evaporated. The crude product was recrystallized from cyclohexane to obtain colorless crystals (1.86 g, 5.24 mmol, 91%). Mp: 99 °C. ^{1}H NMR (500.1 MHz, $CDCl_3$, 300 K, $CHCl_3$): δ 8.21 (d, ^3J = 9.3 Hz, 2 H), 7.79 (s, 1 H), 7.70 (d, ^3J = 7.8 Hz, 1 H), 7.38 (d, ^3J = 7.8 Hz, 1 H), 7.14 (t, ^3J = 7.8 Hz, 1 H), 7.02 (d, ^3J = 9.3 Hz, 1 H), 5.09 (s, 2 H) ppm. ^{13}C NMR (125.1 MHz, $CDCl_3$, 300 K, $CHCl_3$): δ 163.3, 141.9, 137.8, 137.5, 136.3, 130.5, 126.5, 126.0, 114.8, 94.6, 69.6 ppm. MS (EI, 70 eV): *m*/*z* 354 (11), 216 (100), 125 (11) IR: $\tilde{\nu}$ = 3120 (m), 3066 (m), 1609 (m), 1592 (s), 1565 (m), 1502 (s), 1328 (m), 1258 (m), 1173 (s), 1090 (s), 1063 (w), 844 (s), 769 (s) cm^{-1}. Anal. Calcd for $C_{13}H_{10}INO_3$ (355.13): C, 43.97; H, 2.84; N, 3.94. Found: C, 44.12; H, 2.92; N, 4.11. UV (CH_2Cl_2): λ_{max} (log ε) 238 (4.14), 307 (4.15) nm.

1-[[3-(Trimethylsilylethynyl)phenyl]methoxy]-4-nitrobenzene (5). Under a nitrogen atmosphere, a suspension of 1-[(3-iodphenyl)methoxy]-4-nitrobenzene (**4**, 1.85 g, 5.21 mmol), bis-(triphenylphosphine)palladium(II) chloride (73.0 mg, 10 $^{-4}$ mol), copper iodide (9.9 mg, 0.520 μmol), and TMSA (0.9 mL, 6 mmol) in 20 mL of triethylamine was heated to 40 °C for 4 h and was stirred for another 15 h at room temperature. The solution was diluted with 40 mL of dichloromethane, washed with water, extracted with dichloromethane, and washed with brine. The solution was dried over magnesium sulfate and evaporated. The crude product was purified by column chromatography (ethyl acetate/cyclohexane 1:4) to obtain a brown-orange solid (1.43 g, 4.39 mmol, 87%). Mp: 58 °C. ^{1}H NMR (500.1 MHz, $CDCl_3$, 300 K, $CHCl_3$): δ 8.20 (d, ^{3}J = 9.3 Hz, 2 H), 7.53 (s, 1 H), 7.45 (d, ^3J = 6.9 Hz, 1 H), 7.33−7.37 (m, 2 H), 7.01 (d, ^3J = 9.3 Hz, 1 H), 5.12 (s, 2 H), 0.26 (s, 9 H) ppm. ^{13}C NMR (125.1 MHz, $CDCl_3$, 300 K, $CHCl_3$): δ 163.5, 141.8, 135.7, 132.0, 130.8, 128.7, 127.4, 126.0, 123.8, 114.9, 104.4, 95.0, 70.1, 0.1 ppm. MS (EI, 70 eV): *m*/*z* 325 (5), 231 (13), 187 (100). IR: $\tilde{\nu}$ 3085 (w), 2955 (m), 2154 (m), 1607 (m), 1510 (s), 1337 (s), 1242 (m), 1175 (m), 1111 (m), 996 (m), 836 (s), 796 (s), 751 (s) cm^{-1}. Anal. Calcd for $C_{18}H_{19}NO_3Si$ (325.43): C, 66.43; H, 5.88; N, 4.30. Found: C, 66.41; H, 6.08; N, 4.28. UV (CH_2Cl_2): λ_{max} (log ε) 249 (4.30), 260 (4.27), 308 (4.14) nm.

4-(3-Trimethylsilylethynylbenzyloxy)phenylamine (6).[25] Tin-(II) chloride dihydrate (6.43 g, 28.3 mmol) was added to a solution of 1-[(3-(trimethylsilylethynyl)phenyl)methoxy]-4-nitrobenzene (**5**, 0.930 g, 2.83 mmol) in 5 mL of acetic acid and 35 mL of ethanol and heated to 80 °C for 4 h. The solution was poured onto iced water, and potassium hydroxide (30.8 g, 0.549 mol) was added. The two phases were separated and extracted with dichloromethane. The solution was dried over magnesium sulfate and evaporated to obtain an orange-brown oil. The crude product was purified by column chromatography (dichloromethane) to obtain a brown solid that was dissolved in diethyl ether and precipitated with pentane to obtain a colorless solid (0.66 g, 2.23 mmol, 78%). Mp: 58 °C. ^{1}H NMR (500.1 MHz, $CDCl_3$, 300 K, $CHCl_3$): δ 7.53 (s, 1 H), 7.40 (d, ^3J = 7.6 Hz, 1 H), 7.36 (d, ^3J = 7.6 Hz, 1 H), 7.29 (t, ^3J = 7.6 Hz, 1 H), 6.79 (d, ^3J = 9.3 Hz, 2 H), 6.64 (d, ^3J = 9.3 Hz, 2 H), 4.94 (s, 2 H,), 3.24 (s, br, 2 H), 0.26 (s, 9 H) ppm. ^{13}C NMR (125.1 MHz, $CDCl_3$, 300 K, $CHCl_3$): δ 151.9, 140.2, 137.8, 131.3, 130.8, 128.4, 127.5, 123.4, 116.4, 116.1, 104.9, 94.4, 70.3, −0.0 ppm. MS (EI, 70 eV): *m*/*z* 295 (24), 187 (21), 172 (12), 108 (100) IR: $\tilde{\nu}$ 3360 (w), 3040 (w), 2958 (w), 2152 (w), 1605 (m), 1508 (s), 1429 (w), 1376 (w), 1248 (m), 1227 (s), 1121 (m), 916 (m), 839 (s), 758 (s), 690 (m) cm^{-1}. Anal. Calcd for $C_{18}H_{21}NOSi$ (295.45): C, 73.17; H, 7.16; N, 4.74. Found: C, 73.34; H, 7.10; N, 4.90. UV (CH_2Cl_2): λ_{max} (log ε) 248 (4.47), 259 (4.34), 305 (3.41) nm.

1,2-Bis[4-[(3-trimethylsilylbenzyloxy)phenyl]]diazene (7). Copper(I) chloride (156 mg, 1.58 mmol) was suspended in pyridine, stirred for 15 min at room temperature, and filtrated. 4-(3-Trimethylsilylethynylbenzyloxy)phenylamine (**6**, 0.584 g, 1.98 mmol) was dissolved in pyridine, and the Cu(I)/pyridine solution was added. Air was sparged through the solution for 18 h. The residue was dissolved in 50 mL of 1 M hydrochloric acid and extracted with dichloromethane, washed with water, and dried over magnesium sulfate. The solution was evaporated, and the residue was purified by column chromatography (dichloromethane) to obtain an orange solid (0.227 g, 3.87 × 10 $^{-4}$ mol, 39%). Mp: 164 °C. ^{1}H NMR (500.1 MHz, $CDCl_3$, 300 K, $CHCl_3$): δ 7.87 (d, ^3J = 9.0 Hz, 2 H, H-10), 7.57 (s, 1 H, H-6), 7.44 (d, ^3J = 7.6 Hz, 1 H, H-2), 7.40 (d, ^3J = 7.6 Hz, 1 H, H 4), 7.33 (t, ^3J = 7.6 Hz, 1 H, H-3), 7.09 (d, ^3J = 9.3 Hz, 2 H, H-9), 5.10 (s, 2 H, H-7), 0.26 (s, 9 H, H-14) ppm. ^{13}C NMR (125.1 MHz, $CDCl_3$, 300 K, $CHCl_3$): δ 160.6, 147.3, 136.8, 131.7, 130.9, 128.6, 127.5, 124.4, 123.6, 115.1, 104.7, 94.7, 69.7, −0.0 ppm. MS (EI, 70 eV): *m*/*z* 586 (14), 187 (100), 172 (23), 108 (14). IR: $\tilde{\nu}$ 2958 (m), 2898 (m), 2145 (m), 1602 (m), 1581 (m), 1496 (m), 1455 (m), 1241 (s), 1146 (s), 1104 (m), 1052 (m), 922 (m), 837 (m), 785 (m), 754 (m), 687 (m), 645 (m) cm^{-1}. Anal. Calcd for $C_{36}H_{38}N_2O_2Si_2$ (586.87): C, 73.68; H, 6.53; N, 4.77. Found: C, 73.73; H, 6.49; N, 4.82. UV (toluene): λ_{max} (log ε) 358 (4.48) nm.

1,2-Bis[4-[[3-(4,8,12-tris-*n*-propyl-4,8,12-triazatriangulenium benzyloxy)-12c-ethynyl]phenyl]]diazene (9a). A suspension of 1,2-bis[4-[(3-trimethylsilylbenzyloxy)pheny]]diazene (**7**) (150 mg, 2.56 μmol), *n*-propyl-TATA (**8a**) (508 mg, 1.02 mmol), and potassium hydroxide (362 mg, 6.95 mmol) in 50 mL of THF was refluxed for 17 h under nitrogen atmosphere. The solution was poured onto water, extracted with diethyl ether, and dried over magnesium sulfate. The solution was evaporated and purified by column chromatography (bas. Alox, ethyl acetate) to obtain an orange solid (87 mg, 16.9 × 10^{-5} mol, 27%). Mp: 163 °C. ^{1}H NMR (600.1 MHz, C_6D_6, 300 K, benzene): δ 8.03 (d, ^3J = 8.9 Hz, Ar-*H*, 4 H), 7.18 (t, ^3J = 8.2 Hz, Ar-*H*, 6 H), 6.95 (s, Ar-*H*, 6 H), 6.92 (d, ^3J = 7.8 Hz, Ar-*H*, 2 H), 6.87 (d, ^3J = 7.8 Hz, Ar-*H*, 6.65−6.69 (m, Ar-*H*, 6 H), 6.53 (d, ^3J = 8.2 Hz, Ar-*H*, 12 H), 4.24 (s, OCH_2, 4 H), 3.68 (t, ^3J = 7.9 Hz, NCH_2, 12 H); 1.73 (sext., ^3J = 7.7 Hz, CH_2, 12 H), 0.79 (t, ^3J = 7.4 Hz, CH_3,.18 H) ppm. ^{13}C NMR (150.9 MHz, C_6D_6, 300 K, benzene): δ 160.9, 147.7, 141.0, 136.4, 131.2, 130.9, 128.5, 126.3, 124.7, 124.3, 115.2, 110.9, 105.5, 94.7, 83.9, 69.4, 48.1, 30.1, 28.8, 19.2, 11.0 ppm. MS (MALDI-TOF, Cl-CCA): *m*/*z* = 1257. MS (ESI): *m*/*z* = 1257, 408, 365, 280. IR: $\tilde{\nu}$ 3025 (m), 2957 (m), 2921 (m), 2851 (m), 2341 (m), 1735 (w), 1614 (s), 1578 (s), 1483 (s), 1455 (s), 1396 (s), 1230 (s), 1145 (s), 1029 (m), 917 (m), 750 (s), 695 (m) cm^{-1}. Anal. Calcd for $C_{86}H_{80}N_8O_2$ (1257.61): C, 82.13; H, 6.41; N, 8.91. Found: C, 81.86; H, 6.48; N, 8.77. UV (toluene): λ_{max} (log ε) 290 (4.85), 340 (4.59) nm.

DOI: 10.1021/acs.joc.5b02262
J. Org. Chem. 2015, 80, 11233−11236

The Journal of Organic Chemistry Brief Communication

1,2-Bis[4-[[3-(4,8,12-tris-*n*-octyl-4,8,12-triazatriangulenium-benzyloxy)-12c-ethynyl]phenyl]]diazene (9b). A suspension of 1,2-bis[4-[(3-trimethylsilylbenzyloxy)pheny]]diazene (**7**) (50 mg, 8.52 × 10^{-5} mol), *n*-octyl-TATA (**8b**) (132 mg, 1.87 × 10^{-4} mol), and potassium hydroxide (129 mg, 2.30 mmol) in 50 mL of THF was refluxed for 17 h under nitrogen atmosphere. The solution was poured onto water, extracted with diethyl ether, and dried over magnesium sulfate. The residue was filtrated over Florisil (diethyl ether). The crude product was recrystallized from acetone to obtain an orange solid (54.9 mg, 3.27 × 10^{-5} mol, 38%). Mp: 126 °C. ^{1}H NMR (600.1 MHz, C_6D_6, 300 K, benzene): δ8.04 (d, ^3J = 8.9 Hz, Ar-*H*, 4 H), 7.25 (t, ^3J = 8.2 Hz, Ar-*H*, 6 H), 6.99 (s, Ar-*H*, 2 H), 6.97 (d, ^3J = 7.8 Hz, Ar-*H*, 2 H), 6.91 (d, ^3J = 7.6 Hz, Ar-*H*, 2 H), 6.70−6.73 (m, Ar-*H*, 6 H), 6.64 (d, ^3J = 8.2 Hz, Ar-*H*, 12 H), 4.28 (s, NCH_2, 4 H), 3.80 (t, ^3J = 7.8 Hz, CH_2, 12 H), 1.80 (quint, ^3J = 7.4 Hz, CH_2, 12 H), 1.25 (quint, ^3J = 6.5 Hz, CH_2, 12 H), 1.17−1.21 (m, CH_2, 36 H), 0.90 (t, ^3J = 7.20 Hz, CH_3, 18 H) ppm. ^{13}C NMR (150.9 MHz, $CDCl_3$, 300 K, TMS): δ 161.1, 147.8, 141.2, 136.6, 131.6, 131.2, 128.7, 128.4, 126.5, 124.8, 124.4, 115.3, 111.1, 105.7, 94.8, 84.2, 69.2, 46.7, 32.2, 30.2, 29.7, 29.0, 27.2, 26.2, 23.1, 14.4 ppm. MS (MALDI-TOF, Cl-CCA): *m*/*z* 1678 $[M]^+$. IR: $\tilde{\nu}$ 2922 (m), 2853 (m), 1615 (s), 1579 (s), 1483 (s), 1457 (s), 1396 (s), 1236 (s), 1168 (m), 1145 (m), 1010 (w), 912 (w), 772 (m), 750 (s), 690 (m) cm^{-1}. Anal. Calcd for $C_{116}H_{140}N_8O_2$ (1678.41): C, 83.01; H, 8.41; N, 6.68. Found: C, 82.91; H, 8.37; N, 6.52. UV (toluene): λ_{max} (log ε) 340 (4.58) nm.

■ ASSOCIATED CONTENT

Supporting Information

The Supporting Information is available free of charge on the ACS Publications website at DOI: 10.1021/acs.joc.5b02262.

^{1}H NMR, ^{13}C NMR, and UV/vis spectra for compounds **4**−**7** and **9a**,**b** (PDF)

■ AUTHOR INFORMATION

Corresponding Author

*E-mail: rherges@oc.uni-kiel.de.

Notes

The authors declare no competing financial interest.

■ ACKNOWLEDGMENTS

We gratefully acknowledge financial support by the Deutsche Forschungsgesellschaft (DFG) via the collaborative research center SFB 677, “Function by Switching”.

■ REFERENCES

(1) Tegeder, P. *J. Phys.: Condens. Matter* **2012**, *24*, 394001.
(2) Pace, G.; Ferri, V.; Grave, C.; Elbing, M.; von Hänisch, C.; Zharnikov, M.; Mayor, M.; Rampi, M. A.; Samorì, P. *Proc. Natl. Acad. Sci. U. S. A.* **2007**, *104*, 9937−9942.
(3) Bléger, D.; Ciesielski, A.; Samoì, P.; Hecht, S. *Chem. - Eur. J.* **2010**, *16*, 14256−14260.
(4) Love, J. C.; Estroff, L. A.; Kriebel, J. K.; Nuzzo, R. G.; Whitesides, G. M. *Chem. Rev.* **2005**, *105*, 1103−1170.
(5) Evans, S. D.; Johnson, S. R.; Ringsdorf, H.; Williams, L. M.; Wolf, H. *Langmuir* **1998**, *14*, 6436−6440.
(6) Shipway, A. N.; Willner, I. *Acc. Chem. Res.* **2001**, *34*, 421−432.
(7) Tamada, K.; Akiyama, H.; Wei, T. X. *Langmuir* **2002**, *18*, 5239−5246.
(8) Valley, D. T.; Onstott, M.; Malyk, S.; Benderskii, A. V. *Langmuir* **2013**, *29*, 11623−11631.
(9) Jung, U.; Filinova, O.; Kuhn, S.; Zargarani, D.; Bornholdt, C.; Herges, R.; Magnussen, O. *Langmuir* **2010**, *26*, 13913−13923.
(10) Baisch, B.; Raffa, D.; Jung, U.; Magnussen, O. M.; Nicolas, C.; Lacour, J.; Kubitschke, J.; Herges, R. *J. Am. Chem. Soc.* **2009**, *131*, 442−443.
(11) Otte, F. L.; Lemke, S.; Schütt, C.; Krekiehn, N. R.; Jung, U.; Magnussen, O. M.; Herges, R. *J. Am. Chem. Soc.* **2014**, *136*, 11248−11251.
(12) Jung, U.; Kuhn, S.; Cornelissen, U.; Tuczek, F.; Strunskus, T.; Zaporojtchenko, V.; Kubitschke, J.; Herges, R.; Magnussen, O. *Langmuir* **2011**, *27*, 5899−5908 PMID: 21506548.
(13) Ulrich, S.; Jung, U.; Strunskus, T.; Schütt, C.; Bloedorn, A.; Lemke, S.; Ludwig, E.; Kipp, L.; Faupel, F.; Magnussen, O.; Herges, R. *Phys. Chem. Chem. Phys.* **2015**, *17*, 17053−17062.
(14) Lemke, S.; Ulrich, S.; Claußen, F.; Bloedorn, A.; Jung, U.; Herges, R.; Magnussen, O. M. *Surf. Sci.* **2015**, *632*, 71−76.
(15) Kubitschke, J.; Näther, C.; Herges, R. *Eur. J. Org. Chem.* **2010**, *2010*, 5041−5055.
(16) Jung, U.; Schütt, C.; Filinova, O.; Kubitschke, J.; Herges, R.; Magnussen, O. *J. Phys. Chem. C* **2012**, *116*, 25943−25948.
(17) Klajn, R. *Pure Appl. Chem.* **2010**, *82*, 2247−2279.
(18) Alemani, M.; Peters, M. V.; Hecht, S.; Rieder, K.-H.; Moresco, F.; Grill, L. *J. Am. Chem. Soc.* **2006**, *128*, 14446−14447.
(19) Zheng, X.; Mulcahy, M. E.; Horinek, D.; Galeotti, F.; Magnera, T. F.; Michl, J. *J. Am. Chem. Soc.* **2004**, *126*, 4540−4542.
(20) Liu, Y.; Flood, A. H.; Bonvallet, P. A.; Vignon, S. A.; Northrop, B. H.; Tseng, H.-R.; Jeppesen, J. O.; Huang, T. J.; Brough, B.; Baller, M.; et al. *J. Am. Chem. Soc.* **2005**, *127*, 9745−9759.
(21) Hauptmann, N.; Scheil, K.; Gopakumar, T. G.; Otte, F. L.; Schütt, C.; Herges, R.; Berndt, R. *J. Am. Chem. Soc.* **2013**, *135*, 8814−8817.
(22) Shine, H. J.; Chamness, J. T. *J. Org. Chem.* **1963**, *28*, 1232−1236.
(23) Laursen, B. W.; Krebs, F. C. *Chem. - Eur. J.* **2001**, *7*, 1773−1783.
(24) Rau, H. In *Photochemistry and Photophysics*; Rebeck, J. F., Ed.; CRC Press: Boca Raton, 1990; Vol. *2*.
(25) Schmittel, M.; Saha, M. L.; Fan, J. *Org. Lett.* **2011**, *13*, 3916−3919.

DOI: 10.1021/acs.joc.5b02262
J. Org. Chem. 2015, 80, 11233−11236

Laterally mounted azobenzenes on platforms

Melanie Hammerich and Rainer Herges*

Otto Diels-Institute for Organic Chemistry, University of Kiel,
Otto-Hahn-Platz 4, Kiel, D-24119, Germany

Table of contents

I. ^{1}H and ^{13}C NMR of compounds

Spectra of 1-[(3-Iodophenyl)methoxy]-4-nitrobenzene (4)

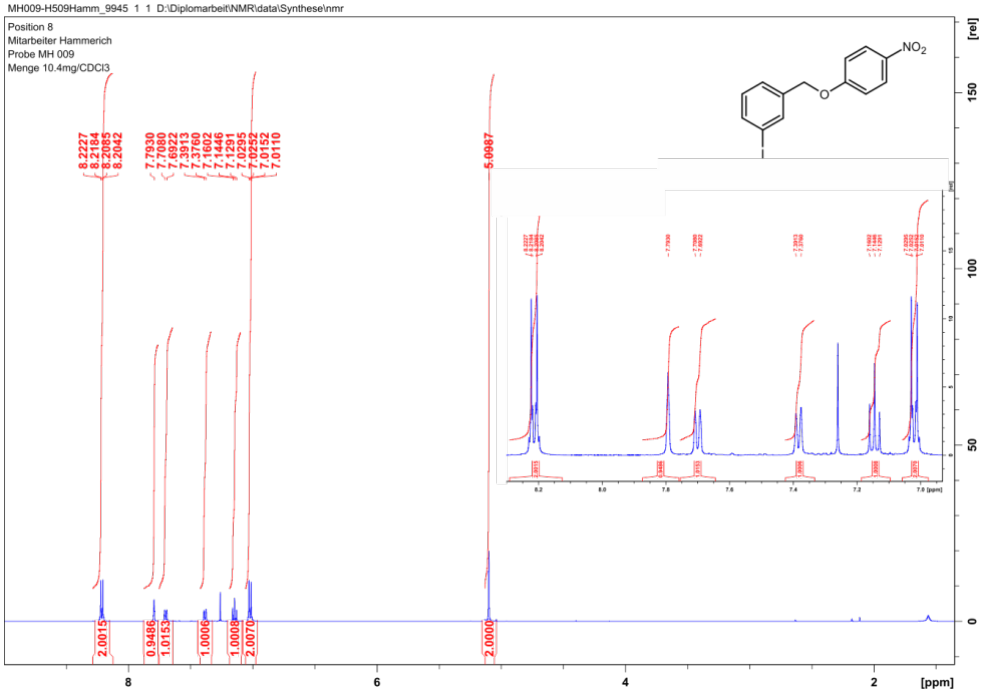

Figure S1 ^{1}H NMR of compound **4**

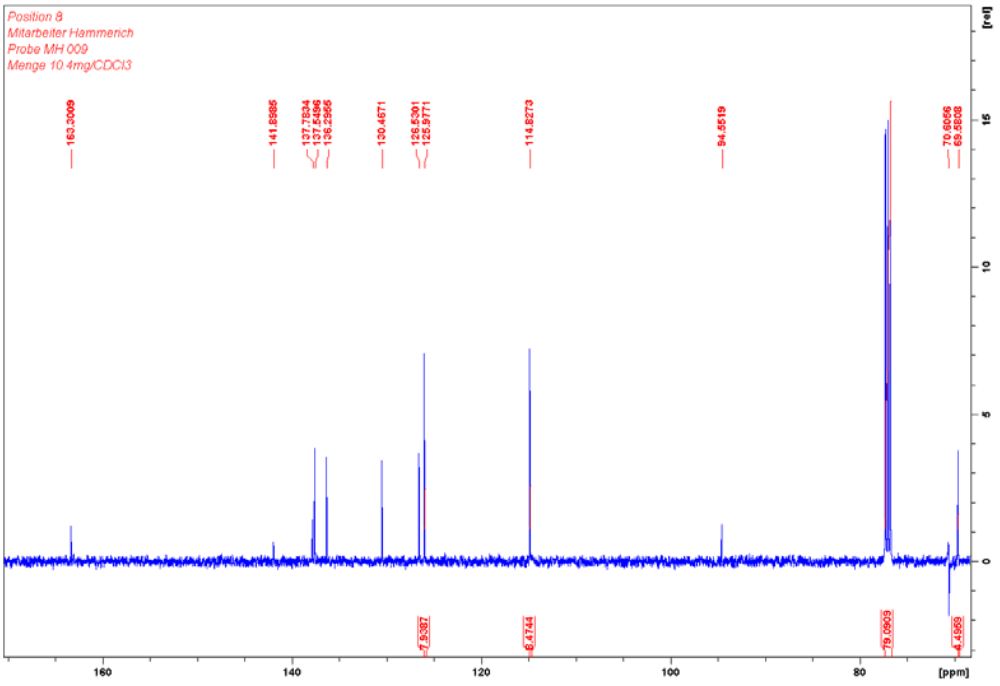

Figure S2 ^{13}C NMR of compound **4**

Spectra of 1-{[3-(Trimethylsilylethinyl)phenyl]methoxy}-4-nitrobenzene (5)

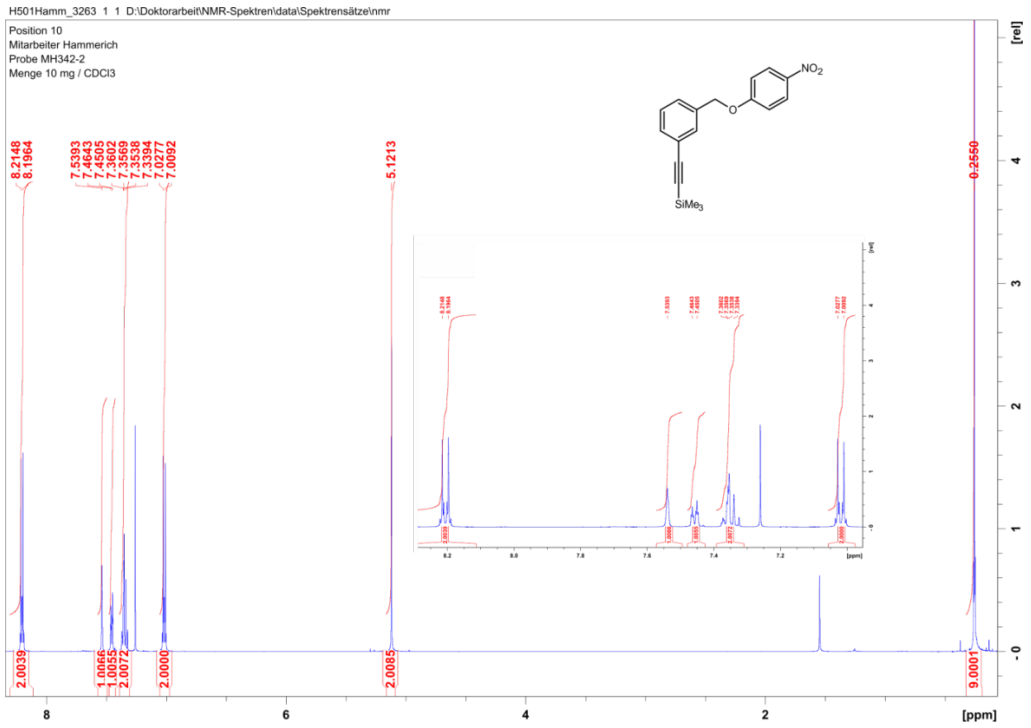

Figure S3 ^{1}H NMR of compound **5**

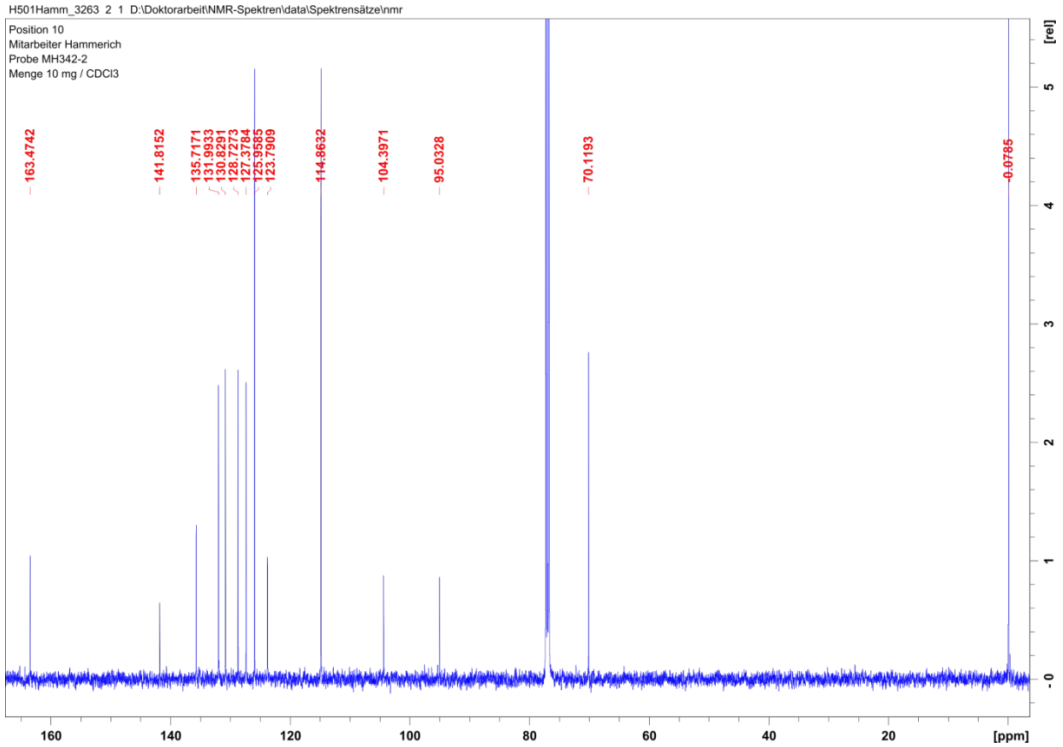

Figure S4 ^{13}C NMR of compound **5**

Spectra of 4-(3-Trimethylsilylethinylbenzyloxy)phenylamine (6)

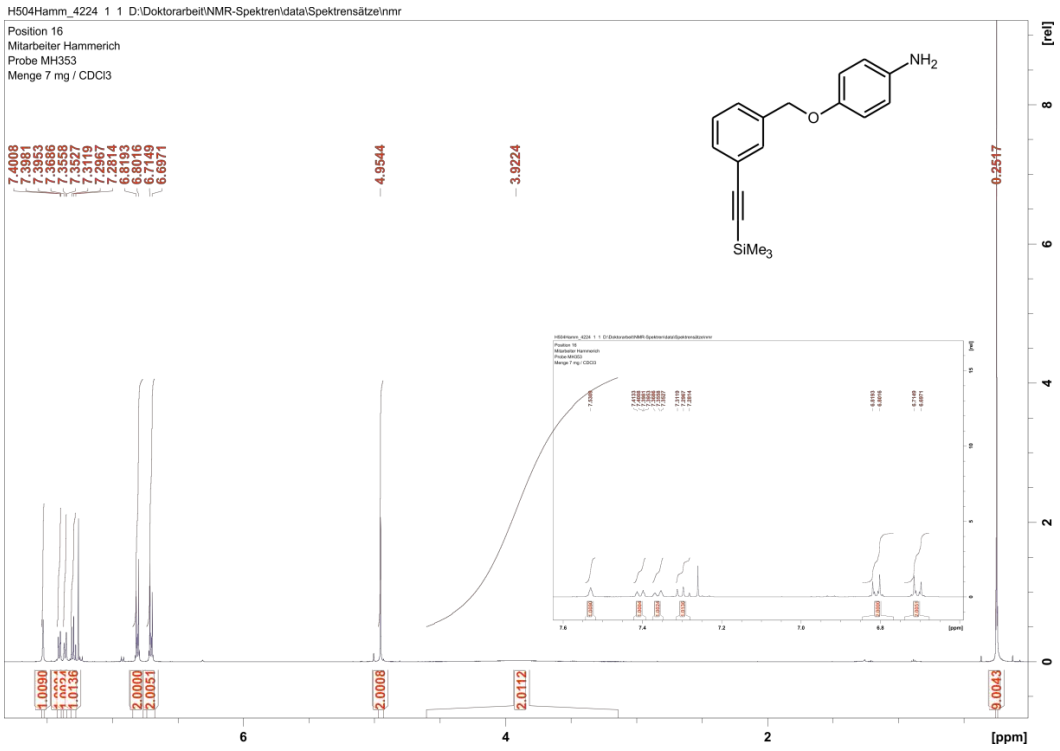

Figure S5 ^{1}H NMR of compound **6**

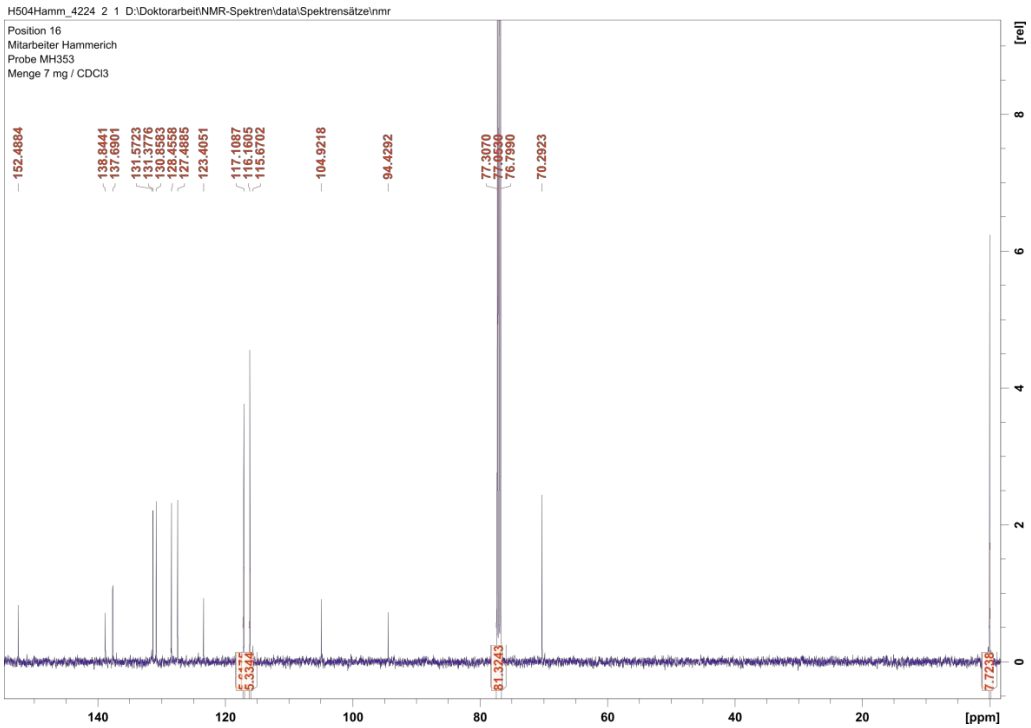

Figure S6 ^{13}C NMR of compound **6**

Spectra of 1,2-Bis{4-[(3-trimethylsilylbenzyloxy)phenyl]}-diazene (7)

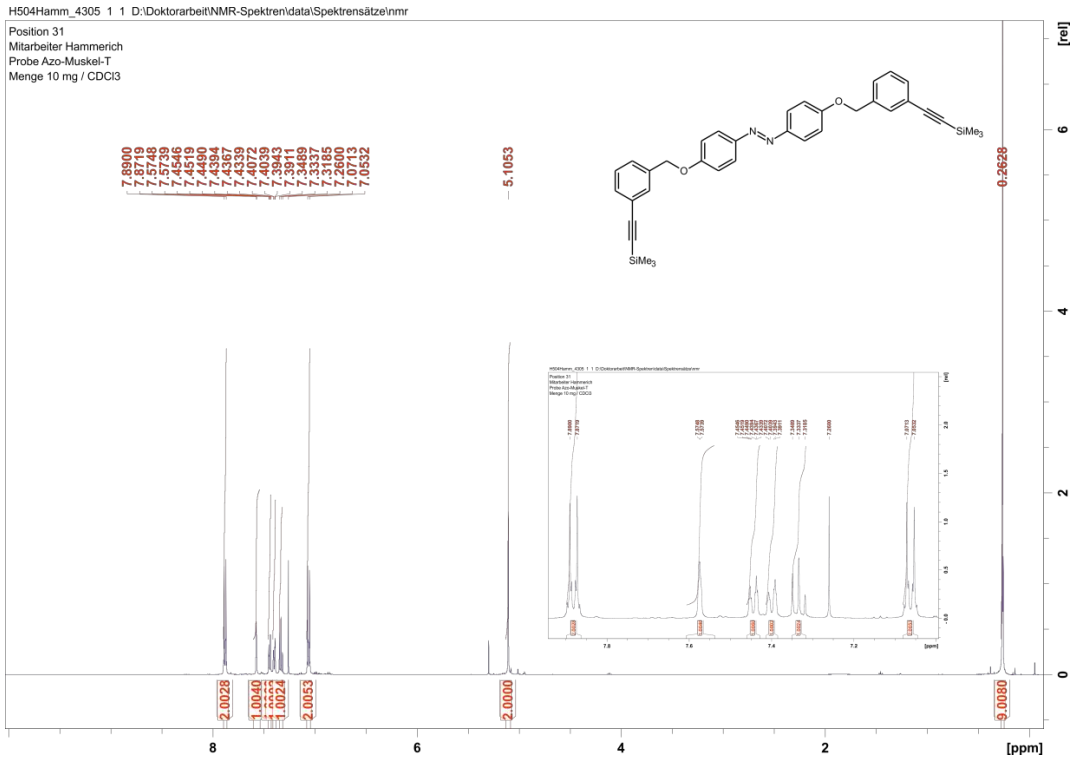

Figure S7 ^{1}H NMR of compound **7**

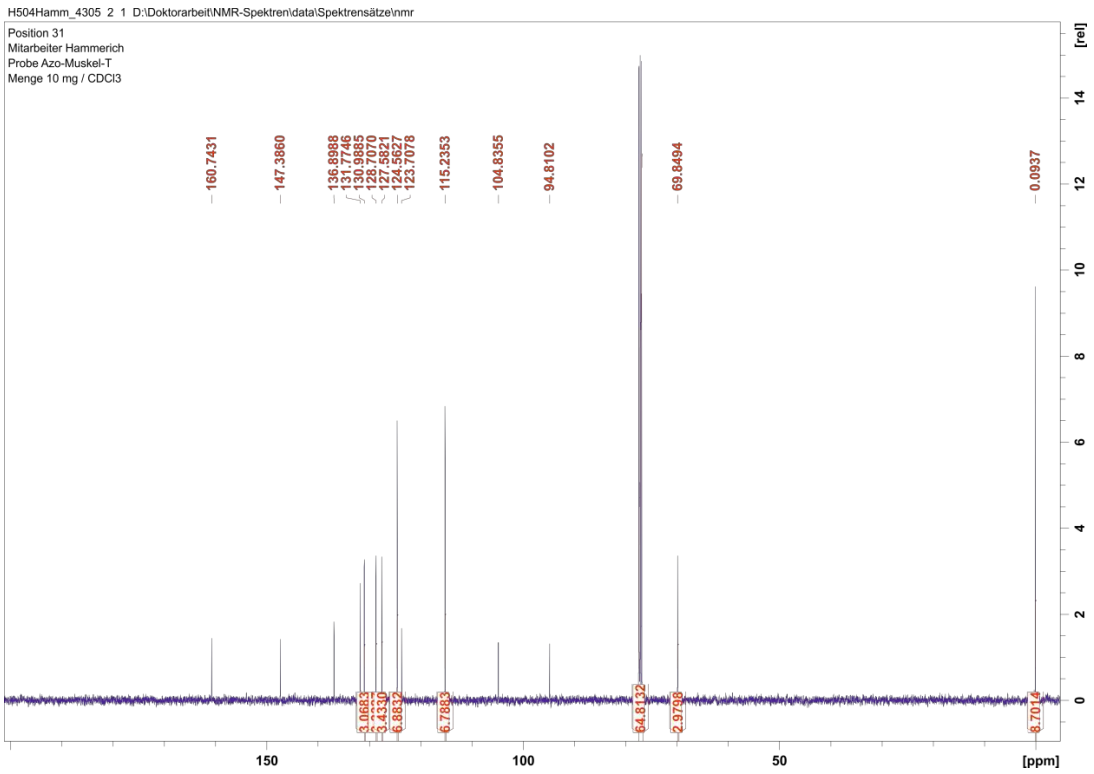

Figure S8 ^{13}C NMR of compound **7**

Spectra of 1,2-Bis-(4-{[3-(4,8,12-tris-*n*-propyl-4,8,12-triazatri-angulenium-benzyloxy]-12c-ethinyl)phenyl})diazene (9a)

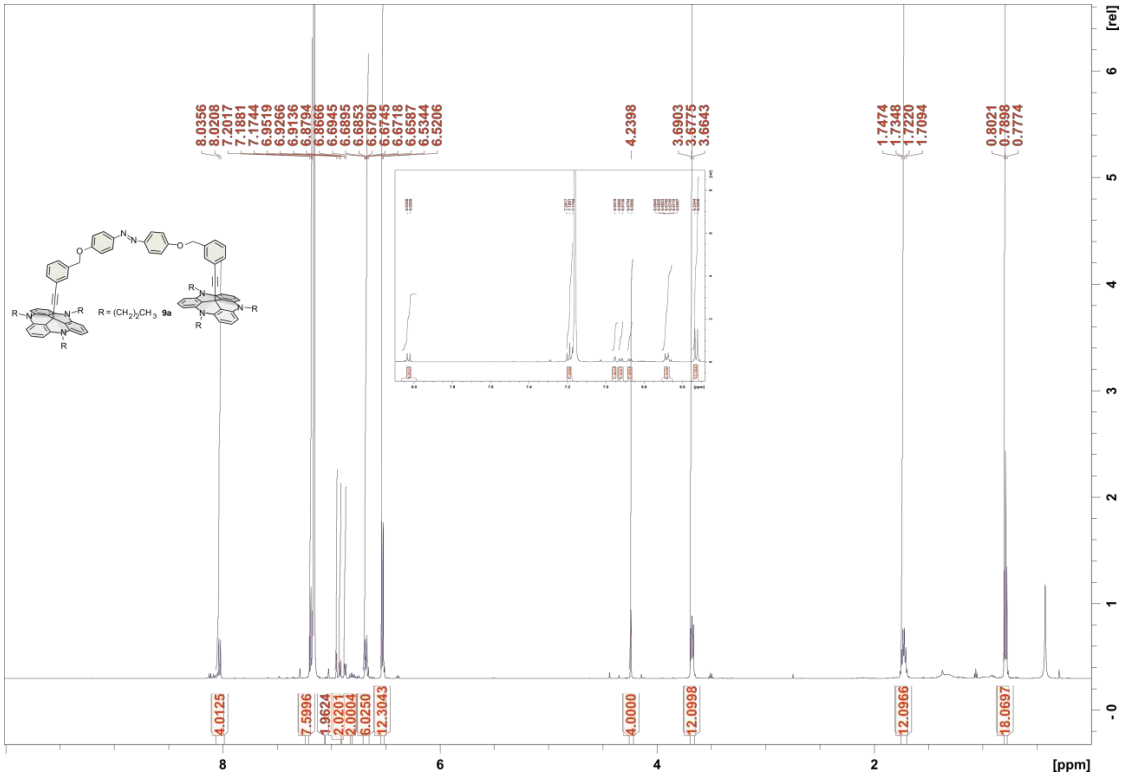

Figure S9 ^{1}H NMR of compound **9a**

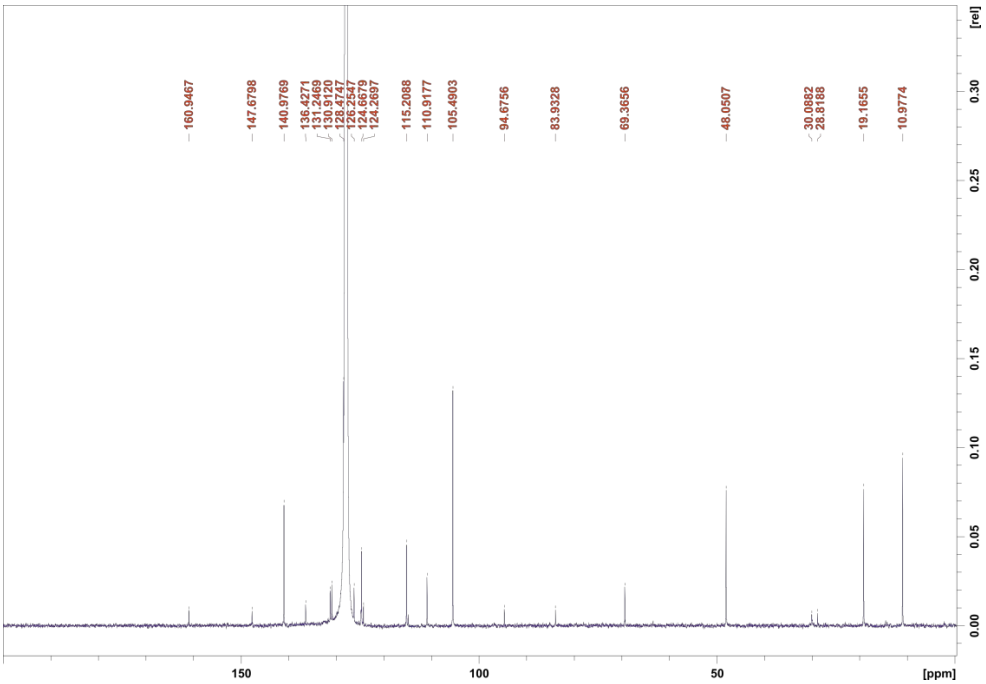

Figure S10 ^{13}C NMR of compound **9a**

Spectra of 1,2-Bis-(4-{[3-(4,8,12-tris-*n*-octyl-4,8,12-triazatriangulenium-benzyloxy]-12c-ethinyl)phenyl})-diazene (9b)

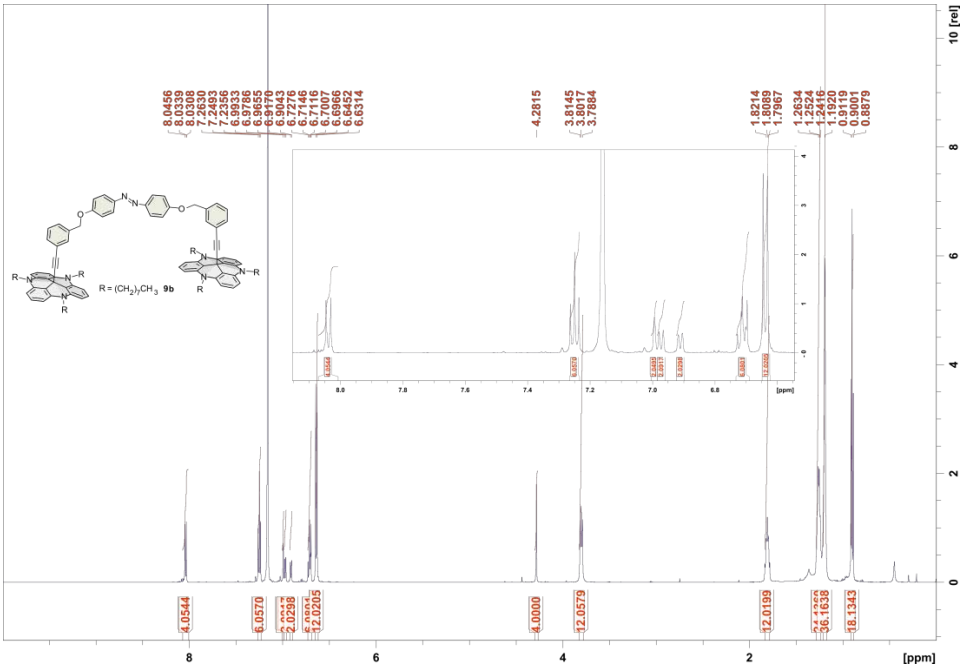

Figure S11 ^{1}H NMR of compound **9b**

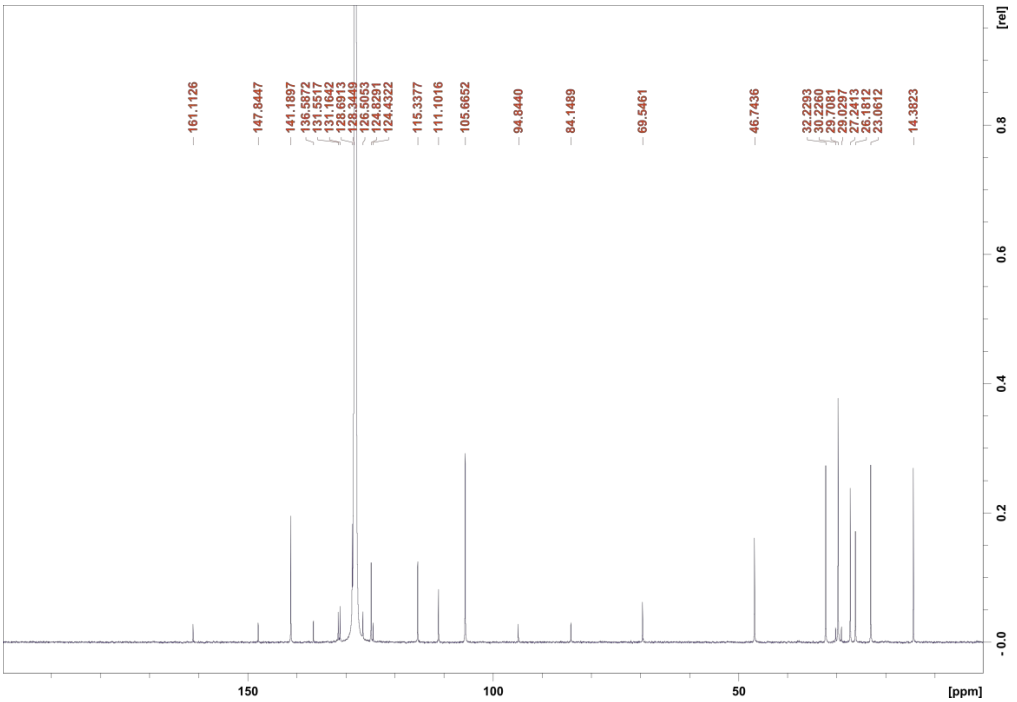

Figure S12 ^{13}C NMR of compound **9b**

II. 1H and 13C NMR of compound 9a and 9b *trans* and *cis*

The ration of *cis* and *trans* isomer were determined by ^{1}H NMR. A solution of the azobenzene was irradiated within the NMR tube with 365 nm (obtaining *cis* isomer) and 470 nm (obtaining *trans* isomer) for 10 min and the ratio of *cis*/*trans* were determined upon the OCH_2 as this signal is well separated for both species.

II.1 ^{1}H NMR of compound **9a** after irradiation

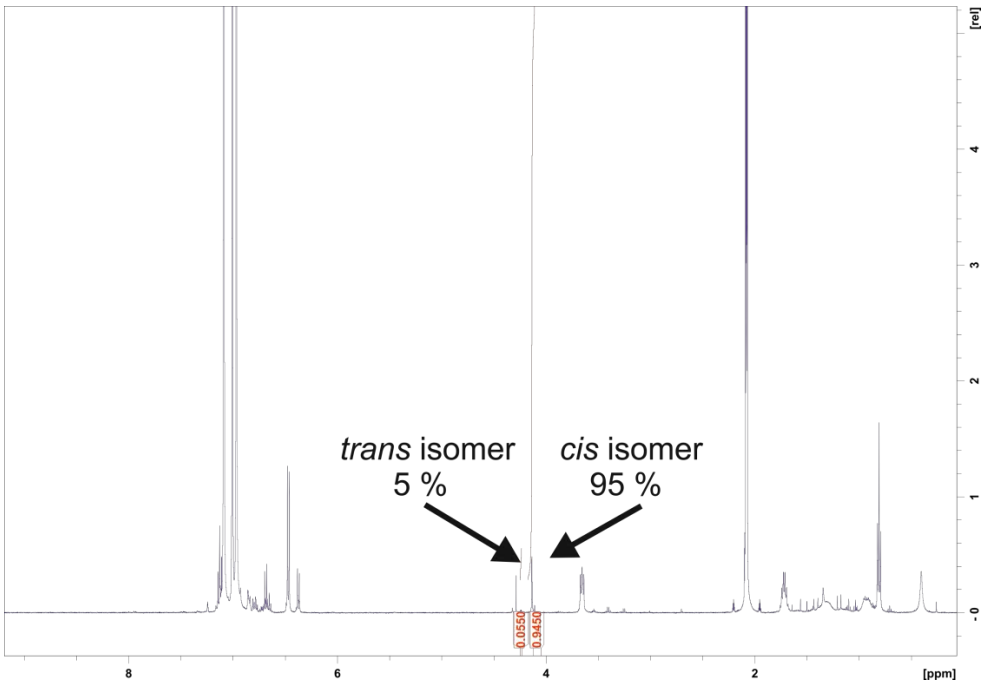

Figure S13 ^{1}H NMR of compound **9a** after irradiation with 365 nm for 10 min.

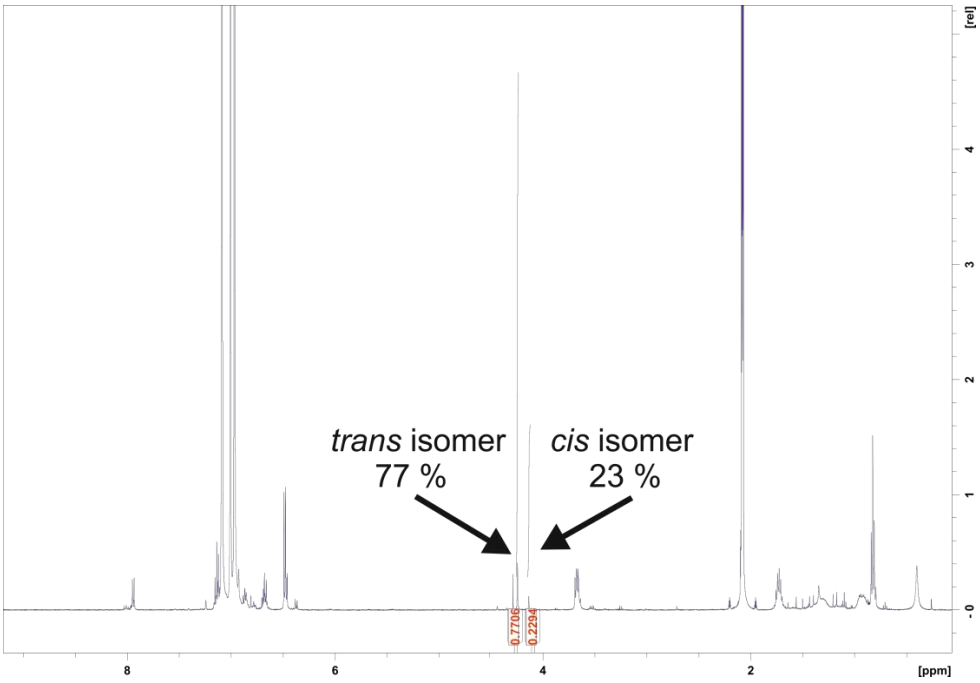

Figure S14 [1]H NMR of compound **9a** after irradiation with 470 nm for 10 min.

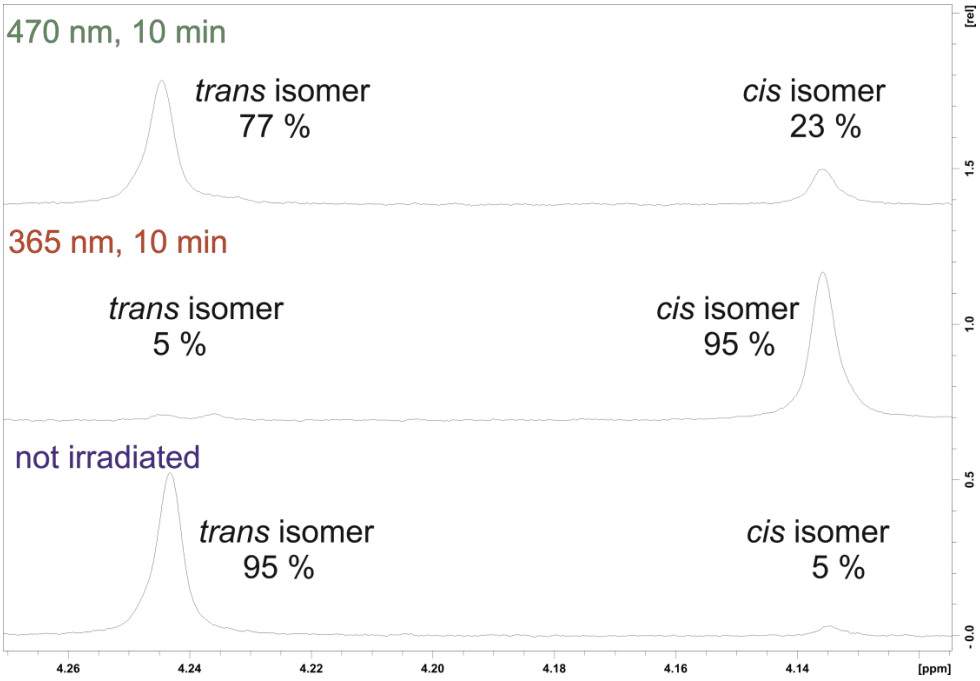

Figure S15 [1]H NMR of compound **9a:** zoom of the OCH_2region not irradiated (blue), irradiated with 365 nm (red) and irradiated with 470 nm (green):

II.2 ^{1}H NMR of compound **9b** after irradiation

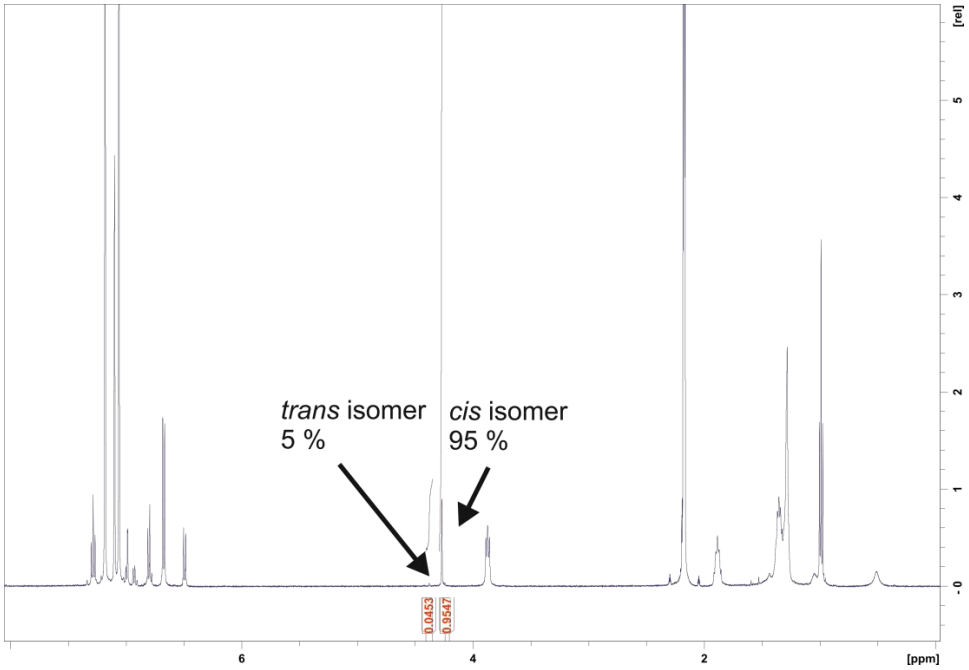

Figure S16 ^{1}H NMR of compound **9b** after irradiation with 365 nm for 10 min.

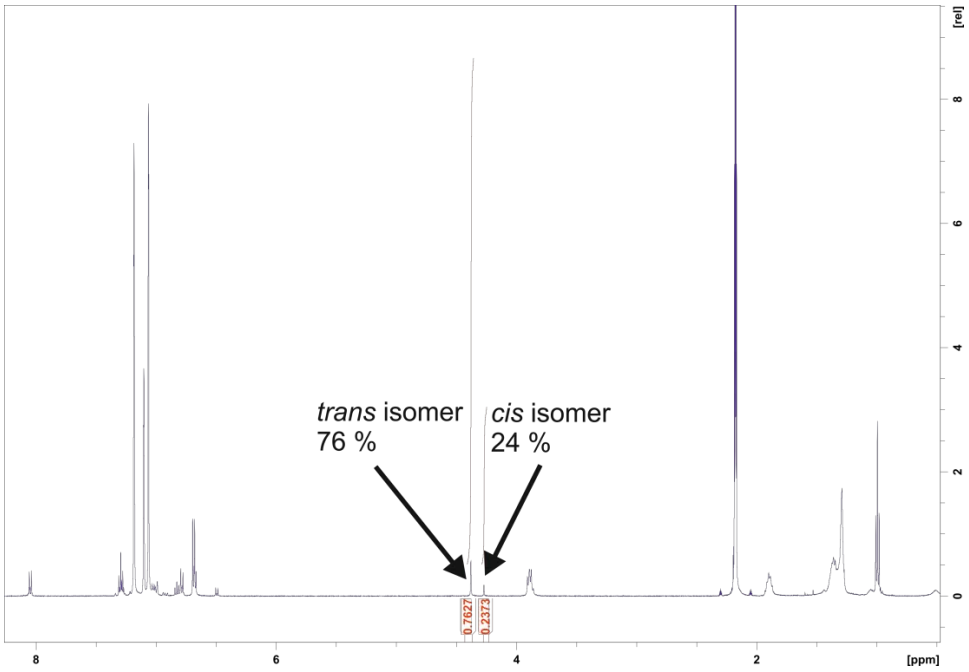

Figure S17 ^{1}H NMR of compound **9b** after irradiation with 470 nm for 10 min.

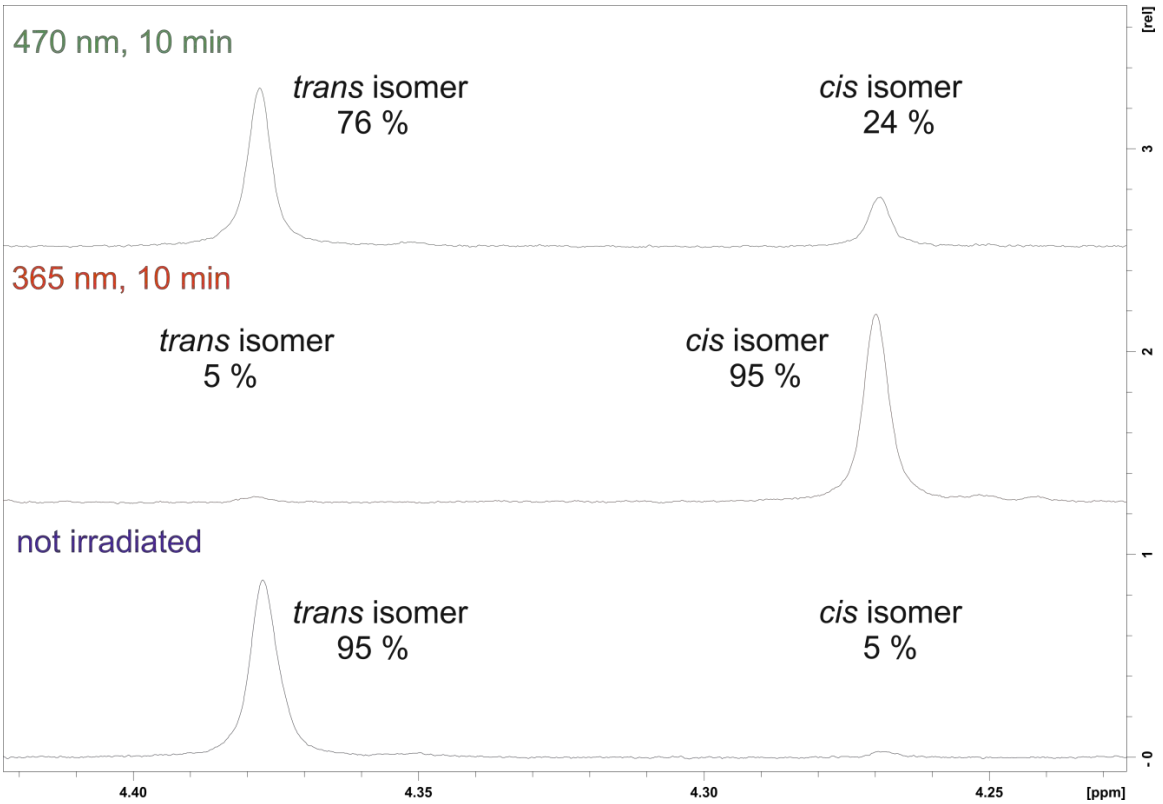

Figure S18 ^{1}H NMR of compound **9b:** zoom of the OCH_2region not irradiated (blue), irradiated with 365 nm (red) and irradiated with 470 nm (green):

II. Thermochemical half-lives of compounds 9a and 9b

Thermochemical half-lives were determined by irradiation a sample of compounds **9a** and **9b** in toluene for 1 h (*trans*→*cis* isomerization), and by subsequent measurement of the ratio of both species at 300 K with ^{1}H NMR several times over a period of five half-lives (*cis*→*trans* isomerization).

II.1 half-life of compound 9a

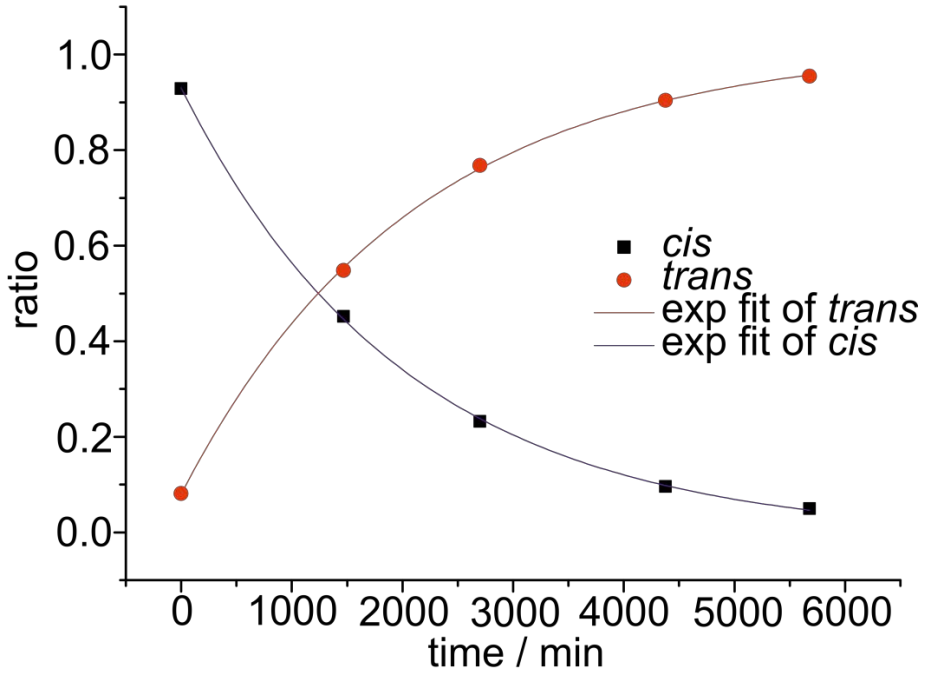

Figure S19 Ratio of *cis* and *trans*-isomer of azobenzene **9a** determined with ^{1}H NMR.

Tab.1: Calculation of thermal thermochemical half-live of compound **9a**.

linear fit $y = A\, e^{\frac{-x}{t_1}} + y_0$	
linear fit of *cis* **9a**	linear fit of *trans* **9a**
A = 0.94123 ± 0.01089 t_1= 2030.93392 ± 60.9791 y_o = 0.01101 ± 0.0095	A = -0.93931 ± 0.01086 t_1= 2088.1232± 62.43992 y_o = 1.01913 ± 0.01002
k= 4.923843 * 10^{-4} mol/ min	k= 4.788989 * 10^{-4} mol/ min
$t_{1/2}$ = 1408 min = 23.5 h	$t_{1/2}$ = 1447 min = 24.1 h
$t_{1/2}$ = 1427 min = 23.8 h	

II.2 half-life of compound 9b

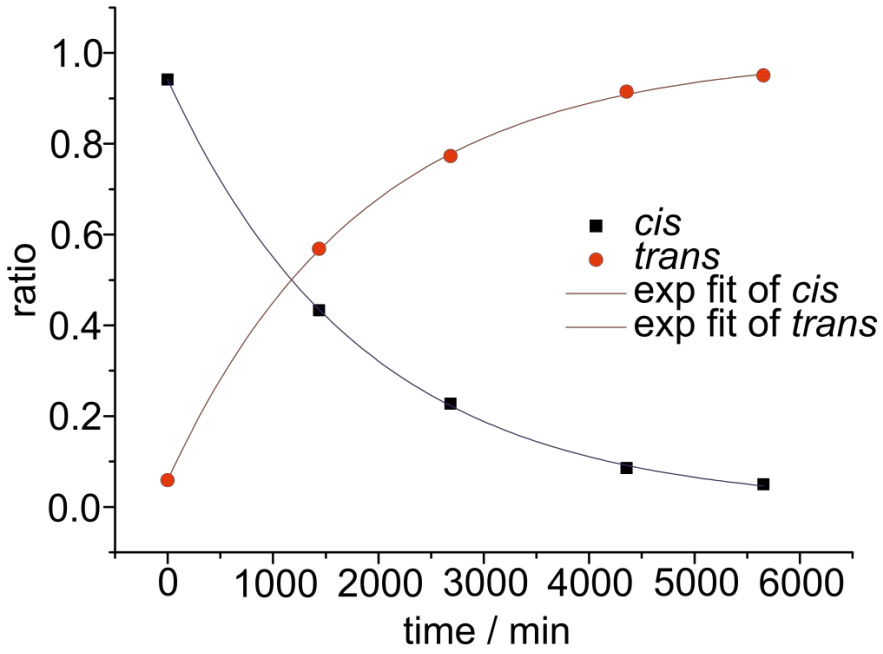

Figure S20 Ratio of *cis* and *trans*-isomer of azobenzene **9b** determined with ^{1}H NMR.

Tab.2: Calculation of thermal thermochemical half-live of compound **9a**.

linear fit $y = A\, e^{\frac{-x}{t_1}} + y_0$	
linear fit of *cis* **9b**	linear fit of *trans* **9b**
A = 0.93951 ± 0.00912 t_1= 1854.79606 ± 47.34129 y_o = 0.00176 ± 0.00791	A =-0.93896 ± 0.0093 t_1= 1849.40284 ± 48.18545 y_o = 0.99758 ± 0.00805
k= 5.391428317*10^{-4} mol/ min	k= 5.407150775*10^{-4} mol/ min
$t_{1/2}$ = 1286 min = 21.4 h	$t_{1/2}$ = 1282 min = 21.4 h
$t_{1/2}$ = 1284 min = 21.4 h	

III.1 UV-vis spectrum of 9a

UV spectra of the pure *trans* isomer and of the photostationary state at 365 nm (~95% cis) of the "muscle" compound **9a** were measured.

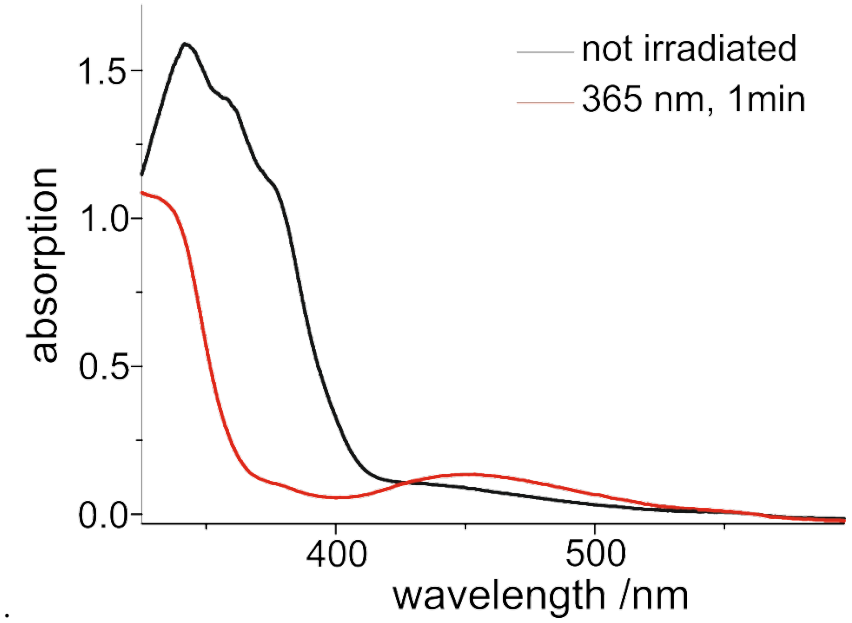

Figure S21 UV spectra of compound **9a**, black curve: pure *trans* isomer, red curve: photostationary equilibrium at 365 nm (~95% *cis*),

III.1 Photostability of compound 9a and 9b

The photostabilities of our compunds **9a** and **9b** were investigated by UV spectroscopy. A solution of the azobenzene in toluene was irradiated alternately with 365 nm and 440 nm for 1 min at every period, and after every switching process a UV spectrum was measured. The compound shows no decay or fatigue.

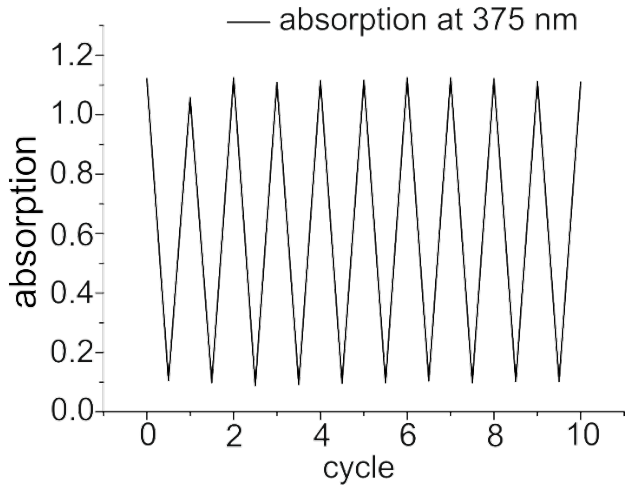

Figure S22 Photostability of compound **9a**, UV spectra were measured after alternating irradiation with 365 nm and 440 nm.

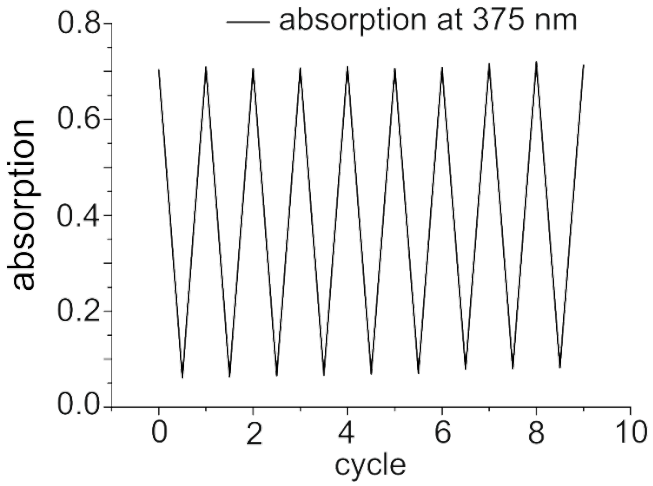

Figure S23 Photostability of compound **9b**, UV spectra were measured after alternating irradiation with 365 nm and 440 nm.

4 Imine-Functionalized TATA Platforms

All photoswitchable TATA platforms that have been synthesized hitherto can perform different kinds of motion but the realization of a unidirectional movement posed a challenge. So far, azobenzenes are most commonly used as photoswitchable units as their photochemical properties are well investigated and reliable. However, both forward and back reaction unfortunately proceed by the same mechanism and, therefore, the time reversal symmetry for the movement cannot be broken. Hence, the efficiency of the switching movement is dramatically decreased. Photoswitchable units that can switch only in one direction would enhance the previous systems accordingly. Advances in this field were made by the development of indane diazocines.[92,99] Those chiral, double bridged diazocines possess the advantage that the *trans* $\rightarrow$ *cis* isomerization can only occur in one direction as the other reaction pathway is sterically hampered. Thus, indane diazocines represent promising candidates to be employed as unidirectional photoswitches.

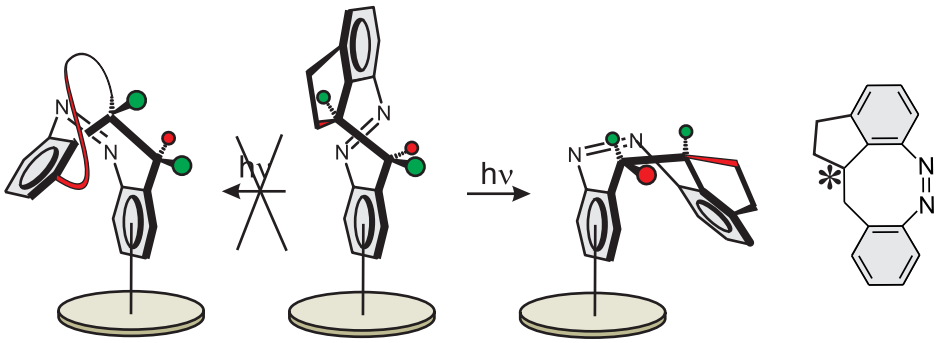

Figure 4.1: By bridging diazocines a second time chiral photoswitches are received that switch only in one direction.[99]

Nevertheless, the synthesis of indane diazocines is very challenging and yields the desired functionalized TATA platforms only in minimal amounts. Hence, a photoswitch with a simplified structure and synthesis would be preferable. LEHN predicted that imines would be ideal candidates as molecular motors as their switching movement occurs unidirectionally.[45,46] An orthogonal imine-functionalized TATA platform monolayer as an artificial ciliated epithelium is a suitable substrate to validate this theory.

4.1 Imine-Functionalized Triazatriangulenium Platforms: Towards an Artificial Ciliated Epithelium

Melanie Hammerich, Talina Rusch, Nicolai R. Krekiehn, Andreas Bloedorn, Olaf M. Magnussen and Rainer Herges

Chem. Phys. Chem **2016**, *17*, 12, 1870–1874.

DOI: 10.1002/cphc.201600147

Scientific contribution to this paper:

All reported syntheses and the photophysical investigations in solution (^{1}H NMR and UV/vis) were performed by me. STM measurements were done by Talina Rusch with preliminary work of Andreas Bloedorn, UV/vis measurements on surface were done by Nicolai Krekiehn. Prof. Dr. O. M. Magnussen, Prof. Dr. R. Herges and I wrote the manuscript.

Summary

We report on the syntheses and photochemical investigations of imine functionalized TATA platforms as a model system of a ciliated epithelium. Like azobenzenzes, imines undergo a photoinduced *trans* → *cis* isomerization after irradiation with UV light (365 nm). Thereby, the isomerization to the *cis* isomer occurs via rotation around the C=N double bond, whereas the thermal back isomerization to the *trans* isomers follows an inversion mechanism. Hence, imines represent the ideal candidates for the unidirectional transport of nanoparticles (Figure 4.2). In this work six different functionalized imine TATA platforms were synthesized by a convergent synthetic route. The synthesis of the imines was achieved by condensation reaction and the following functionalization was conducted by deprotection of the silyl group and *in situ* reaction with the TATA platform. As the photostability of the *cis* isomers is small at room temperature ($t_{1/2}$ = 0.58 s), switching experiments were performed at low temperatures (215–233 K). Formation of the *cis* isomers were observed by UV/vis and ^{1}H NMR spectroscopy. In this process the *cis* isomers could be enriched up to 50 %. The kinetic back isomerization could be verified with ^{1}H NMR and UV/vis spectroscopy and rate constants could be determined for different temperatures. Following the ARRHENIUS approach the activation barrier for the thermal back isomerization was determined as E_A = 61±6 kJ/mol. Formation of SAMs on a Au(111) surface could be proven by STM measurements showing the expected highly ordered hexagonal structure of the TATA platforms. A comparison of the UV/vis spectra in solution and of the monolayer indicated that the compound remains intact after deposition on the Au(111) surface since the absorption bands are nearly identical.

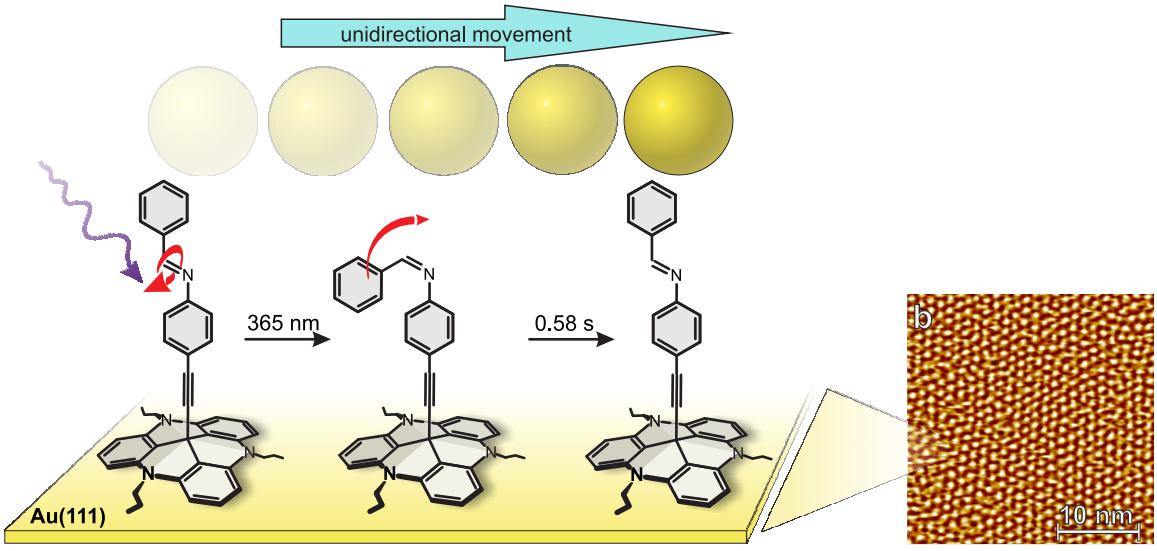

Figure 4.2: Upon irradiation the imine switches *via* rotation around the C=N double bond to the *cis* isomer. With the fast thermal back isomerization that occurs *via* inversion mechanism the starting point is reached in a unidirectional movement.

ChemPubSoc Europe
DOI: 10.1002/cphc.201600147
CHEMPHYSCHEM Articles

Special Issue

Imine-Functionalized Triazatriangulenium Platforms: Towards an Artificial Ciliated Epithelium

Melanie Hammerich,[a] Talina Rusch,[b] Nicolai R. Krekiehn,[b] Andreas Bloedorn,[b] Olaf M. Magnussen,[b] and Rainer Herges*[a]

Triazatriangulenium (TATA) platforms have been used to prepare highly ordered, self-assembled monolayers of free- and vertically standing imines on Au(111) surfaces. Upon irradiation, the imines undergo *trans–cis* isomerization and a fast thermal reaction ($t_{1/2}$ = 0.58 s at 20 °C) back to the more stable *trans* form. It is known that the photochemical reaction proceeds through rotation of the C=N bond and the thermochemical reaction through inversion at the N atom. The imine motors, therefore, should be able to induce a net displacement of particles above the surface similar to cilia epithelia in nature.

1. Introduction

Directed motion is one of the most interesting functions in nanoscience.[1] The majority of approaches pursued so far are based on molecular actuators moving on a passive surface. We propose the reverse assignment: an active surface propelling a passive load. This type of unidirectional motion is abundant in nature. Whip-like structures protruding from the cell wall (flagella or cilia) providing motility probably emerged more than 2 billion years ago[2] and are prevalent in higher organisms. Common examples are the cilia epithelia in our respiratory tract that transport mucous liquid and other substances towards the throat. As Purcell stated 40 years ago,[3] a simple flapping of a flagellum back and forth, or more precisely with a forward motion being the reciprocal of the backward movement, would not induce a net displacement. Cilia break this time-reversal symmetry by performing their periodic motion in two different phases: a power stroke with the tip up and a recovery motion with the tip down. Breaking time-reversal symmetry is the precondition for directed movement. Upon irradiation, simple imines perform such non-reciprocal motion. It is known that the photochemical *trans–cis* isomerization proceeds through a rotation around the C=N double bond,[4–7] whereas the thermal back-reaction mechanism is an inversion at the nitrogen atom via a linear transition state. Based on these arguments, Lehn and Greb suggested to use imines as molecular motors.[8,9] However, before imines can be used as artificial molecular flagella or cilia to build a cilia epithelium, a number of additional preconditions have to be met. 1) The switching units (imines) have to be immobilized as an array on a surface. 2) There must be sufficient free volume for switching. 3) The switching units should be vertically oriented and free standing to achieve maximum power transmission from the switching units to the above load to be transported. 4) If metal surfaces are used, the photoswitchable molecules have to be electronically decoupled from the surface.

These requirements are not well met by adlayers formed through the most popular method used to attach functional molecules to metal surfaces, that is, molecular self-assembly on gold with thiol groups. Here, alkane chains typically serve as spacers, and the functional molecule is attached on top. Although this method allows the facile preparation of close-packed molecular monolayers in which the molecules are standing (almost) upright, the dense packing prevents isomerization. To overcome these problems, a number of more advanced functionalization strategies have been developed.[10] The approach developed by us is a modular molecular system consisting of a platform, a spacer, and the functional unit. Within this "platform approach",[11] the molecular platform (triazatriangulenium, TATA) provides a high affinity to the Au(111) substrate and defines the lateral distances to the next neighbors on the surface. A stiff spacer (phenyl or ethynyl unit) is attached to the central carbon of the platform, which carries the functional molecule on top. Thus, the functional molecules are mounted as freestanding units and rigidly oriented along the surface normal, separating the functional unit spatially from the surface and, moreover, from each other.[12] We could demonstrate the advantages of this concept for azobenzenes: Although in alkanethiol-based monolayers the photochemically switching is clearly hindered, azobenzene-TATA adlayers fully retain the conversion rates (*trans*→*cis*, *cis*→*trans*) and quantum yields that they exhibit in solution.[13] Azobenzenes upon irradiation, however, perform a reciprocal *trans*→*cis* and *cis*→*trans* isomerization. Chiral azobenzenes, which have recently

[a] M. Hammerich, Prof.Dr. R. Herges
Otto Diels-Institute for Organic Chemistry
Christian-Albrechts University Kiel
Otto-Hahn-Platz 4, Kiel 24119 (Germany)
E-mail: rherges@oc.uni-kiel.de

[b] T. Rusch, N. R. Krekiehn, A. Bloedorn, Prof.Dr. O. M. Magnussen
Institut für Experimentelle und Angewandte Physik
Christian-Albrechts University Kiel
Leibnizstraße 11-19, Kiel 24119 (Germany)

Supporting Information for this article can be found under http://dx.doi.org/10.1002/cphc.201600147.

An invited contribution to a Special Issue on Molecular Machines

ChemPubSoc Europe

CHEMPHYSCHEM Articles

been successfully mounted on TATA platforms,[14] allow this problem to be circumvented, but are a bistable system with slow thermal back-isomerization. For realizing artificial molecular cilia, systems with rapid back-switching after optical isomerization are more suitable. This is the case for TATA platforms with imines as functional groups, which we report here.

2. Results and Discussion

As in previous studies, *n*-octyl-TATA **6** was chosen as the platform, because **6**, as a cation and functionalized with a number of different groups, has been proven to form highly ordered self-assembled monolayers (SAMs).[11] In the hexagonal packing, the platforms have a distance of 12.5 Å to their next neighbors on the Au(111) surface. This provides sufficient free volume for the switching of azobenzenes,[15] and should also be sufficient for the very similar imine structures. Ethynyl groups were used as spacers or pillars to electronically decouple the switches from the metal surface, and to provide an upright orientation for the imines attached on top. In this study, we prepared six imines with different head groups. Imines with dimethyl (**5 b**) or *tert*-butyl (**5 c**) head groups were chosen because of steric reasons, as these groups prevent the formation of bilayers. Additionally, imines with amine (NMe_2, **5 e**) and hydrophobic (F, **5 d**) head groups were synthesized. To increase the distance between switching unit and the gold surface, we additionally synthesized an imine with a phenyl ethynyl unit as the spacer group.

2.1. Synthetic Procedure

The functionalization of TATA platforms follows a convergent synthetic route, where the TATA platform and switching unit are prepared separately, and are combined in the last synthetic step. The synthesis of the TATA platform **6** was performed according to the procedure by Laursen and Krebs in a three-step synthesis.[16] The aniline derivative **3** was prepared through a Sonogashira reaction in 90% yield.[17] The syntheses of the imines (**5 a–f**) were achieved by condensation of the corresponding benzaldehydes (**4 a–f**) with the aniline **3** (Figure 1).

The functionalization of the TATA platforms was achieved by deprotecting the silyl group with potassium hydroxide and subsequent in situ reaction with the cationic center of the platform (Figure 2).[18]

Imine–TATA **5 f**, with the elongated phenyl–ethynyl spacer, was analogously prepared. The aniline derivative that is needed for the condensation reaction was synthesized according to a procedure by Seto and co-workers in a three-step procedure with an overall yield of 16% (Figure 3).[19–21]

2.2. Switching Experiments in Solution

The photophysical properties were investigated by using ^{1}H NMR and UV/Vis spectroscopy in solution at low temperatures. To determine the photostationary state with ^{1}H NMR spectroscopy in solution, a sample of the imine-functionalized TATA platform (**7 c**) was dissolved in deuterated acetone and

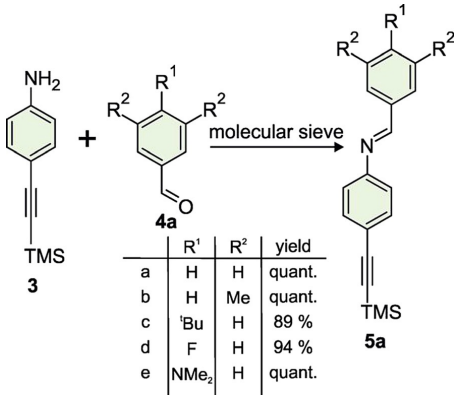

	R^1	R^2	yield
a	H	H	quant.
b	H	Me	quant.
c	^{t}Bu	H	89 %
d	F	H	94 %
e	NMe_2	H	quant.

Figure 1. Syntheses of the imines **5 a–e**.

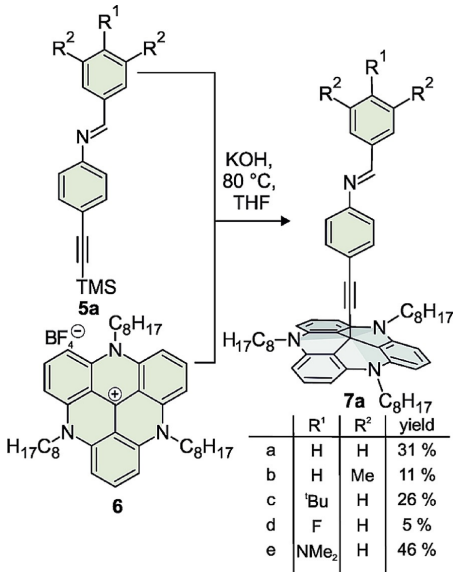

	R^1	R^2	yield
a	H	H	31 %
b	H	Me	11 %
c	^{t}Bu	H	26 %
d	F	H	5 %
e	NMe_2	H	46 %

Figure 2. Functionalization of TATA platforms with imines.

cooled to 195 K with acetone/dry ice. After measuring a reference spectrum of the *trans* isomer at 230 K, the sample was irradiated at 365 nm in a quartz Dewar vessel for 20 min. The sample was rapidly transferred to a precooled NMR spectrometer, and ^{1}H NMR spectra were measured at 230 K. In Figure 4, the aromatic region of compound **7 c** (*tert*-butyl-imine–TATA) is shown before and after irradiation. Upon irradiation, the signals of the *trans* isomer decrease and a set of new signals appears, which proves the formation of the *cis* isomer. Integration of the ^{1}H NMR signals (*trans:* 8.46 ppm; *cis:* 8.30 ppm) yields a ratio of 48% *cis* to 52% *trans* isomer. The thermal back reaction to the *trans* isomer was monitored by measuring

ChemPubSoc Europe
CHEMPHYSCHEM Articles

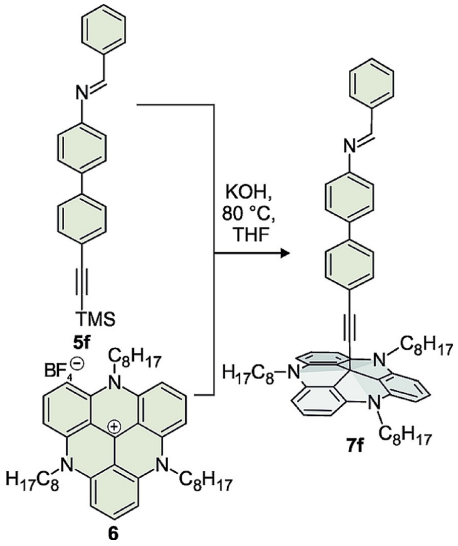

Figure 3. Functionalization of *n*-octyl-TATA with biphenyl-imine **5 f**.

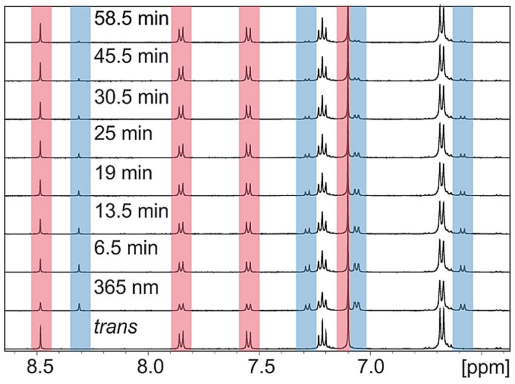

Figure 4. Monitoring of the thermal back reaction of *cis*-**7 c** to the *trans* isomer after irradiation at 365 nm at 230 K. Highlighted in red are the signals of the *trans* isomer. The signals of the *cis* isomer are shaded in blue. All other signals belong to the TATA platform, which remains unaffected during isomerization.

^{1}H NMR spectra in time intervals over several half-lives. As the *cis*→*trans* isomerization follows a reaction of first order, the rate constant *k* could be determined by exponential fitting of the integrals of the *H*-imine proton signals of both species (*trans* red, *cis* blue) as $k = 5.54 \cdot 10^{-4}\ s^{-1}$. The half-life of the *cis* isomer is $t_{1/2} = 21 \pm 1$ min at 230 K (Figure 4). After irradiation, only the signals of the imine protons are shifted, whereas the signals of the TATA platform remain unchanged (non-highlighted signals in Figure 4).

To determine the kinetic parameters of the isomerization reaction, we measured UV/Vis spectra in absolute THF under a nitrogen atmosphere at different temperatures, at intervals between 215 and 233 K. Figure 5 presents the UV spectra of *H*-imine–TATA **7 a** recorded after irradiation with 365 nm at 223 K for 10 min (black curve). Irradiation leads to a distinct decrease in the intensity of the ππ* band (334 nm), whereas the band at 274 nm slightly increases.

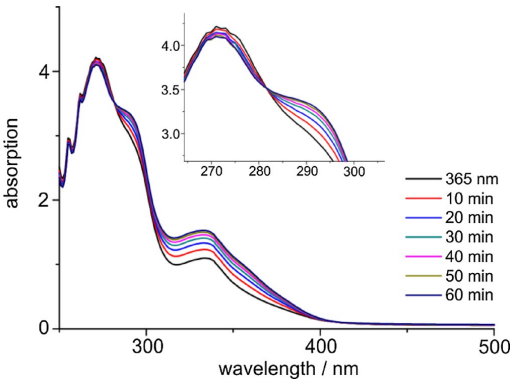

Figure 5. UV/Vis spectra of compound **7 a** in THF at 223 K after irradiation at 365 nm (black curve). The thermal back reaction was monitored in 10 min time intervals (colored curves).

Several spectra were measured with 2 min time intervals until the sample relaxed almost completely back to the *trans* isomer. The exponential increase of the ππ* band was fitted as a function of time. The kinetics were determined at three different temperatures (233, 223, and 215 K). The rate constant and temperature follow an Arrhenius-type relationship. The activation energy for the *cis*→*trans* relaxation was determined by a linear fit of ln(*k*) as a function of 1/*T*. For compound **7 a**, we determined an activation energy of $61.2 \pm 6.4\ kJ\,mol^{-1}$ for the thermal back isomerization, which is somewhat lower than for the parent benzylidene aniline, $70\ kJ\,mol^{-1}$ (Figure 6).[22] Extrapolated to 20 °C, the half-life $t_{1/2}$ of the *cis* isomer is 0.58 s.

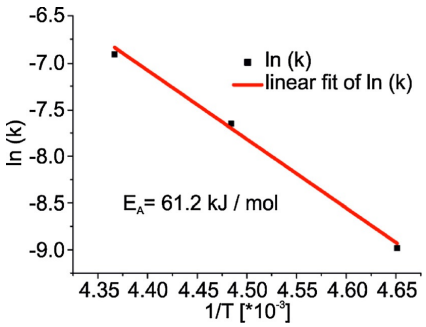

Figure 6. Arrhenius plot for the *cis*→*trans* isomerization of compound **7 a**.

ChemPubSoc Europe

CHEMPHYSCHEM Articles

2.3. STM Measurements

STM measurements at room temperature reveal a hexagonally ordered superstructure with intermolecular distances of (12.5 ± 0.4) Å for **7d** SAMs (Figure 7a) and of (12.3 ± 0.05) Å for **7c**

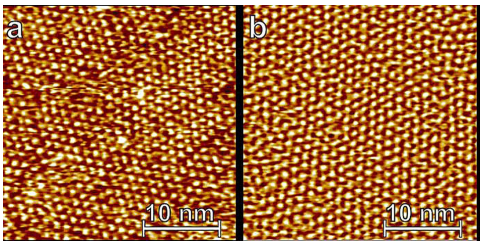

Figure 7. STM images (30 nm × 30 nm) of self-assembled layers of a) **7d** and b) **7c** on Au(111).

SAMs (Figure 7b) on Au (111). The lattice constant and the angles between different rotational domains for both monolayers are in excellent agreement with the $(\sqrt{19}\times\sqrt{19})$ *R*23.4° superstructure, observed previously for SAMs of the pure platform **6** and of **6** with vertically attached azobenzene derivatives.[11,13,15] SAMs prepared from THF solution resulted in well-ordered monolayers, whereas SAMs formed in toluene exhibited a high percentage of bilayer islands as well as a high defect density, especially for the preparation at lower temperatures.

SAMs were prepared after the immersion of Au(111) single crystals for 30–60 min in 100 μM solutions of **7d** and **7c** in toluene or THF at temperatures between 25 and 80 °C. Afterwards, the samples were rinsed with the pure solvent to remove excess molecules physisorbed on top of the SAM.

2.4. UV/Vis Spectroscopic Studies of Adlayers

Spectroscopic studies by using UV/Vis spectroscopy (Figure 8) corroborate that the molecules are present on the Au surface and show that their optical properties are largely unchanged. In the 200–400 nm regime, the difference spectra of **7d** SAMs on thin Au films are almost identical to spectra of the free molecules in solution. In particular, the ππ* transition of the imine moiety at 330 nm is clearly present. The position of this band is identical to that in solution, indicating the absence of pronounced excitonic coupling with neighboring molecules and the metal substrate.

This behavior is similar to that found in previous UV/Vis studies of TATA platforms with vertical azobenzene ligands[23] and can be explained by the decoupling of the freestanding chromophores in these SAMs. In contrast to spectra of the pure cationic platform **6**, the spectrum of the **7d** SAM does not exhibit the broad absorption band around 500 nm. This demonstrates that the imine-functionalized TATA platforms remain intact upon adsorption. The broad band at > 550 nm is located in the spectral range of the Au plasmon resonance. This plasmon band is known to be highly sensitive to the presence of adsorbed species.[24] Its appearance in the difference spectra between the adlayer-covered and the clean Au surfaces can, therefore, be attributed to the adsorption of the molecular layer.

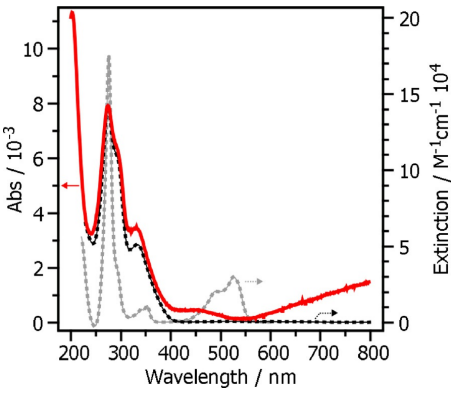

Figure 8. UV/Vis extinction spectra of **6** (dashed grey curve) and **7d** (dashed black curve) in solution (DCM), and absorption spectra of **7d** on a Au substrate (solid red curve). The spectra of the free molecules are limited to wavelengths ≥ 230 nm, owing to the cutoff by the solvent.

In contrast to the behavior found for azobenzene–TATA SAMs,[15] irradiation of the **7d** SAM by UV light (365 nm) at room temperature resulted in no measurable changes in the spectra. This can be readily explained by the fast thermal back-isomerization of the imine–TATAs, found in solution ($t_{1/2}$ = 0.58 s at 20 °C, which is much faster than the time required for recording the UV/Vis spectrum). In fact, the back-isomerization of the SAM may be even faster. In previous studies, we discovered that the rate of the thermal back-reaction (*cis*→*trans*) of azobenzenes mounted on TATA platforms increases by almost three orders of magnitude if the molecules are physisorbed on an Au(111) surface.[15,25] Even though we have no explanation for this phenomenon so far, the same rate acceleration could be operative for the analogous imines, which would be beneficial for application as artificial epithelium, as the frequency of switching cycles would be strongly increased in comparison to azobenzene systems.

3. Conclusions

Aiming at the construction of an artificial cilia epithelium, we synthesized six different imine switches, which were mounted on molecular platforms. By immersion of gold surfaces into dilute solutions, highly ordered self-assembled monolayers were formed. The platforms adsorb on the surface in a defined hexagonally ordered superstructure with intermolecular distances of 12.5 Å. The imines are covalently bound to the central carbon atom of the platform in such a way that they are freestanding and oriented upright. In solution and upon irradiation at 365 nm, the imines perform *trans*→*cis* isomerization. The thermal back-isomerization is very fast at room temperature ($t_{1/2}$ = 0.58 s at 20 °C). As the photochemical reaction and

ChemPubSoc Europe

CHEMPHYSCHEM Articles

the thermochemical back-reaction follow different mechanisms, the imines should function as artificial cilia, which, in principle, could be able to transport particles lying on top of the surface.

Acknowledgements

The authors gratefully acknowledge financial support by the Deutsche Forschungsgesellschaft (DFG) via the collaborative research center SFB 677, "Function by Switching".

Keywords: functionalized surfaces · imines · molecular platforms · photoswitches · self-assembled monolayers

[1] E. R. Kay, D. A. Leigh, F. Zerbetto, *Angew. Chem. Int. Ed.* **2007**, *46*, 72 – 191; *Angew. Chem.* **2007**, *119*, 72 – 196.
[2] P. Satir, D. Mitchell, G. Jékely, *Curr. Top. Dev. Biol.* **2008**, *85*, 63 – 82.
[3] E. M. Purcell, *Am. J. Phys.* **1977**, *45*, 3 – 11.
[4] K. Segawa, O. Kikuchi, T. Arai, K. Tokumaru, *J. Mol. Struct. (THEOCHEM)* **1995**, *343*, 133 – 140.
[5] J. Gálvez, A. Guirado, *J. Comput. Chem.* **2009**, *31*, 520 – 531.
[6] Y. Luo, M. Utecht, J. Dokic, S. Korchak, H.-M. Vieth, R. Haag, P. Saalfrank, *ChemPhysChem* **2011**, *12*, 2311 – 2321.
[7] V. Bonacic-Koutecky, M. Persico, *J. Am. Chem. Soc.* **1983**, *105*, 3388 – 3395.
[8] J.-M. Lehn, *Chem. Eur. J.* **2006**, *12*, 5910 – 5915.
[9] L. Greb, J.-M. Lehn, *J. Am. Chem. Soc.* **2014**, *136*, 13114 – 13117.
[10] R. Klajn, *Pure Appl. Chem.* **2010**, *82*, 2247 – 2279.
[11] B. Baisch, D. Raffa, U. Jung, O. M. Magnussen, C. Nicolas, J. Lacour, J. Kubitschke, R. Herges, *J. Am. Chem. Soc.* **2009**, *131*, 442 – 443.
[12] S. Ulrich, U. Jung, T. Strunskus, C. Schütt, A. Bloedorn, S. Lemke, E. Ludwig, L. Kipp, F. Faupel, O. M. Magnussen, R. Herges, *Phys. Chem. Chem. Phys.* **2015**, *17*, 17053 – 17062.
[13] S. Kuhn, B. Baisch, U. Jung, T. Johannsen, J. Kubitschke, R. Herges, O. M. Magnussen, *Phys. Chem. Chem. Phys.* **2010**, *12*, 4481 – 4487.
[14] T. Tellkamp, J. Shen, Y. Okamoto, R. Herges, *Eur. J. Org. Chem.* **2014**, *2014*, 5456 – 5461.
[15] H. Jacob, S. Ulrich, U. Jung, S. Lemke, T. Rusch, C. Schütt, F. Petersen, T. Strunskus, O. M. Magnussen, R. Herges, F. Tuczek, *Phys. Chem. Chem. Phys.* **2014**, *16*, 22643 – 22650.
[16] B. W. Laursen, F. C. Krebs, *Chem. Eur. J.* **2001**, *8*, 1773 – 1783.
[17] S. Takahashi, Y. Kuroyama, K. Sonogashira, N. Hagihara, *Synthesis* **1980**, *8*, 627 – 630.
[18] J. Kubitschke, C. Näther, R. Herges, *Eur. J. Org. Chem.* **2010**, *26*, 5041 – 5055.
[19] F. Bellamy, K. Ou, *Tetrahedron Lett.* **1984**, *25*, 839 – 842.
[20] J. Xie, C. T. Seto, *Bioorg. Med. Chem.* **2007**, *15*, 458 – 473.
[21] J. Harley-Mason, F. G. Mann, *J. Chem. Soc.* **1940**, 1379 – 1385.
[22] E. Fischer, Y. Frei, *J. Phys. Chem.* **1957**, *27*, 808 – 809.
[23] N. R. Krekiehn, M. Müller, U. Jung, S. Ulrich, R. Herges, O. M. Magnussen, *Langmuir* **2015**, *31*, 8362 – 8370.
[24] M. Müller, U. Jung, V. Gusak, S. Ulrich, M. Holz, R. Herges, C. Langhammer, O. M. Magnussen, *Langmuir* **2013**, *29*, 10693 – 10699.
[25] U. Jung, C. Schütt, O. Filinova, J. Kubitschke, R. Herges, O. Magnussen, *J. Phys. Chem. C* **2012**, *116*, 25943 – 25948.

Manuscript received: February 10, 2016
Accepted Article published: March 27, 2016
Final Article published: April 26, 2016

CHEMPHYSCHEM

Supporting Information

Imine-Functionalized Triazatriangulenium Platforms: Towards an Artificial Ciliated Epithelium

Melanie Hammerich,[a] Talina Rusch,[b] Nicolai R. Krekiehn,[b] Andreas Bloedorn,[b] Olaf M. Magnussen,[b] and Rainer Herges*[a]

cphc_201600147_sm_miscellaneous_information.pdf

I. Analytical equipment

NMR spectroscopy

NMR spectra were measured in deuterated solvents (Deutero). To reference the NMR spectra the following solvent signals were used:

solvent	degree of deuteration	^{1}H signal	^{13}C signal
acetone-d_6	99.8 %	2.05 (quintet)	29.84 (septet)
chloroform-d_1	99.8 %	7.26 (s)	77.16 (triplet)

NMR measurements were performed with a Bruker DRX 500 (^{1}H NMR: 500 MHz, ^{13}C NMR: 125 MHz) and a Bruker AV 600 (^{1}H NMR: 600 MHz, ^{13}C NMR: 150 MHz).

Melting point

Melting points were measured with a Melting Point B-540 (Büchi) in an oneside opened capillary tubule.

Mass spectrometry

The high resolution (HR-EI) mass spectra were measured with an AccuTOF GCv 4G (Joel) with ionization energy of 70 eV. CI spectra were measured with a MAT 8200 (Finnigan) with isobutane gas. MALDI TOF spectra were measured with a Biflex III (Bruker-Daltonics, acceleration voltage: 19 kV, wavelength ionisation laser: 337 nm, matrix: 4-chloro-α-cyanocynnamic acid Cl-CCA)

IR spectroscopy

Infrared spectra were measured on a Perkin-Elmer 1600 Series FT-IR spectrometer with a A531-G Golden-Gate-Diamond-ATR-unit. Signals were abbreviated with w, m, s for weak, medium and strong signal intensity.

UV/Vis spectroscopy

UV-Vis spectra were measured with a Cary 5000 (Agilent Technologies) with CryoVac Kryostat (nitrogen cooling).

Chromatography stationary phases

For column chromatography purifications silica gel (Merck, particle size 0.040-0.063 mm) was used. Rf values were determined by thin layer chromatography on Polygeram® SilG/UV254 (Macherey Nagel, 0.2 mm particle size).

CHNS analyzer

The amount of the elements nitrogen, carbon, hydrogen and sulphur were determined with a CHNS-O-element analysator Euro EA 3000 Series (Euro Vector).

Light source

The irradiation of the samples was performed with LEDs with a wavelength of 365 nm.

II. Experimental procedures

II.1 Synthesis of 4-trimethylsilylethynylaniline (3)

12.4 g (56.6 mmol) 4-iodoaniline was solved under nitrogen atmosphere in 200 mL triethylamine and 820 mg (1.17 mmol) (bis(triphenylphosphine)-palladium(II)-chloride and 228 mg (1.17 mmol) copper(I)iodide were added to this solution. To this suspension 8.9 mL (62.3 mmol) trimethylsilylacetylene was dropped and stirred at 40 °C for 15 h. The solid was removed and the solvent evaporated. The crude product was purified by column chromatography (dichloromethane/pentane, 1:1). The crude product was recrystallized from cyclohexane to obtain colorless crystals (9.63 g, 50.9 mmol, 90 %).

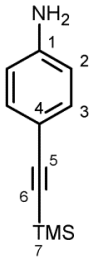

m.p. = 86.8 °C

^{1}H-NMR (500.1 MHz, $CDCl_3$, 300 K, $CHCl_3$) δ = 7.27 (d, ^{3}J = 8.6 Hz, 2 H, *H-3*), 6.57 (d, ^{3}J = 8.6 Hz, 2 H, *H-2*), 3.78 (s, br, 2H, NH_2), 0.22 (s, 9 H, *H-7*) ppm.

^{13}C-NMR (125.1 MHz, $CDCl_3$, 300 K, $CHCl_3$) δ = 146.53 (*C-1*), 133.24 (*C-3*), 114.44 (*C-2*), 112.47 (*C-4*), 105.85 (*C-6*), 91.26 (*C-5*), 0.00 (*C-7*) ppm.

MS (EI, 70 eV): m/z (%) =189.10 $[M]^+$, 174.08 $[M\text{-}NH_2]^+$.

MS (HR) (EI, 70 eV): m/z = calc.: 189.09738, found: 189.09778.

IR: $\tilde{\nu}$ = 3462.98 (m), 3369.99 (m), 3209.18 (w), 2958.79 (w), 2146.47 (m), 1620.22 (m), 1600.41 (m), 1509.24 (s), 1249.20 (m), 1250.83 (m), 1177.13 (w), 1129.92 (w), 829.38 (s), 755.76 (s), 536.89 (m) cm^{-1}.

II.2 Synthesis of 4-trimethylsilylethynyl-*N*-(benzylidene)-aniline (5a)

Under nitrogen atmosphere 160 mg (1.51 mmol) benzaldehyde and 285 mg (1.51 mmol) 4-trimethylsilylethynylaniline were solved in THF and molecular sieve was added. The solution was refluxed for 3 h. The molecular sieve was removed and the solvent was evaporated to obtain a yellow oil that crystallized slowly (416 mg, 1.49 mmol, quant.)

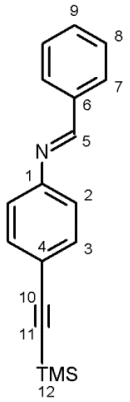

m. p. = 36.4 °C

^{1}H-NMR (500.1 MHz, $CDCl_3$, 300 K, $CHCl_3$) δ = 8.45 (s, 1 H, *H-5*), 7.88 - 7.90 (m, 2 H, *H-7*), 7.47 – 7.50 (m, 5 H, *H-3*, *H-8, H-9*), 7.14 (d, 3J = 8.7 Hz, 2 H, *H-2*), 0.26 (s, 9 H, *H-12*) ppm.

^{13}C-NMR (125.1 MHz, $CDCl_3$, 300 K, $CHCl_3$) δ = 160.70 (C-5),136.00 (C-1), 133.37 (C-6) 132.96 (C-3), 131.61 (C-9), 128.91 (C-8), 128.81 (C-7), 120.86 (C-2), 120.63 (C-4), 105.03 (C-10), 94.40 (C-11), 0.14 (C-12) ppm.

MS (CI, Isobutan): m/z (%) = 334 (19) $[M+iBu]^+$, 278 (100) $[M+H]^+$, 190 (96) $[C_{11}H_{16}NSi]^+$.

IR: ṽ = 2956.22 (m), 2152 (m), 1628.32 (m), 1593.61 (m), 1577.93 (m), 1493.64 (m), 1451.00 (m), 1247.57 (m), 1166.90 (m), 1104.69(w), 859.84 (s), 834.95 (s), 753.30 (s), 691.47 (s), 557.47 (m) cm^{-1}.

EA: $C_{18}H_{19}NSi$ (277.43) calcd C 77.93, H 6.90, N 5.05, found C 77.72, H 6.98, N 5.05.

II.3 Synthesis of 4-trimethylsilylethynyl-*N*-(4'-tert-buylbenzylidene)-aniline (5c)

Under nitrogen atmosphere 92.9 µL (556 µmol) 4-*tert*-butylbenzaldehyde and 105 mg (556 µmol) 4-trimethylsilylethynylaniline were dissolved in dichloromethane and refluxed with molecular sieve for 18 h. The molecular sieve was removed and solvent evaporated and the solid recrystallized form ethanol to obtain 164 mg (495 µmol, 89 %) light yellow solid.

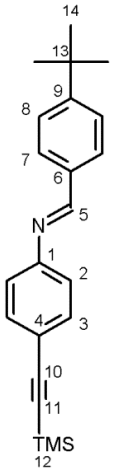

m. p. = 129.5 °C

^{1}H-NMR (500.1 MHz, $CDCl_3$, 300 K, $CHCl_3$) δ = 8.40 (s, 1 H, *H-5*), 7.82 (d, ^{3}J = 8.3 Hz, 2 H, *H-7*), 7.49 (d, ^{3}J = 8.3 Hz, 2 H, *H-8*), 7.48 (d, ^{3}J = 8.6 Hz, 2 H, *H-3*), 7.12 (d, ^{3}J = 8.6 Hz, 2 H, *H-2*), 1.36 (s, 9 H, H-14), 0.26 (s, 9 H, H-12) ppm.

^{13}C-NMR (125.1 MHz, $CDCl_3$, 300 K, $CHCl_3$) δ = 160.58 (C-5), 155.27 (C-9), 152.29 (C-1), 133.39 (C-6), 132.92 (C-3), 128.74 (C-7), 125.76 (C-8), 120.84 (C-2), 120.37 (C-4), 105.09 (C-10), 94.23 (C-11), 35.05 (C-13), 31.17 (C-14), 0.12 (C-12) ppm.

MS (HR) (EI, 70 eV): m/z = calc.: 333.19133, found: 333.19128.

MS (EI, 70 eV): m/z (%) = 333.19 (100) $[M]^+$, 318.16 $[M\text{-}CH_3]^+$.

IR: ṽ = 2957.01 (m), 2152.97 (m), 1622.90 (m), 1592.59 (m), 1497.57 (m), 1248.04 (m), 86185 (s), 832.33 (s), 751.75 (m), 565.24 (m) cm^{-1}.

EA: $C_{22}H_{27}NSi$ (333.54) calcd C 79.22, H 8.16, N 4.20, found C 79.16, H 8.13, N 4.48.

II.4 Synthesis of 4-trimethylsilylethynyl-*N*-(3',5'-dimethylbenzylidene)-aniline (5b)

Under nitrogen atmosphere 105 mg (556 µmol) 4-trimethylsilylethynylaniline and 92.9 µL (556 µmol) 3,5-dimethylbenzaldehyde were dissolved in dichloromethane and refluxed with molecular sieve for 18 h. The molecular sieve was removed and solvent evaporated to obtain 167 mg (550 µmol) light yellow oil.

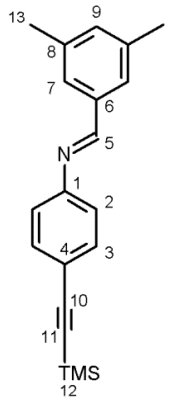

^{1}H-NMR (500.1 MHz, $CDCl_3$, 300 K, $CHCl_3$) δ = 8.36 (s, 1 H, *H-5*), 7.51 (s, 2 H, *H-7*), 7.49 (d, ^{3}J = 8.5 Hz, 2 H, *H-3*), 7.13 (s, 1 H, *H-9*), 7.12 (d, ^{3}J = 8.5 Hz, 2 H, *H-2*), 2.38 (s, 6 H, *H-13*), 0.26 (s, 9 H, *H-12*) ppm.
^{13}C-NMR (125.1 MHz, $CDCl_3$, 300 K, $CHCl_3$) δ = 161.23 (*C-5*), 152.16 (*C-1*) 138.46 (*C-8*), 135.57 (*C-6*), 133.45 (*C-9*), 132.95 (*C-3*), 126.74 (*C-7*),120.84 (*C-2*), 120.37 (*C-4*), 104.73 (*C-10*), 94.35 (*C-11*), 21.15 (*C-13*), 0.00 (*C-12*) ppm.
MS (HR) (EI, 70 eV): m/z = calc.: 305.15998, found: 305.15907.
MS (ESI): m/z = 306.16 $[M+H]^+$.

II.5 Synthesis of 4-ethynyl-*N*-(4-Fluorbenzylidene)aniline (5d)

Under nitrogen atmosphere 115.8 µL (1.05 mmol) 4-fluorobenzaldehyde and 200 mg (1.05 mmol) 4-trimethylsilylethynylaniline was dissolved in 10 mL dichloromethane with molecular sieve (3 Å) and heated under reflux for 18 h. The molecular sieve was removed and the solvent evaporated. The crude product was recrystallized from ethanol to obtain 292 mg (987 µmol, 94 %) of colorless crystals.

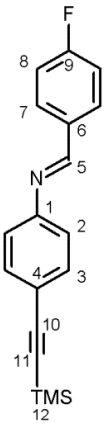

m.p. = 96.0 °C

^{1}H-NMR (500.1 MHz, $CDCl_3$, 300 K, $CHCl_3$) δ = 8.40 (s, 1 H, H-5), 7.90 (dd, ^{3}J = 8.6 Hz, ^{3}J = 5.5 Hz, 2 H, *H-9*), 7.50 (d, ^{3}J = 8.7 Hz, 2 H, *H-3*), 7.16 (t, ^{3}J = 8.6 Hz, 2 H, *H-8*), 7.12 (d, ^{3}J = 8.7 Hz, 2 H, *H-2*), 0.26 (s, 9 H, *H-12*) ppm.

^{13}C-NMR (125.1 MHz, $CDCl_3$, 300 K, $CHCl_3$) δ = 164.86 (*C-9*, ^{1}J = 251 Hz), 159.11 (*C-5*), 151.76 (*C-1*), 133.01 (*C-3*), 132.39 (*C-6*, ^{4}J = 3.3 Hz), 130.91 (*C-9*, ^{3}J = 8.8 Hz), 120.85 (*C-2*), 120.74 (*C-4*), 116.02 (*C-8*, ^{2}J= 22.0 Hz), 104.98 (*C-10*), 94.50 (*C-11*), 0.01 (*C-12*) ppm.

^{19}F-NMR (470.6 MHz, $CDCl_3$, 300 K, TMS) δ = -107.59 ppm.

MS (ESI): m/z = 296.12 $[M+H]^+$

IR: ṽ = 2962.20 (w), 2156.94 (m), 1626.74 (m), 1600.05 (m), 1579.75 (m), 1505.97 (m), 1411.98 (w), 1246.09 (m), 1215.71 (m), 1151.78 (m), 1010.28 (w), 832.00 (s), 758.89 (s), 641.91 (w), 553.07 (m) cm^{-1}.

EA: $C_{18}H_{18}NSiF$(295.43)) calcd C 73.18, H 6.14, N 4.74, found C 73.33, H 6.43, N 4.74

II.6 Synthesis of 4-trimethylsilylethynyl-*N*-(4'-*NN*-dimethylbenzylidene)-aniline (5e)

Under nitrogen atmosphere 105 mg (556 µmol) 4-trimethylsilylethynylaniline and 92.9 µL (556 µmol) 4-dimethylaminobenzaldehyde were dissolved in ethanol and refluxed for 1 h. The solvent was removed to obtain a yellow solid (178 mg, 556 µmol, quant.).

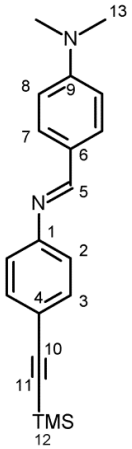

m.p. = 139 °C

^{1}H-NMR (500.1 MHz, $CDCl_3$, 300 K, $CHCl_3$) δ = 8.29 (s, 1 H, *H-5*), 7.76 (d, ^{3}J = 8.9 Hz, 2 H, *H-7*), 7.47 (d, ^{3}J = 8.6 Hz, 2 H, *H-3*), 7.11 (d, ^{3}J = 8.6 Hz, 2 H, *H-2*), 6.73 (d, ^{3}J = 8.9 Hz, 2 H, *H-8*), 3.06 (s. 6 H, *H-13*), 0.26 (s, 9 H, *H-12*) ppm.

^{13}C-NMR (125.1 MHz, $CDCl_3$, 300 K, $CHCl_3$) δ = 160.43 (C-5), 152.96 (C-9), 152.71 (C-1), 132.91 (C-3), 130.68 (C-7), 124.19 (C-6), 120.92 (C-2), 119.51 (C-4), 111.58 (C-8), 105.3 (C-10), 93.86 (C-11), 40.17 (C-13), 0.05 (C-12) ppm.

MS (EI, 70 eV): m/z (%) = = 320.19 (100)$[M]^+$, 305.16 (66) $[M\text{-}CH_3]^+$.

IR: ṽ = 2955.37 (m), 2149.88 (m), 1589.90 (m), 1556.69 (m), 1361.64 (m), 1247.65 (m), 1163.01 (m), 861.72 (m), 835.40 (s), 816.97 (s), 556.82 (m) cm^{-1}.

EA: $C_{20}H_{24}N_2Si$ (320.50) calcd C 74.95, H 7.55, N 8.74, found C 74.44, H 7.60 , N 7.73.

II.7 Synthesis von 4-iodo-4'-nitrobiphenyl

A mixture of 15.0 g (97.4 mmol) biphenyl and 7.50 g (29.6 mmol) iodine was heated up to 100 °C, forming a violet solution. To this solution was added at 100 °C 38 mL of 65 % nitric acid in a period of one hour. After addition the solution was heated for another hour. Afterward the cooled solution was poured onto water. The precipitate was filtrated and washed with water. The obtained solid was heated with ethanol and was filtrated three times. The crude product was recrystallized from toluene to obtain a yellow solid (9.79 g, 30.1 mmol, 31 %, Lit.: 30 %)

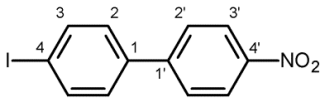

m. p. = 222.3 °C

^{1}H-NMR (500.1 MHz, $CDCl_3$, 300 K, $CHCl_3$) δ = 8.30 (d, ^{3}J = 8.7 Hz, 2 H, H-3'), 7.85 (d, ^{3}J = 8.5 Hz, 2 H, *H-3*),7.71 (d, ^{3}J = 8.7 Hz, 2 H, *H-2'*), 7.36 (d, ^{3}J = 8.5 Hz, 2 H, *H-2*) ppm.

^{13}C-NMR (125.1 MHz, $CDCl_3$, 300 K, $CHCl_3$) δ = 147.33 (C-4'), 146.45 (C-1'), 138.32 (C-3), 138.24 (C-1), 129.06 (C-2'), 127.60 (C-2'), 124.24 (C-3'), 95.16 (C-4) ppm.

MS (EI, 70 eV): m/z (%) =324.97 $[M]^+$, 294.99 $[M\text{-}NO]^+$, 152-07 $[M\text{-}NO_2I]^+$.

IR: ṽ = 2960.7 (w), 2156.3 (w), 1595.01 (m), 1580.46 (m), 1504.57 (s), 1471.59 (m), 1332.72 (m), 1246.34 (m), 1105.80 (m), 998.56 (m), 855.40 (m), 819.73 (s), 751.47 (m), 593.19 (m), 483.05 (m) cm^{-1}.

EA: $C_{12}H_8INO_2$ (325.10) calcd C 44.33, H 2.48, N 4.31, found C 44.62, H 2.45, N 4.48.

II.8 Synthesis of 4-amino-4'-iodobiphenyl

A suspension of 8.50 (26.1 mmol) 4-iodo-4'-nitrobiphenyl and 40.9 (182 mmol) tin(II)chloride dihydrate in 250 mL ethanol was heated for 16 h under reflux. The solution was poured onto ice water and sodium hydrocarbonate solution was added until pH = 9 was reached. After extraction with dichloromethane the organic layer was washed with brine, dried over magnesium sulfate and the solvent was evaporated. The crude product was recrystallized from toluene to obtain a colorless solid (5.60 g, 19.0 mmol, 73 %, Lit.: 70 %).

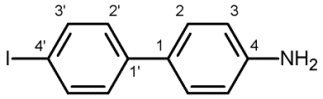

m.p. = 156 °C

^{1}H-NMR (500.1 MHz, $CDCl_3$, 300 K, TMS) δ = 7.70 (d, ^{3}J = 8.4 Hz, 2 H, *H-3'*),7.37 (d, ^{3}J = 8.5 Hz, 2 H, *H-2*), 7.27 (d, ^{3}J = 8.4 Hz, 2 H, *H-2'*), 6.74 (d, ^{3}J = 8.5 Hz, 2 H, *H-3*), 3.75 (s, 2 H, NH_2) ppm.

^{13}C-NMR (125.1 MHz, $CDCl_3$, 300 K, $CHCl_3$) δ = 146.24 (*C-4*), 140.67 (*C-1'*), 137.68 (*C-3'*), 130.23 (*C-1*), 128.25 (*C-2'*), 127.80 (*C-2*), 115.38 (*C-3*), 91.51 (C-4') ppm.

MS (EI, 70 eV): m/z (%) =295.00 $[M]^+$,167.08$[M-I]^+$.

IR: ṽ = 3406.85 (w), 3189.40 (w), 2361.45 (w), 1600.79 (m), 1475.38 (m), 1389.02 (m), 1269.36 (m), 993.55 (m), 808.12 (s), 489.69 (s) cm^{-1}.

EA: $C_{12}H_{10}IN$ (295.12) calcd C 48.84, H 3.42, N 4.75, found C 48.93, H 3.34, N 4.88.

II.9 Synthesis of 4-amino-4'(trimethylsilylethynyl)biphenyl

A suspension of 2.00 g (6.78 mmol) 4-amino-4'-iodobiphenyl, 237 mg (339 µmol) (bis(triphenylphosphine)palladium(II)chloride, 1.05 mL (7.28 mmol) trimethylsilyl-acetylene and 64.5 mg (339 µmol) copper(I)iodide in 60 mL triethylamine and 20 mL THF was heated to 40 °C for 16 h. The solid was removed and the solvent evaporated. The crude product was purified by column chromatography (dichloromethane / pentane 1:1, R_f = 0.25). The solid was recrystallized from cyclohexane to obtain a beige-colored solid (1.30 g, 4.91 mmol, 72 %, Lit.: 70 %).

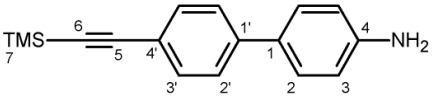

m.p. = 114 °C

^{1}H-NMR (500.1 MHz, $CDCl_3$, 300 K, TMS) δ = 7.48 (m_c, 4 H, *H-2'*, *H-3'*), 7.42 (d, ^3J = 8.5 Hz, 2 H, *H-2*), 6.75 (d, ^3J = 8.5 Hz, 2 H, *H-3*), 3.89 (s, br, 2 H, NH_2), 0.26 (s, 9 H, *H-7*) ppm.

^{13}C-NMR (125.1 MHz, $CDCl_3$, 300 K, $CHCl_3$) δ = 145.92 (*C-4*), 141.07 (*C-1'*), 132.30 (*C-3'*), 130.66 (*C-1*), 127.89 (*C-2*), 125.93 (*C-2'*), 120.80 (*C-4'*), 115.46 (*C-3*), 105.28 (*C-5*), 94.27 (*C-6*), 0.00 (*C-7*) ppm.

MS (EI, 70 eV): m/z (%) = 265.13 $[M]^+$,250.10 $[M\text{-}CH_3]^+$.

IR: ṽ = 3383.10 (w), 2956.31 (w), 2149.62 (m), 1618.10 (m), 1493.85 (m), 1253.10 (m), 862.49 (m), 838.28 (m), 838.28 (s), 810.05 (s), 758.01 (m), 521.26 (s) cm^{-1}.

EA: $C_{17}H_{19}NSi$ (265.42) calcd C 76.93, H 7.22, N 5.28, found C 76.31, H 7.25, N 5.02.

II.10 Synthesis of 4-amino-*N*-(benzylidene)-4'(trimethylsilylethynyl)biphenyl (5f)

In 10 mL ethanol 200 mg (754 µmol) 4-amino-4'-trimethylsilylethynyl)biphenyl and 76.5 µL (754 µmol) benzaldehyde were heated for 1.5 h under reflux. While cooling the solution to room temperature the product precipitates as silvery crystals (182 mg, 516 µmol, 68 %).

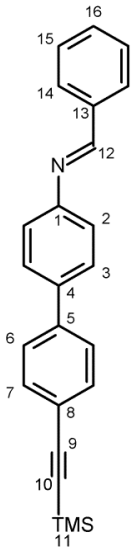

m.p.: 177.3 °C

^{1}H-NMR (500.1 MHz, $CDCl_3$, 300 K, C) δ = 8.67 (s, 1 H, *H-12*), 8.02-7.98 (m, 2 H, *H-14*), 7.76 (d, ^{3}J = 8.6 Hz, 2 H, *H-3*), 7.72 (d, ^{3}J = 8.6 Hz, 2 H, *H-2*), 7.56 (d, ^{3}J = 8.6 Hz, 2 H, *H-7*), 7.55-7.51 (m, 3 H, *H-15*, *H-16*), 7.38 (d, ^{3}J = 8.6 Hz, 2 H, *H-6*), 0.25 (s, 9 H, *H-11*) ppm.

^{13}C-NMR (125.1 MHz, $CDCl_3$, 300 K, $CHCl_3$) δ = 161.23 (*C-12*), 152.64 (*C-1*), 141.52 (*C-5*), 138.20 (*C-8*), 137.51 (*C-13*), 133.17 (*C-7*), 132.27 (*C-16*), 129.67 (*C-14/15*), 129.63 (*C-14/15*), 128.49 (*C-3*), 127.51 (*C-2*), 122.78 (*C-4*), 122.51 (*C-6*), 105.88 (*C-9*), 95.22 (*C-10*), 0.00 (*C-11*) ppm.

MS (EI, 70 eV): m/z (%) = .354.15 (100) $[M]^{+}$, 338.13 (100) $[M\text{-}CH_3]^{+\cdot}$

IR: ṽ = 2959.31 (w), 2160.92 (w), 1624.68 (w), 1573.95 (w), 1485.57 (w), 1251.47 (m), 1202.90 (w), 827.62 (s), 755.69 (s), 715.57 (m), 688.97 (s), 537.93 (s), 409.09 (m) cm^{-1}.

EA: $C_{24}H_{23}NSi$ (353.53) calcd C 81.54, H 6.56, N 3.96, found C 81.61, H 6.68, N 3.95.

II.11 Synthesis of (E)-12c-(4-ethynyl-*N*-(benzylidene)-aniline)-4,8,12-tri-n-octyl-4,8,12-triazatriangulene (7a)

A suspension of 146 mg (529 µmol) 4-trimethylsilylethynyl-*N*-(benzylidene)-aniline, 410 mg (582 µmol) octyl-TATA and 26 mg potassium hydroxide was heated under reflux in 20 mL THF under nitrogen atmosphere for 15 h. The solution was poured onto water and was extracted with diethyl ether. The solution was dried over magnesium sulfate and the solvent was evaporated. The crude product was purified with column chromatography (Florisil, ethyl acetate). The obtained yellow oil was dissolved in few mL toluene and overlaid with pentane and stored at -18 °C. The product precipitates as yellow solid (148 mg, 180 µmol, 31%)

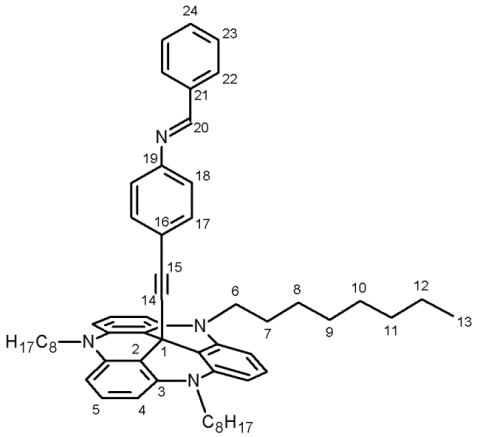

m.p. = 92.5 °C

^{1}H-NMR (500.1 MHz, acetone-d_6, 300 K, acetone) δ = 8.50 (s, 1H, *H-20*), 7.91 (dd, ^{3}J =7. Hz, 2 H, *H-22*), 7.46-7.52 (m, 3H, *H-23*, *H-24*), 7.21 (d, ^{3}J = 8.3 Hz, 3 H, *H-5*), 7.09 (d, ^{3}J = 9.0 Hz, 2 H, H-17), 7.07 (d, ^{3}J = 9.0 Hz, 2 H, H-18), 6.67 (d, ^{3}J = 8.3 Hz, 6 H, *H-4*), 4.02 (t, ^{3}J = 7.5 Hz, 6 H, *H-6*), 1.84 (ps.quint., 6 H, *H-7*), 1.52 (ps.quintt, 6 H, *H-8*), 1.38 (ps.quint., 6 H, *H-9*), 1.32-1.21 (m, 18 H, *H-10*, *H-11*, *H-12*), 0.86 (t, ^{3}J = 6.9 Hz, 9 H, *H-13*) ppm.

^{13}C-NMR (125.1 MHz, acetone-d_6, 300 K, acetone) δ = 161.21 (*C-20*), 152.15 (*C-19*), 141.45 (*C-3*), 137.33 (*C-21*), 133.00 (*C-17*), 132.32 (*C-24*), 129.64 (*C-22*), 129.60 (C-23), 129.34 (*C-5*), 122.0 (*C-16*), 121.77 (*C-18*), 111.28 (*C-2*), 106.10 (*C-4*), 93.50 (*C-14*), 84.15 (*C-15*), 46.72 (*C-6*), 32.61 (*C-11*), 30.11 (*C-9*), 30.10 (*C-10*), 28.84 (*C-1*), 27.51 (*C-8*), 26.81 (*C-7*), 23.32 (*C-12*), 14.40 (*C-13*) ppm.

MS (MALDI-TOF): m/z (%) = 823.80 $[M]^{+}$.

IR: ṽ = 2955.54 (m), 2918.94 (m), 2150.89 (m), 1580.41 (s), 1483.52 (m), 1362.64 (m), 1247.10 (m), 1163.79 (m), 838.26 (s) 753.09 (s), 691.18 (m), 723.37 (m) cm^{-1}.

EA: $C_{58}H_{70}N_4$ (823.20) calcd C 84.62, H 8.57, N 6.81, found C 84.67, H 8.70, N 6.75.

II.12 Synthesis of (E)-12c-(4-ethynyl-*N*-(4-tertbutylbenzylidene)-aniline)-4,8,12-tri-n-octyl-4,8,12-triazatriangulene (7c)

A suspension of 100 mg (300 µmol) 4-ethynyl-N-(4-tertbutylbenzylidene)aniline, 232 mg (330 µmol) n-octyl-TATA and 168 mg potassium hydroxide was heated in 50 mL THF for 15 h under reflux. The solution was poured onto water and extracted with diethyl ether, dried over magnesium sulfate and the solvent was evaporated. The crude product was filtrated over florisil with diethyl ether and recrystallized from ethanol to obtain 68.5 mg (77.9 µmol, 26 %) of a yellow solid.

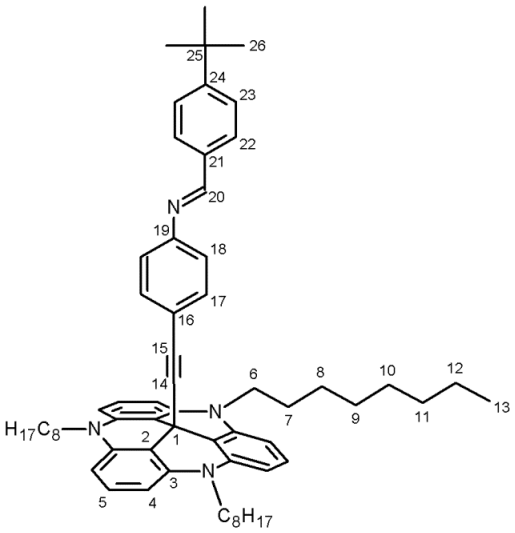

m.p.: 128.4 °C

^{1}H-NMR (500.1 MHz, acetone-d_6, 300 K, acetone) δ = 8.46 (s, 1 H, *H-20*), 7.83 (d, ^3J = 8.4 Hz, 2 H, *H-22*), 7.53 (d, ^3J = 8.4 Hz, 2 H, *H-23*), 7.21 (t, ^3J = 8.3 Hz, 3 H, *H-5*), 7.09 (d, ^3J = 8.8 Hz, 2 H, *H-17*), 7.06 (d, ^3J = 8.8 Hz, 2 H, *H-18*), 6.67 (d, ^3J = 8.3 Hz, 6 H, H-4), 4.02 (t, ^3J = 7.6 Hz, 6 H, *H-6*), 1.85 (ps.quint., 6 H, *H-7*), 1.52 (ps.quintt, 6 H, *H-8*), 1.39 (ps.quint., 6 H, *H-9*), 1.34 (s, 9 H, *H-26*), 1.25-1.32 (m, 18 H, *H-10*, *H-11*, *H-12*), 0.86 (t, ^3J = 6.8 Hz, 9 H, *H-13*) ppm.

^{13}C-NMR (125.1 MHz, acetone-d_6, 300 K, acetone) δ = 160.97 (*C-20*), 155.77 (*C-24*), 152.00 (*C-19*), 141.45 (*C-3*), 134.78 (*C-21*), 132.97 (*C-17*), 129.53 (*C-22*), 129.32 (*C-5*), 126.53 (*C-23*), 121.87 (*C-16*), 121.72 (*C-18*), 111.29 (*C-2*), 106.10 (*C-4*), 94.95 (*C-14*), 84.29 (*C-15*), 46.72 (*C-6*), 35.55 (*C-25*), 32.62 (*C-11*), 31.42 (*C-26*), 30.18 (*C-9*), 30.08 (*C-10*), 28.98 (*C-1*), 27.51 (*C-8*), 26.81 (*C-7*), 23.32 (*C-12*), 14.39 (*C-13*) ppm.

MS (MALDI-TOF, Cl-CCA): m/z (%) = 879.13 $[M]^+$.

IR: ṽ = 2923.58 (m), 1611.45 (m), 1577.96 (m), 1457.32 (m), 1395 (m), 1246.84 (w), 1165.16 (m), 791.23 (w), 749.58 (s), 680.14 (w), 565.32 (w), 498.91 (m), 414.55 (s) cm^{-1}.

EA: $C_{62}H_{78}N_4$ (879.31) calcd C 84.31, H 8.94, N 6.37, found C 84.43, H 8.91, N 6.24.

II.13 Synthesis of (E)-12c-(4-ethynyl-*N*-(3,5-dimethylbenzylidene)-aniline)-4,8,12-tri-n-octyl-4,8,12-triazatriangulene (7b)

A suspension of 100 mg (300 µmol) 4-ethynyl-N-(4-tertbutylbenzylidene)aniline, 232 mg (330 µmol) n-octyl-TATA and 168 mg potassium hydroxide was heated in 50 mL THF for 15 h under reflux. The solution was poured onto water and extracted with diethyl ether, dried over magnesium sulfate and the solvent was evaporated. The crude product was filtrated over florisil with diethyl ether and recrystallized from ethanol to obtain 68.5 mg (77.9 µmol, 26 %) of a yellow solid.

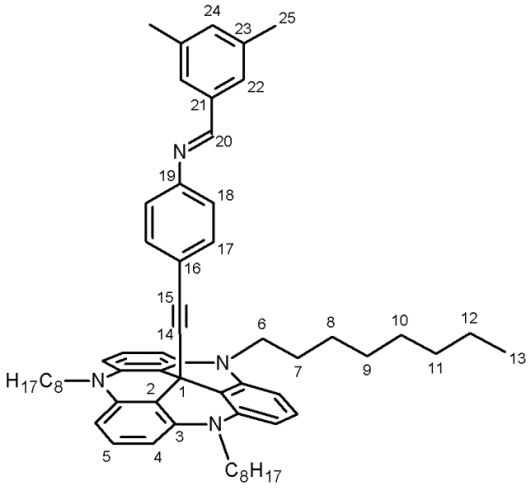

^{1}H-NMR (500.1 MHz, acetone-d_6, 300 K, acetone) δ = 8.40 (s, 1 H, *H-20*), 7.51 (s, 2 H, *H-22*), 7.21 (t, ^3J =8.3 Hz, 3 H, *H-5*), 7.14 (s, 1 H, *H-24*), 7.09 (d, ^3J = 8.8 Hz, 2 H, *H-17*), 7.05 (s, ^3J = 8.8 Hz, *H-18*), 6.67 (d, ^3J = 8.3 Hz, 6 H, *H-4*), 4.02 (t, ^3J = 7.7 Hz, 6 H, *H-6*), 2.33 (s, 6 H, *H-25*), 1.85 (qui., ^3J = 7.5 Hz, 6 H, *H-7*), 1.52 (qui., ^3J = 7.5 Hz, 6 H, *H-8*), 1.39 (qui., ^3J = 7.5 Hz, 6 H, *H-9*), 1.25-1.32 (m, 18 H, *H-10*, *H-11*, *H-12*), 0.86 (t, ^3J = 6.8 Hz, 9 H, *H-13*) ppm.

^{13}C-NMR (125.1 MHz, acetone-d_6, 300 K, acetone) δ = 161.45 (*C-20*), 152.35 (*C-19*), 141.45 (*C-3*), 139.09 (*C-23*), 137.35 (*C-21*), 133.91 (*C-24*), 132.98 (*C-17*), 129.32 (*C-5*), 127.47 (*C-22*), 121.92 (*C-16*), 121.70 (*C-18*), 111.29 (*C-2*), 106.10 (*C-4*), 95.00 (*C-14*), 84.28 (*C-15*), 46.72 (*C-6*), 32.61 (*C-11),* 31.42 (*C-26*), 30.23 (*C-9*), 30.78 (*C-10*), 28.99 (C-1), 27.51 (*C-8*), 26.81 (*C-7*), 23.31 (*C-12*), 21.12 (*C-25*), 14.37 (*C-13*) ppm.

MS (MALDI-TOF, Cl-CCA): m/z (%) = 851.09 $[M]^+$.

II.14 Synthesis of (E)-12c-(4-ethynyl-*N*-(4-fluorobenzylidene)-aniline)-4,8,12-tri-n-octyl-4,8,12-triazatriangulene (7d)

A suspension of 100 mg (339 µmol) 4-trimethylsilylethynyl-*N*-(4-fluorobenzylidene)-aniline, 263 mg (372 µmol)n-octyl-TATA and 151 mg (2.71 mmol) potassium hydroxide in 50 mL THF was heated for 15 h under reflux. The solution was poured onto water and extracted with water, dried over magnesium sulfate and the solvent was evaporated. The crude product was filtrated with diethyl ether over florisil. The obtained oil was dissolved in diethyl ether and precipitated with pentane as colorless solid (14 mg, 17 µmol, 5 %).

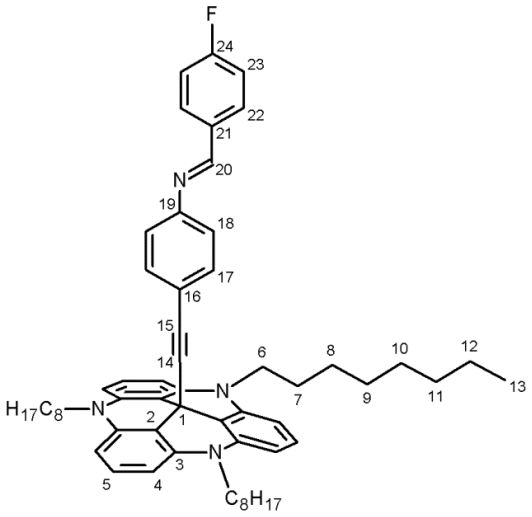

m.p. = 110 °C

^{1}H-NMR (500.1 MHz, acetone-d_6, 300 K, acetone) δ = 8.50 (s, 1 H, *H-20*), 7.96 – 7.98 (m, 2 H, *H-22*), 7.25 (t, ^3J = 8.8 Hz, 2 H, *H-23*), 7.20 (t, ^3J = 8.3 Hz, 3 H, *H-5*), 7.09 (d, ^3J = 9.0 Hz, 2 H, *H-18*), 7.07 (d, ^3J = 9.0 Hz, 2 H, *H-17*), 6.67 (d, ^3J = 8.3 Hz, 6 H, *H-4*), 4.01 (t, ^3J = 7.7 Hz, 6 H, *H-6*), 1.83 (qui., ^3J = 7.5 Hz, 6 H, *H-7*), 1.51 (qui., ^3J = 7.5 Hz, 6 H, *H-8*), 1.38 (qui., ^3J = 7.5 Hz, 6 H, *H-9*), 1.25-1.32 (m, 18 H, *H-10*, *H-11*, *H-12*), 0.86 (t, ^3J = 6.8 Hz, 9 H, *H-13*) ppm.

^{13}C-NMR (125.1 MHz, acetone-d_6, 300 K, acetone) δ = 165.8 (C-24), 159.64 (C-20), 141.38 (C-3), 133.87 (C-21), 132.97 (C-18), 131.87 (C-22), 129.26 (C-5), 121.67 (C-17), 116.50 (C-23, ^2J= 21.6 Hz), 111.17 (C-2), 106.00 (C-4), 84.1 (C-15), 46.72 (*C-6*), 35.40 (*C-25*), 32.61 (*C-11),* 31.42 (*C-26*), 30.23 (*C-9*), 30.78 (*C-10*), 28.99 (C-1), 27.51 (*C-8*), 26.81 (*C-7*), 23.31 (*C-12*), 21.12 (C-25), 14.37 (*C-13*) ppm.

C-14 can't be assigend due to low signal intensity.

^{19}F-NMR (470.6 MHz, $CDCl_3$, 300 K, TMS) δ = -110.01 ppm.

MS (MALDI-TOF, Cl-CCA): m/z (%) = 841.09 $[M]^+$.

IR: ṽ = 3379.00 (w), 2954.38 (m), 2922.33 (m), 2851.29 (m), 1612.55 (s), 1578.62 (s), 1482.24 (s), 1457.44 (s), 1394.20 (s), 1266.86 (s), 1245.10 8s), 1165.52 (s), 912.75 (w), 824.47 (m), 750.64 (s), 524.46 (m) cm^{-1}.

II.15 Synthesis of (E)-12c-(4-ethynyl-*N*-(4-*N,N*-dimethylaminobenzylidene)-aniline)-4,8,12-tri-n-octyl-4,8,12-triazatriangulene (7e)

A suspension of 200 mg (624 µmol) 4-trimethylsilylethynyl-*N*-(4-*N'N'*-dimethylaminobenzylidene)aniline, 484 mg (686 µmol) *n*-octyl-TATA and 244 mg (4.36 mmol) potassium hydroxide in 50 mL THF was heated for 15 h under reflux. The solution was poured onto water and extracted with water, dried over magnesium sulfate and the solvent was evaporated. The crude product was filtrated with diethyl ether over florisil. The obtained oil was dissolved in diethyl ether and precipitated with pentane as pale yellow solid (248 mg, 287 µmol, 46 %).

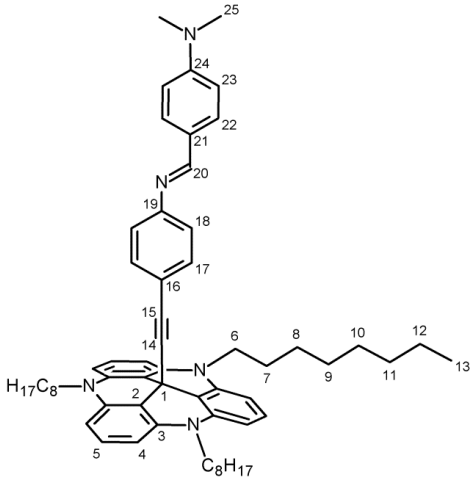

m.p.: 136.4 °C

^{1}H-NMR (500.1 MHz, acetone-d_6, 300 K, acetone) δ = 8.30 (s, 1 H, *H-20*), 7.73 (d, ^3J = 9.0Hz, 2 H, *H-22*), 7.22 (t, ^3J = 8.3 Hz, 3 H, *H-5*), 7.07 (d, ^3J = 8.7 Hz, 2 H, *H-17*), 7.00 (d, ^3J = 8.7 Hz, 2 H, *H-18*), 6.78 (d, ^3J = 9.0 Hz, 2 H, *H-23*), 6.68 (d, ^3J = 8.3 Hz, 6 H, *H-4*), 4.03 (t, ^3J = 7.6 Hz, 6 H, *H-6*), 3.05 (s, 6 H, *H-25*), 1.85 (ps.quint., 6 H, *H-7*), 1.53 (ps.quint., 6 H, *H-8*), 1.40 (ps.quint., 6 H, *H-9*), 1.33-1.23 (m, 18 H, *H-10*, *H-11*, *H-12*), 0.88 (t, ^3J = 6.9 Hz, 9 H, *H-13*) ppm.

^{13}C-NMR (125.1 MHz, acetone-d_6, 300 K, acetone) δ = 160.55 (*C-20*), 153.74 (*C-24*), 153.21 (*C-19*), 141.44 (*C-3*), 132.90 (*C-17*), 131.26 (*C-22*), 129.28 (*C-5*), 125.34 (*C-21*), 121.62 (*C-18*), 120.87 (*C-16*), 112.34 (*C-23*), 111.37 (*C-2*), 106.08 (*C-4*), 94.59 (*C-14*), 84.50 (*C-15*), 46.73 (*C-6*), 40.16 (*C-25*), 32.62 (*C-11*), 30.19 (*C-9*), 30.08 (*C-10*), 28.94 (*C-1*), 27.52 (*C-7*), 26.82 (*C-7*), 23.33 (*C-12*), 14.40 (*C-13*) ppm.

MS (MALDI-TOF, Cl-CCA): m/z (%) = 866.88 $[M]^+$.

IR: ṽ = 2922.2 (m), 2852.21 (m), 2250.9 (w), 1606.85 (s), 1579.0 (s), 1525.9 (m), 1482.3 (s), 1456.1 (m), 1391.2 (m), 1362.2 (m), 1245.7 (m), 1162.2 (s), 833.1 (m), 811.6 (m), 752.1 (s), 722.4 (m), 690.4 (m), 589.2 (w), 408.4 (s) cm^{-1}.

EA: $C_{60}H_{75}N_5$ (866.27) calcd C 83.19, H 8.73, N 8.08, found C 83.73, H 8.91, N 8.21.

II.16 Synthesis of (E)-12c-(4-amino-*N*-(benzylidene)-4'(trimethylsilylethynyl)-biphenyl)-4,8,12-tri-*n*-octyl-4,8,12-triazatriangulene (7f)

A suspension of 100 mg (282 µmol) 4-trimethylsilylethinyl-*N*-(4-*N'N'*-dimethylaminobenzylidene)aniline, 705 mg (311 µmol) *n*-octyl-TATA and 126 mg (2.26 mmol) potassium hydroxide in 50 mL THF was heated for 15 h under reflux. The solution was poured onto water and extracted with water, dried over magnesium sulfate and the solvent was evaporated. The crude product was filtrated with diethyl ether over florisil. The obtained oil was dissolved in diethyl ether and precipitated with pentane as colorless solid (40 mg, 44.4 µmol, 16 %).

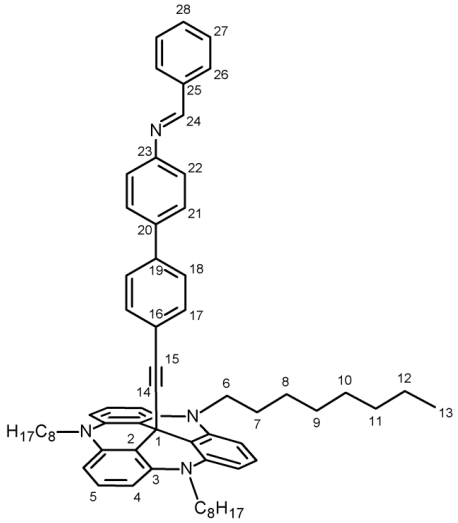

m.p. = 117 °C

^{1}H-NMR (500.1 MHz, acetone-d_6, 300 K, acetone) δ = 8.63 (s, 1 H, *H-24*), 7.97 (d, ^3J = 7.8 Hz, 2 H, *H-26*), 7.63 (d, ^3J = 8.5 Hz, 2 H, *H-21*), 7.55-7.49 (m, 5 H, *H-18*, *H-27*, *H-28*), 7.32 (d, ^3J = 8.5 Hz, 2 H, *H-22*), 7.22 (t, ^3J = 8.4 Hz, 3 H, *H-5*), 7.15 (d, ^3J = 8.4 Hz, 2 H, *H-17*), 6.68 (d, ^3J = 8.4 Hz, 6 H, *H-4*), 4.03 (t, ^3J = 7.6 Hz, 6 H, *H-6*), 1.85 (ps.quint., 6 H, *H-7*), 1.52 (ps.quint., 6 H, *H-8*), 1.38 (ps.quint., 6 H, *H-9*), 1.33-1.23 (m, 18 H, *H-10*, *H-11*, *H-12*), 0.85 (t, ^3J = 6.9 Hz, 9 H, *H-13*) ppm.

^{13}C-NMR (125.1 MHz, acetone-d_6, 300 K, acetone) δ = 160.09 (C-24), 152.39 (C-23), 141.46 (*C-3*), 140.46 (*C-19*), 138.44 (C-20), 137.51 (C-25), 132.61 (*C-17*), 132.24 (C-28), 129.63 (C-26) 129.36 (*C-27*), 129.28 (C-5),128.29 (*C-21*), 127.14 (C-18), 123.40 (C-16), 122.43 (*C-22*), 111.25 (*C-2*), 106.12 (*C-4*), 95.59 (C-14), 84.23 (C-15), 46.71 (*C-6*), 32.62 (*C-11*), 30.02 (*C-9*), 30.00 (*C-10*), 28.91 (*C-1*), 27.52 (*C-8*), 26.83 (*C-7*), 23.32 (*C-12*), 14.38 (*C-13*) ppm.

MS (MALDI-TOF, Cl-CCA): m/z (%) = 899.57 $[M]^+$.

IR: ṽ = 3379.69 (w), 2953.07 (m), 2922.19 (m), 2851.31 (m), 1613.43 (s), 1578.56 (s), 1482.24 (s), 1457.14 (m), 1393.71 (m), 1244.36 (m), 1166.34 (m), 987.45 (w), 913.08 (w), 824.29 (m), 750.50 (s), 524.95 (m) cm^{-1}.

EA: $C_{64}H_{74}N_4$ (899.29) calcd C 83.19, H 8.73, N 8.08, found C 83.73, H 8.91, N 8.21.

III. ^{1}H-NMR spectra of *tert*-butylimine-8-TATA (7c)

A solution of *tert*-butylimine-8-TATA (**7c**) in deuterated acetone was cooled to 230 K and a ^{1}H NMR spectrum was measured. The sample was irradiated with 365 nm for 20 min and several spectra were recorded until the *trans* spectrum was obtained again.

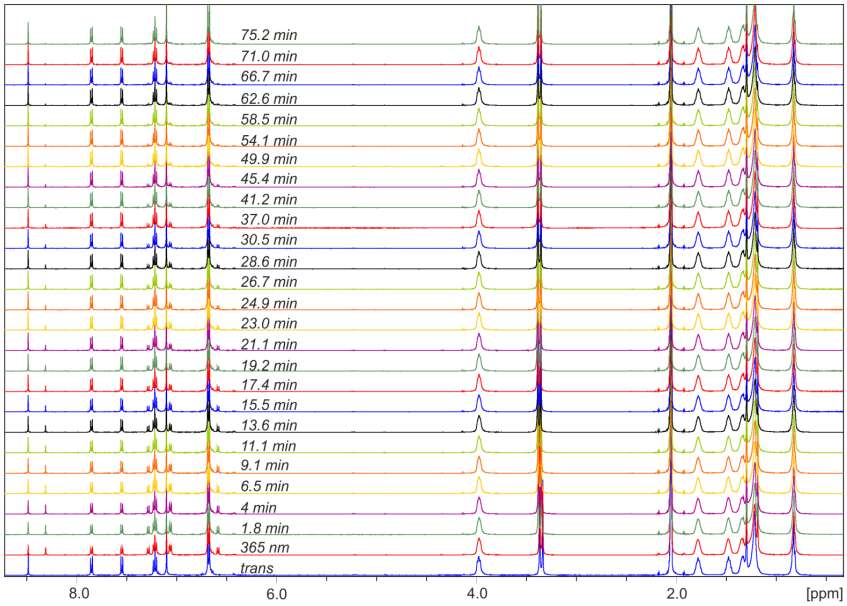

Fig.III.1: ^{1}H NMR spectra of 7c; *trans* spectrum (bottom) and spectra obtained after irradiation with 365 nm for 20 min.

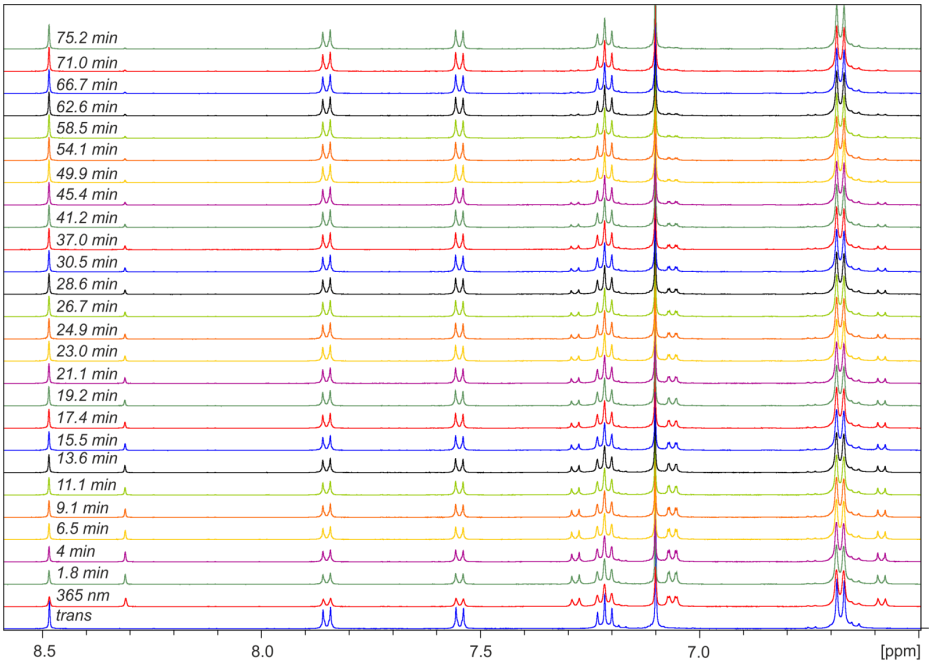

Fig.III.2: aromatic region of ^{1}H NMR spectra of **7c**

20

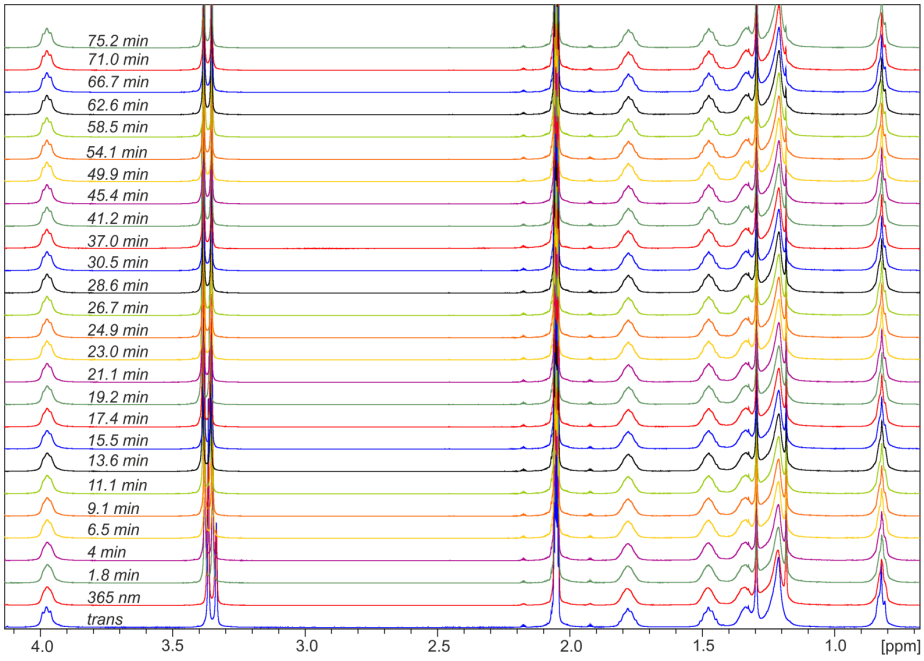

Fig.III.3: aliphatic region of ^{1}H NMR spectra of **7c**

To determine the rate constant of the thermal *cis*→*trans* isomerization the integral of the imine proton (*cis* and *trans*) was plotted against time and fitted exponentially.

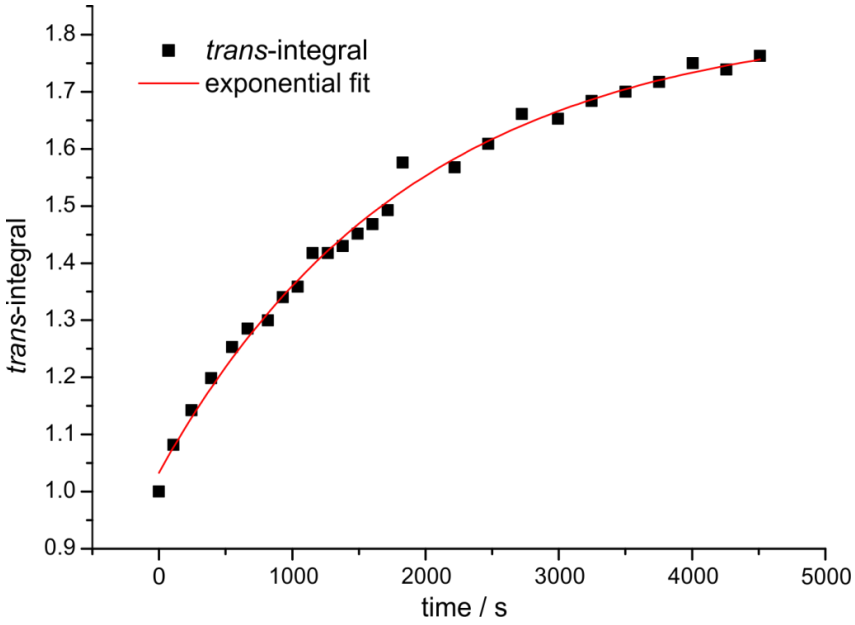

Fig.III.4: aliphatic region of ^{1}H NMR spectra of **7c**

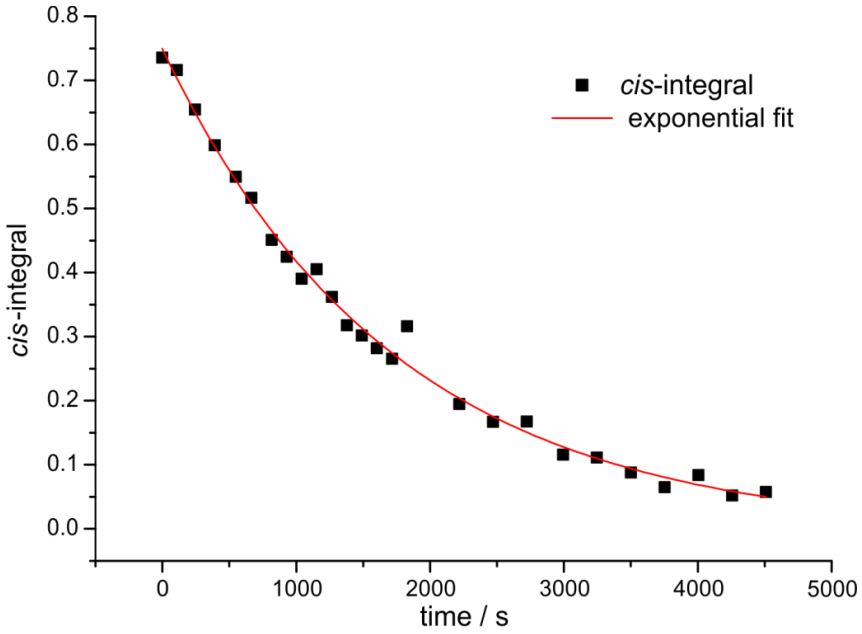

Fig.III.5: aliphatic region of ^{1}H NMR spectra of **7c**

Tab.III.1: calculation of half life of compound **7c**

tert-butylimine-8-TATA 7a	
$y = A\, e^{-\frac{x}{t_1}} + y_0$	
trans (8.46 ppm)	*cis* (8.30 ppm)
A = -0,79704	A = 0,75495
t_1 = 1894.0452	t_1 = 1731.258
y_0 = 1.83003	y_0 = -0.00593
$k = 1/t_1 = 5.27971 \cdot 10^{-4}\ s^{-1}$	$k = 1/t_1 = 5.77615 \cdot 10^{-4}\ s^{-1}$
$t_{1/2}$ = (ln2)/k = 1312.8 s = 21.9 min	$t_{1/2}$ = (ln2)/k = 1200.0 s = 20 min
$t_{1/2}$ = (ln2)/k = 21 min	

IV. UV/Vis spectra

UV/Vis spectra were measured at three different temperatures. A solution of compound **7a** in absolute THF was cooled to the desired temperature. Within the UV/Vis spectrometer the samples was irradiated with 365 nm for 10 min and spectra were measured in two minutes time interval for several half lifes.

IV.1 UV/Vis spectra of 7a at T = 215 K

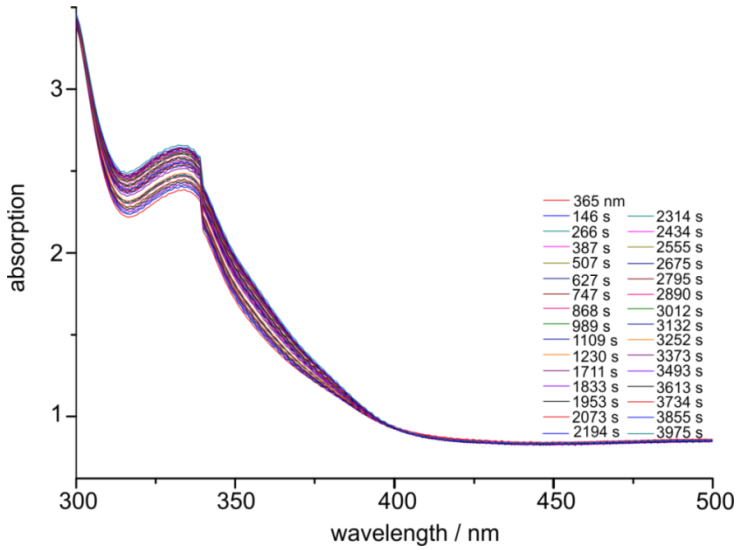

Fig.IV.1: UV/Vis spectra of compound **7a** in THF at 215 K.

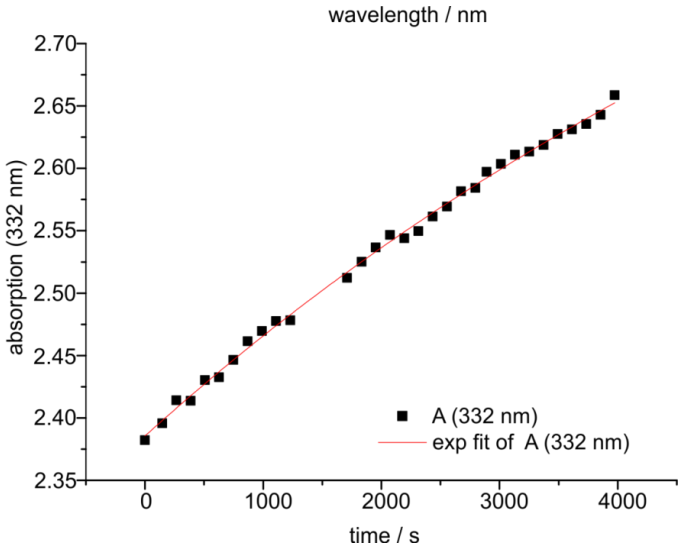

Fig.IV.2: exponential fit of the increase of the ππ*band at 332 nm.

IV.2 UV/Vis spectra of 7a at T = 223 K

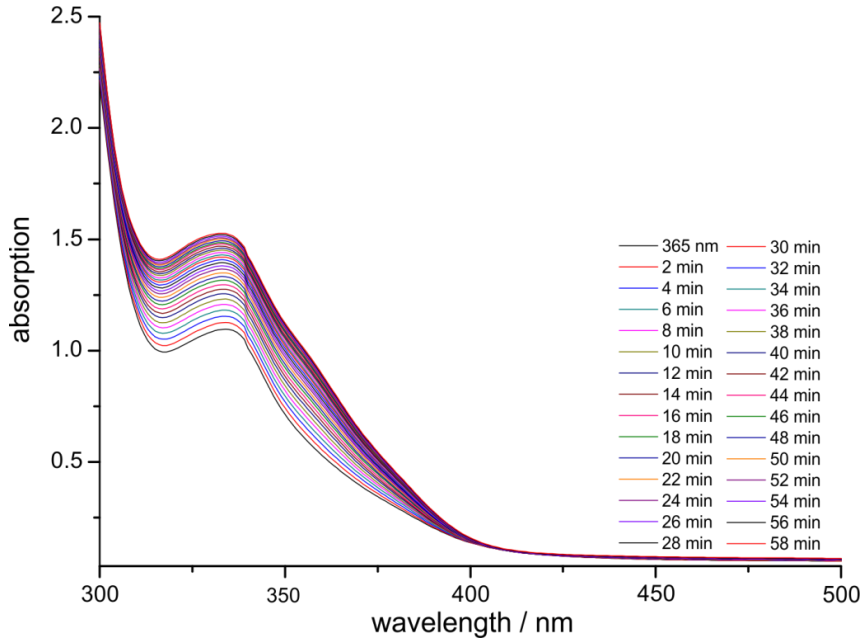

Fig.IV.3: UV/Vis spectra of compound **7a** in THF at 223 K.

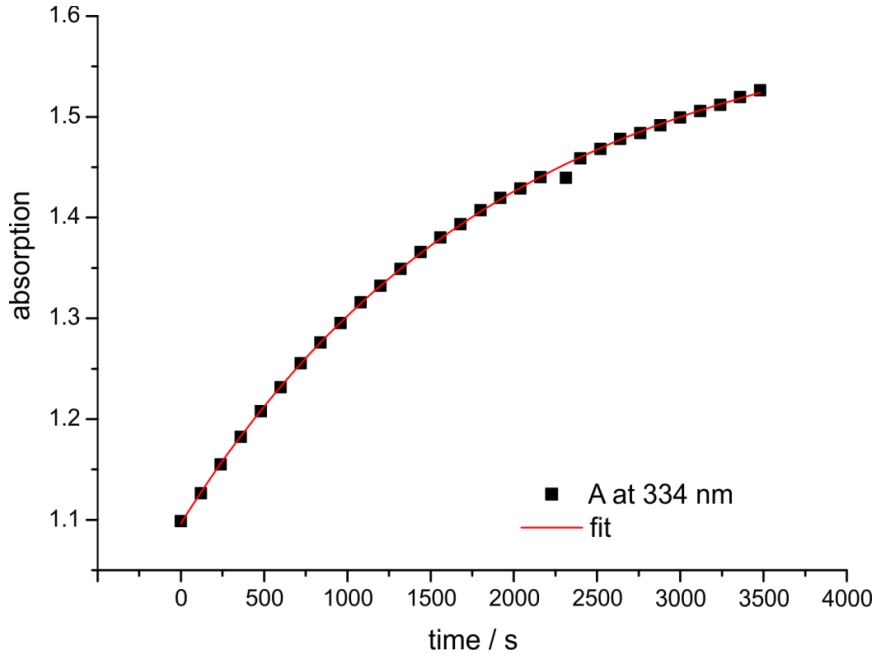

Fig.IV.4: exponential fit of the increase of the ππ*band at 332 nm.

IV.3 UV/Vis spectra at T = 229 K

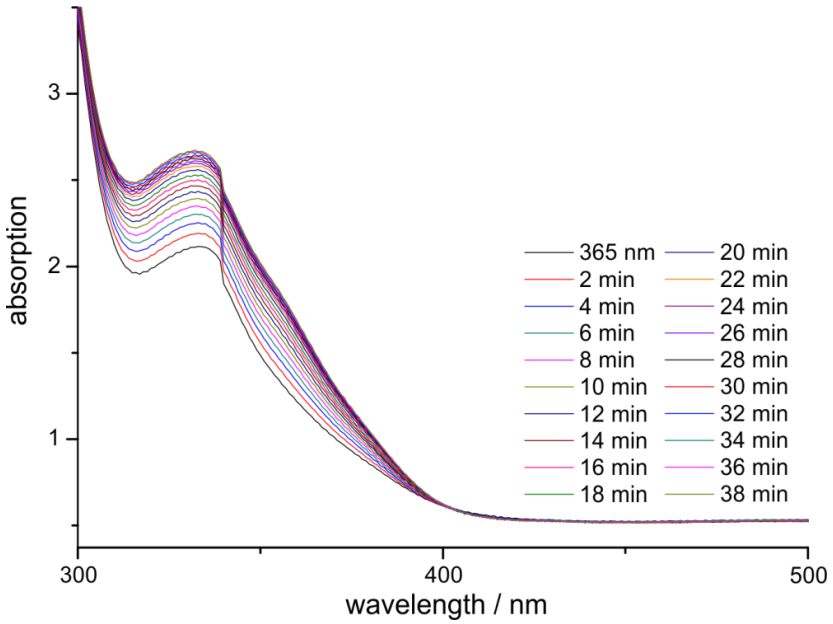

Fig.IV.5: UV/Vis spectra of compound **7a** in THF at 229 K.

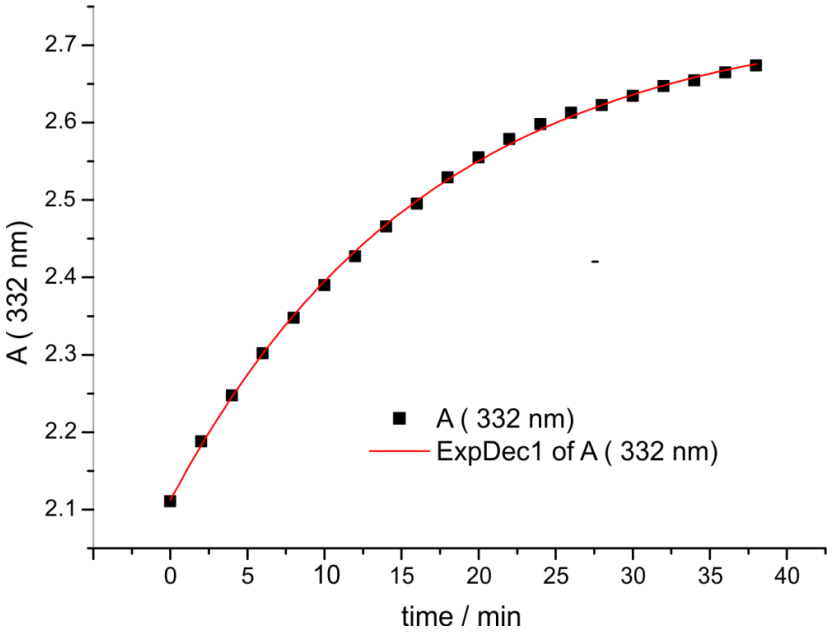

Fig.IV.6: exponential fit of the increase of the ππ*band at 332 nm.

IV. calculation of activation energy for compound 7a

To determine the activation energy for the *cis→trans* isomerization the logarithms of the rate constants were plotted against 1/T.

Tab.IV.1: rate constants for the three different temperatures of compound **7a**.

temperature / K	rate constant / mol s^{-1}
215	$1.255 \cdot 10^{-4}$
223	$5.119 \cdot 10^{-4}$
229	$2.400 \cdot 10^{-3}$

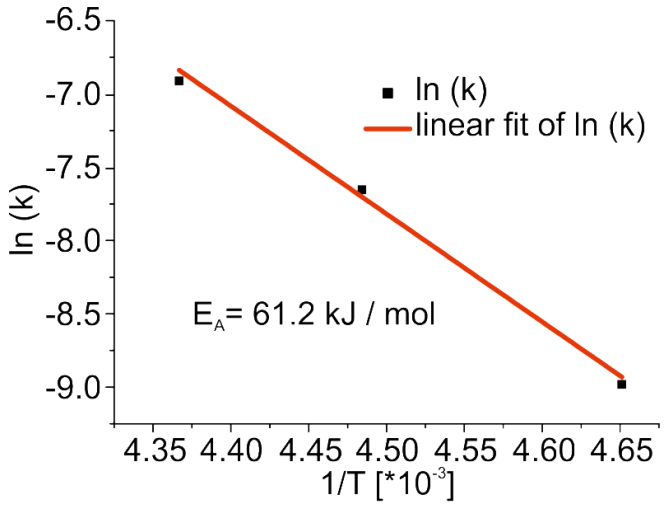

Fig.IV.7: Arrhenius plot for compound **7a**.

Tab.IV.2: calculation of the activation energy of compound **7a**.

y = ax + c		
slope	**- 7362.12144**	**765.18639**
intercept	**25.611**	**3.44508**
E_A = 61.2 ± 6.4 kJ/mol		

IV.4 UV/Vis spectra of 7c at T = 233 K

UV/Vis spectra were measured at two different temperatures. A solution of compound **7c** in absolute toluene was cooled to the desired temperature. Within the UV/Vis spectrometer the samples was irradiated with 365 nm for 10 min and spectra were measured in two minutes time interval for several half lifes.

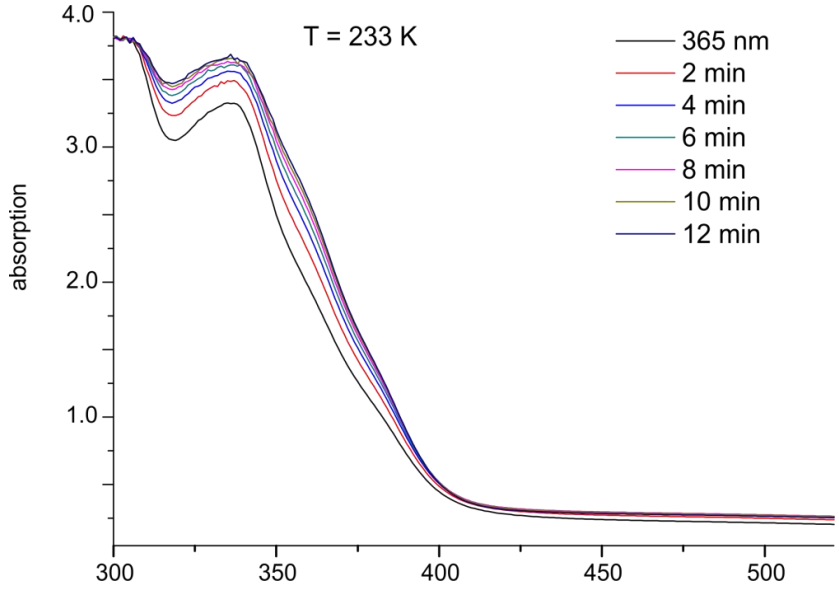

Fig.IV.8: UV/Vis spectra of compound **7c** in toluene at 233 K.

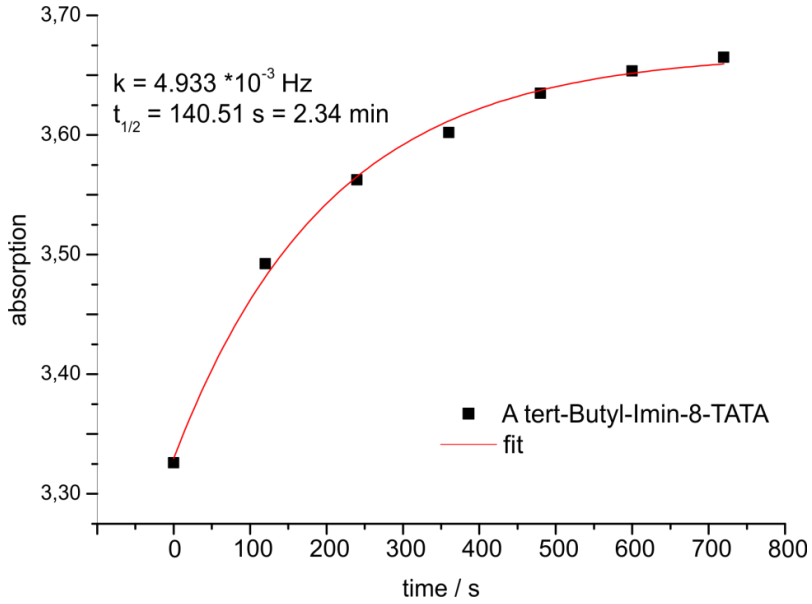

Fig.IV.9: exponential fit of the increase of the ππ*band at 335 nm.

IV.5 UV/Vis spectra of 7c at T = 233 K

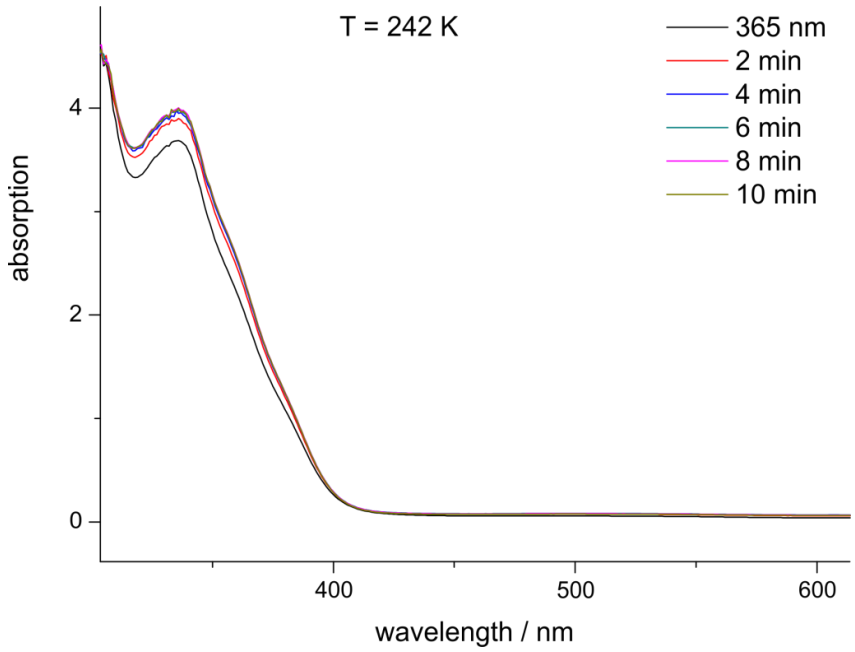

Fig.IV.10: UV/Vis spectra of compound **7c** in toluene at 242 K.

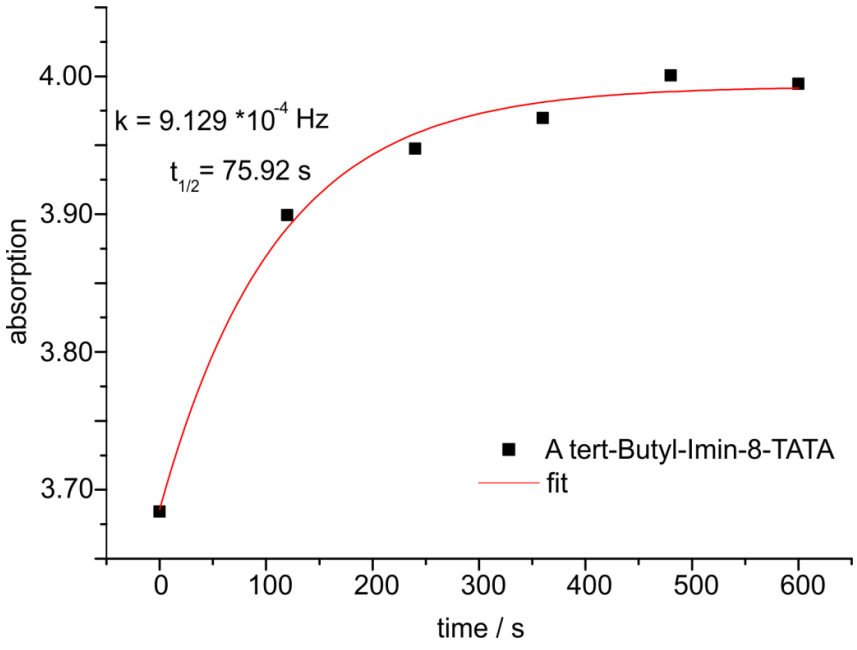

Fig.IV.11: exponential fit of the increase of the ππ*band at 335 nm.

5 Heterodiazocines

Although the properties of the artificial ciliated epithelium on the basis of the platform concept were improved tremendously by using imines as photoswitchable units, some challenges remain. The movement within the switching process occurs unidirectionally as desired but the high flexibility within the photoswitchable unit decreases the efficiency of the stroke movement. As both phenyl rings can rotate around the single bonds, the transport of nanoparticles is impaired as the strength of the induced stroke is not sufficient.

Azobenzenes can be replaced as switching units by more rigid diazocines derivatives. The ethyl bridge of those molecules prevents the rotation and therefore, the resulting stroke motion should be more forceful. Hence, diazocines represent the ideal candidates to be incorporated into an artificial ciliated epithila. However, the effortful synthesis so far hampers the usage of these photoswitches.[57,99,114–116] Thus, the design of easily synthesizeable photoswitchable units that exhibit the excellent photophysical properties of diazocines would be preferable.

5.1 Heterodiazocines: Synthesis and Properties of Photochromic Compounds within the Bio-optical Window

Melanie Hammerich, Christian Schütt, Cosima Stähler, Fynn Röhricht, Ronja Höppner and Rainer Herges

manuscript

Scientific contribution to this paper:

All reported syntheses and the photophysical investigations in solution (^{1}H NMR and UV/vis) were carried out by me, with support of Cosima Stähler during her bachelor thesis and as research assistant. DFT calculations were conducted by Christian Schütt and Fynn Röhricht. Prof. Dr. R. Herges, Christian Schütt and I wrote the manuscript.

Summary

Diazocines exhibit excellent photophysical properties such as high quantum yields, a nearly quantitative conversion to the respective isomer, switching wavelength in the visible region of light and a rigid framework which is beneficial for a photomechanical movement. However, other substitution patterns derived from the parent system were difficult to achieve so far and the ring closure by the azobenzene synthesis only provides unsteady yields. To solve this challenge we developed two heterodiazocines that are accessible by a convenient synthetic route and could furthermore be switched within the bio optical window. Therefore we exchanged one methylene group within the bridging unit with an oxygen or sulfur atom, respectively. The synthesis of the precursors can now be accomplished by (thio)ether formation in good yields in good yields and facilitates the attachment of the desired substituents. The ring closure was performed during the azobenzene synthesis. Using ultrasound, the previously published synthetic route was improved concerning both reaction time and yield. Both molecules exhibit distinct improved photophysical properties with respect to the parent system. Switching to the *trans* isomer proceeds in high yields and the nπ* band is bathochromically shifted by about 125 nm. The *cis* isomer could be obtained by irradiation from 500 nm up to 660 nm. Thus, in the presented novel heterodiazocines, the switching wavelength is located in the bio optical window where blood is transparent (650–1100 nm) (Figure 5.1). Whereas the switching wavelengths of both systems are identical, the investigated compounds exhibit a tremendous difference in the thermal half-life of the metastable configuration. The oxygen diazocine isomerizes back within minutes at room temperature while the sulfur diazocine exhibits a prolonged thermal half-life of 85 h which is distinctively higher than in the parent system ($t_{1/2}$ = 4.5 h). The switching cycles recorded for both substances show no fatigue or decay.

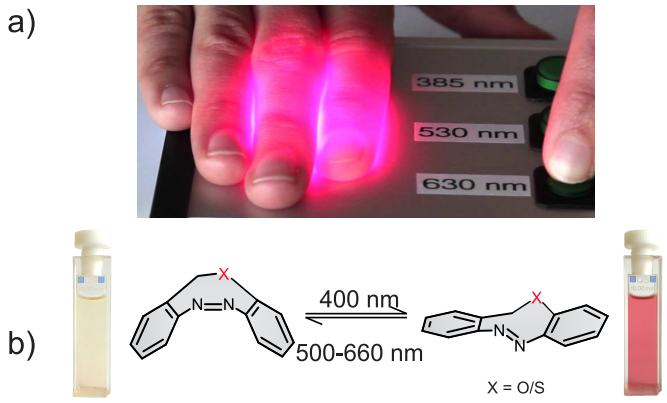

Figure 5.1: a) As red light can penetrate skin and blood, it possesses the ability to shine through the human body; b) by irradiation with 400 nm the yellow, bended *cis* isomer can be switched into the red, slender *trans* isomer, back isomerization can be induced by irradiation with 500 nm – 660 nm.

Heterodiazocines: Synthesis and Properties of Photochromic Compounds Switching within the Bio-optical window

Melanie Hammerich,[†] Christian Schütt,[†] Cosima Stähler,[†] Fynn Röhricht,[†] Ronja Höppner,[#] and Rainer Herges[†]*

[†]*Otto Diels-Institute of Organic Chemistry, Christian Albrechts University Kiel, Otto Hahn Platz 4, 24118 Kiel, Germany. E-mail: rherges@.uni-kiel.de*
[#]*Institute for Physical Chemistry, Christian Albrechts University Kiel, Max-Eyth-Str. 2, 24118 Kiel, Germany*

Supporting Information Placeholder

ABSTRACT: Diazocines, bridged azobenzenes, exhibit superior photophysical properties compared to parent azobenzenes such as high switching efficiencies, quantum yields, and particularly switching wavelengths in the visible range. Synthesis, however, proceeds with low yields, and derivatives are difficult to prepare. We now present two heterodiazocines which are easier to synthesize and to derivatize. Moreover, both compounds can be switched with light in the near infrared (650 nm). Accessibility and photophysical properties make them ideal candidates for applications such as photoswitchable drugs and functional materials.

Azobenzenes are probably the most frequently used photochromic compounds in applications ranging from molecular motors and machines to photoswitchable drugs.[1-4] They are easily accessible and their photochromic function generally is quite reliable. Usually, the stretched *trans* isomer is the most stable configuration. Upon irradiation with UV light the bent *cis* isomer is formed which returns back to the *trans* isomer either upon irradiation with visible light or thermochemically.[5] Aiming at *in vivo* applications, there have been several attempts to shift the switching wavelengths towards the near infrared (λ>650 nm).[6,7] Within the so-called bio-optical window (650-1100 nm) blood supported tissue is transparent (penetration depth ~ 20 mm). Ortho substitution of the azobenzene unit has been successful towards this end, as shown by Woolley et al. (R=OMe, λ(E/Z)=550/450nm) and Hecht et al. (R=F, λ(E/Z)=500/410nm).[8-10] Aprahamian et al. presented BF_2 bridged azobenzenes with λ(E)=710 nm.[11,12] Diazocines (ortho ethylene bridged azobenzenes) are particularly interesting visible light switchable compounds (λ(E/Z)=500/400nm).[13] Bridging of the phenyl groups prevents their rotation, and the rigid molecular framework should improve power transmission of the photomechanical movement onto the environment. This is important in biochemical applications if an efficient detachment from the active site of a protein must be achieved, or if the molecular switching has to be translated into a macroscopic effect in functional materials. Moreover, as opposed to azobenzenes, diazocines are more stable in the *cis* form (Figure 1). This is of considerable advantage in optopharmacological applications. Most photochemically switchable drugs and inhibitors are active in their stretched and slender *trans* configurations, and inactive in their bulgy *cis* forms.[14-17] Mechanistic biochemical studies as well as in vivo applications require that switching to the inactive state is complete, because even remaining traces of the active form can reduce the switching efficiency, whereas an incomplete conversion to the active state can be compensated by an increase of the concentration.[18] In this regard diazocines are superior because they can be quantitatively switched to the inactive *cis* state. Their excellent photophysical properties notwithstanding, applications of diazocines so far have been rather limited. Main obstacles are the notoriously low yields in the final ring closing azo formation and the lack of reproducibility of the synthesis.[19-22] Functionalization of the parent system using standard aromatic substitution reactions is difficult, and the preparation of unsymmetrically substituted diazocines[23] which are important for most applications is even more problematic because all steps are based on homo couplings.[24] We now present two hetero diazocines which are accessible by reliable procedures in reasonable yields. Moreover, both compounds switch efficiently (>99%) from the *trans* to the *cis* isomer upon irradiation with light in the near infrared (650 nm).

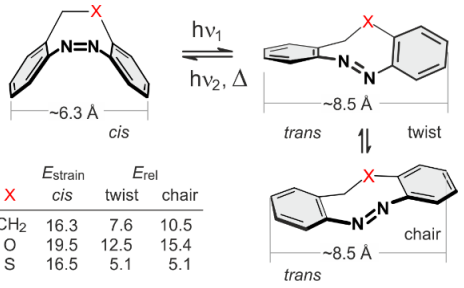

	X	E_{strain} cis	E_{rel} twist	E_{rel} chair
1	CH_2	16.3	7.6	10.5
2	O	19.5	12.5	15.4
3	S	16.5	5.1	5.1

Figure 1. Calculated (B3LYP/6-31G*) strain energies (E_{strain}) of the *cis* isomers of diazocine **1** and hetero derivatives **2** and **3**, and energies (E_{rel}) of *trans* isomers (twist and

chair conformations) of **1**, **2** and **3** relative to the corresponding *cis* isomers in kcal mol^{-1}. Distances are given between the C atoms in *para* position to the azo group.

TD-DFT calculations (see Supporting Information) predict that the nπ* transitions of the *cis* and the *trans* isomers in both hetero diazocines **2**, and **3** are separated by more than 100 nm. Therefore, we expected that efficient photo isomerization with two wavelengths should be possible. However, the *trans* isomer can adopt two different conformations (twist and chair see Figure 1) with markedly different UV-vis spectra. In the parent diazocine **1** and the O-diazocine **2**, the twist conformations are about 3 kcal mol^{-1} more stable than the chair forms, and hence the concentrations of the chair conformers in equilibrium should be very small. Twist and chair conformations in the S-diazocine **3**, however, are almost isoenergetic, and therefore the UV-vis spectrum of *trans*-**3** is a linear combination of the spectra of both conformations.

The oxygen and sulfur bridged diazocines **2** and **3** were obtained by a three step synthesis. In the first synthetic step the bridging unit was formed. This was accomplished for the oxygen system via Williamson ether synthesis with potassium phosphate as base in water with 93 % yield (Scheme 1).[25,26] The thioether precursor **8** was formed by reduction of the disulfide **7** with sodium borohydride and *in situ* reaction with 2-nitrobenzylbromide **4** in 45 % yield.

The main problem hampering the synthesis of diazocines are the low and unreliable yields in the subsequent reductive ring closure of the dinitro precursors. According to our calculations (Figure 1) the ring strains of the parent diazocine **1**, and its hetero derivatives **2** and **3** amount from 16 to almost 20 kcal mol^{-1} (details see SI). Polymer formation, therefore, is the main reaction pathway. Moreover, most reduction methods require strongly basic reaction conditions which lead to deprotonation of the benzylic positions, and consequently cyclization,[27] oxidation and polymer formation. Upon reduction of the corresponding dinitro precursors the O- and S-diazocine **6** and **8** with Zn under basic conditions no traces of the diazocine products could be isolated. Cleavage of the benzyl(thio)ether[27] was observed. To avoid deprotonation at the benzylic positions, and to favour ring closure, heterogeneous reaction conditions[28] under moderately basic pH were applied. A corresponding procedure was published by Yan et al..[19,22] They achieved the reductive ring closure of 2,2'dinitrodibenzyl to the cyclic azoxy compound with lead powder under basic conditions, and subsequently reduced the azoxy compound with trivalent phosphorous to the diazocine. As the reaction time is relatively long with two days, and the solubility of our starting material in methanol was quite low, we improved the synthesis by using high power ultrasound. As main products the azoxy compounds **9a/b** (44%, mainly **9b**) or **10a/b** (32%) were formed, concomitant with small amounts of the desired diazocines **2** and **3**.

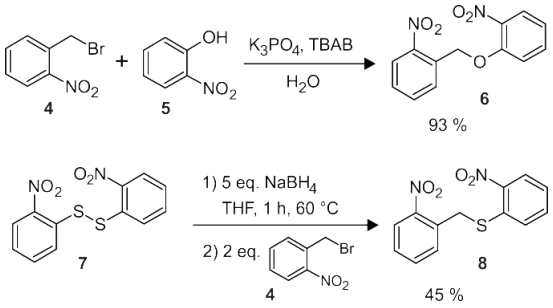

Scheme 1. Synthesis of the dinitro precursors for the diazocine synthesis. (TBAB: tetrabutylammonium bromide)

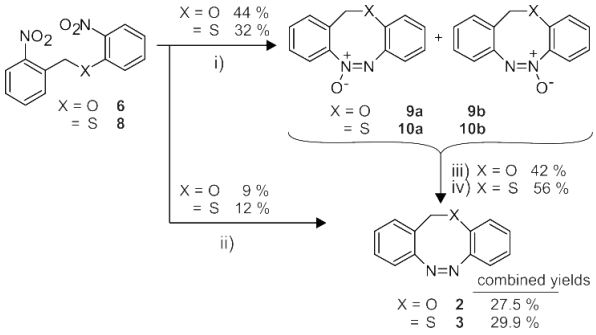

Scheme 2. Reaction conditions: i) and ii) Pb, NEt_3/formic acid/MeOH/H_2O, pH = 9.5, ultrasound; iii) PPh_3, MoO_2Cl_2, iv) Pb, ball mill, 40 Hz, 4 h.

The reduction of the oxygen bridged azoxy compounds **9a/b** to the corresponding diazocine **2** was achieved applying the literature method with triphenylphosphine and a molybdenum catalyst (Scheme 2) (see Supporting Information).[22,29] However, the method was unsuccessful in case of the sulfur bridged analogon **10a/b**. Reduction of the latter azoxy compound was achieved with lead granules in a ball mill.

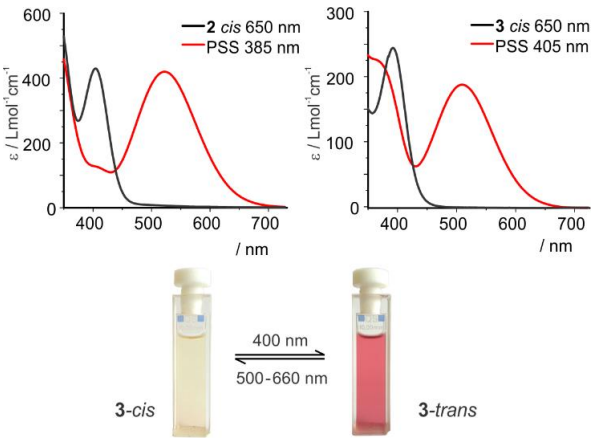

Figure 2. UV spectra of O-diazocine **2** (THF, T = -80°C, left) and S-diazocine **3** (acetonitrile, right), the *cis* spectrum is plotted in black, the spectrum of the *trans* isomer in red, below: solution of S-diazocine **3** before and after irradiation in acetone.

Photophysical properties were investigated with ^{1}H NMR and UV/Vis spectroscopy. The UV/vis spectra of the O-diazocine **2** and S-diazocine **3** are similar to the parent system. The nπ* bands of the *cis* isomers are located at 400 nm. By switching both diazocines to the *trans* isomers, the nπ* excitations are shifted bathochromically to λ_{max} =525 nm. These bands are broad and extend up to 700 nm. Therefore, the back isomerization to the *cis* isomers can be performed with red light (660 nm) (Figure 2). In contrast to the parent diazocine **1** and the O-diazocine **2**, the S-diazocine **3** exhibits an additional strong absorption at 380 nm which we attribute to the chair conformation.

Photostationary states were determined by ^{1}H NMR spectroscopy. In both systems (**2** and **3**) *cis-trans* isomerizations were achieved with 385 or 405 nm (**2**: 80%, **3**: 70%) and *trans-cis* switching with 530 or 660 nm (>99%) (Table 1).

Half-lives of the *trans* compounds were also determined by ^{1}H NMR spectroscopy (X = S, **3**) and UV/Vis spectroscopy (X = O, **2**). Compared to the parent system the oxygen bridged system **2** exhibits a distinctly shorter half-life. Rate constants were determined at four different temperatures (-11, 0, 4, and 9°C) and the half-life at room temperature was extrapolated from the Arrhenius equation (see Supporting information) as $t_{1/2}$ = 89 s (20 °C). In contrast to **2**, the *trans* isomer of the sulphur system **3** exhibits a high thermal stability. With $t_{1/2}$ = 3.5 d the half-life of trans-**3** is considerably longer than the half-life of the parent system **1** ($t_{1/2}$ = 4.5 h). To check the photostability of hetero diazocines **2** and **3** were irradiated with 385 and 530 nm in an alternate sequence. No fatigue was observed over a large number of cycles (Figure 3).

Table 1. Photostationary states and half-lives of heterodiazocines **2** and **3**.

X =	$PSS_{385/405}$ % trans	$PSS_{530/660}$ % cis	$t_{1/2}$
O (**2**)	80 [a]	> 99	89 s (20 °C)
S (**3**)	70 [b]	> 99	3.5 d (27 °C)

a) 385 nm, -70 °C b) 405 nm, 27 °C.

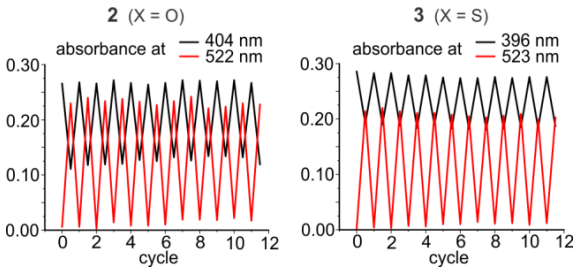

Figure 3. Left: measured absorbances of a solution of **2** at 404 nm (black zig-zag line) and 522 nm (red zig-zag line) in the photostationary states after alternating irradiation at 530 and 385 nm in repeated switching cycles. Right: absorbance of **3** at 396 nm (black) and 523 nm (red) after irradiation at 530 and 405 nm.

ASSOCIATED CONTENT

Supporting Information

DFT-calculations, experimental procedures, ^{1}H- and ^{13}C-NMRs of all compounds, photoswitching experiments (^{1}H-NMR and UV/Vis), web enhanced object (movie) showing the switching of the oxygen diazocine **2**

AUTHOR INFORMATION

Corresponding Author

*E-mail: rherges@oc.uni-kiel.de.

Author Contributions

Notes

The authors declare no competing financial interests.

ACKNOWLEDGMENT

The authors gratefully acknowledge financial support by the Deutsche Forschungsgesellschaft (DFG) within the Sonderforschungsbereich 677, “Function by Switching”.

REFERENCES

(1) Kay, E. R.; Leigh, D. A.; Zerbetto, F. *Angew.Chem.Int.Ed* **2007**, *46*, 72–191.

(2) Feringa, B. L.; Brown, W. R. In *Molecular Switches*; 2nd,, Ed.; Wiley-VCH: Weinheim, 2011.

(3) Merino, E.; Ribagorda, M. *Beilstein J. Org. Chem.* **2012**, *8*, 1071–1090.

(4) Szymanski, W.; Beierle, J. M.; Kistemaker, H. A. V.; Velema, W. A.; Feringa, B. L. *Chem. Rev.* **2013**, *113*, 6114–6178.

(5) Hartley, G. S. *Nature* **1937**, *14*, 281.

(6) Bléger, D.; Hecht, S. *Angew. Chem. Int. Ed.* **2015**, *54*, 11338–11349.

(7) Dong, M.; Babalhavaeji, A.; Samanta, S.; Beharry, A. A.; Woolley, G. A. *Acc. Chem. Res.* **2015**, *48*, 2662–2670.

(8) Beharry, A. A.; Sadovski, O.; Woolley, G. A. *J. Am. Chem. Soc.* **2011**, *133*, 19684–19687.

(9) Bléger, D.; Schwarz, J.; Brouwer, A. M.; Hecht, S. *J. Am. Chem. Soc.* **2012**, *134*, 20597–20600.

(10) Samanta, S.; Beharry, A. A.; Sadovski, O.; McCormick, T. M.; Babalhavaeji, A.; Tropepe, V.; Woolley, G. A. *J. Am. Chem. Soc.* **2013**, *135*, 9777–9784.

(11) Yang, Y.; Hughes, R. P.; Aprahamian, I. *J. Am. Chem. Soc.* **2012**, *134*, 15221–15224.

(12) Yang, Y.; Hughes, R. P.; Aprahamian, I. *J. Am. Chem. Soc.* **2014**, *136*, 13190–13193.

(13) Siewertsen, R.; Neumann, H.; Buchheim-Stehn, B.; Herges, R.; Näther, C.; Renth, F.; Temps, F. *J. Am. Chem. Soc.* **2009**, *131*, 15594–15595.

(14) Pittolo, S.; Gómez-Santacana, X.; Eckelt, K.; Rovira, X.; Dalton, J.; Goudet, C.; Pin, J.-P.; Llobet, A.; Giraldo, J.; Llebaria, A.; Gorostiza, P. *Nat. Chem. Biol.* **2014**, *10*, 813–815.

(15) Broichhagen, J.; Frank, J. A.; Trauner, D. *Acc. Chem. Res.* **2015**, *48*, 1947–1960.

(16) Velema, W. A.; Szymanski, W.; Feringa, B. L. *J. Am. Chem. Soc.* **2014**, *136*, 2178–2191.

(17) Stein, M.; Middendorp, S. J.; Carta, V.; Pejo, E.; Raines, D. E.; Forman, S. A.; Sigel, E.; Trauner, D. *Angew. Chem.* **2012**, *124*, 10652–10656.

(18) Thies, S.; Sell, H.; Bornholdt, C.; Schütt, C.; Köhler, F.; Tuczek, F.; Herges, R. *Chem. Eur. J.* **2012**, *18*, 16358–16368.

(19) Eljabu, F.; Dhruval, J.; Yan, H. *Bioorg. Med. Chem. Lett.* **2015**, *25*, 5594–5596.

(20) Samanta, S.; Qin, C.; Lough, A. J.; Woolley, G. A. *Angew. Chem.* **2012**, *124*, 6452–6455.

(21) Sell, H.; Näther, C.; Herges, R. *Beilstein J. Org. Chem.* **2013**, *9*, 1–7.

(22) Joshi, D. K.; Mitchell, M. J.; Bruce, D.; Lough, A. J.; Yan, H. *Tetrahedron* **2012**, *68*, 8670–8676.

(23) Reissert, A.; Crämer, K. *Chem. Ber.* **1928**, *61*, 2555–2566.

(24) Tellkamp, T.; Shen, J.; Okamoto, Y.; Herges, R. *Eur. J. Org. Chem.* **2014**, *2014*, 5456–5461.

(25) Lellmann, E.; Mayer, N. *Chem. Ber.* **1892**, *25*, 3583–3586.

(26) Wang, H.; Ma, Y.; Tian, H.; Yu, A.; Chang, J.; Wu, Y. *Tetrahedron* **2014**, *70*, 2669–2673.

(27) Machin, J.; Mackie, R. K.; McNab, H.; Reed, G. A.; Sagar, A. J. G.; Smith, D. M. *J. Chem. Soc., Perkin Trans. 1* **1976**, 394–399.

(28) Thorwirth, R.; Bernhardt, F.; Stolle, A.; Ondruschka, B.; Asghari, J. *Chem. Eur. J.* **2010**, *16*, 13236–13242.

(29) Sanz, R.; Escribano, J.; Fernández, Y.; Aguado, R.; Pedrosa, M. R.; Arnáiz, J., Francisco *Synlett* **2005**, 1389–1392.

Authors are required to submit a graphic entry for the Table of Contents (TOC) that, in conjunction with the manuscript title, should give the reader a representative idea of one of the following: A key structure, reaction, equation, concept, or theorem, etc., that is discussed in the manuscript. Consult the journal's Instructions for Authors for TOC graphic specifications.

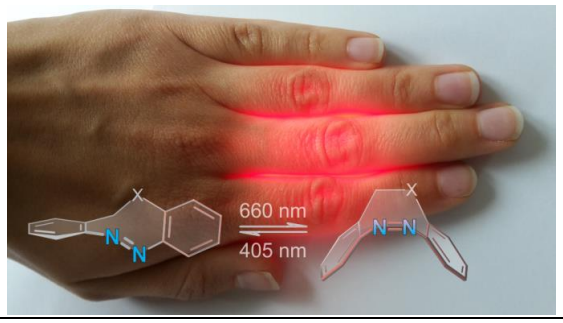

Heterodiazocines: Synthesis and Properties of Photochromic Compounds Switching within the Bio optical window

Melanie Hammerich, Christian Schütt, Cosima Stähler, Fynn Röhricht, Ronja Höppner and Rainer Herges*

Table of contents

I. Analytical equipment

NMR spectroscopy

NMR spectra were measured in deuterated solvents (Deutero). To reference the NMR spectra the following solvent signals were used:

solvent	degree of deuteration	^{1}H signal	^{13}C signal
acetone-d_6	99.8 %	2.05 (quintet)	29.84 (septet)
chloroform-d_1	99.8 %	7.26 (s)	77.16 (triplet)
DMSO-d_6	99.8 %	2.60 (quintet)	39.52 (septet)

NMR measurements were performed with a Bruker DRX 500 (^{1}H NMR: 500 MHz, ^{13}C-NMR: 125 MHz) and a Bruker AV 600 (^{1}H NMR: 600 MHz, 13C NMR: 150 MHz).

Melting point

Melting points were measured with a Melting Point B-540 (Büchi) in an oneside opened capillary tubule.

Mass spectrometry

The high resolution (HR-EI) mass spectra were measured with an AccuTOF GCv 4G (Joel) with ionization energy of 70 eV.

IR spectroscopy

Infrared spectra were measured on a Perkin-Elmer 1600 Series FT-IR spectrometer with an A531-G Golden-Gate-Diamond-ATR-unit. Signals were abbreviated with w, m, s for weak, medium and strong signal intensity. Broad signals are additionally abbreviated with br.

UV-Vis spectroscopy

UV-Vis spectra were measured with a Cary3000 (Agilent Technologies) and with a Lambda 14 spectrometer (Perkin-Elmer) with a (Büchi) thermostat. Quartz cuvettes of 1 cm optical path length were used.

Chromatography stationary phases

For column chromatography purifications silica gel (Merck, particle size 0.040-0.063 mm) was used. R_f values were determined by thin layer chromatography on Polygeram® SilG/UV254 (Macherey Nagel, 0.2 mm particle size).

Light source

UV/Vis and 1H NMR:
The irradiation of the samples was performed with LEDs with a wavelength of 385 nm, 405 nm, 525 nm and 660 nm from Sahlmann Photochemical Solutions.

Movie
The irradiation of the samples was performed with LEDs with a wavelength of 385 nm, 530 nm and 630 nm from Sahlmann Photochemical Solutions.

Ultrasound generator

The synthesis with ultrasound was performed with a Branson Sonifier 450.

II. DFT calculations

II.1 Ring Strain

The standard synthetic procedures to prepare diazocines only proceed in low yields. To find the reason for the inefficient ring closure reaction we calculated the ring strain energies of diazocines **1**, **2** and **3** at the B3LYP/6-31G* level of density functional theory using an isodesmic reaction approach. According to our calculations the ring strain amounts to more than 16 kcal mol^{-1} (see Figure S1) which explains why polymer formation is the main reaction pathway during the reductive azo coupling reaction.

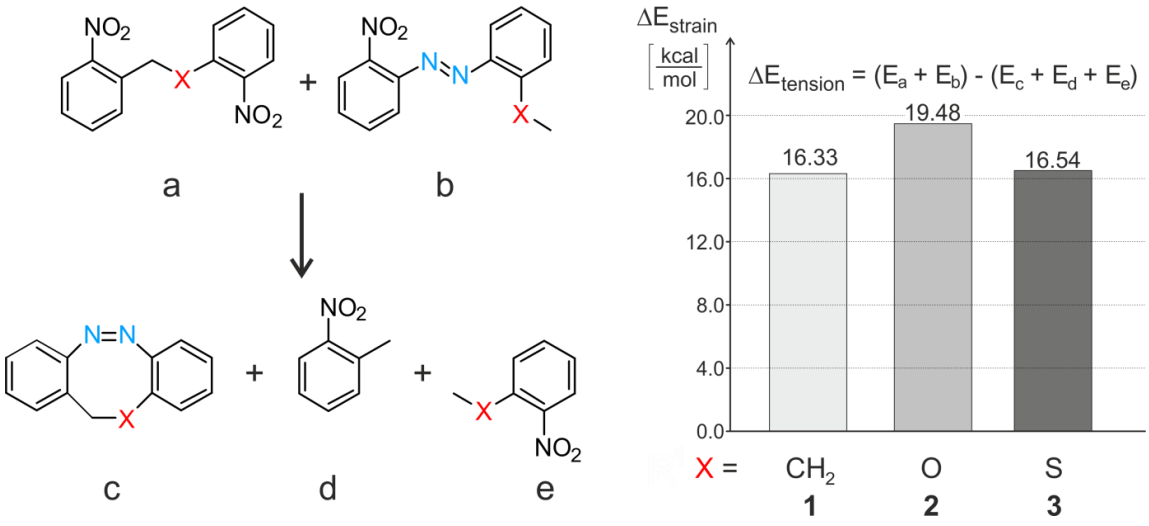

Figure S1. Left: Isodesmic reaction defining the ring strain energy of the diazocines **1**, **2**, and **3**. Right: bar energy diagram of the calculated (B3LYP/6-31G*) ring strain energies of the diazocines **1**, **2** and **3**.

II.2 Calculated UV Spectra

TD-DFT calculations were performed at the B3LYP/6-31G* level of theory using Gaussian 09.D01.[2] Note that all structures in Figure S2 are chiral, however, only one enantiomer is considered. The measured UV-vis spectrum of the parent diazocine **1** exhibits absorption maxima at λ_{max} = 404 nm for the *cis* isomer and at λ_{max} = 490 nm in the *trans* form. The respective calculated n-π* transitions (see Table S2) of **1** are at 433 nm (*cis*) and 533 nm (*trans*-twist). According to our calculations the *trans*-chair is 2.9 kcal/mol less stable than the *trans*-twist conformation and therefore should not contribute to the UV/vis spectrum. As compared to the experiment, theory predicts the n-π* absorptions at higher wavelengths but the distance between the n-π* absorption in *cis* and *trans* isomers as well as the oscillator strength of the n-π* transitions are in good agreement with the experimental results. Hence we assume that this level of theory is suitable to give a semi quantitative estimation of the photochromic properties of the hetero diazocines **2** and **3** (Figure S2).

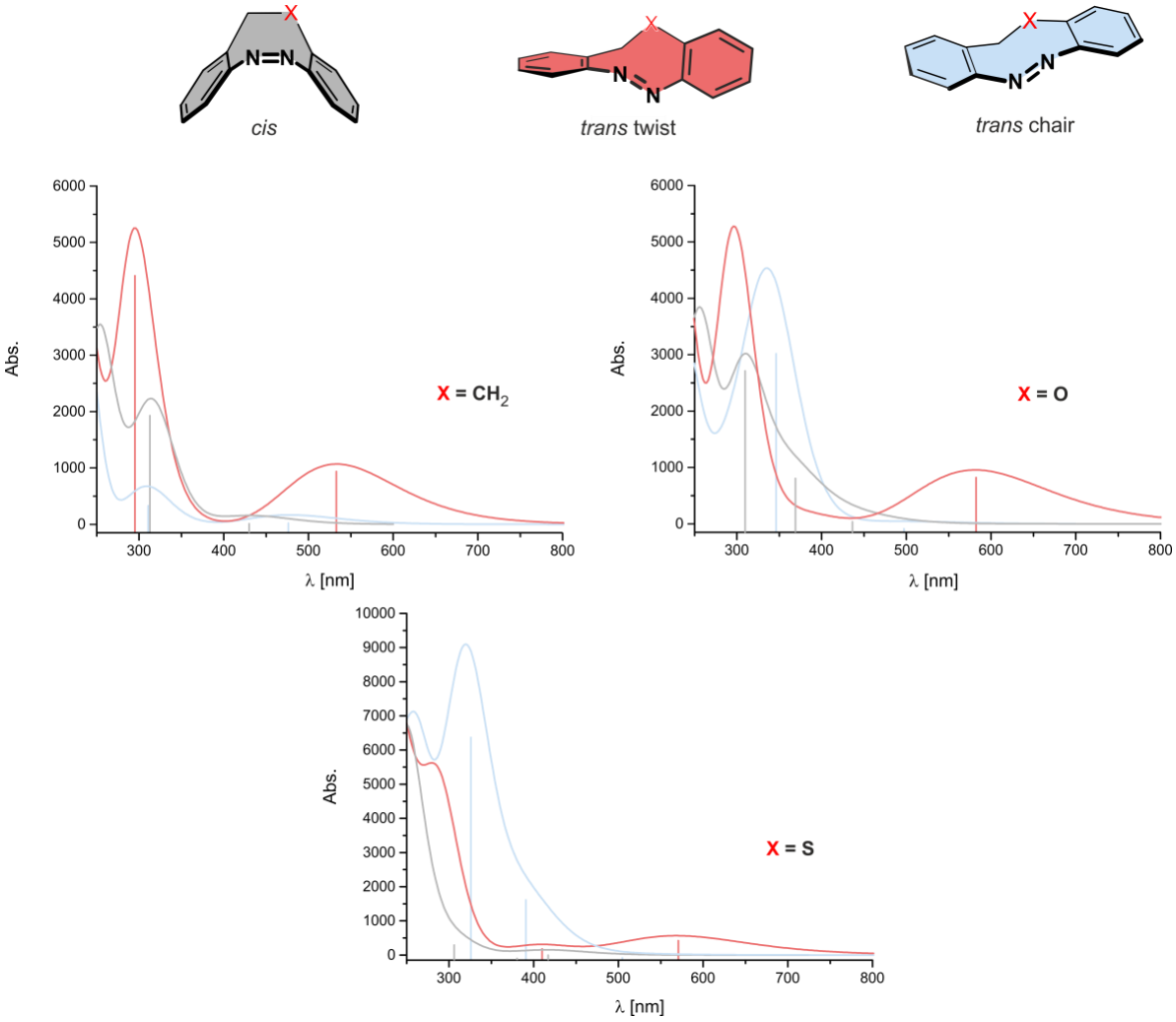

Figure S2. Calculated (TD-B3LYP/6-31G*) UV-vis spectra of the *cis* isomer (black line) and the *trans* twist (red) and *trans* chair conformation (blue) of the parent diazocine **1** (top left) and its oxygen (**2**, top right) and sulfur analogue (**3**, bottom). The bars in the corresponding color which are proportional to the oscillator strength represent the n-π* transitions. The UV spectra are simulated by an overlay of Gaussian functions with a half-width of 0.333 eV.

There is an overlap of the n-π* transition of the *cis* and *trans* twist isomer in the oxygen derivative **2**, which explains the incomplete conversion of the *cis* to the *trans* isomer upon irradiation with 385 nm. The n-π* transition of the *trans* twist isomer is bathochromically shifted with respect to the parent system which is also in agreement with experiment. This also applies for the sulfur analogue **3** in which the distance of the n-π* transitions of *cis* and *trans-twist* increases to 148 nm. However, according to the calculations the *trans*-twist and *trans*-chair conformations of the sulfur bridged azobenzene **3** are almost isoenergetic. Therefore, both *trans* conformations have to be included in the prediction of the UV/vis spectrum. The *chair* conformer of **3** exhibits a n-π* transition with a high oscillator strength (f = 0.0430) at 390 nm resulting in a substantial overlap with the transition of the *cis* isomer (422 nm). Hence, the percentage of the *trans* isomer in the photostationary state of **3** upon irradiation with 405 nm is predicted to be lower in comparison to the parent system **1** and the oxygen analogue **2**. So, we conclude that any measure (e.g. substitution) which disfavors the *trans* chair conformation would improve the photochromic properties of the sulfur bridged diazocine. Generally it can be stated that the *trans* twist conformations are responsible for the unusually bathochromic n-π*absorptions of heterodiazocines **2** and **3**.

Table S1. Calculated (TD-B3LYP/6-31G*) n-π* transitions and oscillator strengths (f) of the *cis*, *trans* twist and *trans* chair configurations of the diazocines **1**, **2** and **3**. Experimental absorption wavelengths are given as λ_{max}.

compound	**isomer/conform.**	**calc. λ [nm]**	***f***	**exp. λ_{max} [nm]**
1 (CH_2)	*trans*-twist	533	0.0264	490
		294	0.1148	
	trans-chair	478	0.0041	
		318	0.0115	
	cis	433	0.0038	404
		317	0.0507	
2 (O)	*trans-twist*	581	0.0236	522
	trans-chair	497	0.0011	
		346	0.0776	
	cis	437	0.0045	404
		367	0.0232	
		311	0.0701	
3 (S)	*trans-twist*	570	0.0139	523
		408	0.0075	
	trans-chair	504	0.0009	
		390	0.0430	
		326	0.1607	
	cis	422	0.0033	396
		379	0.0008	
		312	0.0107	

II.3 XYZ Coordinates of the B3LYP/6-31G* Optimized Isomers of 1, 2 and 3

II.3.1 Parent Diazocine (X = CH_2) (1)

***trans*-twist**

$E_{B3LYP/6-31G*}$ = -650.1492714 Hartree

NImag = 0

C	0.583470	1.549820	0.525660
H	0.168850	1.333220	1.517200
H	0.957570	2.578820	0.581860
C	-4.231370	0.383960	-0.202230
C	-3.100260	1.163680	-0.456600
C	-1.808450	0.661250	-0.268850
C	-1.701310	-0.669420	0.198820
C	-2.819900	-1.440830	0.507780
C	-4.092570	-0.918450	0.281270
C	1.808480	0.661250	0.268800
N	-0.366280	-1.045040	0.511330
N	0.366230	-1.044820	-0.511380
C	1.701330	-0.669420	-0.198880
C	3.100270	1.163700	0.456570
C	4.231380	0.383970	0.202190
C	4.092580	-0.918440	-0.281250
C	2.819900	-1.440850	-0.507760
H	-5.221130	0.801980	-0.363940
H	-3.223340	2.186270	-0.806910
H	-2.684240	-2.444820	0.898840
H	-4.971170	-1.521670	0.492300
H	3.223340	2.186280	0.806900
H	4.971170	-1.521690	-0.492250
H	2.684290	-2.444870	-0.898760
C	-0.583490	1.549930	-0.525560
H	-0.168890	1.333620	-1.517160
H	-0.957640	2.578920	-0.581460

***trans*-chair**

$E_{B3LYP/6-31G*}$ = -650.1446865 Hartree

NImag = 1 (-73 Hz)

C	4.052970	-0.994450	-0.097320
C	2.788010	-1.543450	0.130500
C	1.699650	-0.689780	0.245090
C	4.205970	0.388610	-0.189080
C	3.099270	1.230750	-0.042160
C	1.819130	0.715930	0.182890
C	0.628770	1.634070	0.473060
C	-0.628400	1.633610	-0.473430
C	-1.818840	0.715690	-0.182770
C	-1.699800	-0.690080	-0.244920
C	-3.098860	1.230890	0.042160
C	-4.205820	0.389100	0.189100
C	-4.053270	-0.994010	0.097320
C	-2.788480	-1.543390	-0.130510
N	0.343690	-1.058420	0.523640
N	-0.344020	-1.059570	-0.523340
H	4.913100	-1.649280	-0.206390
H	2.643750	-2.617520	0.198030
H	5.188720	0.816760	-0.365980
H	3.233350	2.308980	-0.097090
H	0.284900	1.445110	1.498310
H	1.018890	2.658460	0.467120
H	-1.018570	2.657980	-0.468360
H	-3.232640	2.309160	0.096950
H	-5.188430	0.817560	0.365990
H	-4.913600	-1.648560	0.206340
H	-2.644570	-2.617510	-0.198110

cis

$E_{B3LYP/6\text{-}31G^*}$ = -650.1613841 Hartree

NImag = 0

C	0.827860	1.803160	1.052080
H	0.785940	1.516210	2.107900
H	1.378820	2.749410	1.009990
C	-3.170580	0.071640	-1.460350
C	-2.321320	1.071110	-0.995070
C	-1.422180	0.867760	0.065200
C	-1.404230	-0.413700	0.649430
C	-2.291200	-1.410290	0.214710
C	-3.155100	-1.183270	-0.849670
C	1.570660	0.744520	0.274760
N	-0.626020	-0.823910	1.800590
N	0.611930	-0.972430	1.756270
C	1.383760	-0.610640	0.596580
C	2.455280	1.055770	-0.763580
C	3.124800	0.055350	-1.468320
C	2.937070	-1.285040	-1.122120
C	2.086980	-1.618000	-0.070110
H	-3.844480	0.274370	-2.288000
H	-2.346670	2.051060	-1.466530
H	-2.277340	-2.367580	0.727580
H	-3.817170	-1.974430	-1.190030
H	2.618960	2.100270	-1.020270
H	3.802850	0.321410	-2.274420
H	3.464740	-2.068690	-1.658640
H	1.953390	-2.650880	0.237920
C	-0.606890	2.063260	0.529860
H	-1.163660	2.597350	1.313520

II.3.2 Oxygen-Diazocine (X = O) (2)

***trans*-twist**

$E_{B3LYP/6-31G*}$ = -686.0350761 Hartree

NImag = 0

C	0.469660	1.463050	0.527200
H	0.052590	1.225130	1.510480
H	0.753710	2.520130	0.536140
C	-4.125770	0.495780	-0.308610
C	-2.949180	1.220110	-0.514740
C	-1.713390	0.636070	-0.239980
C	-1.676610	-0.697270	0.240480
C	-2.852590	-1.395150	0.498630
C	-4.081900	-0.802900	0.203980
C	1.736530	0.639530	0.249560
N	-0.354440	-1.094420	0.581470
N	0.371440	-1.155950	-0.448500
C	1.690440	-0.710500	-0.171320
C	2.993450	1.230950	0.388240
C	4.163550	0.508210	0.137550
C	4.089940	-0.815580	-0.299400
C	2.846880	-1.421580	-0.483040
H	-5.082710	0.958760	-0.532550
H	-2.970140	2.239010	-0.888660
H	-2.795010	-2.404610	0.894850
H	-5.001630	-1.354360	0.375560
H	3.061470	2.273310	0.692300
H	5.130300	0.988380	0.259270
H	4.998470	-1.371910	-0.512180
H	2.765580	-2.443220	-0.841560

***trans*-chair**

$E_{B3LYP/6-31G*}$ = -686.0305104 Hartree

NImag = 0

C	0.567250	1.604580	0.455740
H	0.229360	1.464020	1.487220
H	0.828480	2.657420	0.309560
C	-4.097540	0.589450	0.044780
C	-2.902100	1.305410	-0.036590
C	-1.679020	0.636550	-0.129370
C	-1.688770	-0.787910	-0.143350
C	-2.888370	-1.496160	-0.118060
C	-4.094720	-0.807700	0.000220
C	1.798280	0.745460	0.190120
N	-0.401130	-1.365130	-0.326540
N	0.321590	-0.923460	0.603050
C	1.680010	-0.659100	0.292790
C	3.049240	1.274590	-0.121680
C	4.153970	0.430270	-0.286090
C	4.010450	-0.951780	-0.160830
C	2.759840	-1.512870	0.122180
H	-5.038120	1.127370	0.125220
H	-2.897730	2.390950	-0.050900
H	-2.860850	-2.580950	-0.162130
H	-5.029540	-1.358190	0.051720
H	3.166190	2.350740	-0.228420
H	5.127320	0.855040	-0.514440
H	4.871340	-1.601230	-0.293950
H	2.627110	-2.586820	0.207230

cis

$E_{B3LYP/6\text{-}31G^*}$ = -686.0550130 Hartree

NImag = 0

C	0.633890	1.404790	1.385290
H	0.444770	0.858180	2.315340
H	1.078010	2.369030	1.641610
C	-3.339270	0.508460	-1.249740
C	-2.393020	1.322670	-0.645930
C	-1.412670	0.801560	0.216430
C	-1.398260	-0.588010	0.469580
C	-2.403940	-1.385130	-0.110740
C	-3.345460	-0.865370	-0.985840
C	1.535320	0.635800	0.457960
N	-0.590530	-1.361700	1.394580
N	0.646820	-1.499570	1.313440
C	1.454010	-0.762850	0.390340
C	2.459180	1.292850	-0.363740
C	3.273780	0.578810	-1.239440
C	3.191190	-0.817140	-1.284550
C	2.305510	-1.490720	-0.449780
H	-4.077890	0.945960	-1.915550
H	-2.377320	2.393960	-0.819820
H	-2.409950	-2.439180	0.151140
H	-4.088250	-1.515880	-1.437290
H	2.531870	2.376790	-0.314110
H	3.980500	1.104430	-1.875080
H	3.832300	-1.379890	-1.957310
H	2.252350	-2.575190	-0.441100

II.3.3 Sulfur-Diazocine (X = S) (3)

***trans*-twist**

$E_{B3LYP/6-31G*}$ = -1009.0233672 Hartree

NImag = 0

C	0.776490	1.449660	0.761490
H	0.302970	1.139860	1.693480
H	1.172930	2.456950	0.922860
C	-4.280540	0.098760	-0.205640
C	-3.217650	0.986590	-0.386650
C	-1.900220	0.570560	-0.168110
C	-1.677920	-0.759580	0.249610
C	-2.738800	-1.629460	0.483050
C	-4.044790	-1.205010	0.233080
C	1.932700	0.535620	0.364880
N	-0.317310	-1.041260	0.571940
N	0.408890	-1.130590	-0.448330
C	1.751320	-0.762780	-0.166910
C	3.247270	0.996020	0.493290
C	4.336940	0.199190	0.134300
C	4.129460	-1.072490	-0.403050
C	2.830110	-1.542790	-0.582370
H	-5.296720	0.438160	-0.385380
H	-3.408830	2.011240	-0.692890
H	-2.532170	-2.635750	0.835270
H	-4.874070	-1.888370	0.391410
H	3.422280	1.996670	0.881910
H	5.346380	0.582180	0.254700
H	4.974590	-1.688080	-0.697570
H	2.638820	-2.515850	-1.024710

***trans*-chair**

$E_{B3LYP/6-31G*}$ = -1009.0234590 Hartree

NImag = 0

C	0.973680	1.697760	0.613490
H	0.599150	1.582990	1.632550
H	1.359330	2.717030	0.501720
C	-4.242860	0.257120	0.105480
C	-3.115960	1.079570	0.057310
C	-1.826420	0.538100	-0.053440
C	-1.709160	-0.884960	-0.085410
C	-2.844240	-1.698430	-0.080970
C	-4.110740	-1.131820	0.031650
C	2.061930	0.688580	0.310610
N	-0.415530	-1.445620	-0.209510
N	0.335830	-0.768120	0.537640
C	1.713320	-0.680400	0.286850
C	3.382060	1.034290	0.022450
C	4.330770	0.037460	-0.232620
C	3.965060	-1.311380	-0.235080
C	2.640530	-1.681120	0.007090
H	-5.228490	0.706640	0.189160
H	-3.231630	2.158490	0.086670
H	-2.708960	-2.774510	-0.137170
H	-4.989980	-1.768850	0.063360
H	3.676550	2.080920	0.007090
H	5.361220	0.316980	-0.433840
H	4.710870	-2.075360	-0.436430
H	2.326720	-2.720120	-0.009000

cis

$E_{B3LYP/6\text{-}31G^*}$ = -1009.0315646 Hartree

NImag = 0

C	1.058910	2.000580	0.478000
H	1.138000	2.102700	1.562830
H	1.572720	2.846390	0.013940
C	-3.011880	-0.724630	-1.436860
C	-2.298740	0.458800	-1.264200
C	-1.447260	0.644550	-0.162550
C	-1.318060	-0.407400	0.763370
C	-2.046830	-1.590070	0.594700
C	-2.880790	-1.757330	-0.506730
C	1.649840	0.701560	0.019870
N	-0.569070	-0.311350	1.996840
N	0.674970	-0.374850	2.001650
C	1.412610	-0.466210	0.762930
C	2.456650	0.607770	-1.119930
C	3.021600	-0.608160	-1.501870
C	2.795210	-1.752850	-0.733880
C	2.003910	-1.680860	0.411190
H	-3.663610	-0.839820	-2.298140
H	-2.389810	1.261050	-1.990230
H	-1.952480	-2.368930	1.345880
H	-3.430780	-2.685650	-0.631320
H	2.642170	1.502480	-1.709300
H	3.646360	-0.660160	-2.388810
H	3.240660	-2.701230	-1.020910
H	1.832210	-2.556830	1.029530

III. Syntheses

III. 1 Synthesis of 1-nitro-2-((2'-nitrobenzyl)oxy)benzene (6)

2-Nitrophenol (**5**, 800 mg, 5.75 mmol), 2-nitrobenzylbromide (**4**, 1.49 g, 6.88 mmol), potassium phosphate (2.30 g, 8.63 mmol) and tetra-*n*-butylammonium bromide (TBAB) (940 mg, 2.90 mmol) were stirred in 30 mL water at room temperature for 16 h. The suspension was diluted with water and extracted with 250 mL dichloromethane. The combined organic layers were dried over sodium sulfate. The solution was evaporated and recrystallized from ethanol to obtain colorless crystals (**6**, 1.47 g 5.36 mmol, 93 %).

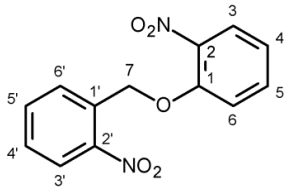

melting point: 156 °C (154 °C)[1]

^{1}H-NMR (500 MHz, acetone-d_6, 300 K): δ = 8.22 (dd, ^{3}J = 8.2 Hz, ^{4}J = 1.2 Hz, 1 H, *H-3'*), 8.01 (d, ^{3}J = 7.9 Hz, 1 H, *H-6'*), 7.94 (dd, ^{3}J = 8.1 Hz, ^{4}J = 1.7 Hz, 1 H, *H-6*), 7.87 (td,^{3}J = 7.6 Hz, ^{4}J = 1.2 Hz, 1 H, *H-5'*), 7.70 (td, ^{3}J = 8.0 Hz, ^{4}J = 1.7 Hz, 1 H, *H-4*), 7.67 (t, ^{3}J = 7.8 Hz, 1 H, *H-4'*), 7.49 (dd, ^{3}J = 8.5 Hz, ^{4}J = 1.0 Hz, 1 H, *H-3*), 7.21 (ddd, ^{3}J = 7.8 Hz, ^{3}J = 7.3 Hz, ^{4}J = 1.1 Hz, 1 H, *H-5*), 5.73 (s, 2 H, *H-7*) ppm.

^{13}C-NMR (125 MHz, acetone−d_6, 300 K): δ = 152.04 (*C-2*), 148.16 (*C-2'*), 141.05 (*C-1*), 135.35(*C-4*), 135.12 (*C-5'*), 133.24 (*C-1'*), 129.92 (*C-4'*), 129.63 (*C-6'*), 126.25 (*C-6*), 125.83 (*C-3'*),122.10 (*C-5*), 116.18 (*C-3*), 68.80 (*C-7*) ppm.

IR (ATR): $\tilde{\nu}$= 3115 (w), 3089 (w), 1604 (m), 1515 (s), 1339 (s), 1248 (s), 1153 (m), 1024 (m), 865(m), 727 (s), 665 (m), 617 (w), 525 (w) cm^{-1}.

MS (EI, 70 eV): m/z = 274.06 $[M]^+$, 152.06 $[M-C_6H_4NO_2]^+$, 136.04 $[M-C_6H_4NO_3]^+$.

MS (HR) (EI, 70 eV): m/z = calc.: 274.05897, found: 274.05894.

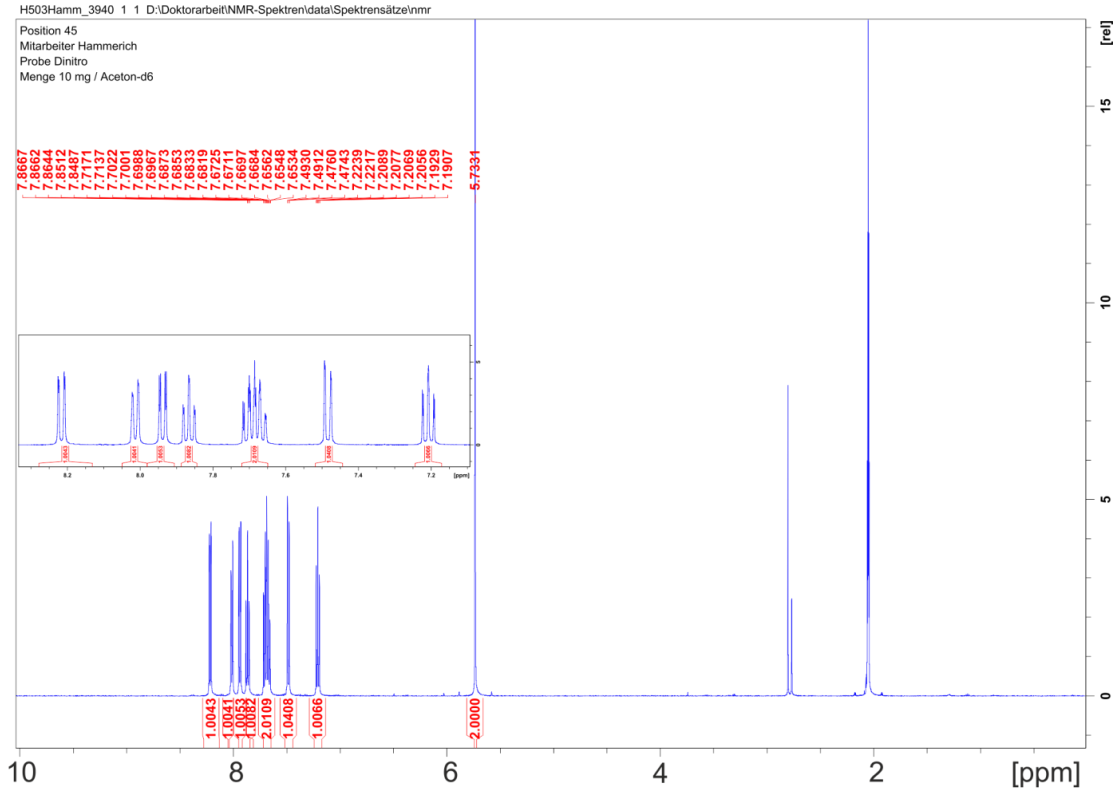

Figure S3: ^{1}H-NMR spectrum of compound **6**.

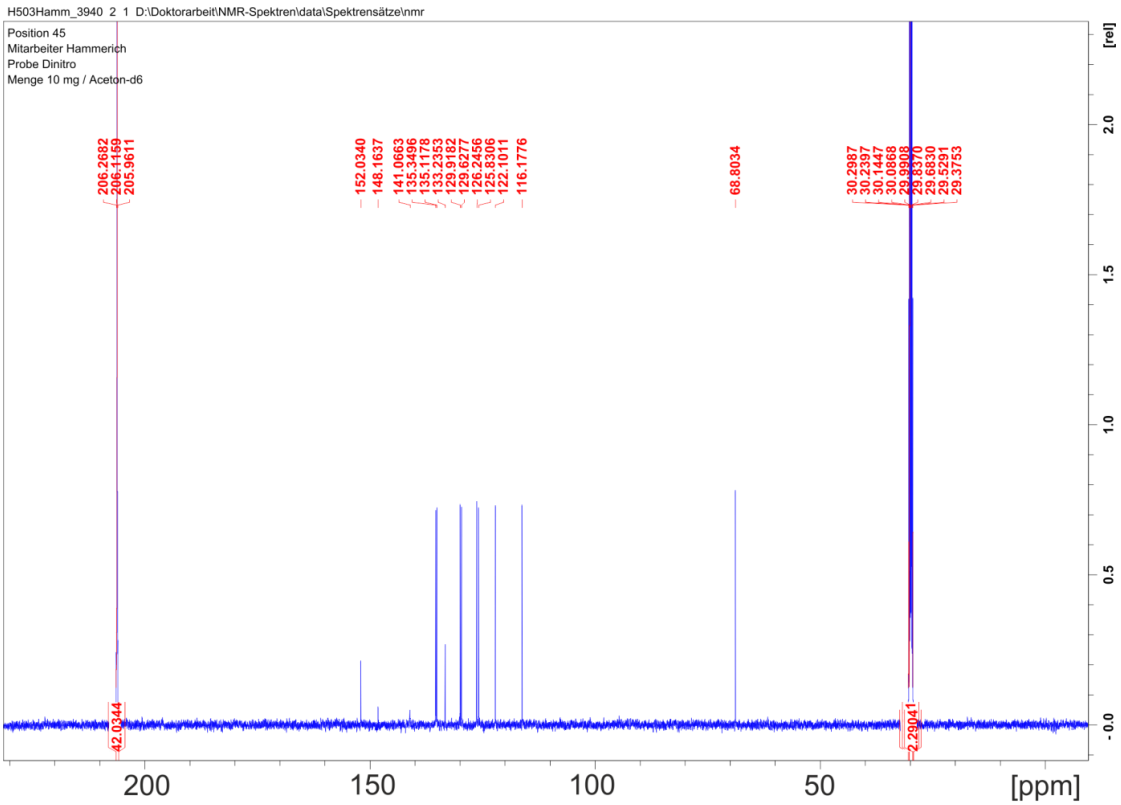

Figure S4: ^{13}C-NMR spectrum of compound **6**.

III.2. Synthesis of 12*H*-dibenzo[*b,f*][1,4,5]oxadiazocine-6-oxide (9 b)

To a solution of triethylamine (22 mL) , methanol (50 mL) , formic acid (1 mL) and water (14 mL) were added 1-nitro-2-((2'-nitobenzyl)oxy)benzene (**6**, 100 mg, 364 µmol) and lead powder (350 mg, 1.69 mmol) and the suspension was treated with ultrasound (450 W) for 5 h. After the first and second hour another portion lead (350 mg, 1.69 mmol) was added. The reaction mixture was filtrated and reduced in vacuo. The residue was extracted with dichloromethane, dried over magnesium sulfate and the solvent was evaporated. The residue was purified by column chromatography (0.040–0.063 mm, dichloromethane, R_f: 0.29) to obtain of a yellow solid (**7a/b**, 36 mg, 160 µmol, 44 %). As a side product the diazocine could be obtained as a yellow solid (**9**, 7 mg, 32 µmol, 9 %).

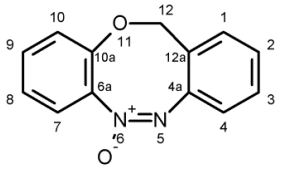

melting point: 141 °C.

^{1}H-NMR (600 MHz, DMSO-d_6:$CDCl_3$(1:1), 300 K, TMS): 7.40 (t, ^{3}J = 7.6 Hz, 1 H, *H-8*), 7.36 (d, ^{3}J = 7.5 Hz, 1 H, *H-10*), 7.26 (m, 2 H, *H-3,9*), 7.21 (d, ^{3}J = 8.2 Hz, 1 H, *H-1*), 7.13 (dd, ^{3}J = 8.2 Hz, 1 H, *H-7*), 7.01 (t, ^{3}J = 7.5 Hz, 1 H, *H-2*), 6.94 (d, ^{3}J = 8.3 Hz, 1 H, *H-4*), 5.27 (d, ^{3}J = 12.3 Hz, 1 H, *H-12*), 5.13 (d, ^{3}J = 12.3 Hz, 1 H, *H-12*) ppm.

^{13}C-NMR (125 MHz, DMSO-d_6:$CDCl_3$(1:1), 300 K, TMS): 145.32 (*C-6a*), 144.44 (*C-4a*), 139.66 (*C-12a*), 130.17 (*C-3*), 129.45 (*C-10*), 128.83 (*C-8*), 126.44 (*C-9*), 124.12 (*C-10a*), 122.01(*C-1*,*2*), 120.15 (*C-7*), 120.07 (*C-4*), 69.28 (*C-12*) ppm.

^{15}N-NMR (600 MHz, DMSO-d_6:$CDCl_3$(1:1), 300 K, TMS): δ = 363.6 (s, 1 N, *N-6*), 342.3 (s, 1 N, *N-5*) ppm.

IR (ATR): $\tilde{\nu}$ = 3037 (w), 2828 (w), 2887 (w), 1597 (w), 1468 (s), 1443 (s), 1343 (m), 1225 (m), 1195 (m), 981 (m), 765 (s), 678 (w), 639 (w), 611 (m) cm^{-1}.

MS (EI, 70 eV): m/z = 226.07 $[M]^+$, 196.07 $[M-CH_2O]^+$, 181.07 $[M-CHO_2]^+$, 141.07 , 120.04 $[M-C_7H_6O]^+$.

MS (HR) (EI, 70 eV):[m/z] = calc.: 226.07423, found: 226.07381

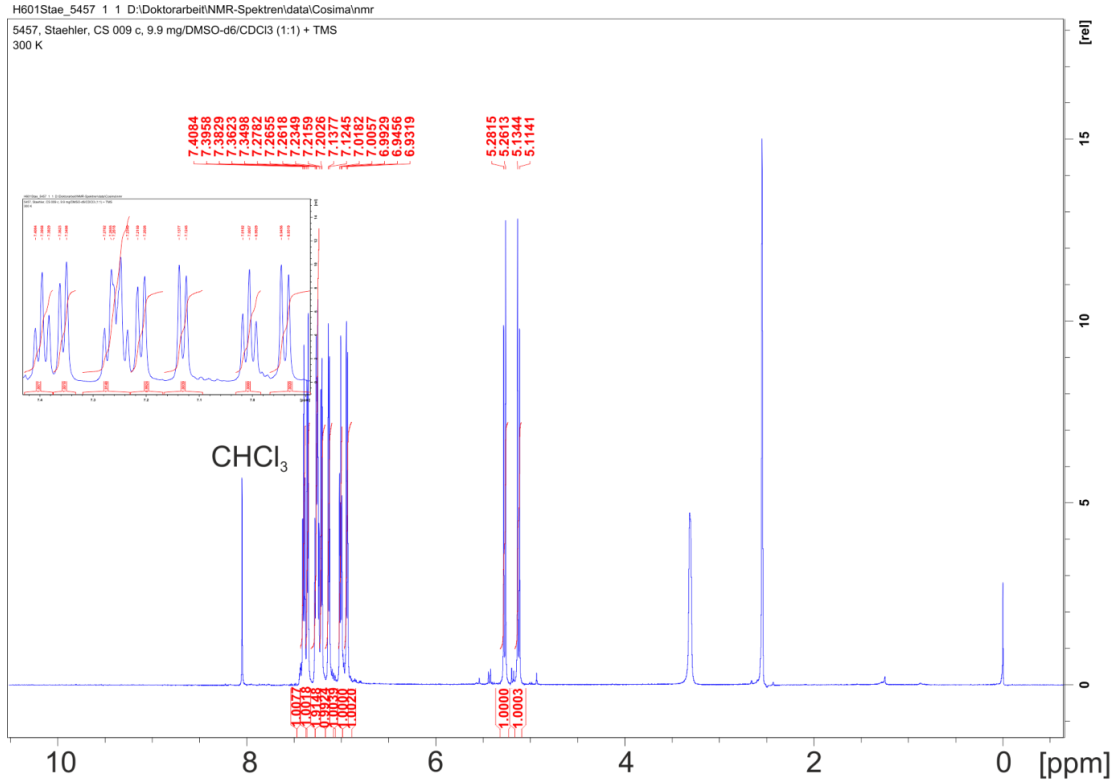

Figure S5: ^{1}H-NMR spectrum of compound **7b**.

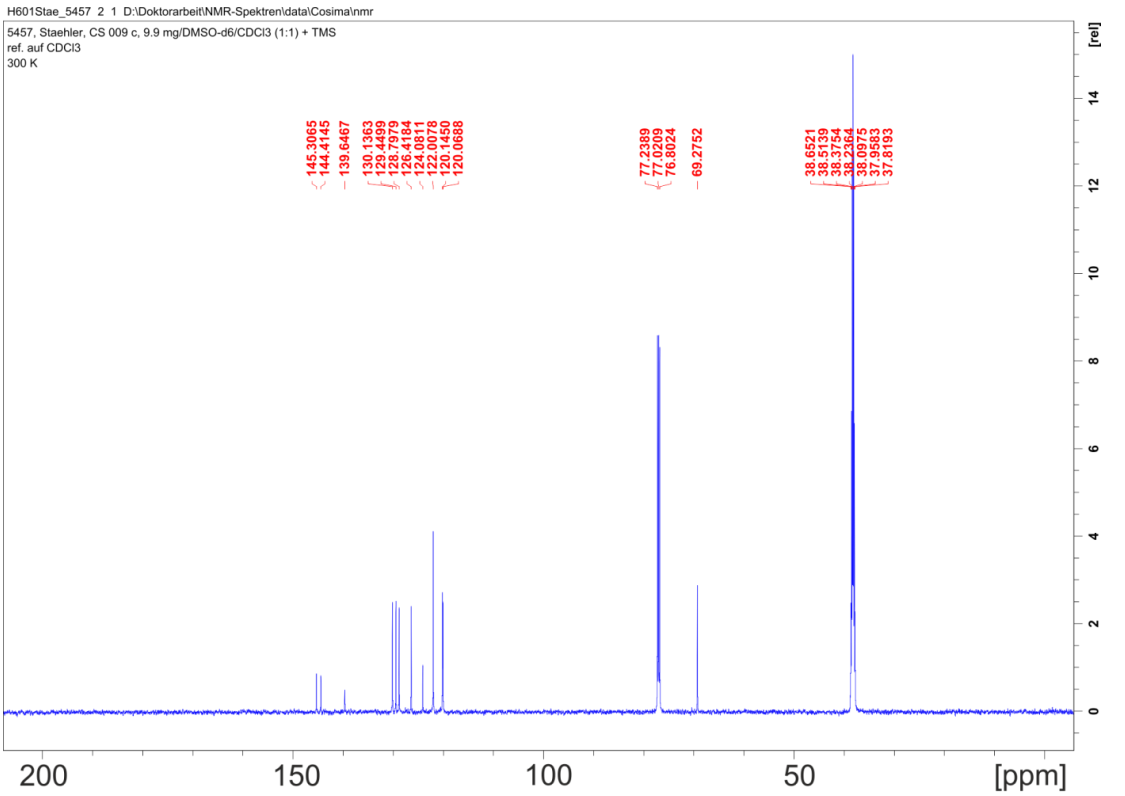

Figure S6: ^{13}C-NMR spectrum of compound **7b**.

III.3 Synthesis of 12*H*-dibenzo[*b,f*][1,4,5]oxadiazocine (2)

12*H*-dibenzo[*b*,*f*][1,4,5]oxadiazocine-6-oxid (**9a/b**, 89.0 mg, 390 µmol) was dissolved under a nitrogen atmosphere in THF (5 mL) and triphenylphosphine (521 mg, 1.99 mmol) and molybdenum(VI)dichloride dioxide (18.0 mg, 91.0 µmol) were added. The solution was refluxed for 3 h, the solvent was evaporated and the residue was purified by column chromatography (0.040–0.063 mm, dichloromethane, R_f: 0.65) to obtain of a yellow solid (34 mg, 163 mmol, 42 %) .

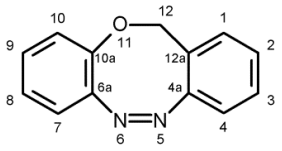

melting point: 106 °C

^{1}H-NMR (500 MHz, acetone-d_6, 300 K): δ = 7.47–7.41 (m, 2 H, *H-1*,*3*), 7.30 (td, ^3J = 7.5 Hz, ^4J = 1.2 Hz, 1 H, *H-2*), 7.20 (dd, ^3J = 7.9 Hz, ^4J = 1.1 Hz, 1 H, *H-4*), 7.09 (td, ^3J = 7.7 Hz, ^4J = 1.8 Hz, 1 H, *H-9*), 6.98 (td, ^3J = 7.6 Hz, ^4J = 1.3 Hz, 1 H, *H-8*), 6.91 (dd, ^3J = 8.0 Hz, ^4J = 1.8 Hz, 1 H, *H-7*), 6.87 (dd, ^3J = 8.2 Hz, ^4J = 1.3 Hz, 1 H, *H-10*), 4.97 (s, 2 H, *H-12*) ppm.

^{13}C-NMR (125 MHz, acetone−d_6, 300 K): δ = 157.87 (*C-4a*), 147.26 (*C-6a*), 144.12 (*C-10a*), 133.21(*C-3*), 130.64 (*C-1*), 129.74 (*C-9*), 129.12 (*C-2*), 123.17 (*C-8*), 123.00 (*C-7*), 122.71 (*C-12a*), 122.13 (*C-10*), 120.81 (*C-4*), 71.94 (*C-12*) ppm.

IR (ATR): $\tilde{\nu}$ = 2908 (w), 1596 (w), 1523 (w), 1465 (m), 1434 (m), 1202 (m), 989 (m), 764 (s) cm^{-1}.

UV/Vis (acetonitrile): λ(lg ε) = 398 (2.72) nm.

MS (EI, 70 eV): m/z = 210.08 $[M]^+$, 181.06 $[M-CH_2O]^+$, 152.06 $[M-CH_2N_2O]^+$, 90.04 $[M-C_7H_6NO]^+$.

MS (HR) (EI, 70 eV):[m/z] = calc.: 210.07931, found: 210.07923.

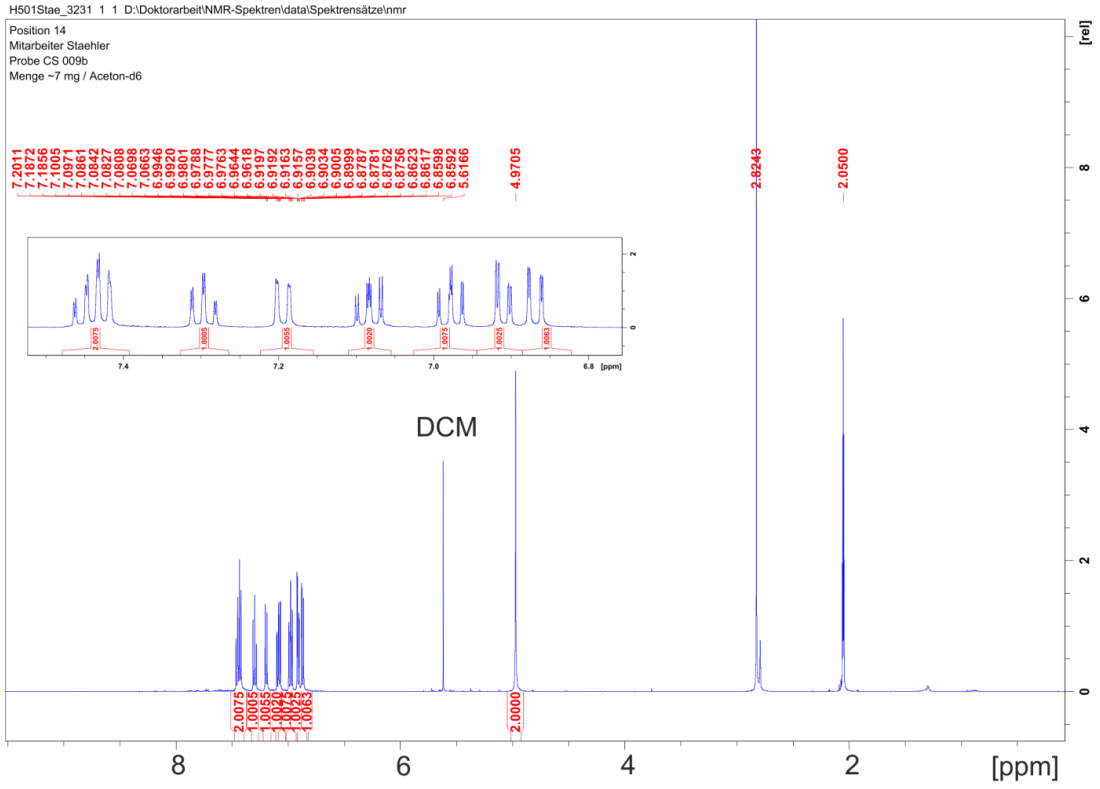

Figure S7: ^{1}H-NMR spectrum of compound **2**.

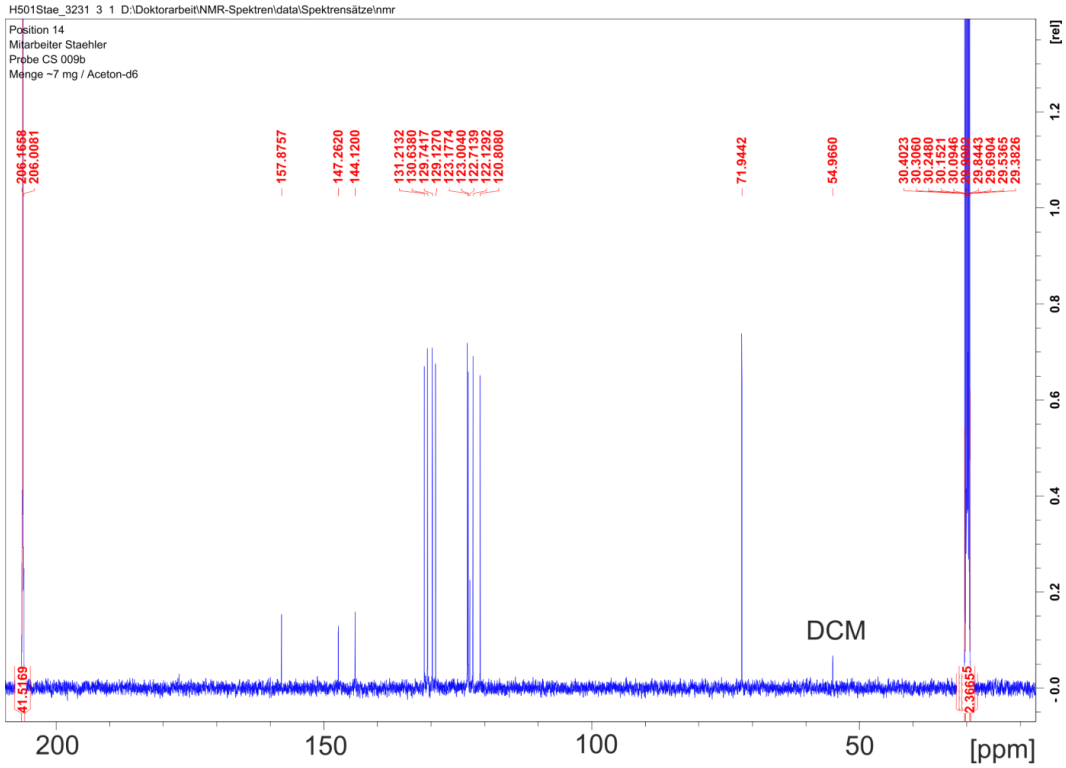

Figure S8: ^{13}C-NMR spectrum of compound **2**.

III.4 Synthesis of 2'-nitrobenzyl-2-nitrophenyl-sulfide (6)

Bis(2-nitrophenyl)disulfide (**7**, 2.00 g, 6.48 mmol) was suspended in THF (40 mL) under nitrogen atmosphere, sodium borohydride (1.22 mg, 32.4 mmol) was added to this suspension (solution turns immediately red) and heated up to 60 °C 1 h. To this solution 2-nitrobenzylbromide (**4**, 2.80 g, 13.0 mmol) was added and stirred 16 h at room temperature (solution turns yellow). The reaction mixture was carefully poured on ice water. The precipitated solid was filtered and washed with water and methanol. The product was obtained as a yellow solid (1.69 g, 5.85 mmol, 45 %).

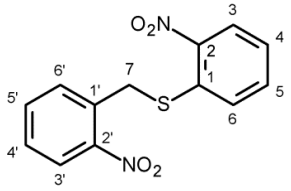

melting point: 165.6 °C

^{1}H-NMR (500 MHz, acetone-d_6, 300 K): δ = 8.18 (dd, ^{3}J = 8.2 Hz, ^{4}J = 1.3 Hz, 1 H, *H-3*), 8.07 (dd, ^{3}J = 8.2 Hz, ^{4}J = 1.2 Hz, 1 H, *H-3'*), 7.77-7.69 (m, 4H, *H-5, 5', 6, 6'*), 7.61 (m_c, 1 H, *H-4'*), 7.47 (ddd, ^{3}J = 8.2 Hz, ^{3}J = 8.3 Hz, ^{4}J = 1.6 Hz, 1 H, *H-4*), 4.71 (s, 2 H, *H-7*) ppm.

^{13}C-NMR (125 MHz, acetone−d_6, 300 K): δ = 150.13(C-2'), 147.94 (C-2), 136.26 (C-1), 134.79 (C-5), 134.47 (C-5'), 133.35 (C-6), 131.78 (C-1'), 130.11 (C-4'), 129.26 (C-6'), 126.81 (C-4), 126.54 (C-3), 126.16 (C-3'), 35.17 (*C*-7) ppm.

IR (ATR): $\tilde{\nu}$ = 3118.33 (w), 1596.24 (w), 1565.58 (m), 1527.51 (m), 1505.15 (s), 1428.01 (m), 1334.40 (s), 1308.91 (s), 1256.71 (m), 1231.44 (m), 1168.31 (w), 1106.66 (m), 1061.87 (w), 1045.75 (m), 954.13 (w), 858.20 (m), 782.28 (s), 734.90 (s), 712.24 (s), 653.32 (s) cm^{-1}.

MS (EI, 70 eV): m/z = 290.04 $[M]^+$, 155.00 $[C_6H_4NO_2S]^+$, 136.04$[C_7H_6NO_2]^+$.

MS (HR) (EI, 70 eV): [m/z] = calc.: 290.03613, found: 290.03624.

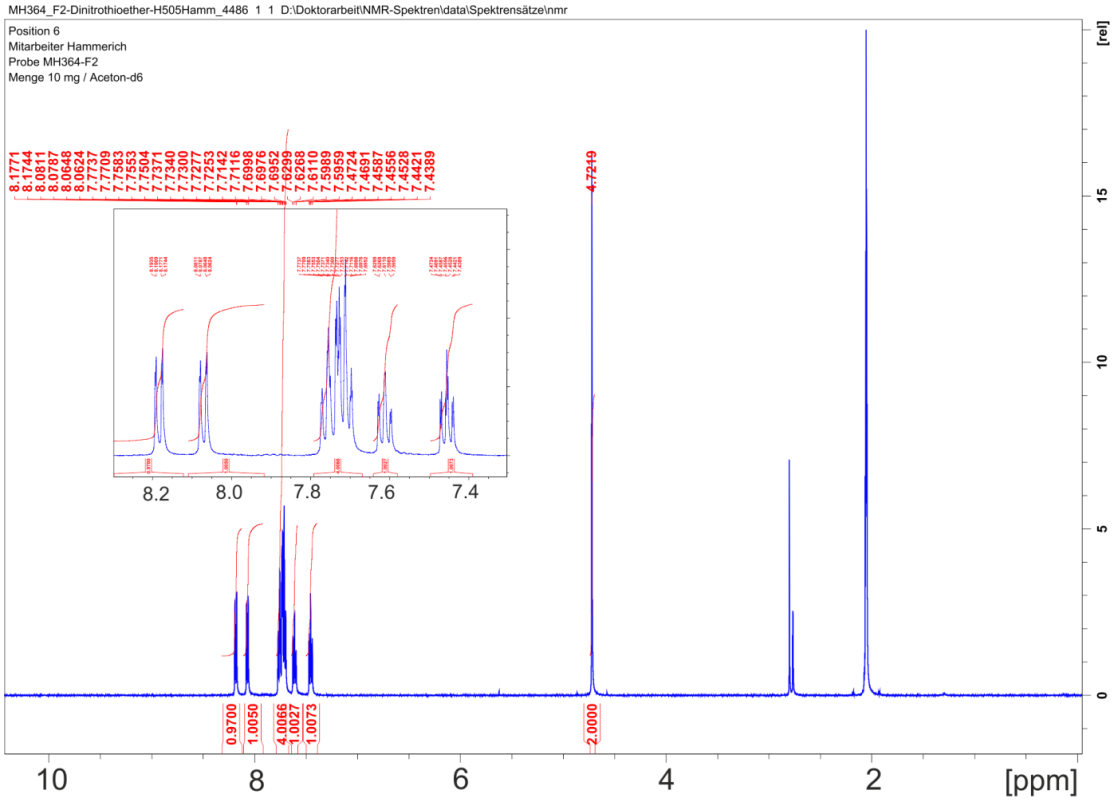

Figure S9: ^{1}H-NMR spectrum of compound **8**.

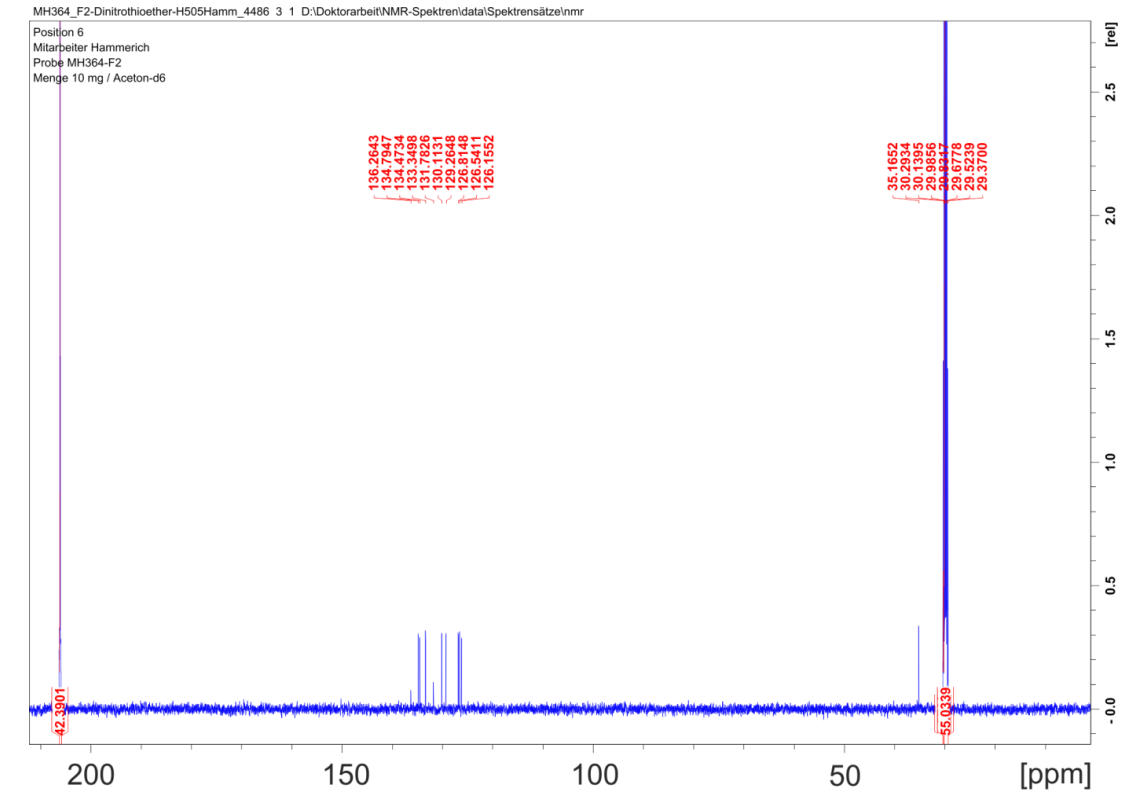

Figure S10: ^{13}C-NMR spectrum of compound **8**.

III.5 Synthesis of 12H-dibenzo[b,f][1,4,5]thiadiazocine 6-oxide (10b) and 12H-dibenzo[b,f][1,4,5]thiadiazocine 5-oxide (10a)

To a solution of triethylamine (22 mL), methanol (50 mL), formic acid (1 mL) and water (14 mL), 2'-nitrobenzyl-2-nitrophenyl-sulfide (**6**, 100 mg, 344 µmol) and lead powder (350 mg, 1.69 mmol) were added, and the solution was treated with ultrasound (450W) for 5 h. After the first and second hour another portions lead (350 mg, 1.69 mmol) were added. The reaction mixture was filtrated and reduced in vacuo. The residue was extracted with dichloromethane, dried over magnesium sulfate and the solvent was evaporated. The residue was purified by column chromatography (0.040–0.063 mm, dichloromethane, R_f: 0.29) to obtain a mixture of the regioisomers of both azoxy compounds (36 mg, 160 µmol, 44 %) as yellow solid. As a side product the diazocine could be obtained as a yellow solid (7 mg, 32 µmol, 9 %).

The azoxy compounds were used for the next synthetic step as a mixture of regioisomers.

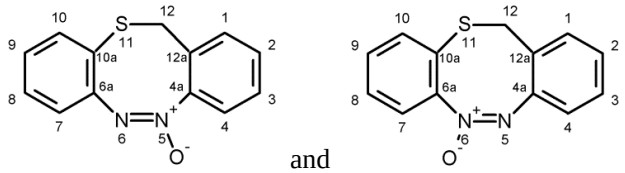

melting point: 129.9 °C

MS (EI, 70 eV): m/z = 242.04 (X) $[M]^+$, 225.04 (100), 184.03, 136.02.

MS (HR) (EI, 70 eV): [m/z] = calc.: 242.05138, found: 242.05127.

IR (ATR): $\tilde{\nu}$ = 3280.52 (m), 3242.53 (m), 3507.86 (m), 1603.56 (w), 1568.61 (s), 1448.77 (s), 1347.71 (m), 1194.35 (w), 1131.15 (w), 1034.00 (w), 924.48 (m), 880.93 (m), 854.04 (m), 809.66 (m), 760.89 (s), 743.84 (s), 743.84 (s), 723.04 (m), 692.78 (m), 660.14 (m), 610.84 (m), 583.58 (m), 564.12 (m), 504.93 (m) cm^{-1}.

II.6 Synthesis of 12H-dibenzo[b,f][1,4,5]thiadiazocine (3)

A mixture of 12H-dibenzo[b,f][1,4,5]thiadiazocine 6-oxide and 12H-dibenzo[b,f][1,4,5]thiadiazocine 5-oxide (**10b**/**10a**, 50 mg, 206 µmol) and lead shots (341 mg, 1.65 mmol) were placed in a ball mill with 20 balls and were shaken for 4 h with 40 Hz. The black powder was extracted with dichloromethane. The solvent was evaporated and the crude product was purified by column chromatography (0.040–0.063 mm, dichloromethane). The product was obtained as yellow solid (26 mg, 115 µmol, 56 %).

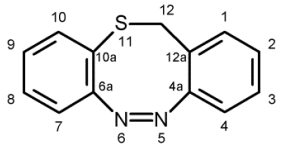

melting point: 112.9 °C

^{1}H-NMR (500 MHz, acetone-d_6, 300 K): δ = 7.52 – 7.20 (m, 3 H, *H-1*, *H-3*, *H-8*), 7.12 (td, ^{3}J = 7.6 Hz, ^{4}J = 1.3 Hz, 1 H, *H-2*), 7.10 (dd, ^{3}J = 7.8 Hz, ^{4}J = 1.2 Hz, 1 H, *H-10*), 6.99 (ddd, ^{3}J = 7.5 Hz, ^{3}J = 7.8 Hz, ^{4}J = 1.4 Hz, 1 H, *H-9*), 6.78 (dd, ^{3}J = 7.6 Hz, ^{4}J = 0.7 Hz, 1 H, H-4), 6.76 (dd, ^{3}J = 7.9 Hz, ^{4}J = 1.4 Hz, 1 H, *H-7*), 3.98 (d, ^{2}J = 11.6 Hz, 1 H, *H-12*), 3.84 (d. ^{2}J = 11.6 Hz, 1 H, *H-12*) ppm.

^{13}C-NMR (125 MHz, acetone−d_6, 300 K): δ = 158.30 (*C-6a*), 158.58 (*C-4a*), 134.28 (*C-10*), 130.31 (*C-1*), 129.27 (*C-3*), 128.80 (*C-8*), 128.29 (*C-2*), 127.86 (*C-9*), 124.97 (*C-12a*), 122.94 (*C-10a*), 120.16, (*C-7*) 117.81 (*C-4*), 35.12 (*C-12*) ppm.

IR (ATR): $\tilde{\nu}$ = 2923.65 (m), 1517.7(w), 1476.23 (m), 1454.55 (m), 1260.02 (m), 1155.28 (m), 1087.98 (m), 1064.49 (m), 1030.39 (m), 954.58 (m), 915.22 (m), 892.30 (s), 801.76 (m), 768.92 (s), 734.28 (s), 691.15 (s), 659.16 (s), 578.66 (m) cm^{-1}.

UV/Vis (acetonitrile): λ(lg ε) = 398 (2.61) nm.

MS (EI, 70 eV): m/z = 226.05 (100) $[M]^{+}$, 199.04 (X) 165.07 (X).

MS (HR) (EI, 70 eV): [m/z] = calc.: 226.05647, found: 226.05602.

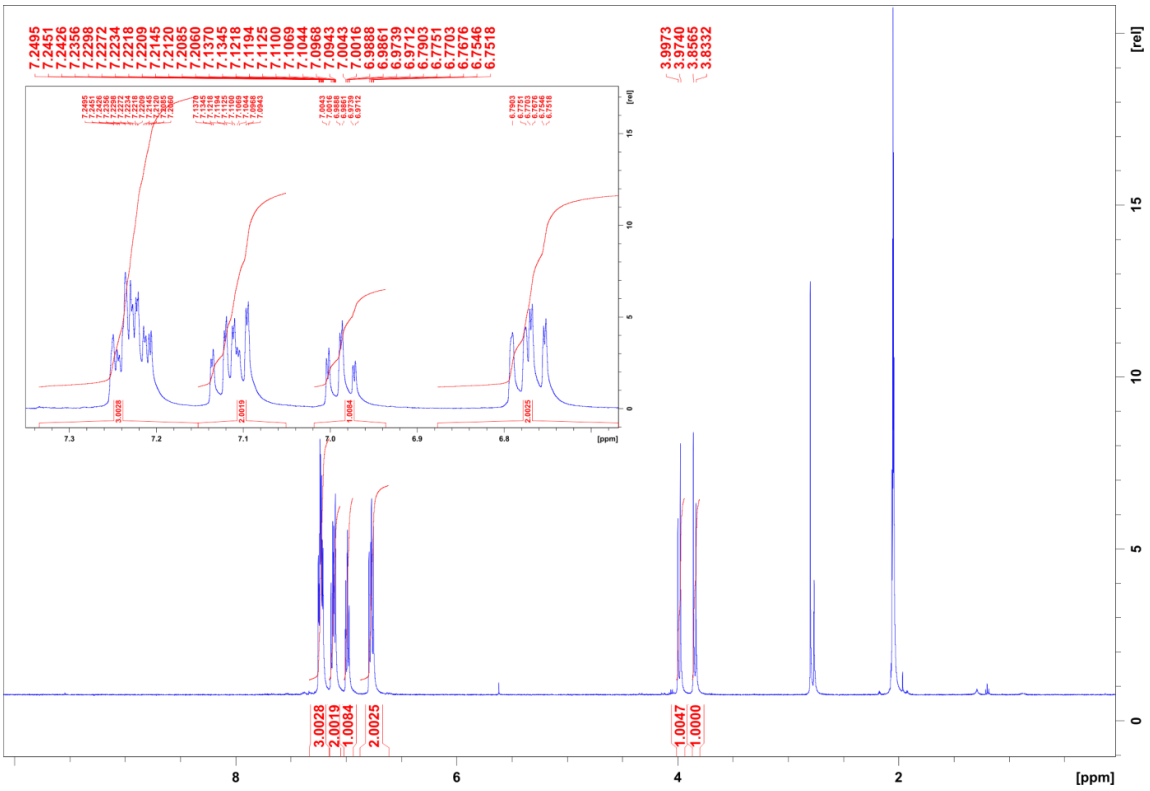

Figure S11: ^{1}H-NMR spectrum of compound **3**

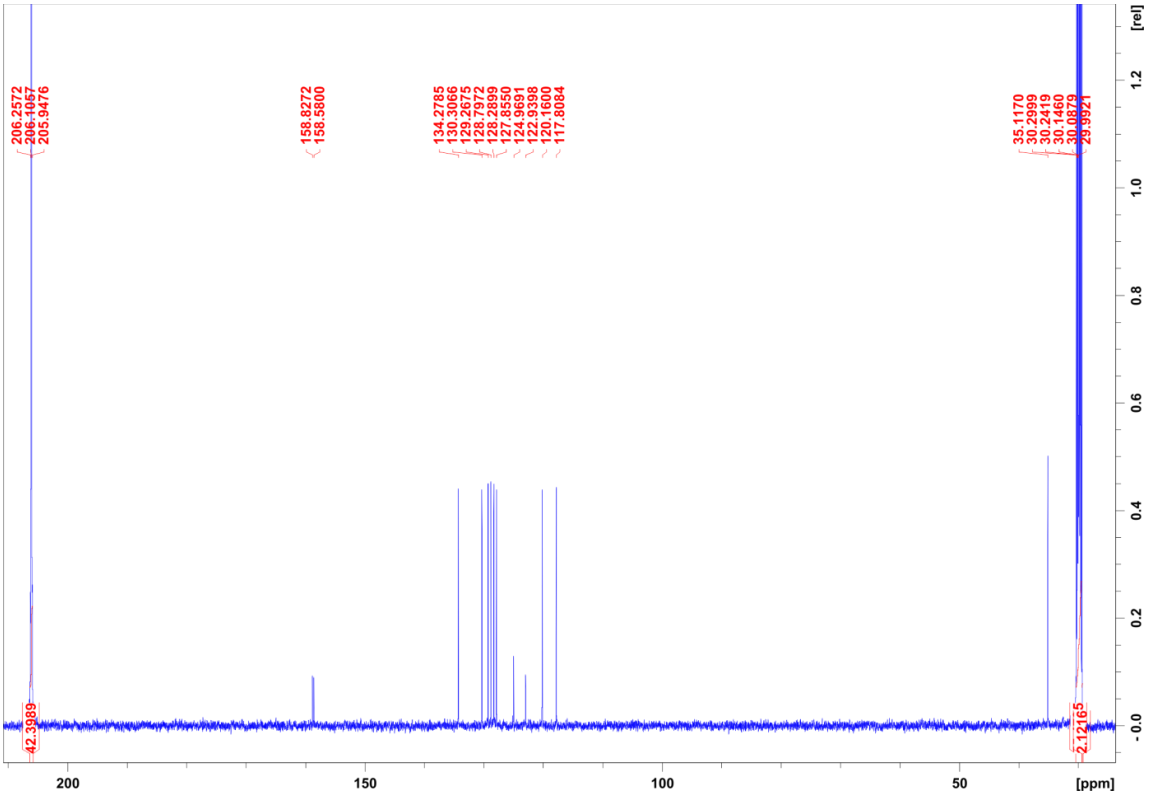

Figure S12: ^{13}C-NMR spectrum of compound **3**

IV. ^{1}H- NMR measurements

IV.1 ^{1} NMR measurements of oxygen diazocine 2 at 198 K

As the rate of the back isomerization (*cis* → trans) of O-diazocine **2** is fast at room temperature, investigations of the photo switching can only be performed at low temperature. Therefore, the sample was cooled within the NMR spectrometer to 198 K. Upon cooling of *cis*-**2** we observe coalescence of the methylene protons in the bridge. We attribute the splitting of the singlet at 4.97 ppm into two doublets to the freezing of the ring inversion of the boat conformation leading to the separation of the signals for the pseudo equatorial and pseudo axial protons.

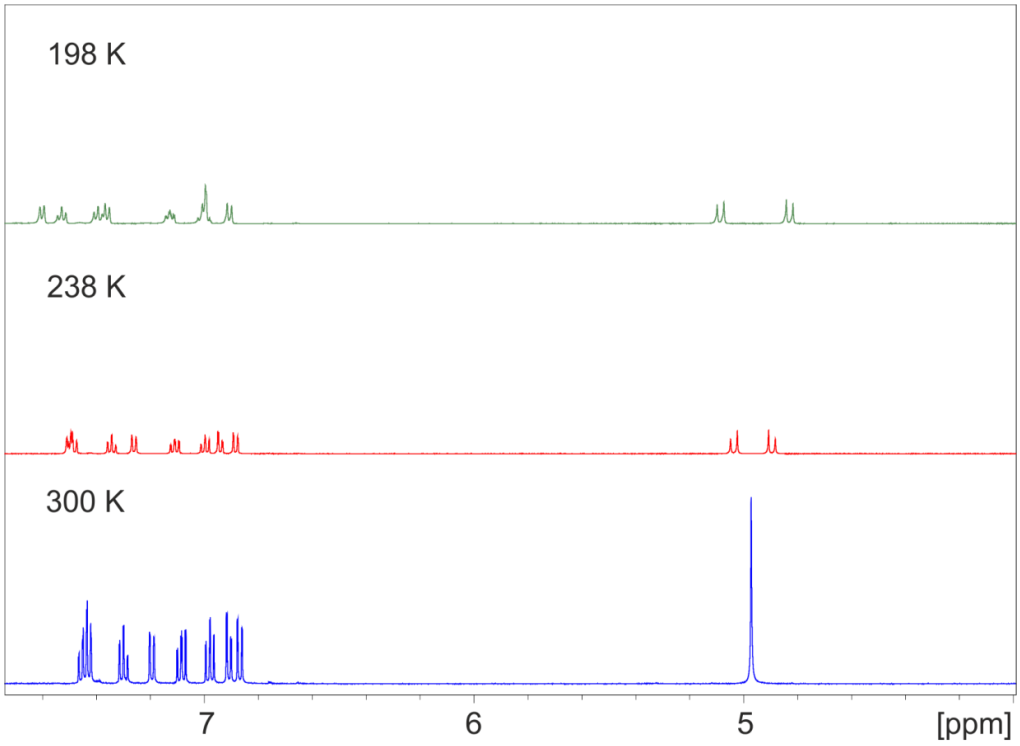

Figure S13: ^{1}H-NMR spectra of oxygen diazocine **2** upon lowering of the temperature from room temperature to 198 K. Ring inversion is fast at room temperature on the NMR time scale. The methylene protons appear as a sharp singlet. At lower temperatures the methylene protons split into two separate signals (doublets) for the pseudo equatorial and pseudo axial protons.

IV.2 Determination of the photostationary state of O-diazocine 2

^{1}H NMR spectra of compound **2** were measured in deuterated acetone at 198 K before and after irradiation with 385 nm for 15 min. The probe was irradiated outside the NMR spectrometer in an NMR tube at 195 K immersed in a quartz Dewar with acetone and dry ice. After irradiation the probe was transferred rapidly to the precooled spectrometer to avoid warming of the sample. According to integration of characteristic signals in ^{1}H NMR spectrum the oxygen diazocine **2** switches to 80 % to the *trans* isomer.

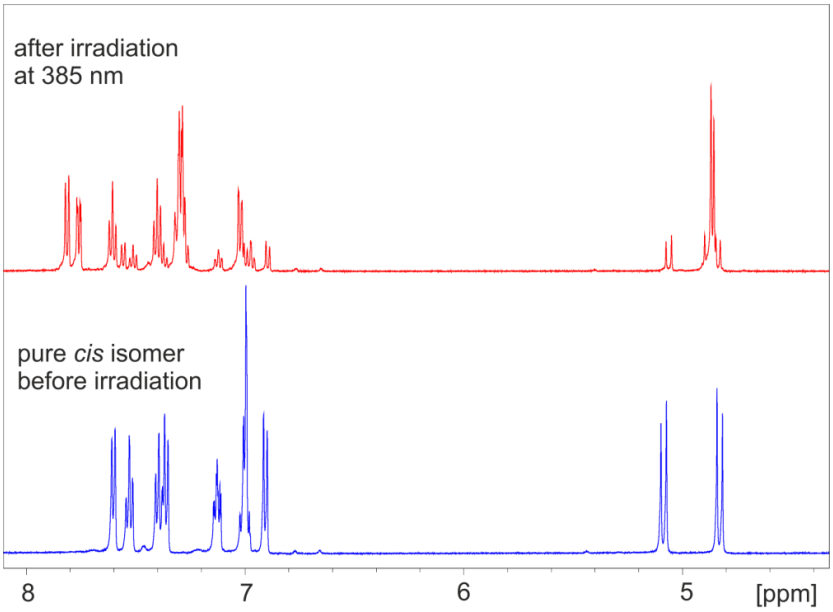

Figure S14: ^{1}NMR spectra of oxygen diazocine **2** at 198 K before (blue) and after irradiation (red).

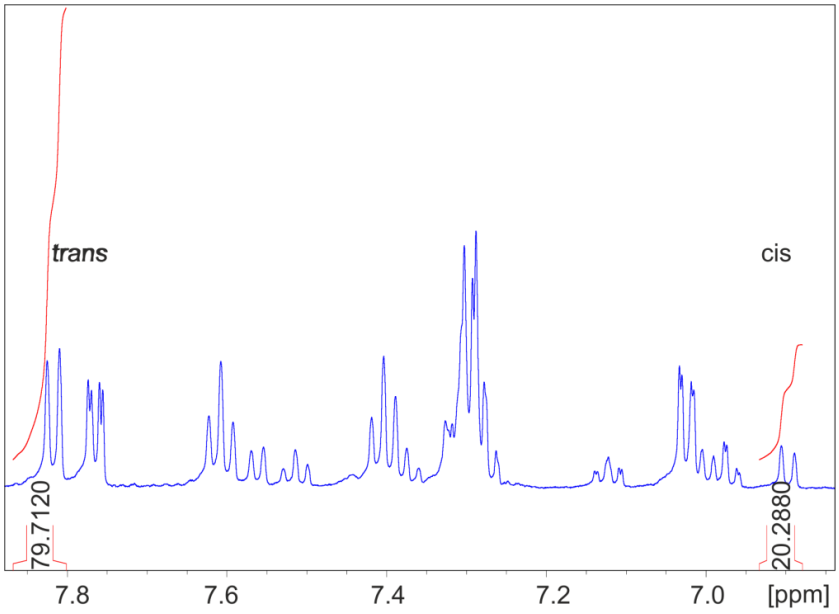

Figure S15: aromatic region of the ^{1}NMR spectrum of oxygen diazocine **2** at 198 K after irradiation.

IV.3 Kinetic measurements of the thermochemical *trans->cis* isomerization of O-diazocine 2

^{1}H NMR spectra of compound **2** were measured in deuterated acetone at 278 K before and after irradiation with 385 nm (Nichia LED's) for 15 min (the probe was irradiated at 195 K with the NMR tube immersed in a quartz Dewar with acetone and dry ice outside the NMR spectrometer). Several spectra were recorded within a period of serveral half-lives (every fifth spectrum is shown in the graphic below, Figure S16 and Figure S17).

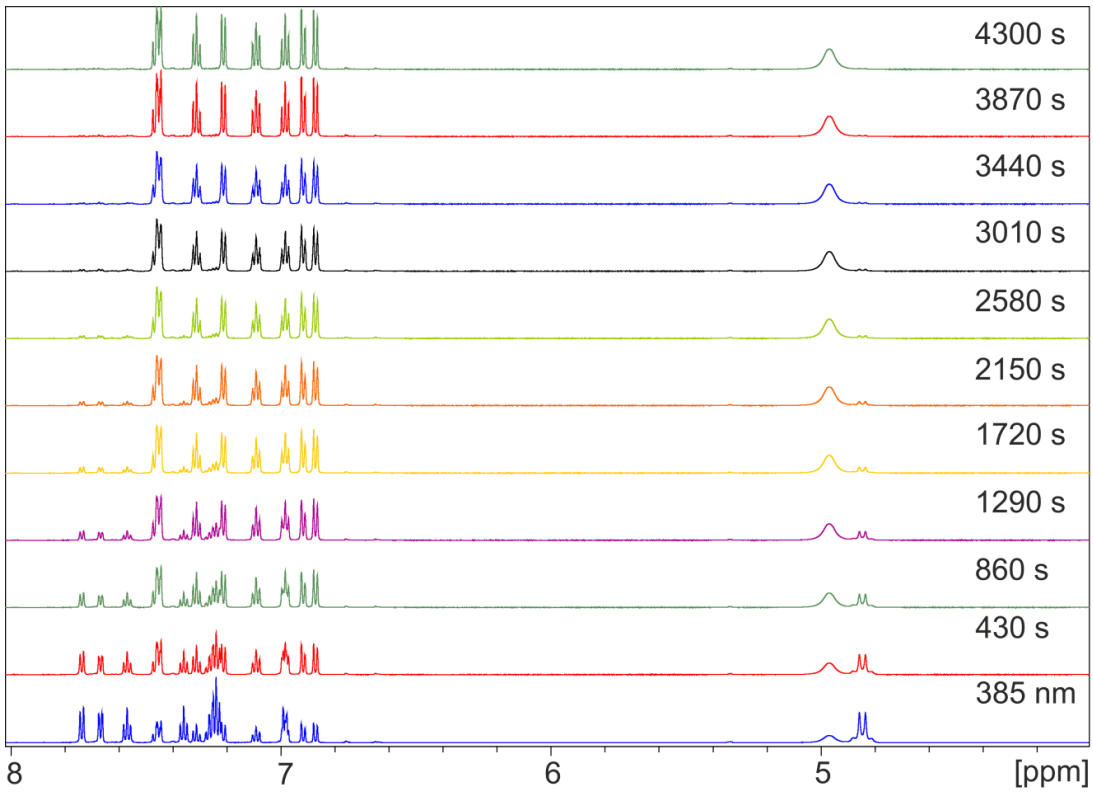

Figure S16: ^{1}H-NMR spectra of oxygen diazocine **2** after irradiation with 385 nm (directly after irradiation: blue spectrum at the bottom) and at regular time intervals after irradiation at 287 K.

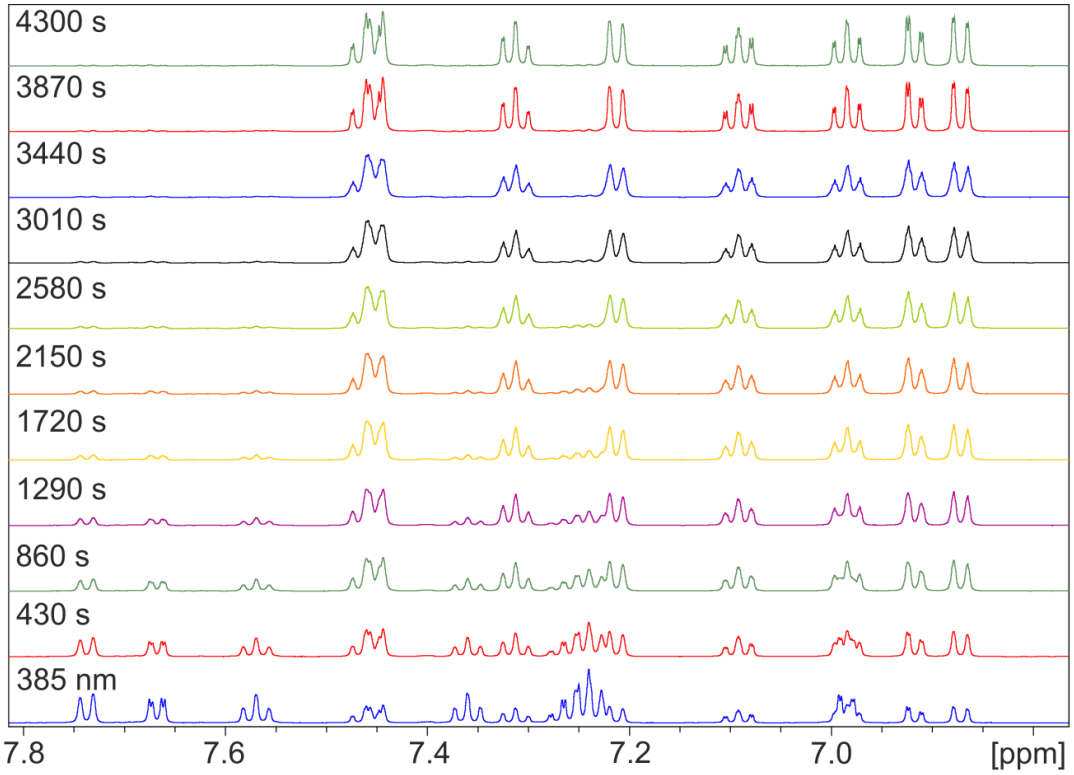

Figure S17: Aromatic region of the ^{1}H-NMR spectra of oxygen diazocine **2** after irradiation with 385 nm (directly after irradiation: blue spectrum at the bottom) and at regular time intervals after irradiation at 287 K.

IV.4 Thermal half-life of O-diazocine 2 determined with ^{1}H-NMR spectroscopy

To determine the half-life of compound **2** with ^{1}H-NMR spectroscopy the integrals of the *cis* and *trans* isomer were plotted against time. The half-life was calculated with an exponential fit.

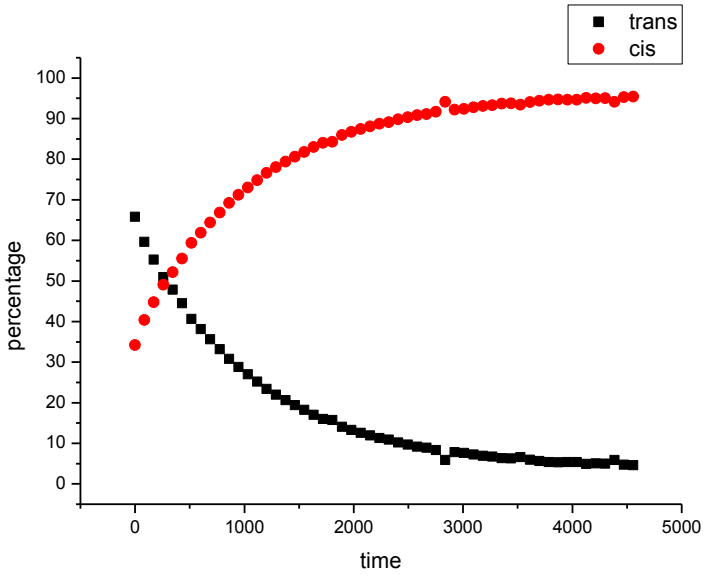

Figure S18: Percentage of *cis* and *trans* isomer of compound **2** plotted as a function of time.

Table S2. Exponential fit of the cis and *trans* signal for the thermal back isomerization to the *cis* isomer.

cis	*trans*
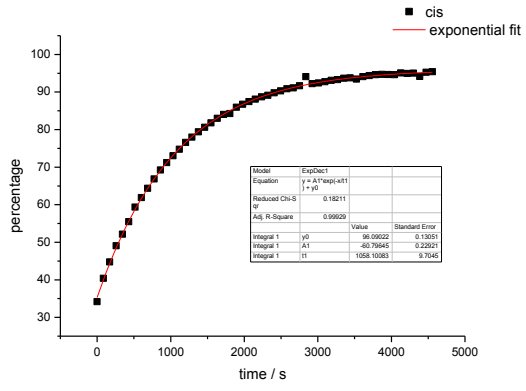	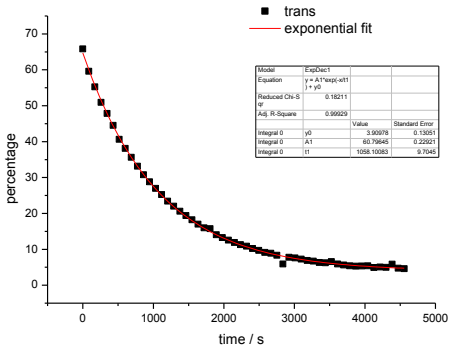
k = 9.45 ± 0.09 *10^{-4} mol/s	k = 9.45±0.09 *10^{-4} mol/s
$t_{1/2}$ = 733±6 s = 12.2±0.1 min	$t_{1/2}$ = 733±6 s = 12.2±0.1 min

IV.5 Determination of the photostationary state of sulfur diazocine 3

^{1}H NMR spectra of compound **3** were measured in deuterated acetone at 300 K before and after irradiation with 405 nm for 15 min. It could be shown, that the sulfur diazocine **3** switches to 70 % to the *trans* isomer.

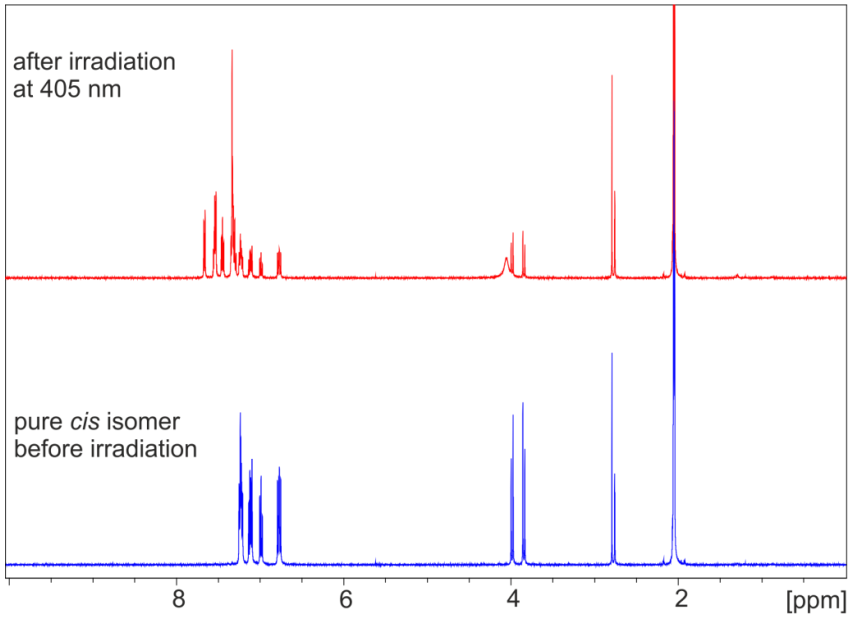

Figure S19: ^{1}NMR spectra of sulfur diazocine **3** before (blue) and after irradiation (red).

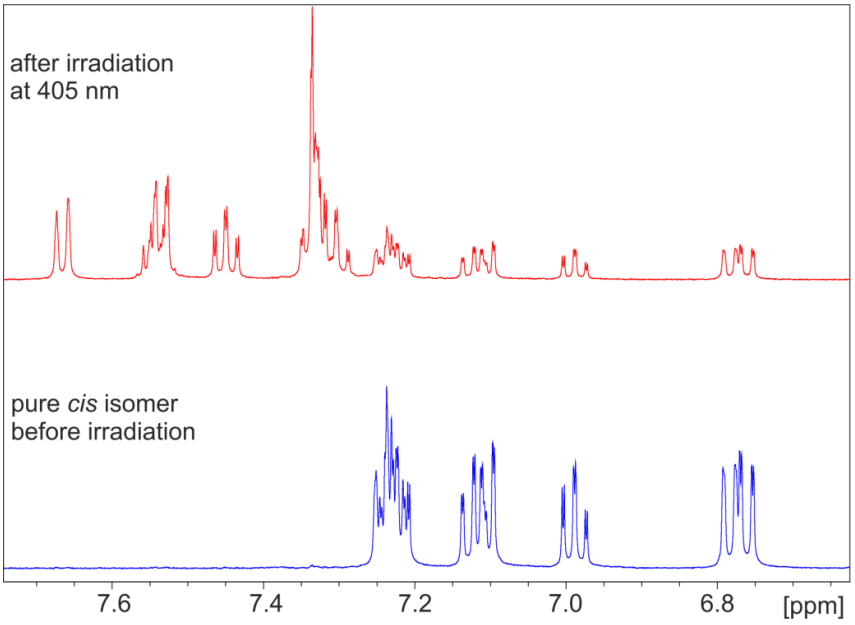

Figure S20: Aromatic regions of the ^{1}NMR spectra of sulfur diazocine **3** before (blue) and after irradiation (red).

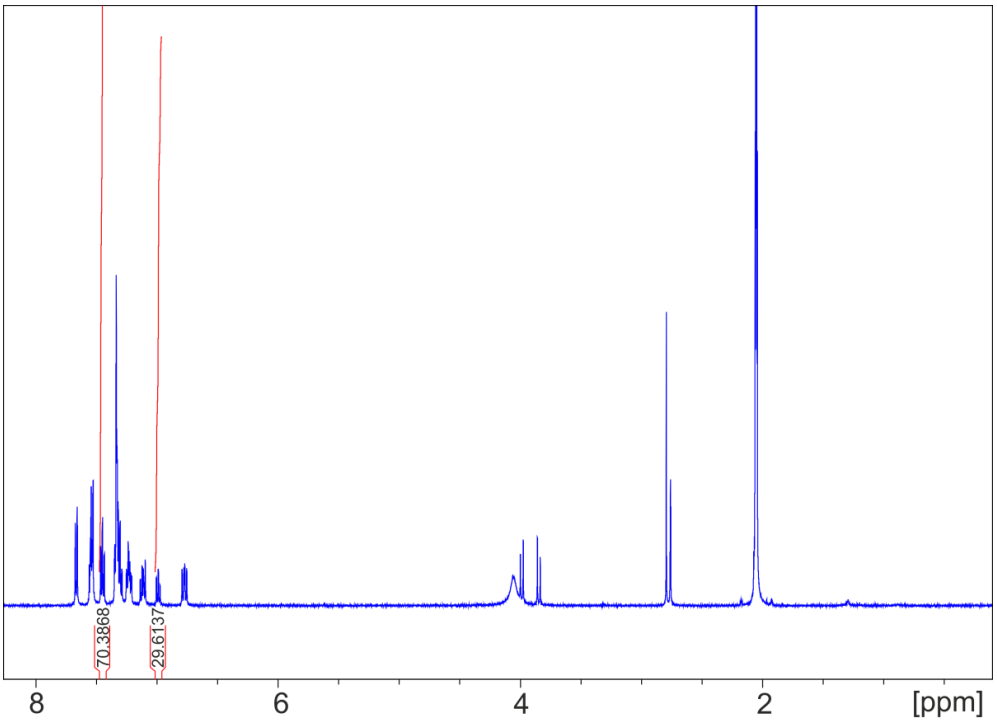

Figure S21: Photostationary state of sulfur diazocine **3** after irradiation with 405 nm (*trans*: 70% and *cis*: 30 %).

IV.6 Kinetic measurements of the thermochemical *trans->cis* isomerization of sulfur diazocine 3

^{1}H NMR spectra of compound **3** were measured in deuterated acetone at 300 K before and after irradiation with 400 nm for 5 min. Several spectra were recorded over several half-lives (every fifth spectrum is shown in the graphic below).

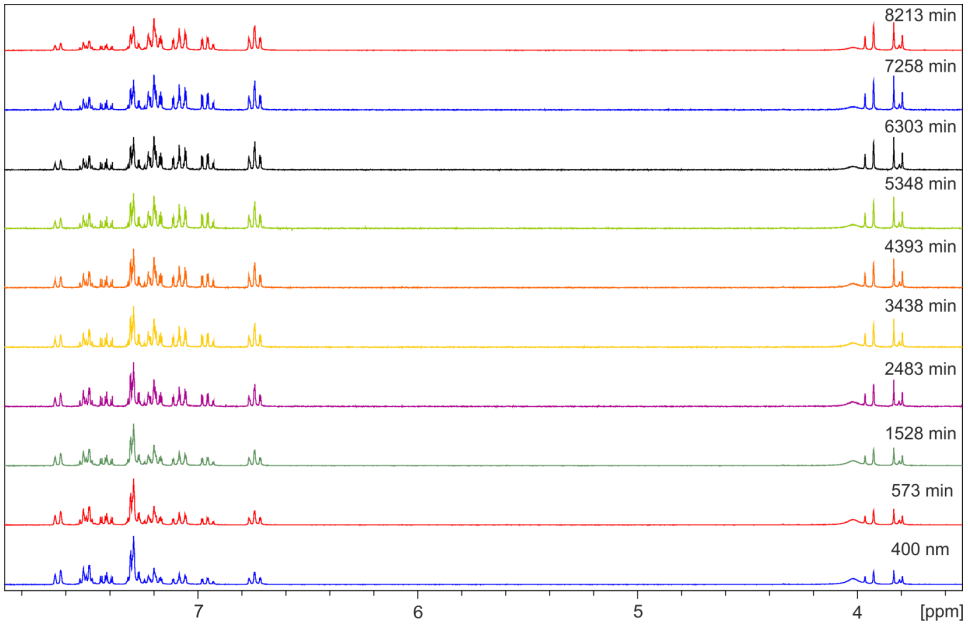

Figure S22: ^{1}H-NMR spectra of sulfur diazocine **3** after irradiation with 405 nm (blue spectrum at the bottom) and spectra measured after regular time intervals at 300 K.

IV.7 Half-life of sulfur diazocine 3 determined with ^{1}H NMR spectroscopy

To determine the half-life of compound **3** with ^{1}H NMR spectroscopy the integrals of two aromatic signals for both isomers were plotted against time. Half-life was calculated with exponential fit.

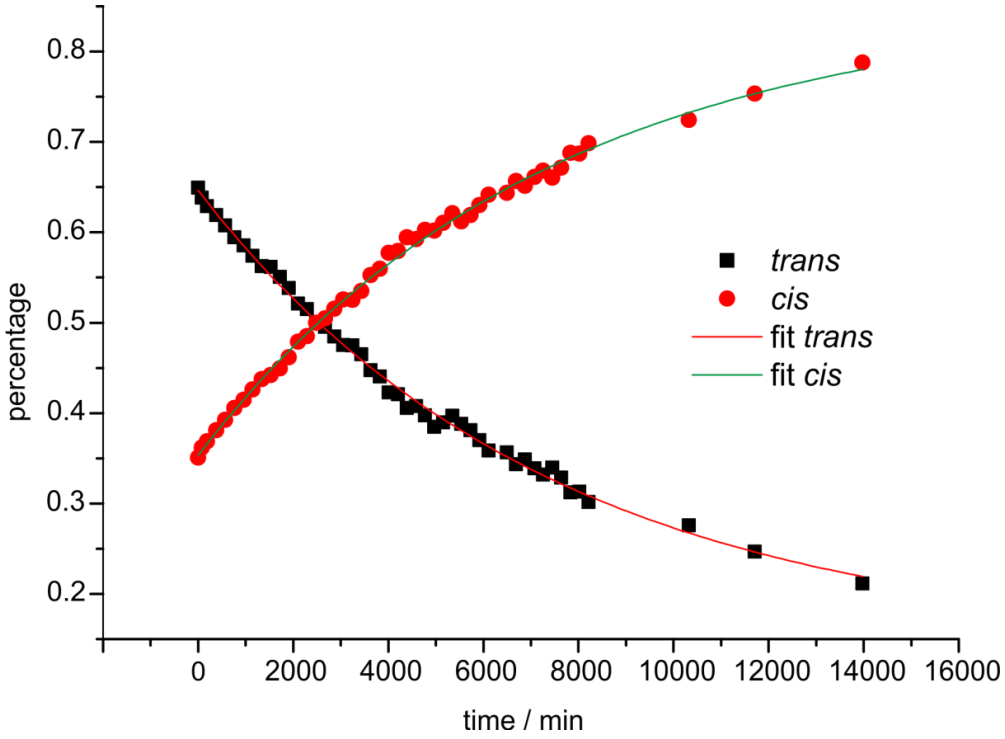

Figure S23: Percentage of *cis* and *trans* isomer of compound **3** plotted against time.

Table S3. Exponential fit of the *cis* and *trans* signal for the thermal back isomerization to the *cis* isomer.

cis	*trans*
k = 1.37±0.048 *10^{-4} mol/min	k = 1.36±0.054 *10^{-4} mol/min
$t_{1/2}$ = 5050±161 min = 84±2.6 h	$t_{1/2}$ = 5093±190 min = 85±3.18 h

V. UV/vis switching experiment

V. I UV/Vis measurements of oxygen diazocine 2

A solution of oxygen diazocine **2** in THF was irradiated with 385 nm for 5 minutes and UV/vis spectra were recorded every two minutes at constant temperatures. The absorption maxima were plotted against time and the reaction time constants were determined.

V.1.1 Temperature T = 262 K

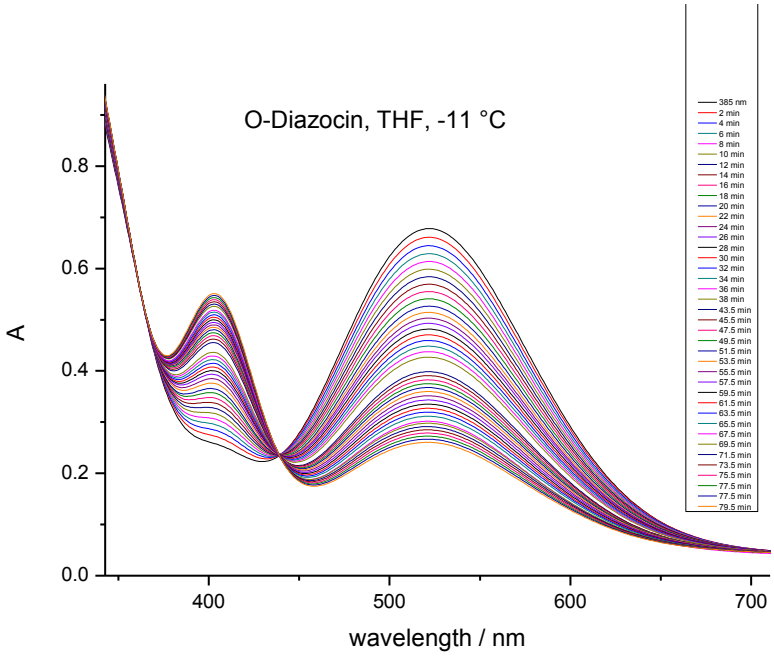

Figure S24: UV/Vis spectra of oxygen diazocine **2** after irradiation with 385 nm at 262 K.

Table S4. Exponential fit of the *cis* and *trans* signal for the thermal back isomerization at 262 K

absorption at 389 nm	absorption at 523 nm
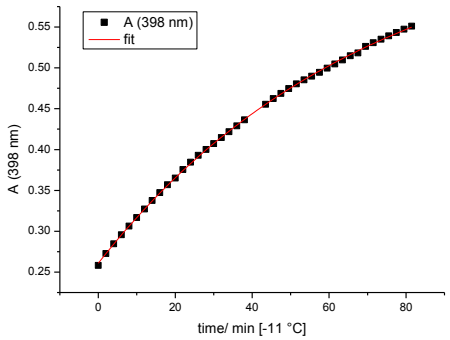	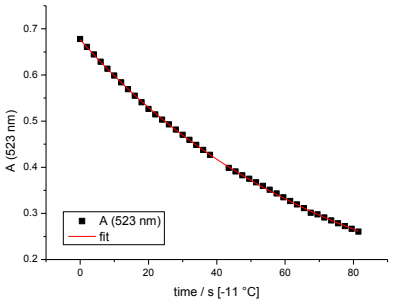
k = 2.39±0.03 *10^{-4} mol/s	k = 2.24±0.03 *10^{-4} mol/s
$t_{1/2}$ = 2902±42 s = 48.3±0.7 min	$t_{1/2}$ = 3096±42 s = 51.6±0.7 min

V1.2 Temperature T = 273 K

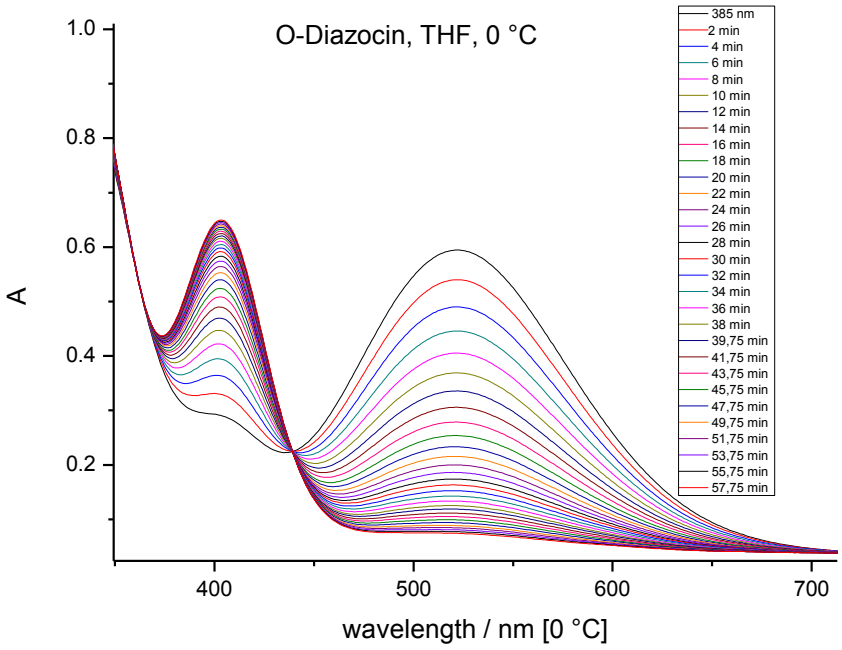

Figure S25: UV/Vis spectra of oxygen diazocine **2** after irradiation with 385 nm at 273 K.

Table S5. Exponential fit of the *cis* and *trans* signal for the thermal back isomerization at 273 K.

absorption at 389 nm	absorption at 523 nm
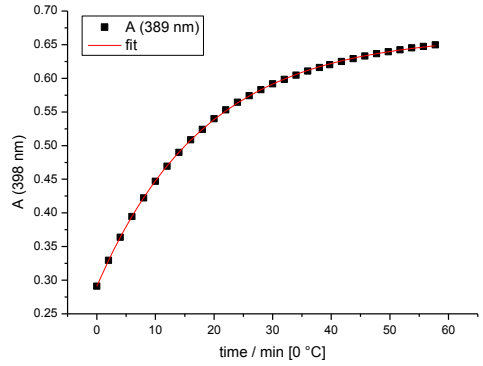	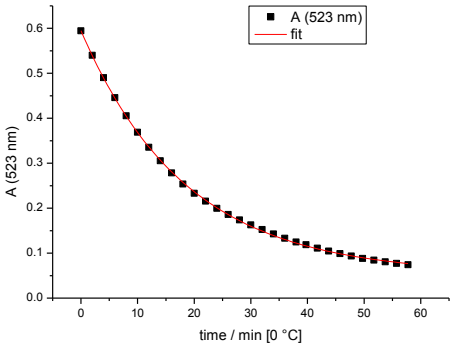
k = 9.07±0.04 *10^{-4} mol/s	k = 9.02±0.07 *10^{-4} mol/s
$t_{1/2}$ = 764±4 s = 12.7±0.06 min	$t_{1/2}$ = 769±7 s = 12.8±0.12 min

V1.3 Temperature T = 277 K

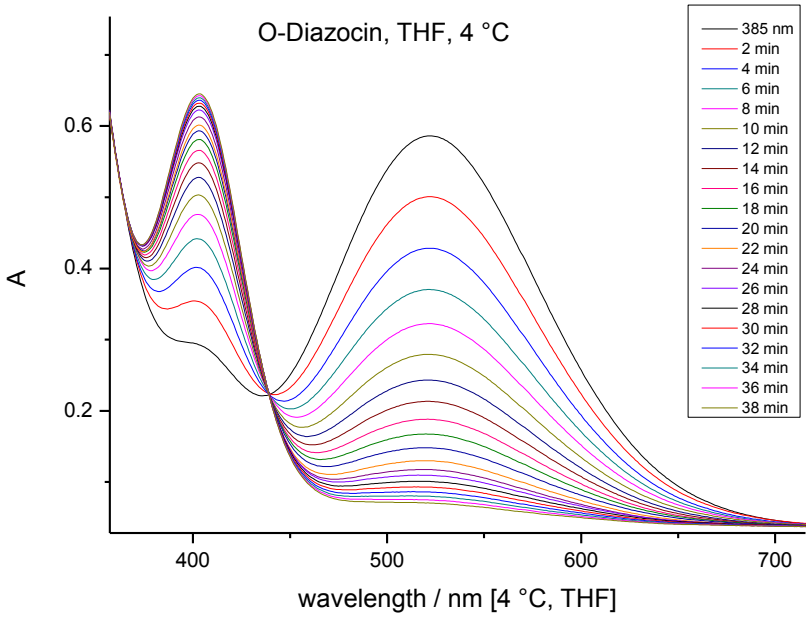

Figure S26: UV/Vis spectra of oxygen diazocine **2** after irradiation with 385 nm at 277 K.

Table S6. Exponential fit of the *cis* and *trans* signal for the thermal back isomerization at 277 K.

absorption at 389 nm	absorption at 523 nm
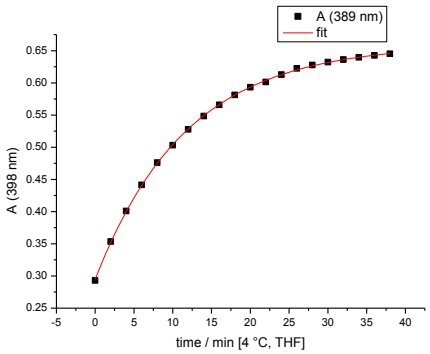	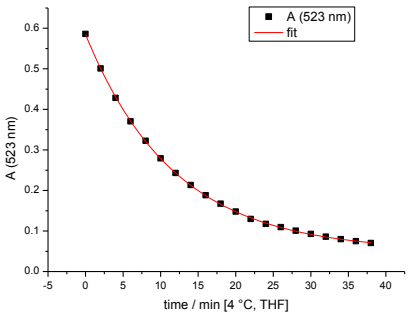
k = 1.42±0.008*10^{-3} mol/s	k = 1.42±0.01 *10^{-3} mol/s
$t_{1/2}$ = 489±4 s = 8.15±0.06 min	$t_{1/2}$ = 490±6 s = 8.16±0.1 min

V1.4 Temperature T = 282 K

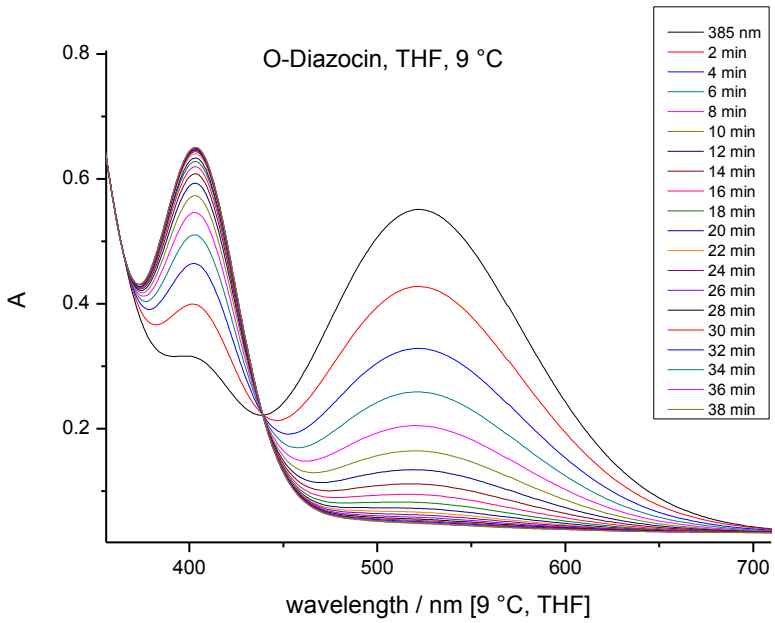

Figure S27: UV/Vis spectra of oxygen diazocine **2** after irradiation with 385 nm at 282 K.

Table S7. Exponential fit of the *cis* and *trans* signal for the thermal back isomerization at 282 K.

absorption at 389 nm	absorption at 523 nm
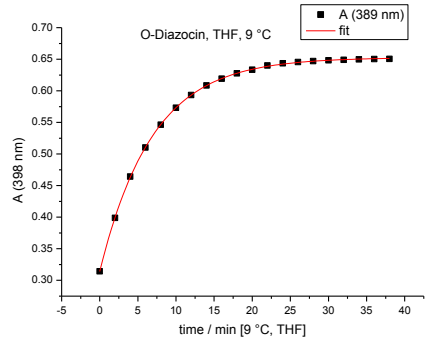	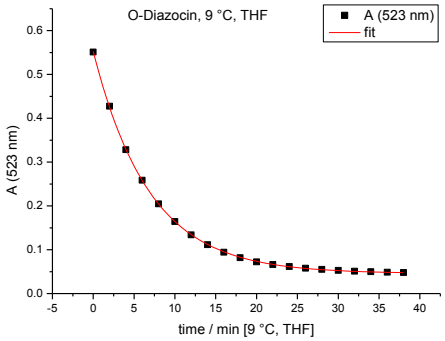
k = 2.42±0.009 *10^{-3} mol/s	k = 2.42±0.009 *10^{-3} mol/s
$t_{1/2}$ = 287±2 s = 4.78±0.03 min	$t_{1/2}$ = 286±2 s = 4.77±0.03 min

V1.5 Experimental determination of activation energy of the oxygen diazocine 2

To determine the activation energy of the switching process the logarithm of the rate constants were plotted as a function of 1/T.

Table S8. Arrhenius plots to determine the activation energy of the thermal back isomerization of the oxygen diazocine **2**.

A = 398 nm	A = 523 nm
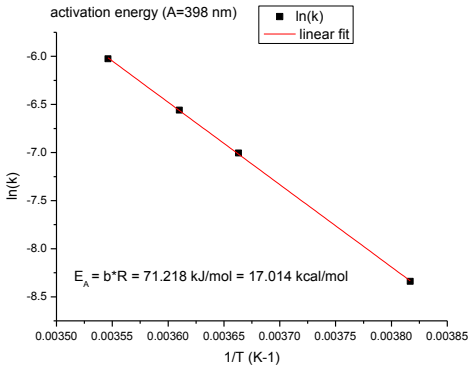	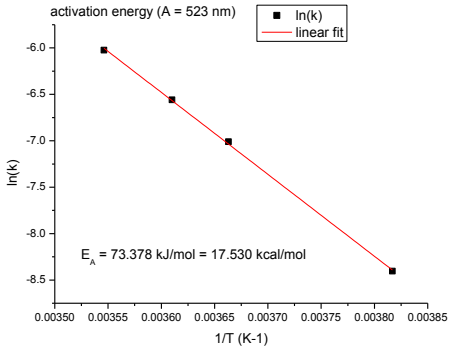
E_A = 71.2±0.49 kJ/mol=17.01±0.11 kcal/mol	E_A = 73.4±1.01 =17.53±0.24 kcal/mol

V.2 UV/Vis measurements of sulfur diazocine 3

A solution of sulfur diazocine **3** in THF was irradiated with 405 nm for 5 minutes at 293 K and UV/vis spectra were recorded every hour. The absorption maxima were plotted against time and the reaction time constants were determined.

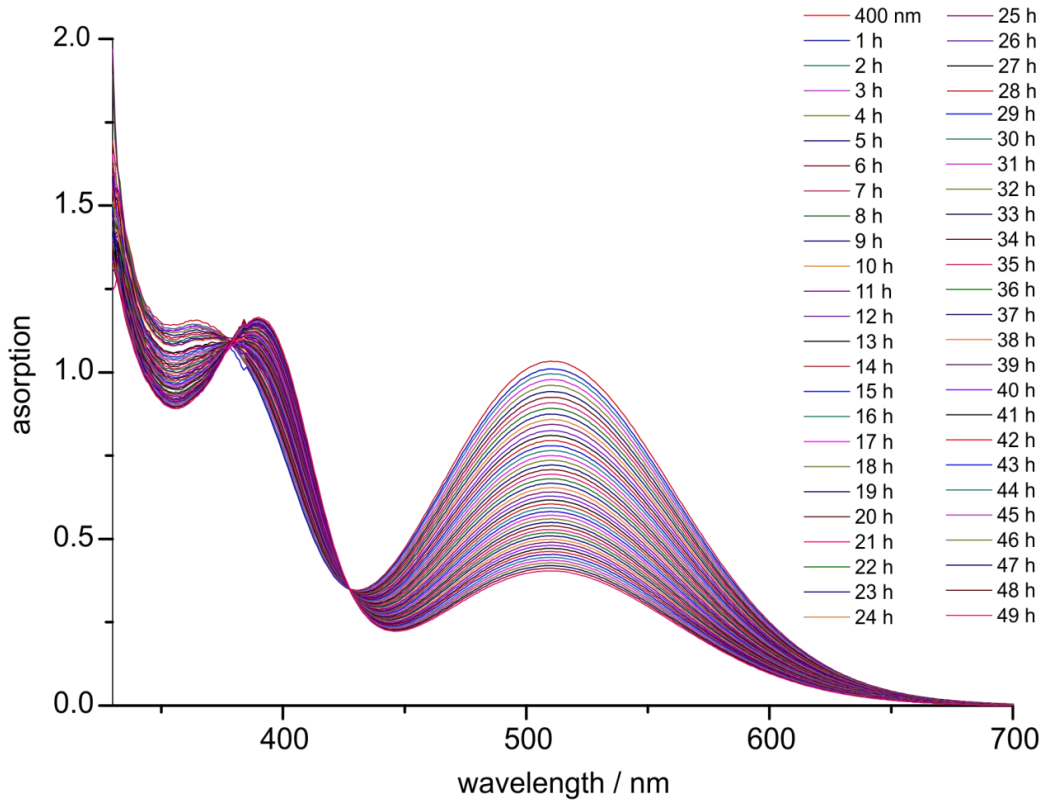

Figure S28: UV/Vis spectra of oxygen diazocine **2** after irradiation with 405 nm at 293 K.

(1) Lellmann, E.; Mayer, N. *Chem. Ber.* **1892**, *25*, 3583–3586.

VI.1 Short explanation of the movie

The movie is shown in real-time (no time-lapse!) The first part of the movie demonstrates that blue (385 nm) and green (530 nm) light don't penetrate the human skin while blood supported tissue is transparent to red light. Then the yellow *cis* isomer of the oxygen diazocine **2** is irradiated with 385 nm (LED light source) demonstrating the very rapid formation of the red *trans* isomer. By irradiation with green light (LED light source) the diazocine **2** isomerizes back to the yellow *cis* isomer within less than a second. The diazocine is switched a second time to the red *trans* isomer, to show the back isomerization to the *cis* configuration with red light.

6 Conclusion

The most common approach to functionalize Au(111) surfaces uses alkane thiols to form densely packed, covalently bound self-assembled monolayers (SAMs) on metal surfaces.[72–74] Due to the tight packing of these SAMs, functional molecules attached to the alkane chains stand nearly perpendicular to the surface.[78] Concomitantly, this is a great disadvantage of the strategy as for sterically demanding reactions (e.g. *cis* → *trans* isomerization) the space between the functional units is not sufficient.[79–83] A more sophisticated approach to realize highly ordered functionalized Au(111) surfaces is the platform concept that was developed by HERGES *et al.* in 2009.[88] It is based on triazatriangulenium (TATA) platforms that which form highly ordered hexagonal SAMs on Au(111), concomitantly providing sufficient free volume for a number of functionalities. The large planar cations offer the possibility of vertical functionalization by reaction of the cationic center with a nucleophile.[94] The advantage of this concept exists in the inherent orthogonal orientation of the functional molecules with respect to the surface.[104] Therefore, sufficient space between the functional units is ensured and isomerization of azobenzene moieties is possible.[103]

In this work three photoswitches were successfully developed as new functional units within the TATA platform concept. All three photoswitchable molecules perform different types of motion during the isomerization process. Both lateral shift and vertical stroke could be realized as motion on a molecular level. Thus, the fundemental work for the design and further development of the TATA platform concept towards molecular machines was achieved.

The first part of this work lays the groundwork for lateral movement of molecules on a Au(111) surface. To this end, two platform units were connected by an azobenzene moiety. This azobezene unit undergoes a conformational change if it is irradiated with 365 nm, which leads to a contraction of the whole molecule. Consequently, molecules of this type were coined molecular muscle.

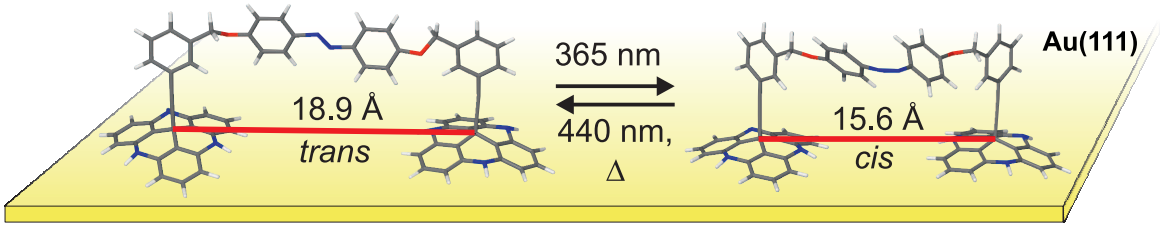

Figure 6.1: Scheme of the functional principle of the molecular muscle: by switching the azobenzene moiety the distance of the centers of the TATA platforms is shortened leading to a lateral movement above the surface.[109]

As TATA platforms bind only by London dispersion forces to Au(111) surfaces the sliding on the surface should have almost no barrier.[89] The design of these molecules was supported by density functional theory (DFT) calculations and the parameters were chosen in such a way that both platform units are able to bind to the metal surface in both configurations. Secondly, to prevent quenching of the photoisomerization by the gold surface,[108] the azobenzene unit needs to be located sufficiently far above the surface (Figure 6.1). Therefore, phenylacetylene was introduced as a vertical spacer unit between the platform and the azobenzene moiety. The synthesis of the best candidates followed a convergent synthetic route, whereby the azobenzene moiety and the TATA platforms were prepared separately and combined in the last step. Investigations of the photophysical properties in solution showed the high potential of the molecular muscles as they could be switched efficiently (95 %) to the metastable *cis* configuration. The *trans* isomers could be obtained again thermally or by irradiation with 440 nm. Switching the molecules between both configurations for several cycles proved the high photochemical stability as no sign of fatigue was observed.[109]

The concept of the molecular muscle enables the molecules to perform a lateral contraction and relaxation of the platform moieties. The second part of this theses focuses on the realization of a transport system for nanoparticles above a functionalized surface. Therefore, a new strategy had to be developed. It is inspired by the ciliated epithelium that transports mucous liquid and particles out of the human respiratory tract by performing a unidirectional stroke movement.[117–119] This movement consists of two separate parts; initially the progressive stroke is performed with a stretched conformation of the cilium followed by the regressive stroke in a bent shape.[120] A similar motion can be realized at the molecular level by an imine–functionalized TATA platform monolayer (Figure 6.2).

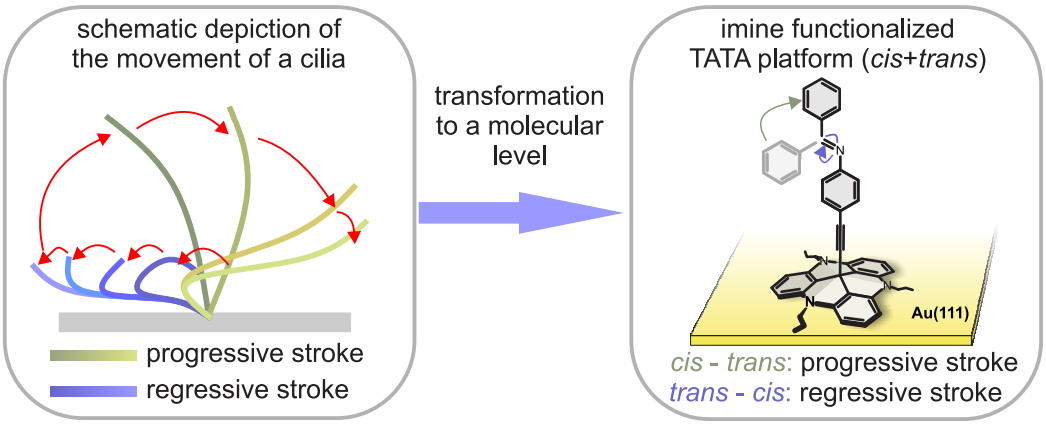

Figure 6.2: Cilia perform a unidirectional movement by adopting different shapes while performing the power stroke and the recovery motion.[121] It was the goal of this work to realize this transport system at the molecular level using imine-functionalized TATA platform monolayers on Au(111) as an artificial ciliated epithelium.[122]

By irradiation with UV light the imines undergo a *trans* → *cis* isomerization *via* a rotation mechanism, which mimics the regressive stroke. The following thermal back isomerization to the *trans* configuration occurs by inversion and, therefore, resembles the progressive stroke.[31–34] While using polarized light for the *trans* → *cis* isomerization, only the molecules with their dipole moment parallel to the incident light beam are switched. Thus, the stroke movement should lead to a net displacement of particles lying on top of the artificial epithelium.

To validate the above assumption six imine–functionalized TATA platforms were synthesized. The syntheses of the imines were achieved by condensation reaction of the corresponding benzaldehyde with the aniline derivative. The obtained imines were connected to the TATA platforms and the photochemical properties were investigated in solution. Experiments had to be performed at low temperatures (215–233 K) as the *cis* configurations are rapidly isomerizing back to the *trans* forms at room temperature ($t_{1/2}$ = 0.58 s). At low temperatures the *cis* configurations could be obtained with a yield of 50 % (^{1}H NMR). Rate constants for the thermal *cis* → *trans* isomerization were determined for different temperatures with UV/vis spectroscopy and extrapolated to room temperature. Scanning tunneling microscopy (STM) investigations show that the imine TATA platforms form highly ordered hexagonal monolayers on Au(111) surfaces with a $\sqrt{19} \times \sqrt{19}$ superstructure. Investigations of these monolayers with UV/vis spectroscopy indicated the integrity of the molecules on the Au(111) surface as the spectra in solution and on surface were nearly identical.[122]

The efficiency of the stroke movement could be enhanced if the high flexibility within the molecules is constrained. This can be accomplished by bridging the two phenyl rings with an ethyl unit, whereby free rotation is prevented. These diazocines exhibit excellent photochemical properties, such as high conversion to the corresponding isomer, high quantum yields and photostability.[49] Therefore, diazocines were developed for the functionalization of TATA platforms. Although the desired molecules have been synthesized and showed the anticipated photochemical properties, the difficult preparation hampered applications so far.[99] The ring closure reactions forming the diazocine azo group are hardly reproducible, difficult to scale up, and low yielding.[57,99,114–116] To simplify the synthetic procedure new bridging units were developed within this thesis. Towards this end, one of the methylene groups in the bridging unit was replaced by an oxygen or sulfur atom, respectively (Figure 6.3).

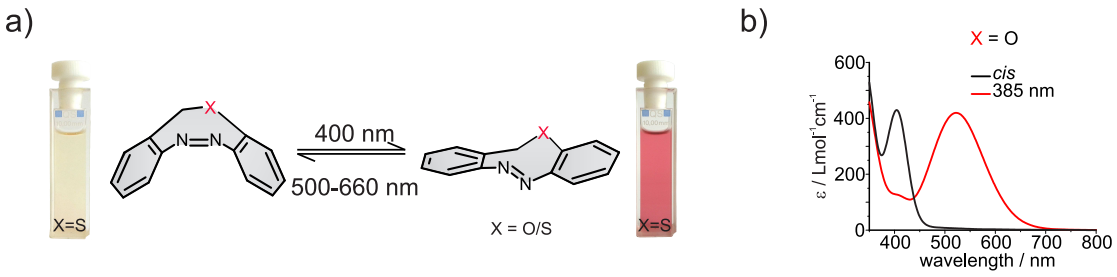

Figure 6.3: a) The metastable, red *trans* isomer can be obtained by irradiation with 400 nm, the back-isomerization to the yellow *cis* configuration is achieved with 500–660 nm, b) The UV/vis spectra of the *cis* and of the *trans* isomer reveal the well separated nπ* bands.

The syntheses of the dinitro precursors were achieved by reaction of the (thio)phenol with the corresponding benzyl bromide in a WILLIAMSON ether synthesis in good yields. The reaction time of the ring closure was drastically reduced using sonication with lead as a reducing agent. The azoxy compounds which are formed in the process were reduced to the diazocines using triphenylphosphine/MoO_2Cl_2 for the O–diazocine and Pb/ball mill for the S–diazocine. The overall yields for the ring closure are approximately 30 %. The oxygen as well as the sulfur diazocine exhibit improved photophysical properties compared to the parent system. Similar to the parent diazocine the *cis* configurations represent the thermodynamically more stable forms, with absorption bands at 400 nm ($n\pi^*$ excitations). After irradiation with blue light the absorption bands of the *trans* isomers are strongly shifted bathochromically with maxima at 525 nm. The $n\pi^*$ bands are broad and extend up to 700 nm. Hence, the back isomerizations to the *cis* configuration can be performed with green (530 nm) and red (660 nm) light. Therefore, these heterodiazocines represent ideal candidates for the application in photopharmacology as blood supported tissue is transparent in the near infrared region (650–950 nm). Although the switching wavelengths are nearly identical, both *trans* diazocines exhibit tremendous differences in their half-lives. Whereas the *trans* configuration of the oxygen diazocine has a short half-life of 89 s (20 °C, acetone), the sulfur diazocine has a distinctly higher thermal stability ($t_{1/2}$ = 85 h, 27 °C, acetone), compared to the parent system ($t_{1/2}$ = 4.5 h, 28.5 °C, *n*-hexane). Both diazocines can be switched several times, without noticeable fatigue or decay.

7 Prospect

This thesis lays the groundwork to further develop the TATA platform concept to realize a unidirectional movement and transport on the surface. As a next step towards this goal the presented compounds have to be investigated by scanning tunneling microscopy (STM) and atomic force microscopy (AFM) to gain further insight into their properties after deposition onto a surface. This is a crucial step for their future application as molecular machines.

The molecular muscle is capable of a light-induced reversible contraction. Consequently, irradiation results in a non-directional motion. The molecule can be enhanced towards a unidirectional movement on the surface by incorporation of a chiral photoswitchable unit. The great advantage of these molecules is the intrinsic unidirectional movement within the switching process.[123–126] A well known example for the realization of a directed motion is the so-called molecular car that was introduced by FERINGA *et al.*.[127] The directed locomotion of the molecular car that is induced by inelastic electronic tunneling using a STM tip was demonstrated on a Cu(111) surface. Concomitantly, with a STM tip only a single molecule could be addressed at the same time. Contrary to this, light is a promising external stimulus to address a large number of molecules simultaneously. However, there is no example of a light-induced unidirectional transport on a surface to date.

One approach towards this goal is the replacement of the azobenzene moiety by a chiral imine. LEHN suggested that this class of photoswitches is a promising candidate to be employed as a molecular motor since the light-induced *trans* $\rightarrow$ *cis* isomerization can only occur in one direction.[45] For one thing imines possess two isomerization pathways for forward and back reaction (rotation and inversion), and for another the rotation of the light-induced *trans* $\rightarrow$ *cis* isomerization could only occur in one direction while a chiral center is located next to the switching unit. A molecular motor that is based on this concept could already be realized but only works in solution and not on surfaces.[46] Thus, the replacement of the azobenzene unit of the molecular muscle by the Lehn Motor may facilitate a light-induced unidirectional movement. The resulting so-called molecular caterpillar is depicted in Figure 7.1.

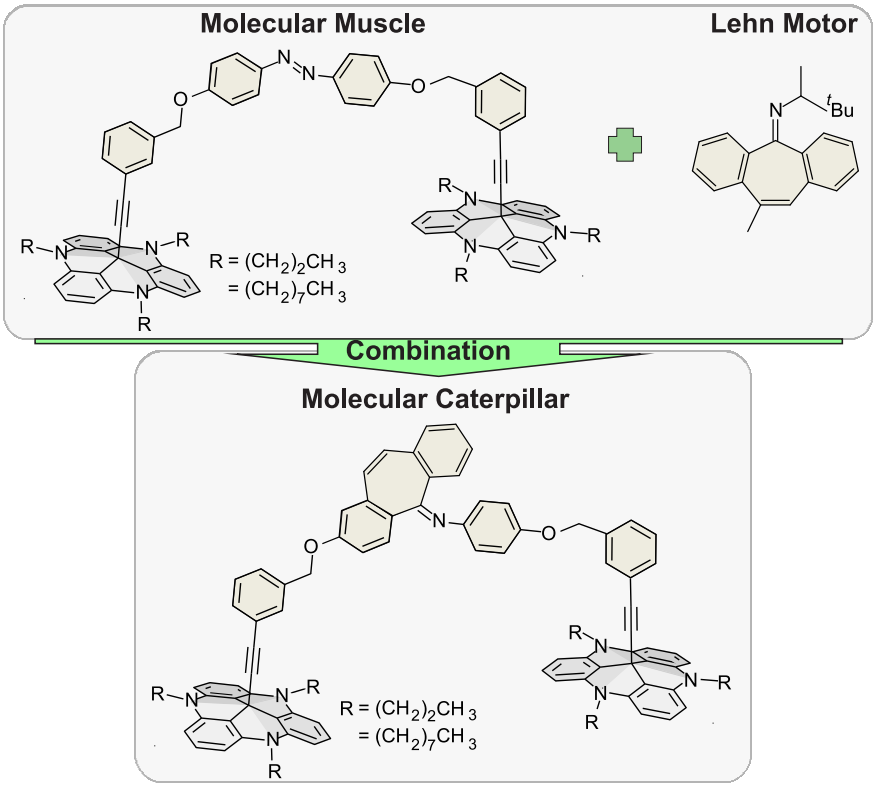

Figure 7.1: Implementation of a LEHN motor analogue[46] into the molecular muscle framework results in a molecular caterpillar that facilitates a unidirectional motion on the Au(111).

Furthermore, this chiral switching units are potential candidates to facilitate a directed transport on a surface based on the TATA platform concept. The switching process of the artifical ciliated epithelium that was presented in this thesis is already unidirectional. However, the rotation that is performed during the isomerization process may occur clockwise or counterclockwise. This can be circumvented by the implementation of a chiral center into the switching unit (e.g. indanediazocine or the lehn motor). Consequently, irradiation with polarized light induces an aligned rotation of all molecules. Thus, the stroke motion is more efficient and the transport velocity increases.

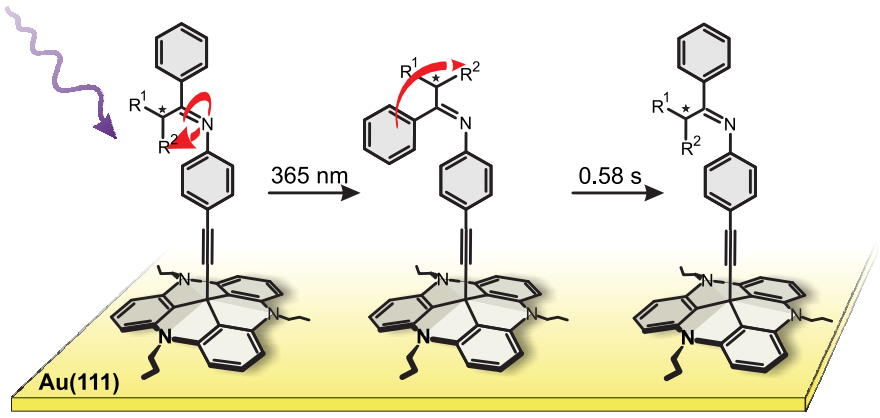

Figure 7.2: Implementation of a chiral center into the imine epithelium results in a strongly enhanced transport rate as all molecules perform an aligned rotation/inversion mechanism.

The superior photochemical properties of the heterodiazocines that were presented in the last part of the thesis open up a great variety of new possible applications. The developed synthetic route permits an easier access to unsymmetric diazocines. Consequently, the artificial ciliated epithelium designed by TELLKAMP are now available in larger yields and less effortful syntheses. Thus, future works focus on the syntheses of an indanediazocine derivative following the synthetic approach that was developed in this thesis to obtain an chiral and rigid photoswitch in high yields (Figure 7.3).

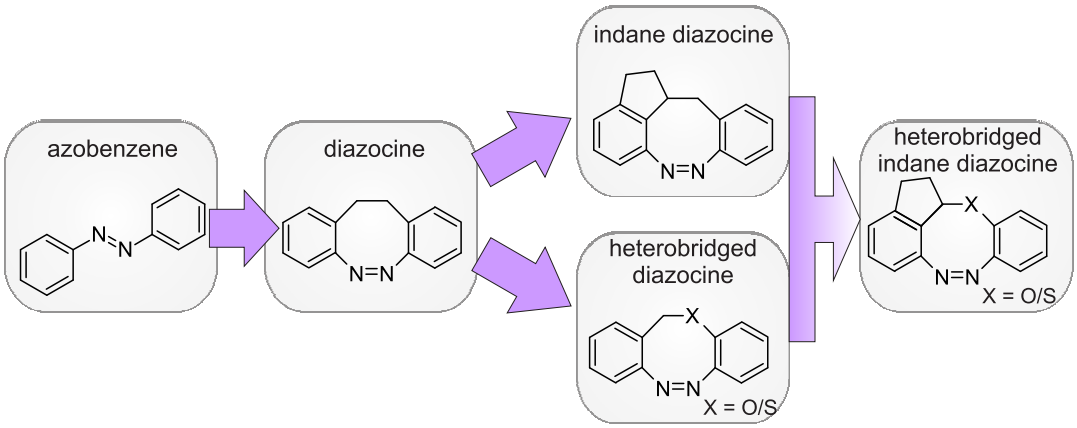

Figure 7.3: Diazocines could be further enhanced by a combination of heterobridge and indane diazocines to obtain chiral, rigid and easily obtainable photoswitches.

With their outstanding property to switch within the biooptical window heterodiazocines are predestinated for the application in photopharmaceuticals. This field of pharmacology has become of great interest in recent years as it provides promising approaches to answer urgent questions about the mechanisms of action and side effects of pharmaceuticals. Poor drug selectivity is one of the great challenges in the development of pharmaca as it is the main reason for side effects and dosage problems. A second drawback of the currently employed pharamaceuticals is the development of multiple drug resistances. To gain a deeper understanding of how these resistances emerge and how to avoid them is one of the most investigated issues in pharmacology. Photopharceuticals can be utilized to provide further insight into this matter since they can be switched repeatedly between an active and an inactive state and thus, allow the investigation of pharmacological processes by novel methods.[128–132] The incorporation of a nitrogen atom into the bridging unit results in a promising candidate for these investigations since the resulting photoswitchable molecules bear a strong resemblance to tricyclic antidepressants e.g. imipramine and desipramine (Figure 7.4). Additionally, the corresponding derivatives of this novel diazocine may be employed as model systems to gain a deeper understanding of the binding mechanism of antidepressants into the neuronal gap.[133] Furthermore, molecules of this type can be utilized as light-responsive activators for neurons.

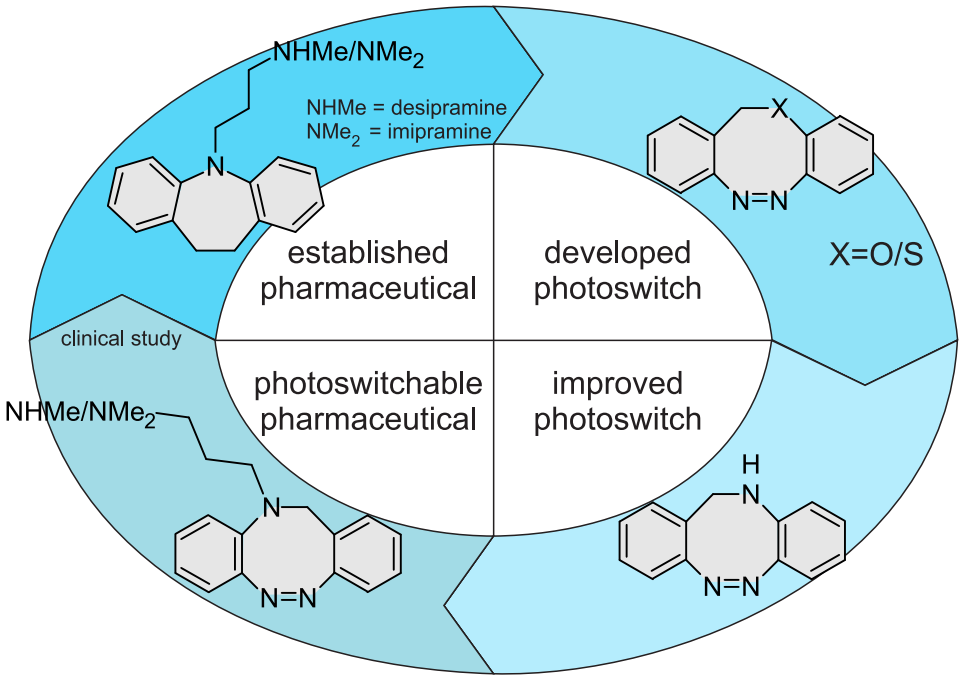

Figure 7.4: A photoswitchable antidepressant could eventually be developed by further modification of the heterodiazocines. By implementation of a nitrogen atom the photoswitch already resembles commercially available antidepressants. Combination of both structures would result in the design of a photopharmaceutical compound (neurotransmitter uptake inhibitor).

8 Bibliography

[1] K. Padian, *Nature* **2016**, *530*, 416–417.

[2] M. Wilkinson, *Restless Creatures: The Story of Life in Ten Movements*, Basic Books **2016**.

[3] S. Childress, A. Hosoi, W. W. Schultz, Z. J. Wang, *Natural Locomotion In Fluids and on Surface, Swimming, Flying, and Sliding*, Springer Science+Business Media New York **2012**.

[4] E. M. Purcell, *Am. Chem. J. Phys.* **1977**, *45*, 3–11.

[5] A. Najafi, R. Golestanian, *Phys. Rev. E* **2004**, *69*, 1–4.

[6] Y. Hirshberg, E. Fischer, *J. Chem. Phys.* **1955**, *23*, 1723–1723.

[7] B. L. Feringa, W. R. Brown, *Molecular Switches*, Wiley-VCH: Weinheim **2011**.

[8] D. H. Waldeck, *Chem. Rev.* **1991**, *91*, 415–436.

[9] E. Merino, M. Ribagorda, *Beilstein J. Org. Chem.* **2012**, *8*, 1071–1090.

[10] M. Irie, *Chem. Rev.* **2000**, *100*, 1685–1716.

[11] B. S. Lukyanov, M. B. Lukyanova, *Chem. Heterocycl. Compd.* **2005**, *41*, 281–311.

[12] G. S. Hartley, *Nature* **1937**, *140*, 281–281.

[13] A. Mostad, C. Rømming, C. Rømming, S. Hammarström, R. J. J. C. Lousberg, U. Weiss, *Acta Chem. Scand.* **1971**, *25*, 3561–3568.

[14] J. J. de Lange, J. M. Robertson, I. Woodward, *Proc. R. Soc. A* **1939**, *171*, 398–410.

[15] G. C. Hampson, J. M. Robertson, *J. Chem. Soc.* **1941**, 409.

[16] H. Knoll, *CRC Handbook of Organic Photochemistry and Photobiology Vol. 2 nd Edition*, CRC Press, Boca Rota, London, New York, Washington DC **1989**.

[17] G. S. Kumar, D. C. Neckers, *Chem. Rev.* **1989**, *89*, 1915–1925.

[18] J.-A. Andersson, R. Petterson, L. Tegnér, *J. Photochem.* **1982**, *20*, 17–32.

[19] P. Haberfield, P. M. Block, M. S. Lux, *J. Am. Chem. Soc.* **1975**, *97*, 5804–5806.

[20] A. Shaabani, M. Zahedi, *J. Mol. Struct. (Theochem.)* **2000**, *506*, 257–261.

[21] A. Cembran, F. Bernardi, M. Garavelli, L. Gagliardi, G. Orlandi, *J. Am. Chem. Soc.* **2004**, *126*, 3234–3243.

[22] N. Tamai, H. Miyasaka, *Chem. Rev.* **2000**, *100*, 1875–1890.

[23] T. Sueyoshi, N. Nishimura, S. Yamamoto, S. Hasegawa, *Chem. Lett.* **1974**, 1131–1134.

[24] T. Schultz, J. Quenneville, B. Levine, A. Toniolo, T. J. Martínez, S. Lochbrunner, M. Schmitt, J. P. Shaffer, M. Z. Zgierski, A. Stolow, *J. Am. Chem. Soc.* **2003**, *125*, 8098–8099.

[25] P. Cattaneo, M. Persico, *Phys. Chem. Chem. Phys.* **1999**, *1*, 4739–4743.

[26] T. Ishikawa, T. Noro, T. Shoda, *J. Chem. Phys.* **2001**, *115*, 7503–7512.

[27] H. Rau, E. Lueddecke, *J. Am. Chem. Soc.* **1982**, *104*, 1616–1620.

[28] H. M. D. Bandara, S. C. Burdette, *Chem. Soc. Rev.* **2012**, *41*, 1809–1825.

[29] C. Ciminelli, G. Granucci, M. Persico, *J. Chem. Phys.* **2005**, *123*, 1–10.

[30] G. S. Hartley, *J. Chem. Soc.* **1938**, 633–642.

[31] E. Fischer, Y. Frei, *J. Phys. Chem.* **1957**, *27*, 808–809.

[32] V. Bonacic-Koutecky, M. Persico, *J. Am. Chem. Soc.* **1983**, *105*, 3388–3395.

[33] K. Segawa, O. Kikuchi, T. Arai, K. Tokumaru, *J. Mol. Struct. (Theochem)* **1995**, *343*, 133–140.

[34] J. Gálvez, A. Guirado, *J. Comput. Chem.* **2009**, *31*, 520–531.

[35] L. M. N. Saleem, *Org. Magn. Reson.* **1982**, *19*, 176–180.

[36] G. Wettermark, E. Wallström, *Acta Chem. Scand.* **1968**, *22*, 675–680.

[37] Y. Luo, S. Korchak, H.-M. Vieth, R. Haag, *ChemPhysChem* **2010**, *12*, 132–135.

[38] H. B. Bürgi, J. D. Dunitz, C. Züst, *Acta Cryst. B* **1968**, *24*, 463–464.

[39] H. Jaffé, S.-J. Yeh, R. Gardner, *J. Mol. Spectrosc.* **1958**, *2*, 120–136.

[40] L. R. Knöpke, A. Spannenberg, A. Brückner, U. Bentrup, *Spectrochim. Acta, Part A* **2012**, *95*, 18–24.

[41] K. Maeda, K. A. Muszkat, S. Sharafi-Ozeri, *J. Chem. Soc., Perkin Trans. 2* **1980**, 1282–1287.

[42] V. de Gaouck, R. J. W. Le Févre, *J. Chem. Soc.* **1938**, 741–745.

[43] V. Baliah, M. Uma, *Tetrahedron* **1963**, *19*, 455–464.

[44] W. Gajewski, H. Wendt, R. Wolfbauer, *Ber. Bunsenges. Phys. Chem.* **1972**, *76*, 450–456.

[45] J.-M. Lehn, *Chem. Eur. J.* **2006**, *12*, 5910–5915.

[46] L. Greb, J.-M. Lehn, *J. Am. Chem. Soc.* **2014**, *136*, 13114–13117.

[47] H. Duval, *Bull. Soc. Chim. Fr.* **1910**, *7*, 727–732.

[48] F. Gerson, E. Heilbronner, A. van Veen, B. M. Wepster, *Helv. Chim. Acta* **1960**, *43*, 1889–1898.

[49] R. Siewertsen, H. Neumann, B. Buchheim-Stehn, R. Herges, C. Näther, F. Renth, F. Temps, *J. Am. Chem. Soc.* **2009**, *131*, 15594–15595.

[50] R. Siewertsen, J. B. Schönborn, B. Hartke, F. Renth, F. Temps, *Phys. Chem. Chem. Phys.* **2011**, *13*, 1054–1063.

[51] N. O. Carstensen, *Phys. Chem. Chem. Phys.* **2013**, *15*, 15017–15026.

[52] H. Rau, *J. Photochem.* **1984**, *26*, 221–225.

[53] S. Helmy, S. Oh, F. A. Leibfarth, C. J. Hawker, J. Read de Alaniz, *J. Org. Chem.* **2014**, *79*, 11316–11329.

[54] S. Helmy, F. A. Leibfarth, S. Oh, J. E. Poelma, C. J. Hawker, J. Read de Alaniz, *J. Am. Chem. Soc.* **2014**, *136*, 8169–8172.

[55] D. Bléger, S. Hecht, *Angew. Chem. Int. Ed.* **2015**, *54*, 11338–11349.

[56] S. Fredrich, R. Göstl, M. Herder, L. Grubert, S. Hecht, *Angew. Chem. Int. Ed.* **2015**, *55*, 1208–1212.

[57] M. Dong, A. Babalhavaeji, S. Samanta, A. A. Beharry, G. A. Woolley, *Acc. Chem. Res.* **2015**, *48*, 2662–2670.

[58] Y. Yang, R. P. Hughes, I. Aprahamian, *J. Am. Chem. Soc.* **2014**, *136*, 13190–13193.

[59] E. D. Sternberg, D. Dolphin, C. Brückner, *Tetrahedron* **1998**, *54*, 4151–4202.

[60] S. Stolik, J. Delgado, A. Pérez, L. Anasagasti, *J. Photochem. Photobiol. B* **2000**, *57*, 90–93.

[61] A. A. Beharry, O. Sadovski, G. A. Woolley, *J. Am. Chem. Soc.* **2011**, *133*, 19684–19687.

[62] D. Bléger, J. Schwarz, A. M. Brouwer, S. Hecht, *J. Am. Chem. Soc.* **2012**, *134*, 20597–20600.

[63] J. Moreno, M. Gerecke, L. Grubert, S. A. Kovalenko, S. Hecht, *Angew. Chem.* **2015**, *128*, 1569–1573.

[64] S. Castellanos, A. Goulet-Hanssens, F. Zhao, A. Dikhtiarenko, A. Pustovarenko, S. Hecht, J. Gascon, F. Kapteijn, D. Bléger, *Chem. Eur. J.* **2015**, *22*, 746–752.

[65] C. Knie, M. Utecht, F. Zhao, H. Kulla, S. Kovalenko, A. M. Brouwer, P. Saalfrank, S. Hecht, D. Bléger, *Chem. Eur. J.* **2014**, *20*, 16492–16501.

[66] Y. Yang, R. P. Hughes, I. Aprahamian, *J. Am. Chem. Soc.* **2012**, *134*, 15221–15224.

[67] C. Vericat, M. E. Vela, G. Benitez, P. Carro, R. C. Salvarezza, *Chem. Soc. Rev.* **2010**, *39*, 1805–1834.

[68] S. Barlow, R. Raval, *Surf. Sci. Rep.* **2003**, *50*, 201–341.

[69] S. De Feyter, F. C. De Schryver, *Chem. Soc. Rev.* **2003**, *32*, 139–150.

[70] F. Schreiber, *Prog. Surf. Sci.* **2000**, *65*, 151–257.

[71] J. A. A. W. Elemans, S. Lei, S. De Feyter, *Angew. Chem. Int. Ed.* **2009**, *48*, 7298–7332.

[72] A. Ulman, *Chem. Rev.* **1996**, *96*, 1533–1554.

[73] F. Schreiber, *J. Phys.: Condens. Matter* **2004**, *16*, 881–900.

[74] J. C. Love, L. A. Estroff, J. K. Kriebel, R. G. Nuzzo, G. M. Whitesides, *Chem. Rev.* **2005**, *105*, 1103–1170.

[75] C. D. Bain, J. Evall, G. M. Whitesides, *J. Am. Chem. Soc.* **1989**, *111*, 7155–7164.

[76] C. D. Bain, E. B. Troughton, Y. T. Tao, J. Evall, G. M. Whitesides, R. G. Nuzzo, *J. Am. Chem. Soc.* **1989**, *111*, 321–335.

[77] D. K. Schwartz, *Annu. Rev. Phys. Chem.* **2001**, *52*, 107–137.

[78] M. D. Porter, T. B. Bright, D. L. Allara, C. E. D. Chidsey, *J. Am. Chem. Soc.* **1987**, *109*, 3559–3568.

[79] D. T. Valley, M. Onstott, S. Malyk, A. V. Benderskii, *Langmuir* **2013**, *29*, 11623–11631.

[80] G. Pace, V. Ferri, C. Grave, M. Elbing, C. von Hänisch, M. Zharnikov, M. Mayor, M. A. Rampi, P. Samorí, *Proc. Natl. Acad. Sci. USA* **2007**, *104*, 9937–9942.

[81] T. Weidner, F. Bretthauer, N. Ballav, H. Motschmann, H. Orendi, C. Bruhn, U. Siemeling, M. Zharnikov, *Langmuir* **2008**, *24*, 11691–11700.

[82] S. D. Evans, S. R. Johnson, H. Ringsdorf, L. M. Williams, H. Wolf, *Langmuir* **1998**, *14*, 6436–6440.

[83] V. Ferri, M. Elbing, G. Pace, M. D. Dickey, M. Zharnikov, P. Samorì, M. Mayor, M. A. Rampi, *Angew. Chem.* **2008**, *120*, 3455–3457.

[84] S. J. Stranick, A. N. Parikh, Y.-T. Tao, D. L. Allara, P. S. Weiss, *J. Phys. Chem.* **1994**, *98*, 7636–7646.

[85] K. Tamada, H. Akiyama, T. X. Wei, *Langmuir* **2002**, *18*, 5239–5246.

[86] K. Tamada, M. Hara, H. Sasabe, W. Knoll, *Langmuir* **1997**, *13*, 1558–1566.

[87] R. Klajn, *Pure Appl. Chem.* **2010**, *82*, 2247–2279.

[88] B. Baisch, D. Raffa, U. Jung, O. M. Magnussen, C. Nicolas, J. Lacour, J. Kubitschke, R. Herges, *J. Am. Chem. Soc.* **2009**, *131*, 442–443.

[89] N. Hauptmann, K. Scheil, T. G. Gopakumar, F. L. Otte, C. Schütt, R. Herges, R. Berndt, *J. Am. Chem. Soc.* **2013**, *135*, 8814–8817.

[90] S. Lemke, S. Ulrich, F. Claußen, A. Bloedorn, U. Jung, R. Herges, O. M. Magnussen, *Surf. Sci.* **2015**, *632*, 71–76.

[91] J. Kubitschke, *PhD thesis*, Kiel University **2010**.

[92] T. Tellkamp, *PhD thesis*, Kiel University **2014**.

[93] S. Kuhn, B. Baisch, U. Jung, T. Johannsen, J. Kubitschke, R. Herges, O. M. Magnussen, *Phys. Chem. Chem. Phys.* **2010**, *12*, 4481–4487.

[94] J. Kubitschke, C. Näther, R. Herges, *Eur. J. Org. Chem.* **2010**, *26*, 5041–5055.

[95] U. Jung, C. Schütt, O. Filinova, J. Kubitschke, R. Herges, O. Magnussen, *J. Phys. Chem. C* **2012**, *116*, 25943–25948.

[96] F. L. Otte, *PhD thesis*, Kiel University **2012**.

[97] F. L. Otte, S. Lemke, C. Schütt, N. R. Krekiehn, U. Jung, O. M. Magnussen, R. Herges, *J. Am. Chem. Soc.* **2014**, *136*, 11248–11251.

[98] N. Hauptmann, L. Groß, K. Buchmann, K. Scheil, C. Schütt, F. L. Otte, R. Herges, C. Herrmann, R. Berndt, *New J. Phys.* **2015**, *17*, 1–8.

[99] T. Tellkamp, J. Shen, Y. Okamoto, R. Herges, *Eur. J. Org. Chem.* **2014**, *2014*, 5456–5461.

[100] Z. Wei, X. Wang, A. Borges, M. Santella, T. Li, J. K. Sørensen, M. Vanin, W. Hu, Y. Liu, J. Ulstrup, G. C. Solomon, Q. Chi, T. Bjørnholm, K. Nørgaard, B. W. Laursen, *Langmuir* **2014**, *30*, 14868–14876.

[101] N. R. Krekiehn, M. Müller, U. Jung, S. Ulrich, R. Herges, O. M. Magnussen, *Langmuir* **2015**, *31*, 8362–8370.

[102] U. Jung, S. Kuhn, U. Cornelissen, F. Tuczek, T. Strunskus, V. Zaporojtchenko, J. Kubitschke, R. Herges, O. Magnussen, *Langmuir* **2011**, *27*, 5899–5908.

[103] H. Jacob, S. Ulrich, U. Jung, S. Lemke, T. Rusch, C. Schütt, F. Petersen, T. Strunskus, O. M. Magnussen, R. Herges, F. Tuczek, *Phys. Chem. Chem. Phys.* **2014**, *16*, 22643–22650.

[104] S. Ulrich, U. Jung, T. Strunskus, C. Schütt, A. Bloedorn, S. Lemke, E. Ludwig, L. Kipp, F. Faupel, O. M. Magnussen, R. Herges, *Phys. Chem. Chem. Phys.* **2015**, *17*, 17053–17062.

[105] M. Alemani, M. V. Peters, S. Hecht, K.-H. Rieder, F. Moresco, L. Grill, *J. Am. Chem. Soc.* **2006**, *128*, 14446–14447.

[106] X. Zheng, M. E. Mulcahy, D. Horinek, F. Galeotti, T. F. Magnera, J. Michl, *J. Am. Chem. Soc.* **2004**, *126*, 4540 –4542.

[107] Y. Liu, A. H. Flood, P. A. Bonvallet, S. A. Vignon, B. H. Northrop, H.-R. Tseng, J. O. Jeppesen, T. J. Huang, B. Brough, M. Baller, S. Magonow, S. D. Solares, W. A. Goddard, C.-M. Ho, J. F. Stoddart, *J. Am. Chem. Soc.* **2005**, *127*, 9745–9759.

[108] P. Tegeder, *J. Phys.: Condens. Matter* **2012**, *24*, 394001.

[109] M. Hammerich, R. Herges, *J. Org. Chem.* **2015**, *80*, 11233–11236.

[110] R. Wang, T. Iyoda, K. Hashimoto, A. Fujishima, *J. Phys. Chem.* **1995**, *99*, 3352–3356.

[111] R. Wang, L. Jiang, T. Iyoda, D. A. Tryk, K. Hashimoto, A. Fujishima, *Langmuir* **1996**, *12*, 2052–2057.

[112] G. Haberhauer, C. Kallweit, *Angew. Chem.* **2010**, *122*, 2468–2471.

[113] C. J. Bruns, J. F. Stoddart, *Acc. Chem. Res.* **2014**, *47*, 2186–2199.

[114] H. Sell, C. Näther, R. Herges, *Beilstein J. Org. Chem.* **2013**, *9*, 1–7.

[115] D. K. Joshi, M. J. Mitchell, D. Bruce, A. J. Lough, H. Yan, *Tetrahedron* **2012**, *68*, 8670–8676.

[116] F. Eljabu, J. Dhruval, H. Yan, *Bioorg. Med. Chem. Lett.* **2015**, *25*, 5594–5596.

[117] R. Xue, Q. Ma, M. A. B. Baker, F. Bai, *Adv. Sci.* **2015**, *2*, 1500129.

[118] B. Bhushan, *Phil. Trans. R. Soc. A* **2009**, *367*, 1445–1486.

[119] I. Ibanez-Tallon, *Hum. Mol. Genet.* **2003**, *12*, 27R–35.

[120] J. Gray, *Proc. R. Soc. A* **1922**, *93*, 104–121.

[121] G. Winkel, R. Wiedemann, K. Thomaier, *Paramecium caudatum (Pantoffeltierchen) Arbeitshilfe Nr. 15.17*, Bd. 2, Landeshauptstadt Hannover Fachbereich Bibliothek und Schule **1992**.

[122] M. Hammerich, T. Rusch, N. R. Krekiehn, A. Bloedorn, O. M. Magnussen, R. Herges, *ChemPhysChem* **2016**, *17*, 1870–1874.

[123] N. Koumura, E. M. Geertsema, A. Meetsma, B. L. Feringa, *J. Am. Chem. Soc.* **2000**, *122*, 12005–12006.

[124] G. Haberhauer, C. Kallweit, *Angew. Chem.* **2010**, *122*, 2468–2471.

[125] G. T. Carroll, G. London, T. F. Landaluce, P. Rudolf, B. L. Feringa, *ACS Nano* **2011**, *5*, 622–630.

[126] K.-Y. Chen, O. Ivashenko, G. T. Carroll, J. Robertus, J. C. M. Kistemaker, G. London, W. R. Browne, P. Rudolf, B. L. Feringa, *J. Am. Chem. Soc.* **2014**, *136*, 3219–3224.

[127] T. Kudernac, N. Ruangsupapichat, M. Parschau, B. Macá, N. Katsonis, S. R. Harutyunyan, K.-H. Ernst, B. L. Feringa, *Nature* **2011**, *479*, 208–211.

[128] J. Broichhagen, J. A. Frank, D. Trauner, *Acc. Chem. Res.* **2015**, *48*, 1947–1960.

[129] W. A. Velema, W. Szymanski, B. L. Feringa, *J. Am. Chem. Soc.* **2014**, *136*, 2178–2191.

[130] A. A. Beharry, G. A. Woolley, *Chem. Soc. Rev* **2011**, *40*, 4422–4437.

[131] O. Babii, S. Afonin, M. Berditsch, S. Reisser, P. K. Mykhailiuk, V. S. Kubyshkin, T. Steinbrecher, A. S. Ulrich, I. V. Komarov, *Angew. Chem.* **2014**, *126*, 3460–3463.

[132] M. Stein, S. J. Middendorp, V. Carta, E. Pejo, D. E. Raines, S. A. Forman, E. Sigel, D. Trauner, *Angew. Chem.* **2012**, *124*, 10652–10656.

[133] A. Mourot, I. Tochitsky, R. H. Kramer, *Front. Mol. Neurosci.* **2013**, *6*, 1–15.